Catalytic Oxy-aminomethylation of Alkenes

Inaugural-Dissertation

zur

Erlangung des Doktorgrades

der Mathematisch-Naturwissenschaftlichen Fakultät

der Universität zu Köln

vorgelegt von

María de los Ángeles Guillén Moralejo

aus Barcelona (Spanien)

Köln 2025

A mi familia

Acknowledgements

I feel profoundly privileged to have had the opportunity to pursue my doctoral studies in Germany, at one of the world's foremost institutes for chemical catalysis. This journey has shaped me in countless ways, and I'm genuinely grateful for the experiences and for all the people who have been part of these past 4 years.

First, I would like to thank my PhD advisor Prof. Dr. Benjamin List, for your support and trust throughout my doctoral studies. Your mentorship has provided the perfect balance between guidance and independence, allowing me to explore my ideas freely while challenging me to aim high. This experience has pushed me to grow both as a chemist and as a person, and I am deeply grateful for your influence on my journey.

I would also like to thank Prof. Dr. Stephanie Kath-Schorr for accepting to review this thesis, and Prof. Dr. Alex Klein and Dr. Monika Lindner for serving on my defense committee.

Next, I would like to thank my collaborators on the research presented in this dissertation, Dr. Sensheng Liu and Dr. David D. Díaz-Oviedo, for all your help and insightful contributions to the oxy-aminomethylation of styrenes project. I would especially like to thank Dr. Markus Leutzsch for all the NMR experiments, scientific discussions, and his constant support throughout the hetero-cycloaddition project. I am truly grateful for your patience and for being so helpful at every stage of the process. Special thanks to those who assisted in proofreading this thesis and offered important constructive criticism: Dr. Roberta Properzi, Dr. Sebastian Brunen, Nils Frank, Wencke Leinung, and Jan Samsonowicz-Górski.

I sincerely acknowledge the excellent service provided by the technician team of the List laboratory in the synthesis of catalysts and intermediates. I also extend my gratitude to all the analytical departments at our institute, especially the HPLC and GC teams, for their assistance in separating chiral compounds.

Thank you to Bruni, Wencke, Mathias, Luc, Markus, and Jan, not only for being brilliant scientists but also for being wonderful colleagues. I deeply appreciate the great companionship both in and outside the lab, the chats, drinks, parties, and all the unforgettable moments. I am very happy to have crossed paths with you during our PhD studies and to have shared incredible memories together.

I would not have reached this point without the incredible support, guidance, and friendship of some of the people I met here. First, I would like to thank David for the invaluable mentorship you offered me at the beginning of the PhD. Your knowledge, advice, and positive attitude really helped me thrive the first months in the List group. Second, I would like to thank my older but smaller sister Gabyta for your friendship, support, and always being so caring with me since I arrived in Mülheim. I am truly grateful that I can always rely on you. Gracias, hermanita. Third, I would like to especially thank Roberta

for the precious friendship over these years. Thank you for being there in my lowest and highest moments, for being so attentive, for your wise advice, for all the conversations and moments shared, and for being part of my life. I am very grateful to have met you here.

Lastly, I would like to thank my family, most especially my parents, for their unconditional support from over thousands of kilometers away throughout my PhD studies.

Table of Contents

Abstract

The direct difunctionalization of C=C bonds is a particularly powerful strategy for the transformation of feedstock olefins into structurally complex building blocks. Olefin 1,2-functionalizations take an important place in chemical synthesis, with dihydroxylation and aminohydroxylation serving as notable examples of their significance. The transformation of olefins into 1,3-dioxygenated moieties through their reaction with aldehydes (Prins reaction) has been extensively documented and several catalytic methodologies thereof are available nowadays. Nonetheless, an analogous, straightforward strategy that enables the oxy-aminomethylation of alkenes remains underexplored, despite its significant potential for the synthesis of marketed blockbuster antidepressant drugs such as duloxetine, fluoxetine, and atomoxetine.

The first part of this PhD work discloses the three-component reaction of aryl olefins, formaldehyde, and ammonia surrogates, such as sulfonamides or carbamates, to yield the corresponding 1,3-oxazinanes using the strong Brønsted acid HPF_6 as catalyst. The proposed transformation not only contributes to the field of olefin functionalization but also benefits from the wide availability of sulfonamides and carbamates, which are common and widely used pharmacophores. This method affords a variety of 1,3-oxazinanes in moderate to good yields under mild reaction conditions. Mechanistic investigations suggest the intermediacy of an in situ generated 1,3,5-dioxazinane and a subsequent reaction with the olefin.

The second part of this PhD work discloses the highly enantioselective, inverse-electron-demand hetero-Diels−Alder reaction of olefins with in situ generated *N*-Boc-formaldimine catalyzed by strong and confined Brønsted acids. This transformation provides direct access to valuable enantioenriched oxazinanones, common motifs in biologically active molecules and direct precursors of 1,3-amino alcohols. The synthetic utility of the obtained cycloaddition products has been demonstrated by the multigram-scale synthesis of the antidepressant (*R*)-fluoxetine hydrochloride. Isotope labeling studies and kinetic analysis reveal an unusual mechanism involving an oxazinium intermediate and a catalyst order greater than one.

Kurzzusammenfassung

Die direkte Difunktionalisierung von C=C-Bindungen ist eine besonders leistungsfähige Strategie zur Umwandlung von Olefinen in strukturell komplexe Bausteine. 1,2-Difunktinoalisierung nehmen einen wichtigen Platz in der chemischen Synthese ein, wobei Dihydroxylierungen und Aminohydroxylierungen herausragende Beispiele für ihre Bedeutung darstellen. Die Umwandlung von Olefinen in 1,3-Dioxy-Strukturen durch ihre Reaktion mit Aldehyden (Prins-Reaktion) ist ausführlich dokumentiert, und mehrere katalytische Methoden hierfür sind heutzutage verfügbar. Trotz ihres erheblichen Potenzials für die Synthese bedeutender Antidepressiva wie Duloxetin, Fluoxetin und Atomoxetin jedoch ist die analoge Oxy-Aminomethylierung von Alkenen bisher noch nicht bekannt.

Der erste Teil dieser Doktorarbeit beschreibt die Drei-Komponenten-Reaktion von Aryl-Olefinen, Formaldehyd und Ammoniak-Derivaten wie Sulfonamiden oder Carbamaten zur Synthese von 1,3-Oxazinanen unter Verwendung der starken Brønsted-Säure HPF_6 als Katalysator. Die untersuchte Transformation trägt nicht nur zum Bereich der Olefin-Funktionalisierung bei, sie wird auch durch die breite Verfügbarkeit von Sulfonamiden und Carbamaten begünstigt, die gängige und weit verbreitete Pharmakophore sind. Diese Methode liefert eine Vielzahl von 1,3-Oxazinanen in moderaten bis guten Ausbeuten unter milden Reaktionsbedingungen. Mechanistische Untersuchungen deuten auf die Zwischenstufe eines in situ erzeugten 1,3,5-Dioxazinan und einer anschließenden Reaktion mit dem Olefin hin.

Der zweite Teil dieser Doktorarbeit beschreibt die hochenantioselektive Hetero-Diels–Alder-Reaktion mit inversem Elektronenbedarf von Olefinen mit in situ erzeugtem *N*-Boc-Formaldimin, katalysiert durch starke und sterisch umzäunte Brønsted-Säuren. Diese Transformation ermöglicht den direkten Zugang zu synthetisch relevanten, enantiomerenangereicherten Oxazinanonen, die häufige Motive in biologisch aktiven Molekülen und direkte Vorstufen von 1,3-Aminoalkoholen darstellen. Der synthetische Nutzen der erhaltenen Cycloadditionsprodukte wurde durch die Multigramm-Synthese des Antidepressivums (*R*)-Fluoxetin-Hydrochlorid demonstriert. Isotopenmarkierungsstudien und kinetische Analysen deuten auf einen unerwartet Mechanismus, der ein Oxazinium-Intermediat und eine Katalysatorordnung größer als eins beinhaltet.

List of Abbreviations

Ac	acyl
AcO	acetoxy
aq.	aqueous
Ar	aryl, aromatic
Alk	alkyl
atm	atmosphere(s)
BINOL	1,1'-bi-2-naphthol
Bn	benzyl
Boc	*tert*-butoxycarbonyl
Bu	butyl
Cbz	benzyloxycarbonyl
cat.	catalyst
conv.	conversion
COSY	correlated spectroscopy
CPA	chiral phosphoric acid
Cy	cyclohexyl
d	day(s) or doublet
DCE	1,2-dichloroethane
DCM	dichloromethane
(DHQD)$_2$-PHAL	hydroquinidine 1,4-phthalazinediyl diether
DIBAL	diisobutylaluminum hydride
DIPEA	diisopropylethylamine, Hünig's base
DMA	dimethylacetamide
DMF	dimethylformamide
DMSO	dimethyl sulfoxide
DNA	deoxyribonucleic acid
DOPA	3,4-dihydroxyphenylalanine
DTBM-SEGPHOS	5,5′-bis-[di-(3,5-di-*tert*-butyl-4-methoxyphenyl)-phosphino]-4,4′-bi-1,3-benzodioxol
d.r.	diastereomeric ratio
DSI	disulfonimide
e$^-$	electron
EDG	electron-donating group
e.e.	enantiomeric excess
EI	electron impact
equiv.	equivalent(s)
e.r.	enantiomeric ratio
ESI	electrospray ionization
Et	ethyl
EWG	electron-withdrawing group

Fmoc	fluorenylmethoxycarbonyl
GC	gas chromatography
GDH	glucose dehydrogenase
h	hour(s)
hept	heptet
HMDS	hexamethyldisilazane
HMBC	heteronuclear multiple bond correlation
HOMO	highest occupied molecular orbital
HPLC	high performance liquid chromatography
HRMS	high-resolution mass spectrometry
HSQC	heteronuclear single quantum coherence
i	iso
IDP	imidodiphosphate
IDPi	imidodiphosphorimidate
IEDDA	inverse-electron-demand Diels–Alder
*i*IDP	iminoimidodiphosphate
JINGLE	1,1'-binaphthyl-2,2'-bis(sulfuryl)imide
L	ligand
LC-MS	liquid chromatography coupled with mass spectrometry
LG	leaving group
LUMO	lowest unoccupied molecular orbital
m	multiplet
m	*meta*
M	metal or molar
Me	methyl
min	minute(s)
MS	mass spectrometry or molecular sieves
MTBE	methyl *tert*-butyl ether
NADP	nicotinamide adenine dinucleotide phosphate
naphth	naphthyl
NMR	nuclear magnetic resonance
NLE	nonlinear effects
NTPA	*N*-triflyl phosphoramide
Nu, H–Nu	nucleophile
o	*ortho*
p	pentet
p	*para*
P, Pro	product
PADI	phosphoramidimidate
PG	protecting group
Ph	phenyl

P-Phos	dipyridylphosphine
Piv	pivaloyl
PMB	*para*-methoxybenzyl
Pr	propyl
p-TsOH	*para*-toluenesulfonic acid
q	quadruplet
quant.	quantitative
rac	racemic
[Red]	reduction
ROESY	rotating frame Overhauser enhancement spectroscopy
rt	room temperature
s	singlet
sat.	saturated
SEGPHOS	5,5′-bis-(diphenylphosphino)-4,4′-bi-1,3-benzodioxol
SM	starting material
S_N	nucleophilic substitution
SNRI	serotonin-norepinephrine reuptake inhibitor
SSRI	selective serotonin reuptake inhibitors
t	time or triplet
t, *tert*	tertiary
T, Temp	temperature
Tf	trifluoromethylsulfonyl
TFA	trifluoroacetic acid
THF	tetrahydrofuran
TLC	thin layer chromatography
TMS	trimethylsilyl
TOCSY	total correlation spectroscopy
TON	turnover number
TPP	tetraphenylporphyrinato
TRIP	3,3'-bis(2,4,6-triisopropylphenyl)-1,1'-binaphthyl-2,2'-diyl hydrogenphosphate
Ts	tosyl
TS	transition state
v	volume
VTNA	variable time normalization analysis

1. Introduction

"L'univers est un ensemble dissymétrique et je suis persuadé que la vie, telle qu'elle se manifeste à nous, est fonction de la dissymétrie de l'univers ou des conséquences qu'elle entraîne. L'univers est dissymétrique."

— Louis Pasteur (1874)

The insightful reflections of Pasteur, articulated over a century ago, have profoundly shaped the landscape of stereochemistry. In contemporary chemistry, the concept of chirality serves as a crucial descriptor of this dissymmetry, referring to the geometric property of molecules that are non-superimposable on their mirror images. This non-superimposability gives rise to enantiomers—two stereoisomers that share identical physical properties yet exhibit distinct interactions within chiral environments.

The handedness of enantiomers plays a crucial role at the intersection of biology and chemistry. With a few exceptions, most amino acids, nucleotides, and sugars are typically found in nature as single enantiomers. While the reasons behind this phenomenon remain a topic of discussion,[1] it is generally accepted that the specific chirality of these fundamental building blocks leads to the production of enantiomerically pure biological macromolecules, such as enzymes and nucleic acids. As a result, biological systems are predominantly homochiral and respond differently to enantiomers of chiral compounds, resulting in varied physiological effects.[2]

An interesting example of the above difference is L-DOPA, a crucial medication in the treatment of Parkinson's disease, a neurodegenerative disorder characterized by the loss of dopamine-producing neurons. The active drug in the treatment of Parkinson's disease is dopamine, which is produced from L-DOPA through in vivo decarboxylation. L-DOPA is administered as a prodrug since it can effectively cross the blood-brain barrier to reach the central nervous system. Conversely, the D-DOPA enantiomer is pharmacologically inactive and cannot be metabolized by the body's enzymes, rendering it ineffective in restoring dopamine levels (Figure 1).[3]
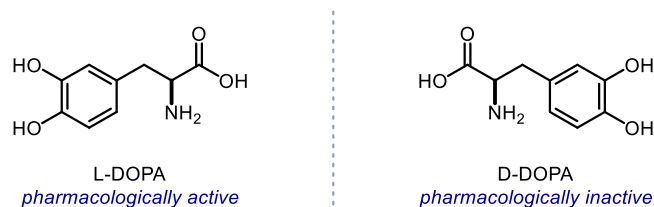

Figure 1. Enantiomers of DOPA.

Enantiopure compounds can be synthesized through three primary methods: (a) resolution of racemic mixtures, which yields a maximum of 50% enantiopure product; (b) chiral pool synthesis, where a

stoichiometric amount of enantiopure starting material is utilized; (c) asymmetric synthesis, which generates stereogenic centers from achiral precursors using an enantiopure reagent in stoichiometric (auxiliary) or catalytic amounts. Among these methods, asymmetric catalysis offers the highest efficiency, allowing for the synthesis of enantiopure compounds while using only small quantities of chiral catalysts to attain enantioselectivity.

In addition to enzymatic catalysis and chiral transition metal catalysis, organocatalysis has emerged as the third pillar of asymmetric catalysis, particularly following the discovery of List[4] and Macmillan[5] in the early 2000s. Unlike transition metal catalysis, which relies on chiral organic ligands and metal complexes, organocatalysis employs low-molecular-weight chiral organic molecules as catalysts to achieve enantioselective chemical transformations. The advantages of organocatalysts, particularly their cost-effectiveness and sustainability compared to metal-based catalysts, have made them increasingly appealing in the synthesis of pharmaceuticals and fine chemicals. Their accessibility, robustness, and low toxicity further contribute to their growing use in industrial applications.[6-7]

The following chapter will provide an organized summary of the existing literature, divided into three primary sections. First, the advancement of asymmetric organocatalysis will be discussed, with particular emphasis on the emergence of chiral Brønsted acid catalysis. The second section will focus on the difunctionalization of olefins, highlighting its significance and the various methodologies employed in organic synthesis. Finally, the prevalence and synthetic strategies for 1,3-amino alcohols will be examined, underlining their significance in the synthesis of natural products and pharmaceuticals.

2. Literature Background

2.1. Asymmetric Organocatalysis

We are constantly deepening our understanding of the implications of chirality, ranging from weak bosons in nuclear physics to the origins of life on Earth and the structure of DNA's double helix.[8] Since the early 1980s, the chirality of drugs has become a major theme in the design, discovery, development, patenting, and marketing of new pharmaceuticals. In his 1984 paper, Ariëns asserted that neglecting stereoselectivity in the action of drug molecules led to "*highly sophisticated scientific nonsense*".[9] This renewed recognition of the importance of drug stereochemistry, along with new methods for producing enantiomerically pure materials, has resulted in a shift in regulatory perspectives on chiral drugs.[10]

Asymmetric synthesis, which allows precise control of the three-dimensional structure of molecular architecture, has revolutionized chemistry in the second half of the 20th century. Among the various approaches to generating enantiomerically enriched products, catalytic methods—where chemical transformations are guided by small amounts of chiral compounds—are regarded as the most attractive.

A catalyst can be defined as a substance present in the reaction mixture that remains chemically unchanged and increases the reaction rate by reducing the activation energy required for the transformation.[11] Although it does not affect the thermodynamic energies of reactants or products, it interacts with reactants and intermediates, facilitating the reaction through an alternative pathway with lower energetic requirements. The aim of asymmetric catalysis however is to preferentially promote the kinetic formation of one enantiomeric product over the other. Since the two enantiomeric products resulting from a catalytic asymmetric reaction are identical in Gibbs free energy, this selectivity can be achieved through the participation of energetically distinct diastereomeric transition states (Figure 2).
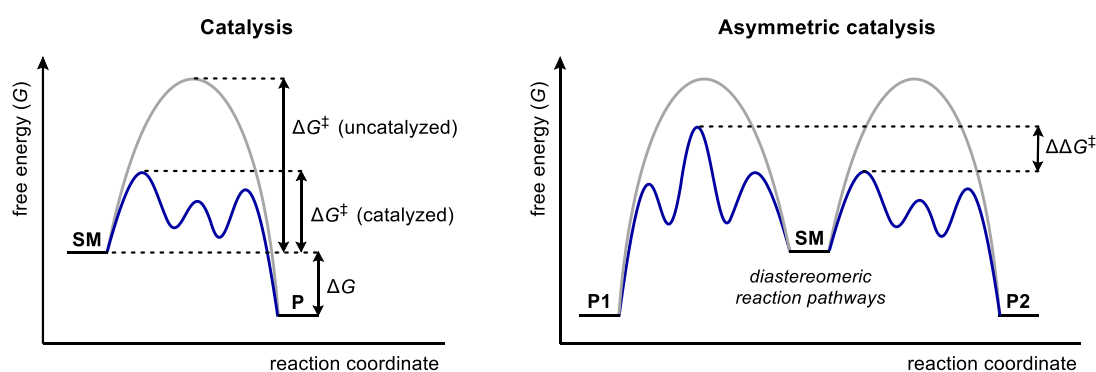

Figure 2. Energy diagrams for catalysis and asymmetric catalysis.

The crucial importance and potential economic advantages of this approach are underscored by the three Nobel prizes awarded in the last 23 years for breakthroughs in asymmetric catalysis, reflecting the efforts of synthetic chemists to enable the selective synthesis of mirror image products.[6]

2.1.1. Foundations of Organocatalysis

Organocatalysis can be defined as the use of small organic molecules, where a metal is not part of the active principle, to catalyze organic transformations. Although organocatalysis has only been recognized as a widely applicable tool for asymmetric transformations in the past two decades, the use of small organic molecules as catalysts has been known for over a century.

The first organocatalytic process, though not asymmetric, was reported by Justus von Liebig in 1860.[12] In 1912, Bredig and Fiske reported the first asymmetric organocatalytic reaction. The authors described the asymmetric addition of HCN to benzaldehyde in the presence of cinchona alkaloids to give the cyanohydrine product with low but reproducible enantiomeric excess (<10% e.e.). A similar strategy was applied by Pracejus in 1960, who investigated the reaction between ketene **1** and methanol (**2**) and under the influence of an analogous cinchona alkaloid **3**, to yield the corresponding ester **4** with good enantiomeric ratio (Scheme 1).[13]
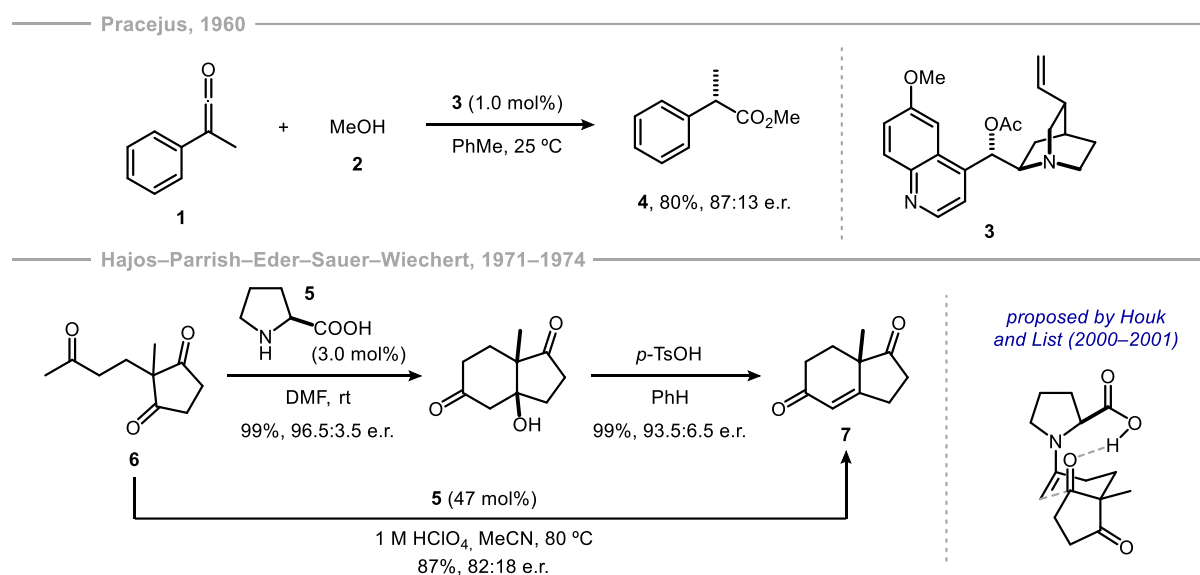

Scheme 1. Initial developments in asymmetric organocatalysis.

Another remarkable example was reported by Eder, Sauer, and Wiechert in 1971 and Hajos and Parrish in 1974, respectively. Both groups independently investigated the use of naturally occurring amino acid L-proline (**5**) as a catalyst in the intramolecular aldol condensation reactions of triketone **6**, leading to the formation of bicyclic enone **7** with excellent yields and very high enantioselectivities (Scheme 1). Computational and experimental studies by Houk and List proposed a chiral enamine as the reactive intermediate.[14-15] Noteworthy, the so-called Hajos–Parrish–Eder–Sauer–Wiechert process toward enantioenriched enones could have direct application in the synthesis of steroid hormones and other natural products.[16]

Perhaps due to an insufficient understanding of the underlying reaction mechanisms, it was not until 2000 that the groundbreaking studies of List and MacMillan opened the field of organocatalysis.

The enlightening report by List, Lerner, and Barbas in 2000 emphasized the immense synthetic potential of using small organic molecules as catalysts in asymmetric transformations.[4] The authors disclose the L-proline-catalyzed intermolecular aldol reaction of acetone (**8**) with isobutyraldehyde (**9**) via the proline-derived acetone enamine (Scheme 2). Later that year, MacMillan reported the asymmetric Diels–Alder reaction of cyclopentadiene (**10**) and unsaturated aldehydes **11** employing a phenylalanine-derived imidazolidinone catalyst **12** (Scheme 2).[5] Moreover, the term "organocatalysis" was coined by MacMillan to define this novel and fundamental concept of enantioselective catalysis. The advancement of the field culminated in 2021, when the Nobel Prize was awarded to List and MacMillan for "*the development of asymmetric organocatalysis*".
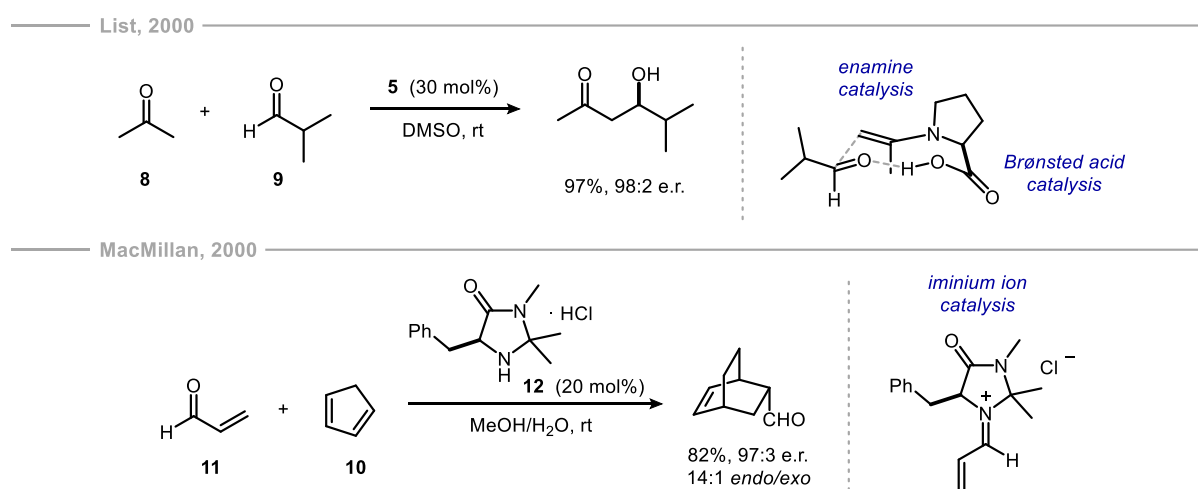
Scheme 2. Pioneer reports on asymmetric organocatalysis by List and MacMillan.[4-5]

The seminal reports by List and MacMillan exemplify two catalytic activation modes when using chiral amines as organocatalysts. Enamine catalysis involves the formation of an enamine intermediate, which raises the highest occupied molecular orbital (HOMO) of the carbonyl compound, making it more nucleophilic. In proline-catalyzed aldol reactions, the electrophile is simultaneously activated via Brønsted acid catalysis by the carboxyl group of the amino acid. Iminium catalysis lowers the lowest unoccupied molecular orbital (LUMO) of the electrophile, enhancing its electrophilicity and making it more susceptible to nucleophilic attack. Over the years, continued investigation expanded the scope of organocatalysts, demonstrating their ability to activate substrates through various mechanisms and tackle increasingly challenging reactions. The rapid growth of research in the field emphasized the demand for a classification system. In 2005, List defined four primary classes of organocatalysis according to the nature of the substrate-catalyst interaction: Brønsted acid, Brønsted base, Lewis acid, and Lewis base catalysis.[17]

2.1.2. Asymmetric Brønsted Acid Organocatalysis

Acids are dominant catalysts in countless chemical processes, spanning both biological and industrial contexts. Among them, chiral Lewis acid catalysts are highly effective tools for asymmetric synthesis. Chiral Lewis acid catalysis is based on a Lewis acidic central atom (metal or metalloid) that is bonded to or coordinated with a chiral ligand. The central atom is able to activate an electrophilic substrate by lowering the energy of its lowest unoccupied molecular orbital, thus enhancing its reactivity toward nucleophilic reagents. The stereochemical information of such transformations resides in the chiral ligand framework around the metal center. When the central Lewis acidic atom is a proton, which constitutes the simplest form of a Lewis acid, the process is classified as asymmetric Brønsted acid catalysis.[18]

Depending on the acidity of the catalyst and the basicity of the substrate, Brønsted acid catalysis can be divided into two subtypes: general acid catalysis and specific acid catalysis (Figure 3).[18] In general catalysis, low to moderately acidic catalysts engage with electrophiles through hydrogen bonding rather than protonation. Examples of such catalysts include hydrogen-bond donors like thioureas, diols, and squaramides.[19-21] This activation mode is commonly found in enzymes, which often use hydrogen bonding networks to help catalyze reactions. In specific catalysis, highly acidic catalysts activate the substrate through direct protonation, resulting in a more pronounced ion pair character of the intermediate. Common examples of these catalysts are phosphoric acids, carboxylic acids, sulfonamides, sulfonic acids, C–H acids, and phosphorimidic acids along with its derivatives.
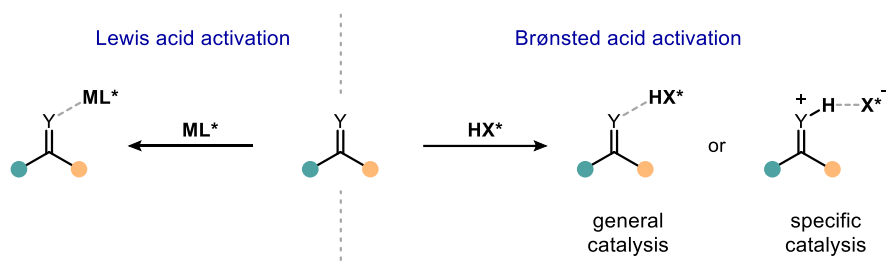

Figure 3. Lewis and Brønsted acid activation of organic molecules.

While chiral small-molecule hydrogen-bond donors have proven effective as asymmetric organocatalysts in recent years, this approach is inherently limited to activating certain substrates, primarily imines and carbonyl compounds. To enhance the activation of less Lewis basic substrates, a stronger acid-base interaction is necessary. As a result, a variety of organocatalysts with a broad range of acidity has been investigated.

Since Akiyama and Terada independently introduced chiral phosphoric acids (CPA) as asymmetric Brønsted acid catalysts in 2004,[22-23] enantioselective Brønsted acid catalysis has garnered significant attention as an effective tool for asymmetric synthesis (Scheme 3). Akiyama and coworkers described the enantioselective Mannich-type reaction of aldimine **11** with silyl ketene acetals **12**, yielding the *syn*-

isomer of β-amino esters **13** with excellent enantiocontrol. Meanwhile, Terada and coworkers reported the asymmetric addition of acetylacetone (**14**) to *N*-Boc-protected imine **15**, producing β-amino ketone **16** under mild reaction conditions. Subsequent findings by the Ishihara group revealed that the catalytic species in Terada's report was not the free acid, but the corresponding calcium salt formed during purification.[24-26] Drawing inspiration from Noyori's groundbreaking work with binaphthyl-based ligands for asymmetric hydrogenation reactions, both groups chose axially chiral phosphoric acids **17** and **18** as potential catalysts due to their unique characteristics. Firstly, the phosphorus atom and the BINOL backbone form a seven-membered ring which prevents free rotation around the P–O bond and therefore fixes the conformation of the Brønsted acid. Secondly, the phosphoryl oxygen atom in CPAs offers an additional Lewis basic site, allowing CPAs to function as bifunctional catalysts. Moreover, chiral phosphoric acids bearing different substituents at the 3,3'-positions can be easily synthesized in a few steps using commercially available BINOL as starting material. These substituents add steric hindrance around the active site and, based on their electron-donating or electron-withdrawing properties, modulate the electron density throughout the catalyst. One of the most widely utilized phosphoric acid catalysts, the 2,4,6-triisopropylphenyl-substituted CPA (commonly known as TRIP), was first reported by the List group in 2005 and continues to have extensive applications in research today.[27]
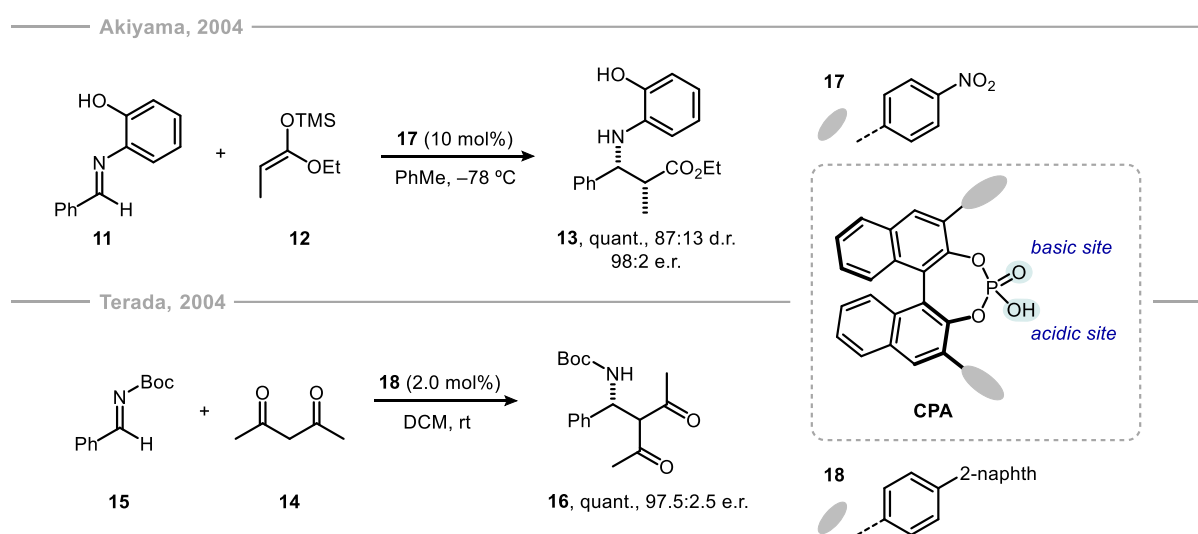
Scheme 3. Reports using BINOL-based chiral phosphoric acids by Akiyama and Terada.[22-23] Note: catalyst **18** was later shown to be the corresponding chiral calcium phosphate salt.

2.1.3. Strong and Confined Brønsted Acid Catalysis

While BINOL-derived phosphoric acids have seen widespread success, two significant obstacles persist: (a) the reliance on relatively Lewis-basic substrates for effective activation, and (b) limited stereocontrol with small, nonbiased substrates. To address these limitations, research efforts have focused on developing more acidic catalysts capable of protonating less reactive substrates, and designing catalysts that offer a more confined chiral environment around the active site to enhance stereoselectivity.

The acidity of Brønsted acid catalysts can be effectively compared when measured under consistent conditions (Figure 4). While CPAs ($pK_a > 13$ in MeCN) are notably more acidic than thioureas and similar hydrogen bond donors,[28] it soon became evident that their application was restricted to reactive substrates. In 2002, Yagupolskii first proposed the idea of enhancing the acidity of phosphate-based catalysts by replacing oxygen atoms with N-(EWG) groups, which has proven to be an effective strategy.[29] The molecular structure of N-triflyl phosphoramides (NTPAs) exemplifies the single Yagupolskii modification of a CPA, which was first explored by Yamamoto in 2006.[30] Their application in asymmetric Diels–Alder reactions showcases the advantages of increased acidity, with average pK_a values of approximately 6–7 in MeCN, which allows them to outperform traditional CPA catalysts.[28] List explored the replacement of the second oxo group in NTPAs in 2016, resulting in the development of highly active Brønsted acid organocatalysts known as phosphoramidimidates (PADIs). The increased acidity facilitates more intricate reactions, exemplified by the Friedel–Crafts alkylation of isophytol with hydroquinone to produce α-tocopherol, albeit with moderate enantioselectivity.[31]

Moving beyond phosphorus-containing acids, a new class of more acidic chiral Brønsted acids, disulfonimides (DSI, $pK_a \sim 8.4$ in MeCN),[28] was independently introduced by List[32] and Giernoth[33] in 2009. This notable catalytic motif has demonstrated efficacy in various C–C bond-forming reactions, including Mukaiyama aldol, Mukaiyama–Mannich, hetero-Diels–Alder, Hosomi–Sakurai, and cyanosilylation of aldehydes, to name just a few.[34] Even higher acidities were achieved by replacing the disulfonimide unit with bis(sulfuryl)imides, referred to as JINGLEs, $pK_a \sim 5.2$ in MeCN),[28] as introduced by Berkessel and coworkers.[35]
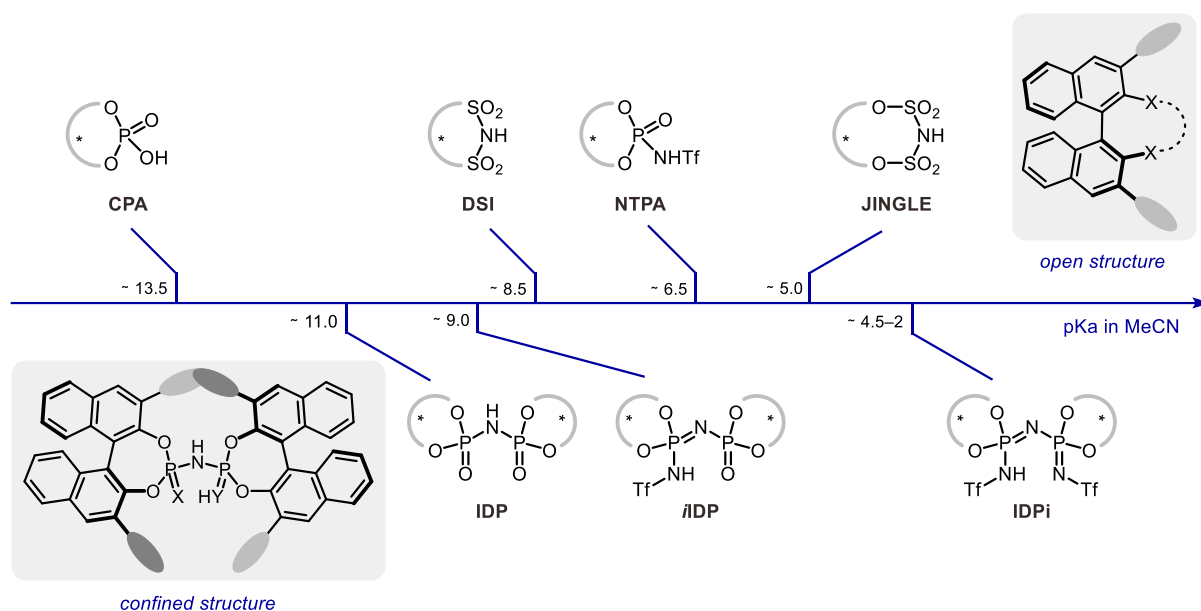

Figure 4. pK_a values of BINOL-based Brønsted acid organocatalysts.

Although these catalysts facilitate the activation of less basic substrates such as ketones and aldehydes, attaining high enantioselectivity with JINGLE-based catalysts continues to be a challenge. This

leads to the inquiry of whether achieving highly selective transformations of very unreactive substrates is possible. In biocatalysis, enzymes exemplify the selective functionalization of unactivated molecules, thanks to their well-defined microenviroment around the active center. This confined space facilitates the pre-organization of substrates into higher-energy conformers, thus enhancing their reactivity.[36] Over the past decade, research by List and colleagues has led to the development and synthesis of a new class of dimeric chiral phosphoric acids (IDP, pK_a ~ 11.3 in MeCN), often referred to as *confined Brønsted acid organocatalysts*. By incorporating two identical BINOLs with bulky 3,3′-substituents that hinder the rotation of the imidodiphosphate unit, the confined catalytic scaffold restricts the variety of catalytically active conformations. This enables the stabilization of only a few selected transition states, resulting in unprecedented chemo-, regio-, and stereoselectivity.

List's novel catalyst design enabled the highly enantioselective intramolecular spiroacetalization of small, unbiased aliphatic cyclic alcohols.[37] Increased reactivity was achieved through Yakupolskii-type modifications, where an oxo group in one of the P=O moieties at the active site was replaced with =NTf.[38] This modification led to the creation of a new family of confined, C_1-symmetric stronger acids known as iminoimidodiphosphates (*i*IDPs), which have a pK_a of approximately 9.0 in MeCN. The incorporation of a second electron-withdrawing group toward the imidodiphosphorimidate structure (IDPi) leads to an even more pronounced increase in acidity, resulting in pK_a values from 4.5 to 2.0 for the corresponding acids. Recent studies from our group have demonstrated that IDPis function not only as potent Brønsted acids but also as precursors for chiral, strong silylium Lewis acid catalysts.[38] The outstanding stereochemical control in IDPi-catalyzed reactions has already been shown in the asymmetric Friedel–Crafts reaction of unactivated arenes,[39] catalytic enantiocontrol over a non-classical carbocation,[40] cyanosilylation of small ketones,[41] or polyene cyclization of homofarnesol to ambrox,[42] among others (Scheme 4). This revolutionary catalyst design opened the door to asymmetric transformations of substrates once considered inaccessible, such as simple olefins and cyclopropanes. Even nearly a decade later, the privileged IDPi catalyst framework continues to expand the limits of asymmetric Lewis and Brønsted acid catalysis.
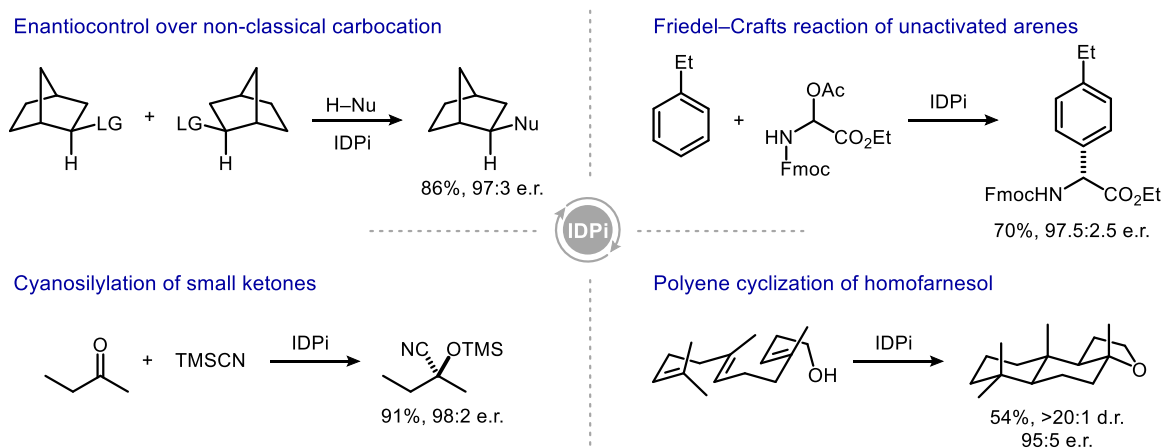
Scheme 4. Examples of IDPi-catalyzed reactions.

2.2. Toward Olefin Functionalization

Carbon-carbon (C–C) double bonds are among the most versatile and prevalent functionalities in organic chemistry. Short-chain olefins, such as ethylene, propylene, or isobutene, are produced in substantial quantities through steam or catalytic cracking of petroleum fractions. Adjusting the reaction temperature can also enable the production of benzene from crude oil.[43] For instance, in 2022, ethylene
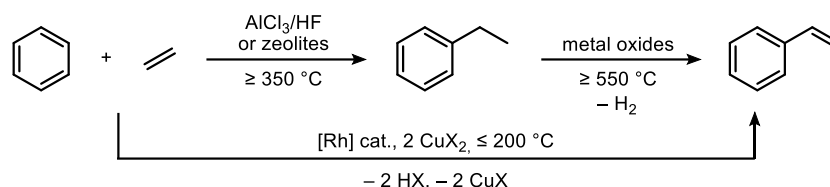
Scheme 5. Processes for the preparation of styrene from benzene and ethylene.

production exceeded 225.5 million tons globally, while propene production reached around 150 million tons.[44-45] Styrene is another versatile precursor in industry, essential for producing plastics, elastomers, and surfactants, highlighting its crucial role in everyday products. It is commonly produced through the dehydrogenation of ethylbenzene, which itself is formed via a Friedel–Crafts reaction between benzene and ethylene.[46] Recent alternative methods for the production of vinyl arenes include the direct and single-step oxidative arene vinylation (Scheme 5).[47]

Consequently, the development of efficient functionalization of such scaffolds has attracted sinificant interest, resulting in a diverse array of olefin transformations that have become fundamental in organic synthesis (Figure 5). Indeed, several Nobel Prizes in chemistry highlight the significance of
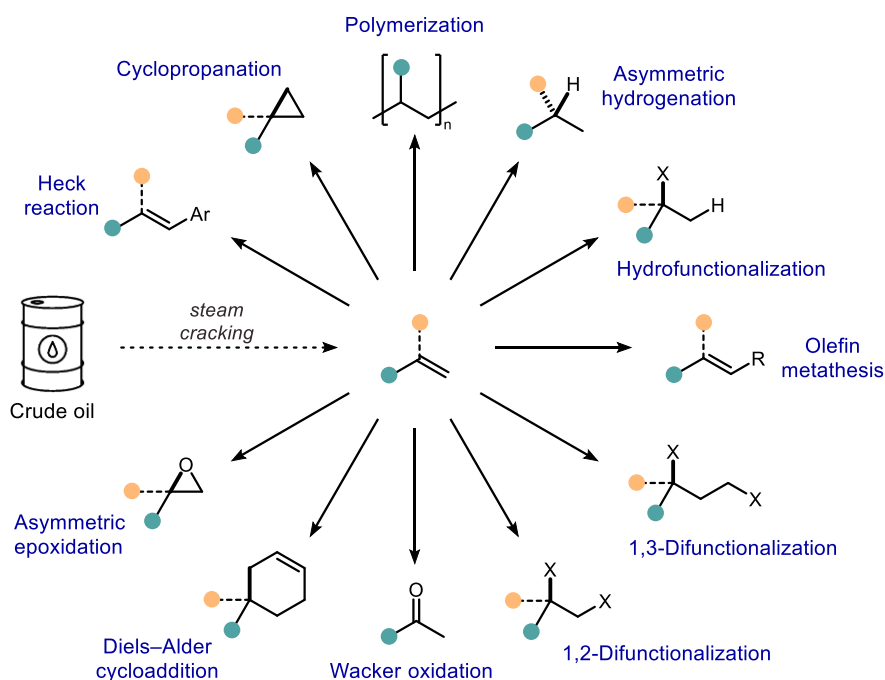

Figure 5. Overview of fundamental transformations of olefins in organic synthesis.

alkene functionalization, with notable laureates including K. Alder, H. C. Brown, O. Diels, R. H. Grubbs, R. F. Heck, W. S. Knowles, G. Natta, R. Noyori, R. R. Schrock, K. B. Sharpless, and K. W. Ziegler.[48] These recognitions underline the crucial role of C=C bonds in advancing molecular complexity and shaping the field of organic chemistry.

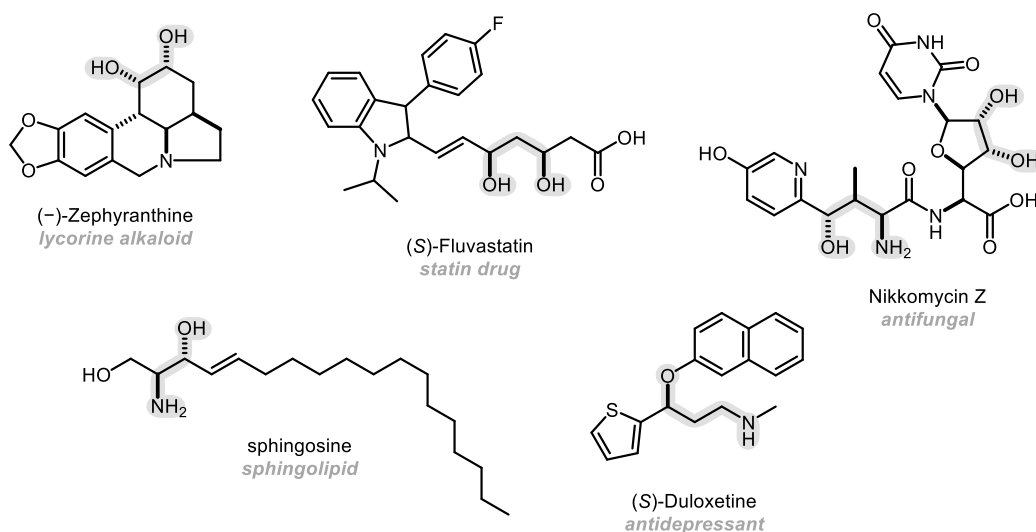### 2.2.1. Alkene Difunctionalization

The ubiquity of oxygen and nitrogen-based scaffolds in biologically active compounds continues to drive the advancement of existing methodologies and the development of new chemical tools (Figure 6a).[49] Hence, incorporating oxygenated and nitrogenated species into C–C double bonds represents a particularly diverse class of chemical reactions that provide industrially feasible and synthetically advantageous methods for increasing the structural complexity of simple feedstocks.

While Sharpless asymmetric dihydroxylation and aminohydroxylation are widely recognized methods for alkene difunctionalization,[50-52] strategies toward the formal oxy-oxymethylation and oxy-aminomethylation of olefins are less known (Figure 6b). The development of such methodologies would greatly enhance the synthetic toolbox of organic chemists, as it enables the incorporation of 1,3-difunctionalized fragments from simple, readily accessible olefins. One of the most notable studies involves the recent work by List and collaborators, which describes the catalytic, asymmetric, intermolecular reaction between aryl olefins and paraformaldehyde, enabled by sterically-confined *i*IDP Brønsted acid catalysts.[53] On a different note, the proof of principle for the aminomethylation of styrenes was first documented by Hartough and coworkers in 1956.[54] Their work presents the condensation of styrene with formaldehyde and ammonium chloride at 80 °C to furnish 6-phenyltetrahydro-1,3-oxazine (**19**) and its *N*-bis-methylene derivative in low and moderate yields, respectively. Alternative approaches to formal oxy-aminomethylation of olefins utilize preformed *N*-acyl and *N*-carbamoyl iminium ions as 4π components in the inverse-electron-demand Diels–Alder (IEDDA) cycloadditions; however, these methods remain relatively scarce. A more detailed discussion of these reactions will be provided in Section 2.2.2.

Mechanistic studies suggest that both Sharpless' asymmetric dihydroxylation and aminohydroxylation likely proceed through concerted transition states, where the olefin serves as the 2π-component in hetero-[3 + 2] cycloaddition reactions.[55] In a similar manner, research on List's oxy-oxymethylation reaction indicates that it follows a concerted, highly asynchronous hetero-[4 + 2] cycloaddition-type pathway, with the olefin also serving as the 2π-component.[53] The driving force of cycloaddition reactions is the release of energy from the formation of new, more stable σ-bonds from π-bonds, facilitated by effective orbital overlap and the stabilization of a cyclic transition state. The concerted nature of their transition state often makes them particularly suitable for constructing complex, cyclic structures with precise control over chirality.
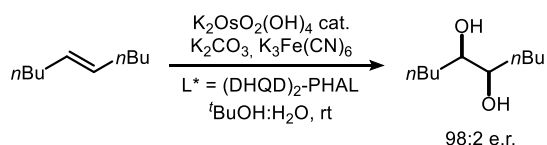
The next section will delve into a subtype of [4 + 2]-cycloaddition reactions, specifically IEDDA reactions, and will explore their unique mechanisms and applications in organic synthesis.

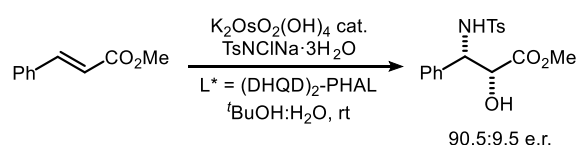**a.** Structural diversity of diols and amino alcohols

(−)-Zephyranthine
lycorine alkaloid

(*S*)-Fluvastatin
statin drug

Nikkomycin Z
antifungal

sphingosine
sphingolipid

(*S*)-Duloxetine
antidepressant

b. Asymmetric functionalization of olefins (diols and amino alcohols)

Dihydroxylation │ Sharpless, 1992

nBu ⟶ $K_2OsO_2(OH)_4$ cat. K_2CO_3, $K_3Fe(CN)_6$ / L* = (DHQD)$_2$-PHAL / $^tBuOH:H_2O$, rt ⟶ 98:2 e.r.

Aminohydroxylation │ Sharpless, 1996

Ph ⟶ CO_2Me / $K_2OsO_2(OH)_4$ cat. TsNClNa·3H$_2$O / L* = (DHQD)$_2$-PHAL / $^tBuOH:H_2O$, rt ⟶ 90.5:9.5 e.r.

Oxy-oxymethylation │ List, 2021

Ph + (HCHO)$_n$ ⟶ *i*IDP (2.5 mol%) / CyH, rt ⟶ 89%, 95.5:4.5 er
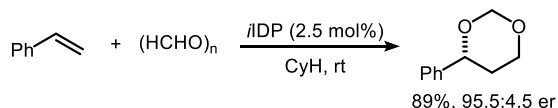
Oxy-aminomethylation │ Hartough, 1956

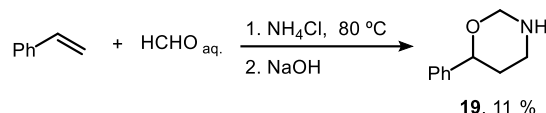Ph + HCHO aq. ⟶ 1. NH$_4$Cl, 80 °C / 2. NaOH ⟶ **19**, 11 %

Figure 6. (a) Representative biologically active diols and amino alcohols. (b) Olefins as versatile building blocks for the synthesis of 1,2- and 1,3-difunctionalized molecules.

2.2.2.   Inverse-Electron-Demand Diels–Alder (IEDDA) Reactions

The Diels−Alder reaction, celebrated for its extensive synthetic versatility, stands as a cornerstone in modern organic chemistry for the construction of six-membered rings. Since its discovery by Otto Diels and Kurt Alder in 1928,[56] the Diels−Alder reaction has seen significant advancement, cementing its status as a fundamental tool in organic synthesis. This powerful reaction has been extensively utilized in constructing complex biologically active molecules and in the synthesis of natural products, under-scoring its critical role in the development of intricate organic structures.[57] As early mentioned, the driving force behind these reactions is the conversion of two π-bonds into two more stable σ-bonds. In general, Diels−Alder reactions can be classified into two types of suprafacial [4π + 2π] cycloadditions based

on the relative energies of the frontier molecular orbitals of the diene and the dienophile in the Hückel molecular orbital model:[58] the normal $HOMO_{diene}$-controlled reaction, and the inverse-electron-demand or $LUMO_{diene}$-controlled reaction (Figure 7). In a Diels−Alder with normal-electron-demand, the dienophile typically bears an electron-withdrawing group, while the diene is electron-rich. Reversely, the IEDDA reaction is characterized by an electron-poor diene and an electron-rich dienophile.

Shortly after its discovery, the normal Diels–Alder reaction was rapidly adopted in the field due to its capability to generate all-carbon six-membered ring systems with predictable regio- and stereochemical control. In contrast, the IEDDA reaction took longer to become established.
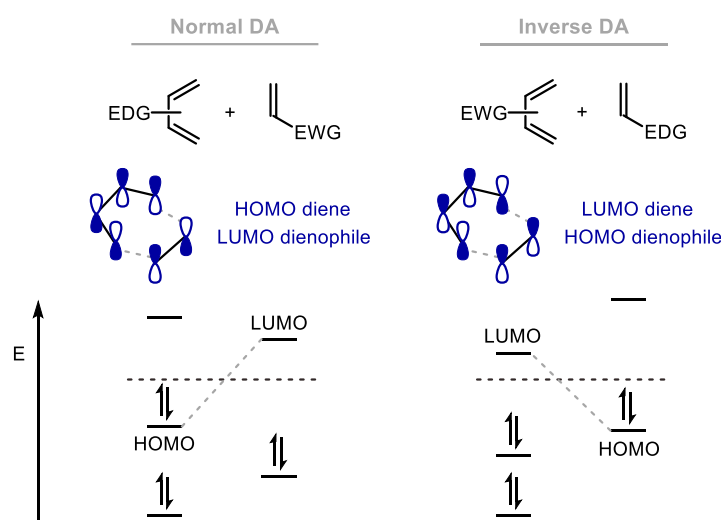

Figure 7. Classification of Diels–Alder reactions.

Understanding the factors that influence cycloaddition rates is crucial for optimizing their effectiveness in practical chemical reactions. The kinetics of a Diels–Alder reaction is determined by the energy gap between the frontier molecular orbitals, specifically the HOMO of one cycloaddend and the LUMO of the other. A smaller energy difference between these orbitals will therefore result in a faster reaction. In inverse-electron-demand cycloadditions, the reaction rate is typically accelerated by the presence of electron-donating groups on the dienophile and electron-withdrawing groups on the diene.[59] Commonly used dienes in IEDDA reactions include oxo- and aza-butadienes, triazines, tetrazines, azo-alkenes, and *N*-acyl imines, while dienophiles often feature strained systems such as norbornene and cyclopropenes, or electron-rich double bonds such as vinyl ethers, silyl enol ethers, vinyl sulfides, and enamines (Figure 8).
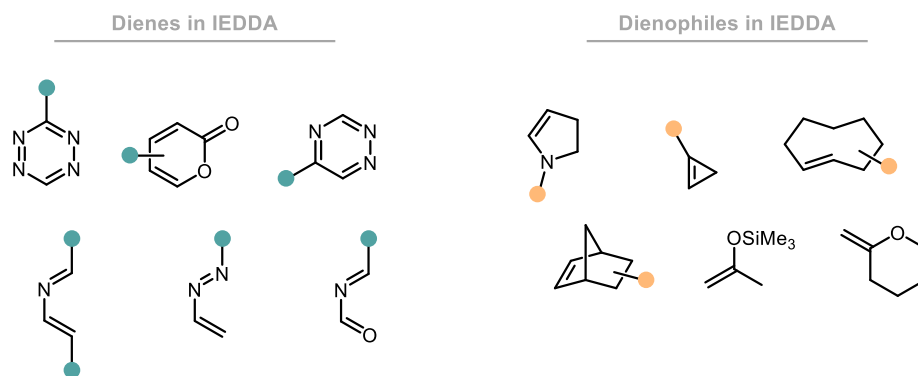
Figure 8. Commonly used dienes and dienophiles in IEDDA reactions.

As for the case of normal Diels–Alder reactions, the regioselectivity of the inverse-electron-demand cycloadditions can typically be predicted using zwitterionic models or frontier molecular orbital analysis.[60] In these models, the atom with the highest LUMO coefficient is anticipated to react with the atom that has the highest HOMO coefficient, and interactions are favored between atoms with opposite formal charges.

2.2.2.1. Olefins as Dienophiles in IEDDA Reactions

A significant challenge in employing unbiased olefins as dienophiles in IEDDA reactions is their inherent low-energy HOMO. The absence of electron-donating groups results in lower electron density in the π-system, thereby preventing the elevation of the HOMO energy level. Consequently, the orbital overlap between the HOMO of the alkene and the LUMO of the diene is less efficient, thereby diminishing the probability of a successful cycloaddition reaction.

HOMO energy can be directly correlated with nucleophilicity, where higher HOMO energy reflects increased availability of electrons for a nucleophilic donation. The nucleophilicity scale developed by Mayr[61] clarifies the relatively disadvantaged position of unbiased olefins as nucleophiles (or dienophiles in IEDDA) compared to electron rich-substituted alkenes (Figure 9).[I] Considering that the Mayr equation indicates a logarithmic relationship between nucleophilicity (N) and the rate constant, it is evident that silyl ketene acetals ($N \sim 12$ to 8) and silyl enol ethers ($N \sim 7$ to 3) are significantly more nucleophilic than allylsilanes (e.g., allyl-TMS: $N = 1.68$) and aryl olefins like styrene ($N = 0.78$). In comparison, highly activated dienes such as Danishefsky's diene ($N = 8.57$) are several orders of magnitude more nucleophilic than less activated 1,3-butadiene ($N = –0.87$). As anticipated, alkyl olefins, such as 1-hexene ($N = –2.77$), are among the least nucleophilic, just above $C(sp^3)$–H bonds in alkanes. Consequently,

---

[I] Note that while using Mayr's nucleophilicity scale for comparison with the HOMO energies of alkenes, it is important to acknowledge that this scale may not provide a fully accurate reflection of HOMO energy levels. The comparison is intended as a general reference rather than an exact measurement.

the application of olefins in IEDDA reactions remains constrained, even with the development of advanced catalytic systems.
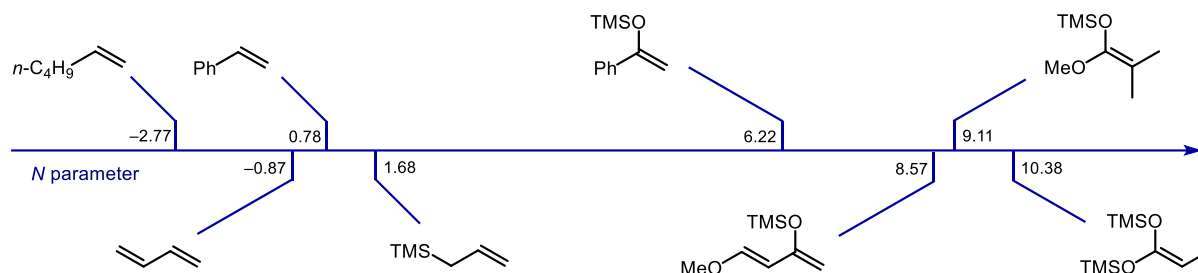

Figure 9. Mayr nucleophilicity scale of several C=C bond-containing compounds, based on their *N* values.

2.2.2.2. IEDDA between Olefins and *N*-Acyl or *N*-Carbamoyl Iminium Ions

N-Acyliminium ions are highly reactive electrophiles that have been extensively utilized in organic synthesis to construct a wide variety of structurally diverse compounds. Their electrophilic nature allows trapping with a variety of carbon and heteroatom nucleophiles, facilitating carbon–carbon and carbon–heteroatom bond formation in the α-position of an amide or carbamate. Since early studies in the 1950s, an impressive number of synthetic examples have been reported using *N*-acyliminium ions for the synthesis of natural products and biologically active molecules.[62] Among the various named reactions involving *N*-acyliminium ions, the Mannich and Pictet–Spengler reactions are the two most extensively studied, particularly in the pursuit of alkaloids containing indole and isoquinoline scaffolds.[63-64]

Conventional methods for *N*-acyliminium ion generation include the Brønsted or Lewis acid-promoted removal of a leaving group at the α-position of the nitrogen atom. While activated hydroxyl groups are the most commonly employed leaving groups, others such as halogen, alkoxy, acetoxy, arylsulfonyl, carbamate, and benzotriazolyl groups have also been successfully utilized.[65] Stoichiometric amounts of the acid are often required, as the catalyst tends to degrade in the presence of water or alcohol byproducts. Other approaches toward *N*-acyliminium ion generation include direct condensation between an amide or carbamate and an aldehyde, protonation of an enamide, or the "cation-pool" method,
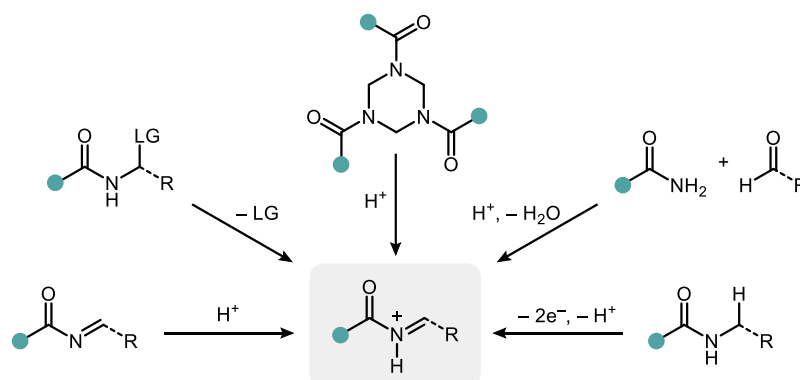

Figure 10. Generation of *N*-acyliminium ions.

characterized by the irreversible generation and accumulation of carbocations by low-temperature electrochemical oxidation (Figure 10).[66]

A less widely recognized characteristic of *N*-acyliminium ions and structurally related compounds is their capacity to serve as 4π components in cationic IEDDA reactions. The acid-promoted, in situ generation of *N*-acyliminium ions provides an enhancement of the electron-deficient nature of the aza-diene system, thereby facilitating its participation in formal [4 + 2]-cycloadditions with electron-rich or electron-neutral dienophiles. These cycloadditions would proceed in a regiospecific manner with the most nucleophilic carbon of the dienophile attaching to the expected electrophilic site of the iminium ion. In his pioneering work, Schmidt reported the synthesis of 5,6-dihydro-4*H*-1,3-oxazines **20** by the reaction between olefins and *N*-(chloromethyl)benzamide (**21**), promoted by Lewis acid activation. The author proposed classifying these reactions as polar cycloadditions with a concerted, though likely asynchronous transition state (Scheme 6).[67] Later investigations by Giordano and collaborators demonstrated that the same cycloadduct products **20** can be obtained by using 1,3,5-triacylhexahydro-1,3,5-triazine reactant **22** or via the three-component condensation reaction of aryl amides and paraformaldehyde, at high temperatures and in the presence of acid and the olefin. The necessity for high temperatures suggests that the reaction rate is limited by the differing rates at which the various systems equilibrate with the crucial *N*-acyliminium ion.[68-69]
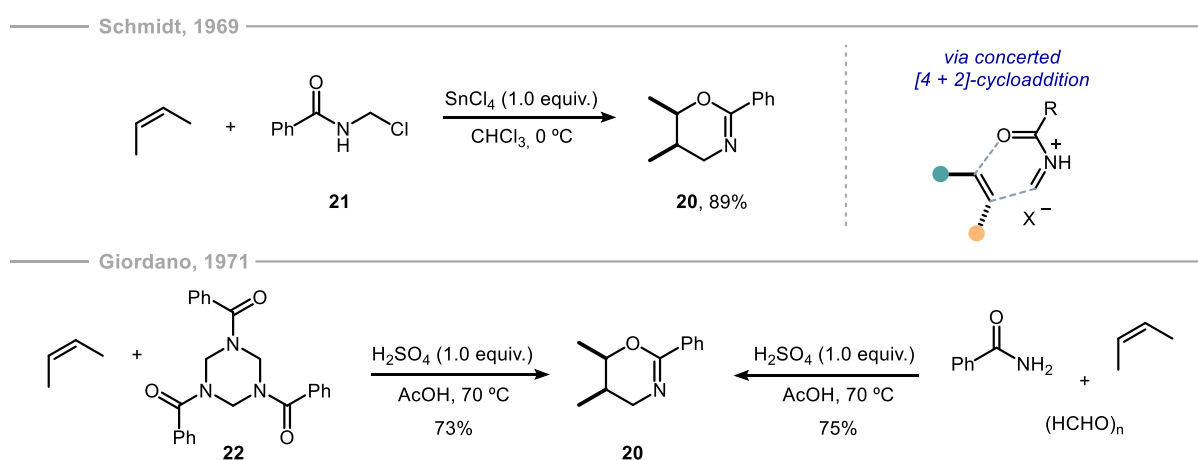

Scheme 6. Inverse-electron-demand hetero-cycloaddition of styrenes by Schmidt and Giordano.[67, 69]

More recent studies on the use of *N*-acyliminium ions as dienes in hetero-Diels–Alder reactions include the work of Terada and collaborators (Scheme 7). The authors report the asymmetric transformation between alkenes and *N*-benzoyl aldimine **23**, achieving excellent diastereo- and enantioselectivities under catalysis by CPA **24** incorporating perfluorophenyl groups at the 3,3'-postitions.[70] Years later, the methodology could be expanded to the use of α-fluorostyrenes **25** as dienophiles in the cycloaddition reaction. Further manipulation of the enantioenriched heterocycle **26** with silyl enol ether, in the presence of a BiCl3 catalyst, afforded the substitution product **27** while retaining the dihydro-4*H*-1,3-oxazine framework.[71]
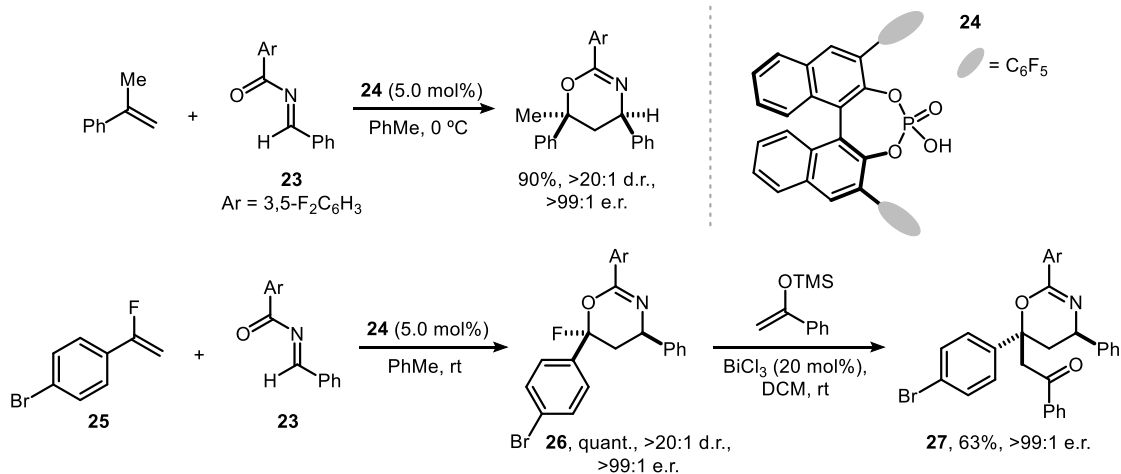
Scheme 7. CPA-catalyzed hetero-cycloaddition reactions of styrenes by Terada.[70-71]

Ishihara and coworkers designed a chiral magnesium potassium binaphthyldisulfonate **28** cluster as a chiral Brønsted acid catalyst for the cycloaddition reaction between styrenes and *N*-Boc-aldimine **15**,[72] which had been originally developed by Hossain[73] in an achiral manner using HBF$_4$·Et$_2$O as the catalyst. The literature conditions reportedly deliver the desired products **29** in excellent yields and diastereo- and enantioselectivities (Scheme 8). To the best of our knowledge, no other reports have been published on the catalytic asymmetric variant of the [4 + 2]-cycloaddition between non-benzaldehyde-derived imines and olefins to date.
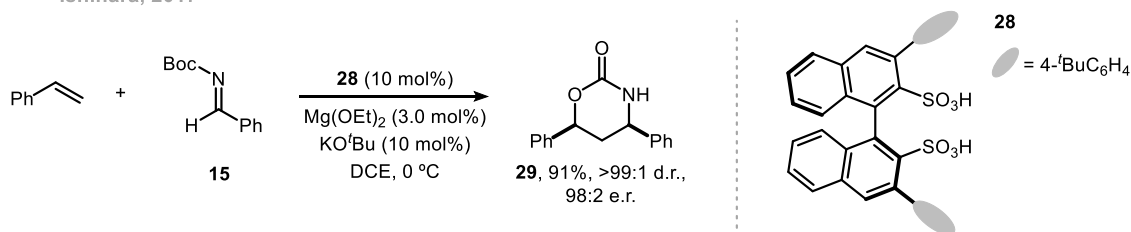
Scheme 8. Asymmetric [4 + 2]-cycloaddition reactions of styrenes and *N*-Boc-aldimines by Ishihara.[72]

2.3.   Chiral 1,3-Amino Alcohols

Chiral 1,3-amino alcohols represent a crucial class of organic compounds that have garnered significant attention in both academic and industrial research due to their versatile reactivity and broad applicability. They are key building blocks in the synthesis of a wide array of biologically active molecules, including pharmaceuticals, natural products, and agrochemicals (Figure 11).

Remarkably, 1,3-amino alcohols and their derivatives are key components in some of the world's best-selling pharmaceuticals, including fluoxetine (Prozac) and duloxetine (Cymbalta), both widely used as antidepressants. Fluoxetine, a selective serotonin reuptake inhibitor (SSRI), was named one of *Fortune* magazine's "Pharmaceutical Products of the Century" in 1999, and achieved peak annual sales of \$2.8 billion in 1998.[74] Duloxetine, a serotonin-norepinephrine reuptake inhibitor (SNRI), reached \$5.8 billion in sales by 2012, placing it among the top ten selling drugs globally.[75] Other examples of the medical significance of 1,3-amino alcohols are tramadol (analgesic),[76] efavirenz (antiretroviral),[77] negamycin (antibiotic),[78] nikkomycin Z (antifungal),[79] as well as the Sedum alkaloids allosedridine and sedamine (Figure 11).[80] Beyond their biological activity, 1,3-amino alcohols are also valuable in synthetic chemistry, serving as chiral ligands, resolving agents, and phase transfer catalysts.[81]
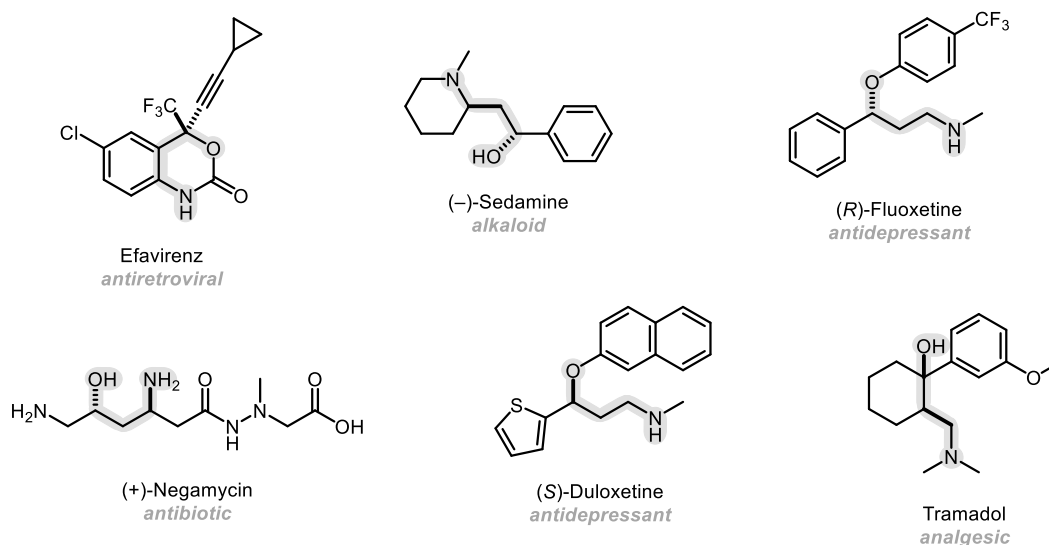

Figure 11. Biologically active molecules containing the chiral 1,3-amino alcohol motif.

2.3.1.   General Synthetic Pathways to Enantioenriched 1,3-Amino Alcohols

The enantioselective synthesis of 1,3-amino alcohols remains a dynamic and essential field for both synthetic and pharmaceutical chemists, with numerous innovative methodologies developed by research groups worldwide to date. The synthetic analysis presented in Figure 12 illustrates the key disconnections and strategic approaches used in their synthesis. Methods for chiral 1,3-amino alcohol synthesis often involve the construction of a 1,3-difunctionalized fragment, followed by hydride reductions. In

this section, the most significant examples of the formation of 1,3-difunctionalized fragments, along with the subsequent reduction step when necessary, will be discussed. Examples of the inverse-electron-demand [4 + 2]-cycloaddition reaction toward 1,3-amino alcohol are highlighted in Section 2.2.2.2.
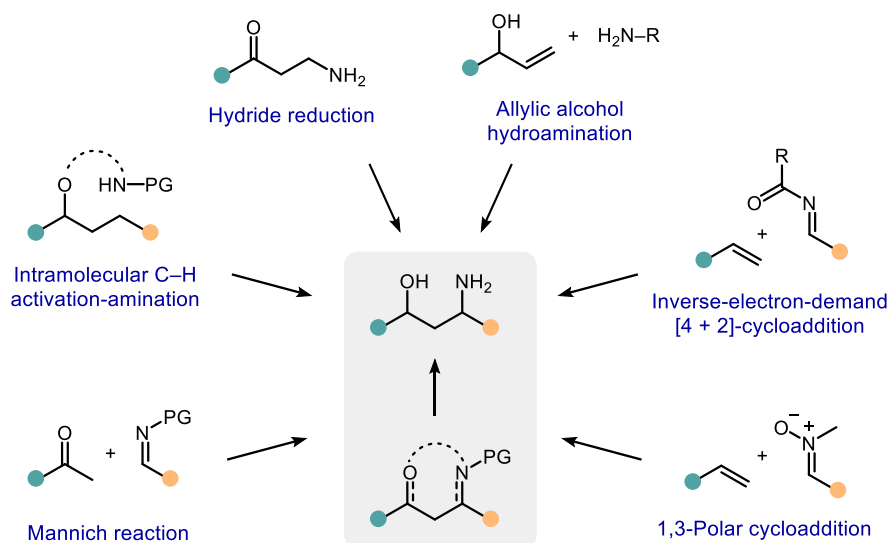

Figure 12. Approaches for the synthesis of enantioenriched 1,3-amino alcohols.

2.3.1.1. Asymmetric Hydride Reduction

Methods commonly employed for chiral 1,3-amino alcohol synthesis involve C–C, C–O, or C–N bond-forming reactions of preoxidized fragments to produce β-hydroxy imines or β-amino ketones, which can be subsequently subjected to enantioselective hydride reductions.

Initial work in the transition-metal-catalyzed asymmetric hydrogenation of β-amino ketone derivatives was disclosed by Achiwa in 1991 by using a chiral rhodium complex.[82] The reported catalyst **30** enabled the successful synthesis of (*R*)-fluoxetine through the enantioselective reduction of 3-(methylbenzylamino)-1-phenyl-1-propanone hydrochloride (**31**), achieving an enantiomeric ratio of 95.4:4.6 with low catalyst loadings (Scheme 9). However, lower enantioselectivity (89:11 e.r.) was observed for the reduction of 3-(methylamino)-1-phenyl-1-propanone hydrochloride (**32**).

Recent advancements by Ye and coworkers led to the development of iridium catalyst **33** with chiral tridentate ferrocene-based phosphine ligands bearing unsymmetrical vicinal diamine scaffolds, which achieved excellent yields and enantioselectivities and TON up to 48500 (Scheme 9). The method was successfully applied for the generation of various chiral γ-amino alcohols, including diverse γ-tertiary-amino and γ-secondary-amino alcohol intermediates of (*S*)-duloxetine, (*R*)-fluoxetine, and (*R*)-atomoxetine on a gram scale (**34**).[83]
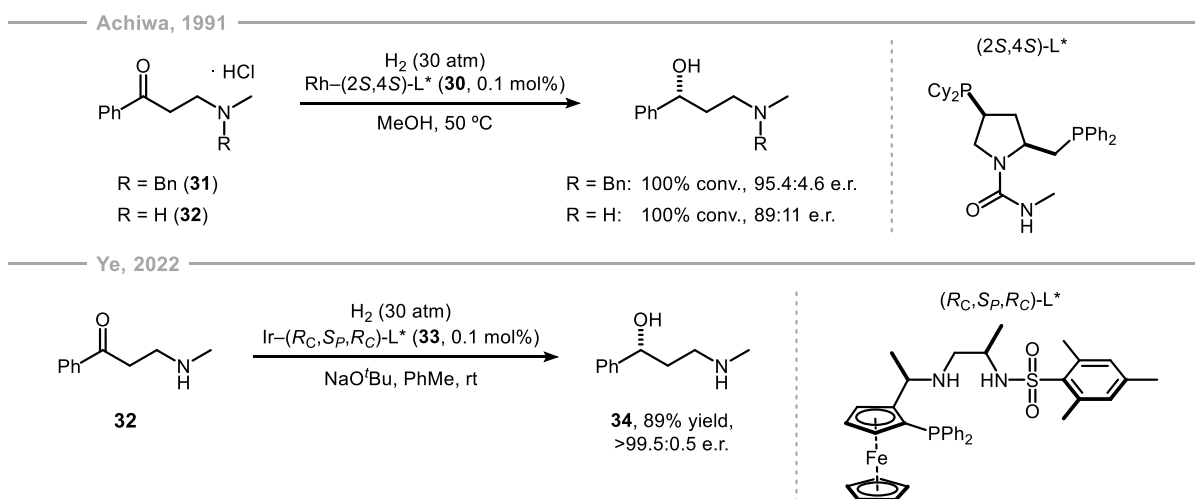
Scheme 9. Asymmetric hydrogenation of β-amino ketones by Achiwa and Ye.[82-83]

Due to the versatility conferred by the halogen, which readily serves as an effective leaving group, enantiomerically enriched halo alcohols serve as essential building blocks for the synthesis of various structurally diverse compounds, including chiral diols, epoxides, and amino alcohols. Li and coworkers published a report detailing the copper-catalyzed enantioselective hydrosilylation of various halo ketones **35** to afford the corresponding chiral alcohols with high selectivity (Scheme 10).[84] The dipyridylphosphine ligand was used with a copper metal center along with the stoichiometric hydride donor PhSiH$_3$ to construct a key chiral alcohol building block **36** for the synthesis of (*S*)-duloxetine.

A chemoenzymatic strategy was developed by the Zheng group to access the (*S*)-duloxetine key intermediate.[85] By employing the RtSCR$_9$ enzyme mined from newly isolated *Rhodosporidium toruloides* in the enantiodetermining step, 1,3-amino alcohol **37** was obtained with high substrate loading (1000 mM), as well as exceptional yield and enantioselectivity (Scheme 10).
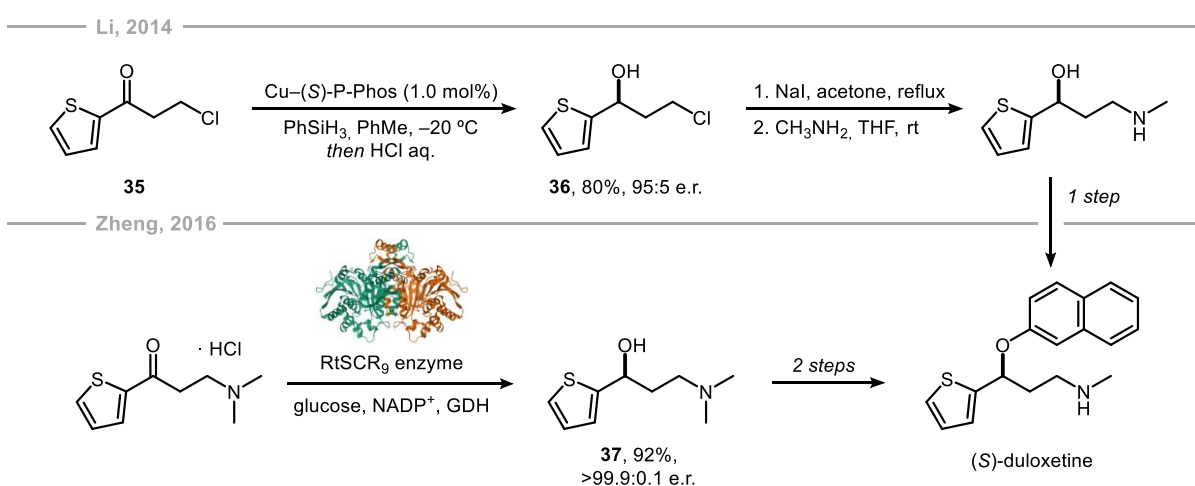
Scheme 10. Asymmetric hydrosilylation of halo ketones by Li and enzymatic carbonyl reduction by Zheng.[84-85]
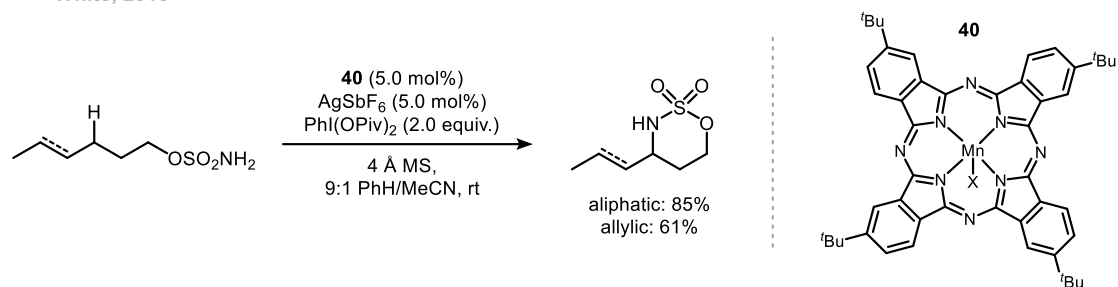
2.3.1.2. Mannich Reaction

Recognized as the traditional approach for preparing β-amino ketones and aldehydes, the asymmetric Mannich reaction is a key method for C–C bond formation in organic synthesis. Introduced by List in 2000,[86-87] the three-component proline-catalyzed Mannich reaction has demonstrated its value as a widely used transformation in the preparation of natural products, pharmaceuticals, and various chiral amino acids. The development of the intermolecular Mannich reaction faced challenges like undesired side products and poor control over regio- and stereoselectivity. To address these issues, preformed Mannich reagents, such as imines and iminium salts, have been successfully introduced. For instance, the List group identified acetaldehyde (**38**) as an effective nucleophile in asymmetric, proline-catalyzed Mannich reactions with *N*-Boc-imine **15**, resulting in β-amino aldehyde **39** with remarkably high enantioselectivities (Scheme 11).[88] The work also demonstrates the synthetic utility of such 1,3-difunctionalized scaffolds with several derivatizations, including oxidation of the aminoaldehyde with sodium chlorite to the corresponding *N*-Boc-amino acid, or NaBH$_4$ reduction of the aldehyde to the amino alcohol without loss of enantiopurity.
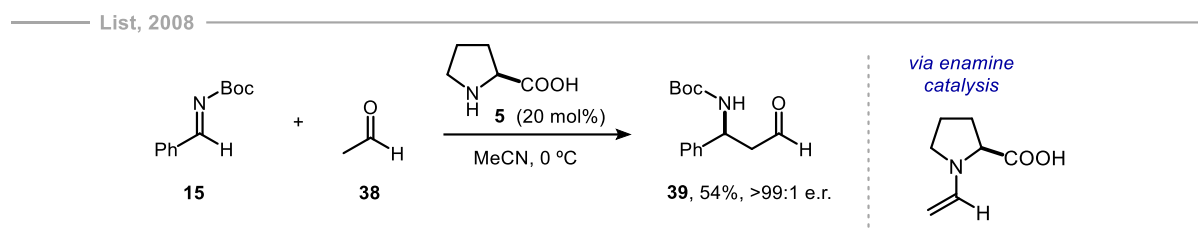
Scheme 11. Proline-catalyzed Mannich reaction of acetaldehyde by List.[88]

2.3.1.3. Intramolecular C–H Amination

Reactions that directly introduce nitrogen into C–H bonds of complex molecules are important due to their ability to alter the chemical and biological properties of the target compound. Following the pioneering work by Breslow,[89] who showed that Fe(TPP)Cl (TPP = tetraphenylporphyrinato) could effectively aminate both aliphatic and benzylic C–H bonds, the field of metal nitrenoid-mediated C–H amination has advanced significantly, leading to the development of a wide range of catalysts based on different transition metals. In 2015, the White group reported a manganese *tert*-butylphthalocyanine catalyst (**40**) capable of aminating a wide range of C–H bonds with greater reactivity and chemoselectivity than previous nitrene-based systems (Scheme 12). The sulfamate esters in the substrate serve as directing groups for catalyst coordination, offering high selectivity for the *syn*-diastereomer while displaying excellent chemoselectivity in the presence of π-functionality.[90]

Scheme 12. Metallonitrene C–H amination by White.[90]

2.3.1.4. Allylic Alcohol Hydroamination

As previously discussed, methods that utilize Mannich reactions or chiral auxiliary-directed addition reactions[91] typically require a subsequent stereoselective reduction of the carbonyl or imine substructures to yield the desired enantioenriched 1,3-amino alcohols. Conversely, asymmetric hydroamination of unprotected allylic alcohols represents a highly atom-economic method for accessing chiral 1,3-amino alcohols, as recently demonstrated by Buchwald and coworkers.[92] The methodology provides access to the amino alcohol motif with the stereogenic center adjacent to the nitrogen atom (**41**) from simple precursors with excellent levels of regio- and enantioselectivity (Scheme 13).
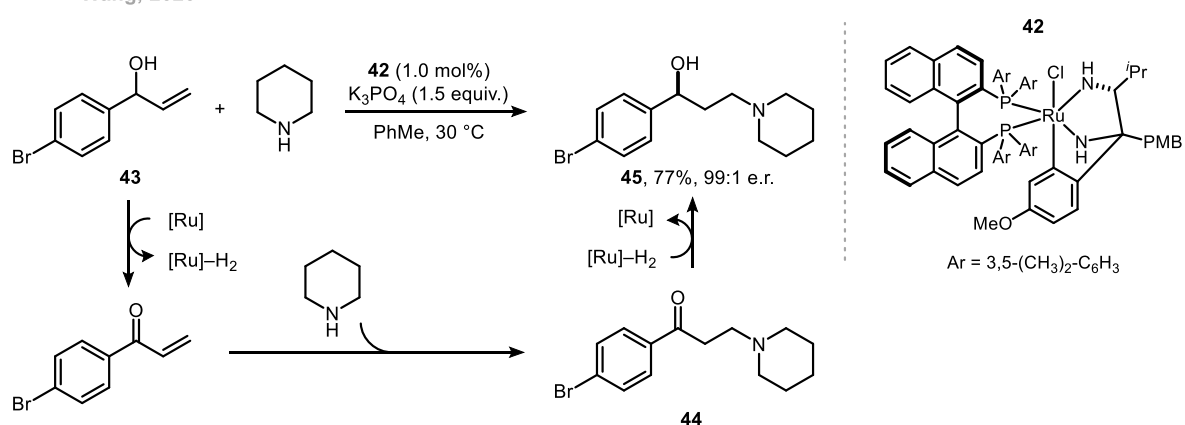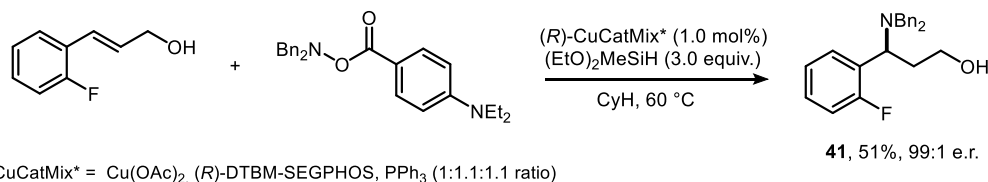
Scheme 13. Strategies for allylic alcohol hydroamination developed by Buchwald and Wang.[92-93]

On the other hand, the Wang group established an asymmetric borrowing-hydrogen strategy for the formal *anti*-Markovnikov addition of nitrogen-based nucleophiles to allyl alcohols.[93] The privileged Ru-diamine-diphosphine catalyst **42** enables the dehydrogenation of a racemic secondary allylic alcohol **43**

as well as the subsequent asymmetric hydrogenation of the resulting amino ketone intermediate **44**, thus furnishing enantiomerically enriched 1,3-amino alcohol **45** with the stereogenic center adjacent to the hydroxyl group (Scheme 13).

2.3.1.5. 1,3-Dipolar Cycloaddition Reaction

The addition of an alkene to a 1,3-dipole for the synthesis of five-membered heterocycles is a classic reaction in organic chemistry, with its broad application established through Huisgen's groundbreaking research in the 1960s.[94] Nitrones and nitrile oxides are important dipolar species which have been used in 1,3-dipolar cycloadditions to constitute 5-membered isoxazole ring systems. One key reason for the successful synthetic application of nitrones is that, contrary to the majority of other 1,3-dipoles, nitrones are generally stable compounds that do not require in situ formation. As an example, MacMillan's group demonstrated that chiral imidazolidinone catalyst **12** can effectively promote the highly enantioselective 1,3-dipolar cycloaddition of nitrone **46** with crotonaldehyde (**47**), yielding the *endo*-cycloadduct **48** (Scheme 14).[95] While isoxazolidines are useful in their own right, they can also be easily converted to 1,3-amino alcohols by hydrogenation in the presence of Pd(OH)$_2$.[96]

In 2014, Kang and colleagues developed a self-hydride transfer method for N–O bond cleavage, which was applied in a cascade 1,3-dipolar cyclization of alkenes with *N*-methyl nitrone **49**, followed by an *N*-demethylative rearrangement (Scheme 14).[97] This approach efficiently produces synthetically valuable *N*–H 1,3-oxazinanes from unbiased styrenes, which could not be otherwise synthesized via the conventional dipolar cycloaddition of readily available *N*-methyl nitrones. The *cis*-1,3-oxazinane product **50** can be further transformed to the corresponding *syn*-1,3-amino alcohol **51** by treatment with NH$_2$OH·HCl in wet methanol. A catalytic asymmetric adaptation of this transformation would be of considerable interest.
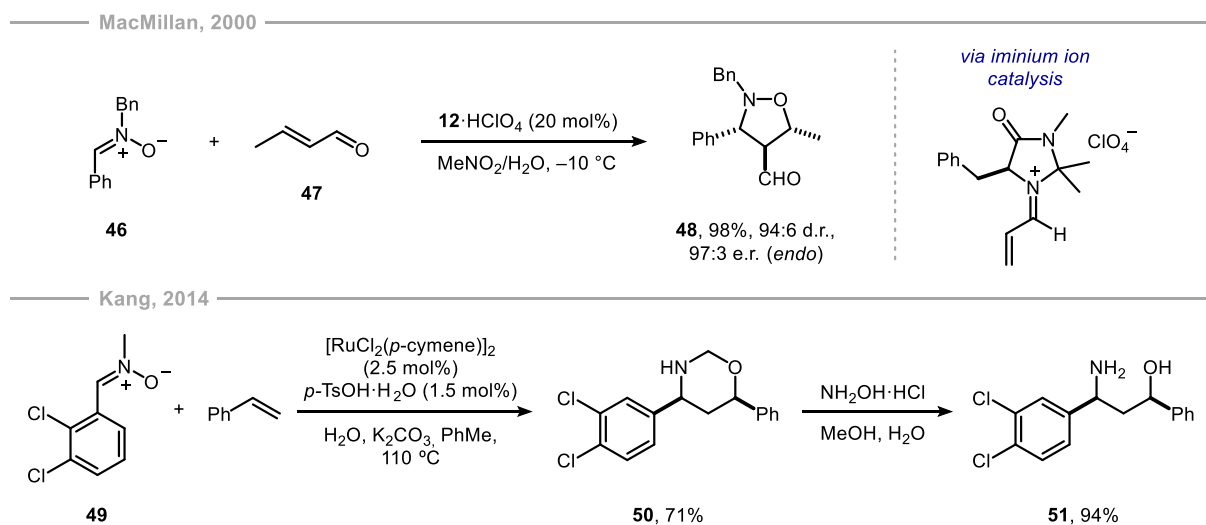
Scheme 14. 1,3-Dipolar cycloaddition reactions with nitrones by MacMillan and Kang.[95, 97]

2.4. Summary and Outlook

As inexpensive and abundant materials, olefins have become pivotal for chemical synthesis. Readily available in bulk from both petrochemical feedstocks and renewable resources, olefins are among the most versatile classes of organic compounds, capable of undergoing a wide range of transformations and serving as key intermediates in diverse synthetic applications. The direct functionalization of olefins has proven to be a particularly useful method for the synthesis of 1,2- and 1,3-difunctionalized molecules. Namely, olefin dihydroxylation, aminohydroxylation, and oxy-oxymethylation are well-established methods for the synthesis of 1,2-diols, 1,2-amino alcohols, and 1,3-diols, respectively. However, an analogous oxy-aminomethylation of alkenes toward 1,3-amino alcohols remains elusive, with only a few reports of non-asymmetric variants in the literature to date. Such enantiopure 1,3-amino alcohols are highly valuable building blocks toward pharmaceuticals, especially for the synthesis of marketed blockbuster antidepressants such as (*S*)-duloxetine, (*R*)-fluoxetine, and (*R*)-atomoxetine. Classic approaches toward 1,3-amino alcohols involve the asymmetric reduction of Mannich reaction products. Other recent strategies include hydroamination of allylic alcohols, intermolecular C–H amination of prefunctionalized substrates and hetero-cycloaddition reactions. Nevertheless, reports on the synthesis of 1,3-amino alcohols through alkene functionalization are scarce. In this regard, we recognized that the ability of strong Brønsted acids to promote reaction with unbiased olefins could serve as a platform toward the privileged 1,3-difunctionalzed scaffold. Building on our group's efforts to explore the chemical transformations of unfunctionalized hydrocarbon feedstocks, we aimed to address this gap by developing two methods for obtaining 1,3-amino alcohols from unbiased olefins, providing a streamlined and efficient route to these important intermediates in drug development.
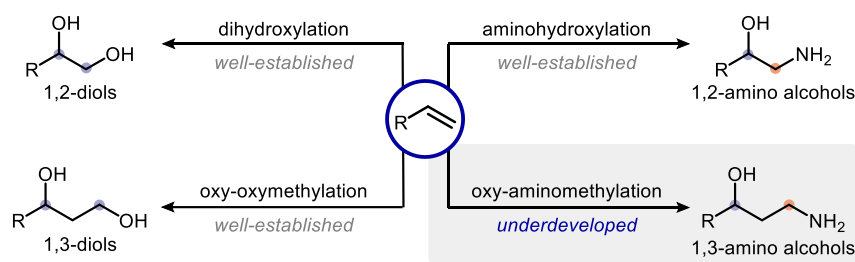
3. Objectives

1,3-Amino alcohols and their derivatives are common structural motifs in a wide range of naturally occurring molecules and medicinal compounds. These structures are particularly significant in several of the world's top-selling pharmaceuticals, such as fluoxetine and duloxetine (commonly known as Prozac and Cymbalta, respectively), underscoring their importance in drug development and therapeutic innovation.

Among the numerous methodologies available for 1,3-amino alcohol synthesis, the direct functionalization of unbiased olefins is particularly attractive due to their low cost and wide availability, making them ideal substrates for building molecular complexity. Direct 1,2-functionalizations of olefins take an important place in chemical synthesis, with dihydroxylations and aminohydroxylations serving as notable examples of their significance. The Prins reactivity enables the formation of 1,3-diols through alkene oxy-hydroxymethylation. However, the corresponding oxy-aminomethylation of olefins has remained underdeveloped to date (Figure 13a).

The goal of this doctoral work is to develop catalytic methods for the transformation of alkenes into valuable 1,3-amino alcohol intermediates by means of Brønsted acid catalysis. Direct olefin functionalization will be explored through two different projects (Figure 13b). The first project involves the three-component reaction of aryl olefins, formaldehyde, and ammonia surrogates, such as sulfonamides or carbamates, catalyzed by strong Brønsted acids. The second project focuses on the asymmetric inverse-electron-demand hetero–Diels–Alder reaction of olefins and in situ generated *N*-Boc-formaldimine, catalyzed by strong and confined IDPi catalysts.
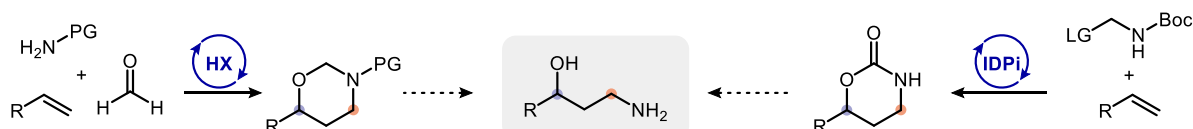

Figure 13. (a) Olefins as building blocks for the synthesis of 1,2- and 1,3-difunctionalized molecules. (b) Our approach: strong Brønsted acid-catalyzed difunctionalization of olefins toward 1,3-amino alcohols.

4. Results and Discussion

The results and discussion of this doctoral thesis are divided into two main sections. The first part addresses the development of a three-component Brønsted acid-catalyzed reaction utilizing aryl olefins, formaldehyde, and ammonia surrogates. This section covers the optimization of the reaction, an examination of its scope, and mechanistic studies aimed at elucidating the reaction pathway of the transformation.

The second part focuses on investigating methods for the strong and confined chiral Brønsted acid-catalyzed hetero-[4 + 2] cycloaddition between styrenes and 1,1-disubstituted alkenes with in situ generated *N*-Boc-formaldimine. Within the section, the broad reaction scope, examples of the applicability of the methodology, and thorough mechanistic studies supporting an inverse-electron-demand hetero-Diels–Alder pathway with unusual kinetics will be discussed.

4.1. Acid-Catalyzed Oxy-aminomethylation of Styrenes

The work presented in this chapter was conducted in collaboration with Dr. S. Liu and Dr. C. D. Díaz-Oviedo.

The Prins reaction and the aza-version thereof stand out for facilitating the direct synthesis of 1,3-difunctionalized moieties, which are prevalent in pharmaceutically relevant molecules. The Prins reaction has been extensively investigated, and several catalytic methodologies are available nowadays.[53, 98-99] Analogously, the aza-Prins reaction of an alkene, formaldehyde, and ammonia represents a straightforward approach to converting olefins into 1,3-amino alcohols. Formally, this reaction would involve the formation of a formaldehyde-derived imine, which is subsequently attacked by the nucleophilic olefin, and the intermediate β-amino carbocation could be trapped with water to yield the corresponding 1,3-amino alcohol (Scheme 15).
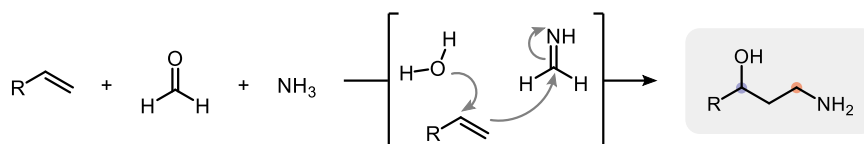

Scheme 15. Synthesis of 1,3-amino alcohols from olefins via a three-component aza-Prins reaction.

Despite the considerable synthetic potential of this transformation, it has remained surprisingly underexplored, with only a few reports in the literature to date. These studies either feature a highly limited substrate scope,[54, 100] rely on biased substrates with tethered nucleophiles to capture reactive intermediates,[101] or utilize preformed electrophiles, limiting the process to a two-component reaction.[102] We sought to address this gap by investigating the Brønsted acid-catalyzed three-component reaction involving aryl olefins, formaldehyde, and ammonia surrogates such as sulfonamides or carbamates. By incorporating these common pharmacophores, our approach aims to broaden the synthetic scope and improve the efficiency of producing 1,3-amino alcohols for potential pharmaceutical applications.

4.1.1. Reaction Design and Optimization Studies

At the onset of our studies, we tested the reaction of styrene (**52a**) with *sym*-trioxane (1,3,5-trioxane, **53**) and *p*-toluenesulfonamide (**54a**) using several common Brønsted- or Lewis acids as catalysts. When substrates **52a**, **53**, and **54a** were mixed in a 1:1.5:3 ratio, the use of a weak Brønsted acid catalyst such as acetic acid (AcOH) led to the formation of 1,3-oxazinane **55a** in poor yield after 24 h at 60 °C (Table 1, entry 1). The use of either *p*-toluenesulfonic acid (*p*-TsOH) or trifluoromethanesulfonic acid (TfOH) resulted in higher conversions, thus affording the product in 38% and 32% yield, respectively (entries 2–3). Conducting the reaction under Lewis acidic conditions resulted in a decrease in reactivity (entries 4–6). As anticipated, the selection of catalyst is critical, as other established strong Brønsted

acids demonstrated lower efficiency. For instance, using bis(trifluoromethane)sulfonamide (Tf₂NH) as catalyst resulted in a complex mixture, yielding only 10% of the desired product (entry 7).
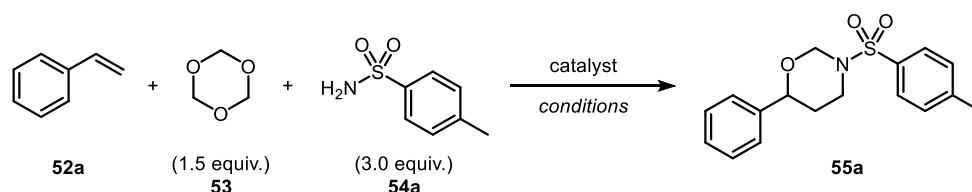
Entry	Catalyst (mol%)	Solvent	Temp (°C)	Yield (%)[a]
1	AcOH (20 mol%)	DCM	60	<5
2	p-TsOH (20 mol%)	DCM	60	38
3	TfOH (20 mol%)	DCM	60	32
4	Fe(OTf)₃ (20 mol%)	DCE	60	26
5	Cu(OAc)₂ (20 mol%)	DCE	60	0
6	CrCl₃ (20 mol%)	DCE	25	0
7	Tf₂NH (20 mol%)	DCM	60	10
8	HPF₆ (10 mol%)	DCE	60	58
9	-	DCM	60	0
10	HPF₆ (20 mol%)	DCM	60	68

Table 1. Optimization of reaction conditions for styrene (**52a**) as substrate. [a]All yields were determined by ¹H NMR spectroscopy.

In contrast, employing the strong Brønsted acid hexafluorophosphoric acid (HPF₆) in catalytic amounts led to the formation of 1,3-oxazinane **55a** with a yield of 58% after 24 hours at 60 °C (entry 8). In the absence of acid catalyst, no product was observed (entry 9). Increasing the HPF₆ loading to 20 mol% resulted in increased product formation (68%, entry 10).
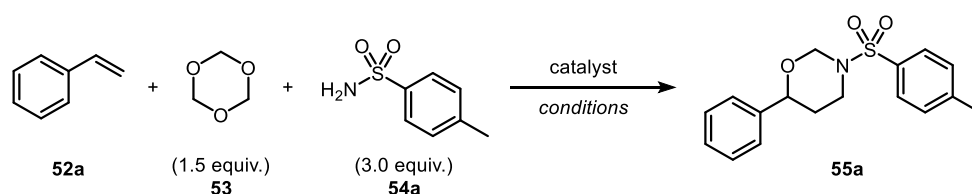

Entry	Catalyst (mol%)	Solvent	Temp (°C)	Yield (%)[a]
1	HPF₆ (20 mol%)	DCE	60	58
2	HPF₆ (20 mol%)	DCE	40	49
3	HPF₆ (20 mol%)	CHCl₃	60	78
4	HPF₆ (20 mol%)	CHCl₃	25	12
5	HPF₆ (20 mol%)	MeCN	60	5
6	HPF₆ (20 mol%)	PhMe	100	20
7[b]	HPF₆ (20 mol%)	CHCl₃	60	68

Table 2. Solvent and temperature optimization. [a]All yields were determined by ¹H NMR spectroscopy. [b]On 10 mmol scale.

Subsequently, the choice of solvents and reaction temperature was also investigated (Table 2, entries 1–6). Upon screening several solvents, the use of chloroform proved beneficial and resulted in an increased yield (78%, entry 3). Remarkably, the HPF$_6$-catalyzed reaction also proceeded at room temperature, although with a considerably reduced rate (entry 4). Higher reaction temperatures did not lead to an improvement in yield (entry 6). Satisfactorily, the reaction could be performed on a larger scale (10 mmol of olefin) to provide 2.2 g of product **55a** (isolated yield of 68%, entry 7).

Finally, the formaldehyde source was furthermore investigated. We compared *sym*-trioxane with other HCHO sources, such as paraformaldehyde and formalin (aqueous 37% *w/w* solution of formaldehyde) in the reaction using HPF$_6$ as catalyst. While *sym*-trioxane demonstrated positive effects on the reaction, a notable drop in reactivity was observed with the use of paraformaldehyde or formalin (Table 3, entries 2–3). Consequently, we opted to use *sym*-trioxane as the formaldehyde source for the oxy-aminomethylation reaction in our investigations.
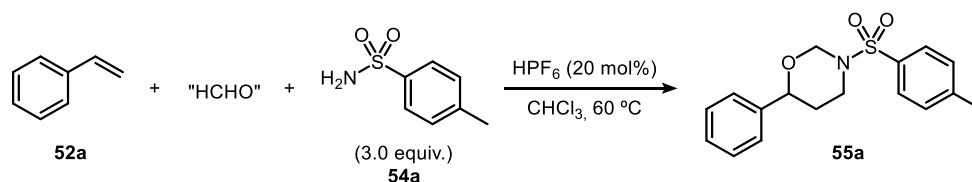
Entry	Formaldehyde source (equiv.)	Solvent	Temp (°C)	Yield (%)[a]
1	*sym*-Trioxane (1.5 equiv.)	CHCl$_3$	60	78
2	Paraformaldehyde (4.5 equiv.)	CHCl$_3$	60	7
3	Formalin (4.5 equiv.)	CHCl$_3$	60	traces

Table 3. Formaldehyde source optimization. [a]All yields were determined by ^{1}H NMR spectroscopy.

4.1.2.   Reaction Scope

Having identified the optimal reaction conditions for the model substrate, we explored several other olefins and protecting groups as potential substrates for this transformation.

4.1.2.1.   Olefin Scope

With respect to the olefin component, it was observed that terminal styrenes bearing *para*-substituents, whether weakly electron-withdrawing (CH$_2$Cl, F, Cl, Br) or electron-donating (Me, ^{t}Bu), delivered the corresponding 1,3-oxazinanes in moderate to good yields (**55b–e** and **55f–g**, Figure 14). *Meta*- and *ortho*-substituted styrenes also proved to be suitable substrates, resulting in the formation of products **55h** and **55i**. Notably, 1,3,5-trimethyl-2-vinylbenzene (**52j**), featuring a challenging double *ortho*-substitution pattern, was successfully converted into the corresponding 1,3-oxazinane **55j** with moderate yield. The methodology was successfully extended to a naphthyl-substituted olefin, yielding product

55k in 38% yield. Remarkably, cyclic and internal aryl olefins also demonstrated compatibility with the transformation. For instance, 1*H*-indene reacted to afford product **55l** exclusively as the *cis*-diastereomer, while dialin gave product **55m** in 32% yield as a diastereomeric mixture (*cis/trans* ratio = 1:1). *Trans*-β-methylstyrene (***trans*-52n**) underwent reaction to yield 1,3-oxazinane **55n** as a mixture of *trans*- and *cis*-isomers in a 2:1 ratio, while the isomeric ***cis*-52n** olefin remained unreactive under identical conditions. Furthermore, the methodology demonstrated high selectivity for aryl olefins, as evidenced by substrate **52o**, which contained both an alkyl and an aryl olefin. In this case, only product **55o** was formed in 53% yield.

Reaction Scope of Aryl Olefins
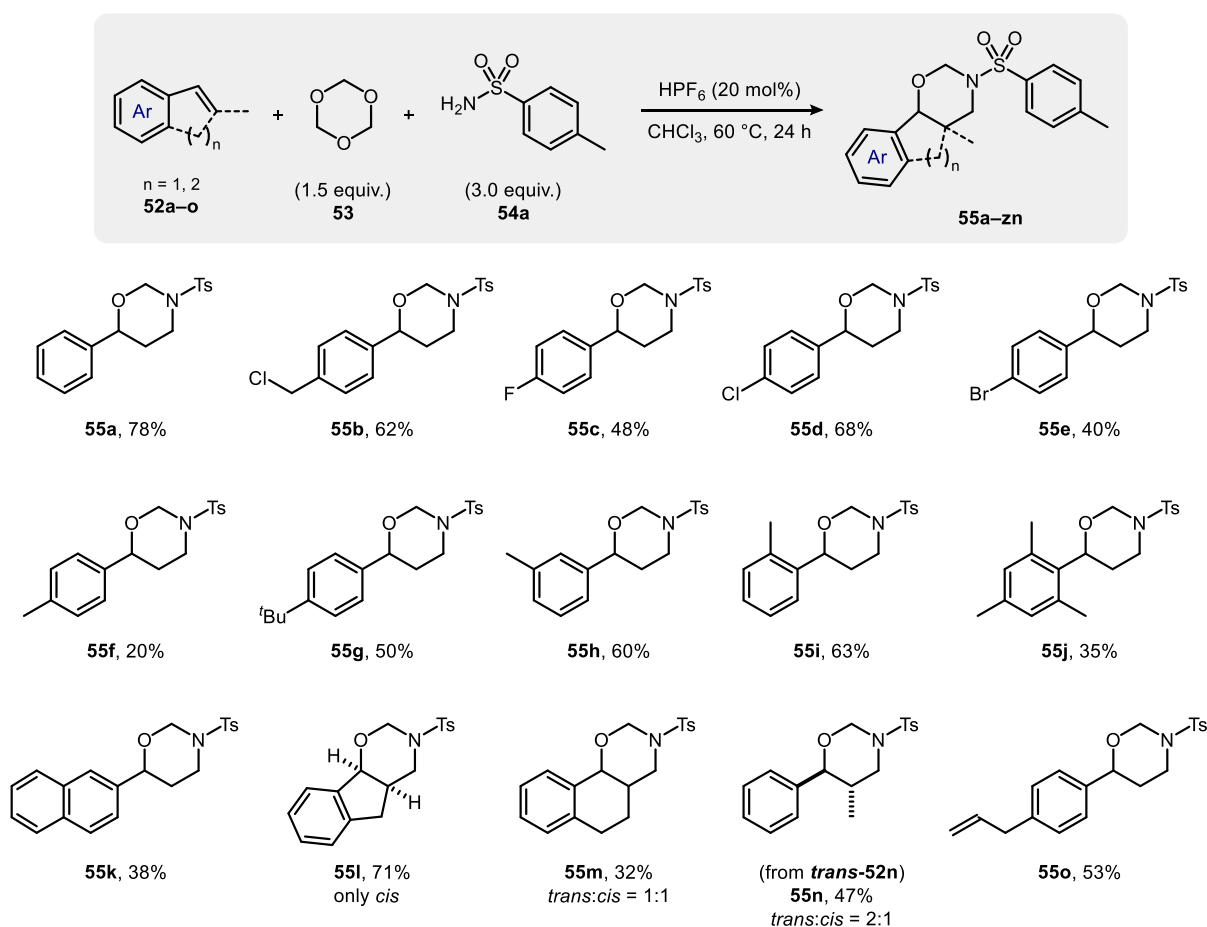
Figure 14. Olefin scope in the three-component transformation. Isolated yields after chromatographic purification.

4.1.2.2. Sulfonamide Scope

Next, the investigation was extended to explore a range of sulfonamides, given their broad availability and versatility as substrates. As illustrated in Figure 15, benzenesulfonamide (**54b**) and its derivatives with electron-donating groups (Me, *t*Bu, OMe) were found to be suitable substrates, yielding the corresponding products **55p–s**. Additionally, a wide range of benzenesulfonamides containing electron-withdrawing groups (F, Cl, Br, NO_2, CF_3) at various positions on the aromatic ring were also

successfully converted into the corresponding 1,3-oxazinanes **55t–ze** in moderate to good yields. The naphthalene-derived sulfonamide underwent reaction to yield the corresponding heterocycle **55zf** in 48% yield. Remarkably, the reaction also proceeded with aliphatic sulfonamides to provide the corresponding products **55zg–zj** in good yields. It is important to highlight that products **55za** and **55zg**
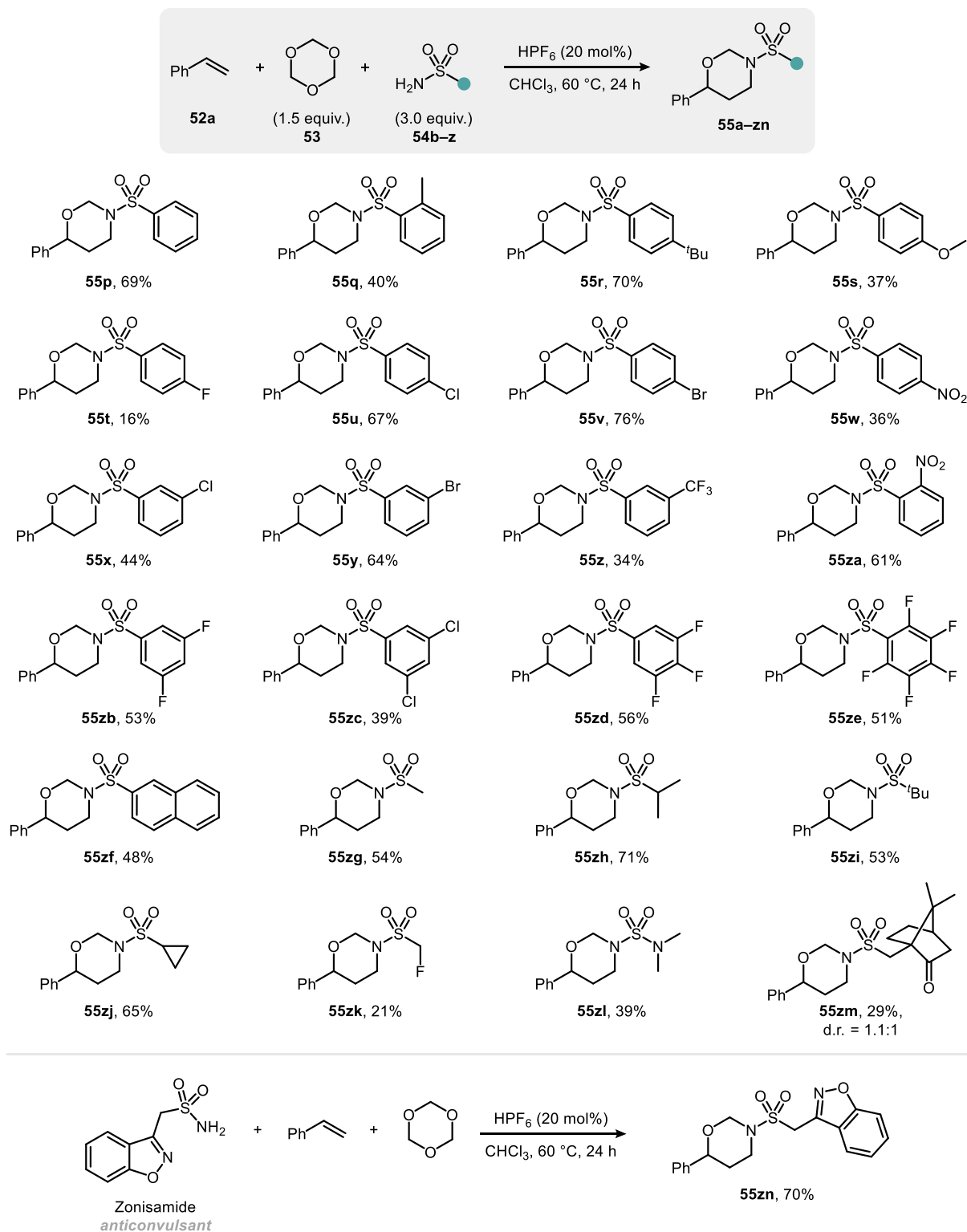

Figure 15. Sulfonamide scope in the three-component reaction. Isolated yields after chromatographic purification.

incorporate nosylate and mesylate groups, respectively, which are commonly used as protecting groups with established deprotection strategies available for their removal. Furthermore, it is worth to mention that the reaction with fluoromethanesulfonamide (**54w**) resulted in the expected oxazinane **55zk** being formed in 21% yield, along with 46% of 4-phenyl-1,3-dioxane, a product of the Prins reaction between styrene and formaldehyde. This occurrence may be attributed to the reduced nucleophilicity of the sulfonamide, which hinders its reaction with trioxane to generate the oxy-aminomethylating species. Using *N,N*-dimethylsulfamide, the desired product **55zl** could be isolated in 39% yield. Given the commercial availability of enantiopure camphorsulfonic acid and its derivatives, which are widely used as chiral auxiliaries and resolving agents, we opted to utilize (1*S*)-10-camphorsulfonamide in our three-component transformation.[103-104] The reaction produced compound **55zm** in a yield of 29%, albeit with minimal diastereoselectivity (d.r. = 1.1:1). Moreover, due to the wide variety of sulfonamide-based drugs, we aimed to investigate whether our methodology could be applied to the derivatization of pharmaceutically active molecules containing this functional group as a late-stage modification strategy.[105-106] Zonisamide, a medication used to manage symptoms of epilepsy and Parkinson's disease,[107] underwent reaction to yield product **55zn** in 70% yield.

4.1.2.3. Carbamate Scope

Considering the widespread application of carbamates (such as Boc, Cbz, Fmoc, and others) as protecting groups (PGs) in peptide synthesis, we recognized the potential of *N*-carbamoyl-protected oxazinanes for generating modified or unnatural peptide derivatives. As exemplified in Figure 16, carbamates also proved to be suitable nitrogen nucleophiles for the multicomponent transformation, although with moderately lower yields than those observed for sulfonamides. When phenyl carbamate (**56a**) was

Reaction Scope of Carbamates

PG = CO$_2$Ph (**57a**), 34%
PG = Cbz (**57b**), 23%
PG = Fmoc (**57c**), 37%

PG = Cbz (**57d**), 39%
PG = Fmoc (**57e**), 35%

PG = Cbz (**57f**), 15%
PG = Fmoc (**57g**), 45%

PG = Cbz (**57h**), 27%
PG = Fmoc (**57i**), 28%

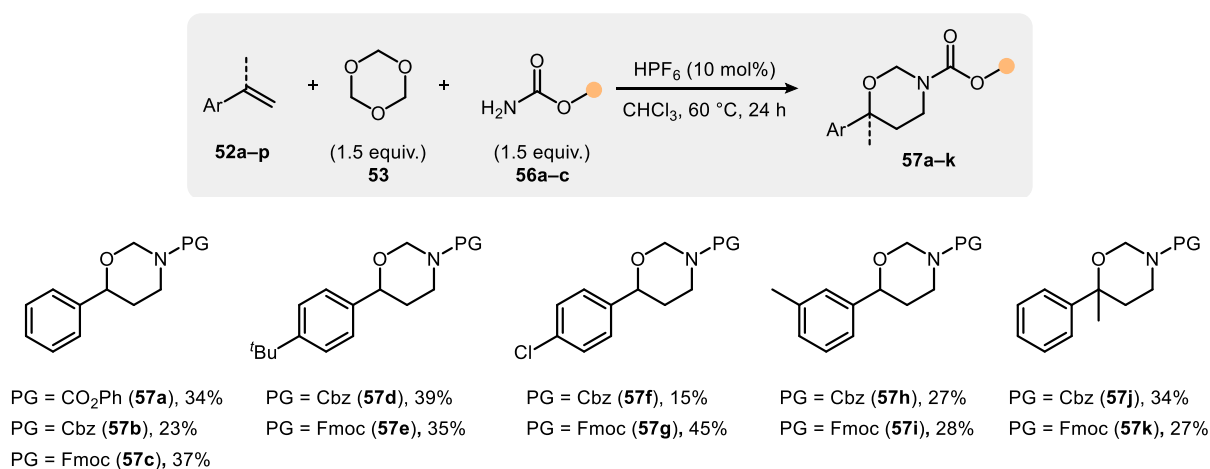PG = Cbz (**57j**), 34%
PG = Fmoc (**57k**), 27%

Figure 16. Carbamate scope in the three-component reaction. Isolated yields after chromatographic purification.

used as the ammonia surrogate, product **57a** was isolated in a yield of 34%. Gratifyingly, both benzyl carbamate (**56b**) and 9-fluorenylmethyl carbamate (**56c**) successfully participated in the HPF$_6$-catalyzed three-component reaction with *sym*-trioxane and styrene, yielding the corresponding *N*-Cbz-protected (**57b**) and *N*-Fmoc-protected (**57c**) 1,3-oxazinanes in 23% and 37% yield, respectively. Similarly, terminal styrenes **52b**, **52f**, **52h**, and **52p** also proved to be suitable substrates for this methodology, yielding the *N*-carbamoyl-protected products **57d–k** in moderate yields. In our attempt to prepare an *N*-Boc-protected oxazinane, *tert*-butyl carbamate was found to be incompatible with the strongly acidic catalyst.

4.1.3. Current Scope Limitations

Several olefins were identified as challenging substrates in the transformation due to their extreme reactivity profiles (Figure 17). Highly electron-rich styrenes, such as *p*-methoxystyrene (**52q**) and 5-vinyl-benzo[*d*][1,3]dioxole (**52r**), exhibited excessive reactivity, leading to complex product mixtures. In contrast, styrenes with strong electron-withdrawing substituents at the *para*-position, like **52s–v**, demonstrated very low reactivity, yielding only trace amounts of the product. It can be rationalized that the presence of electron-deficient groups on the aromatic ring leads to a decrease in the nucleophilicity of the olefin moiety, which is reflected in lower reaction rates. Additionally, terminal alkyl olefins **58a–c**, which possess significantly reduced nucleophilicity compared to aryl olefins (as illustrated by Mayer's scale in Section 2.2.2.1), showed no product formation.
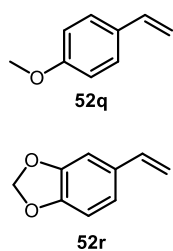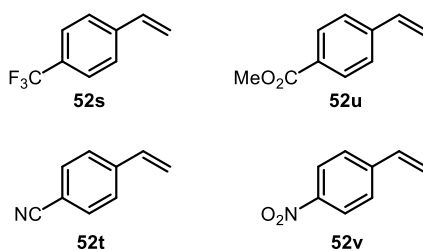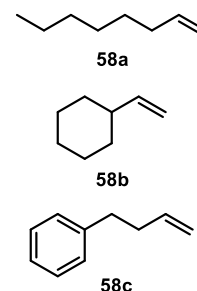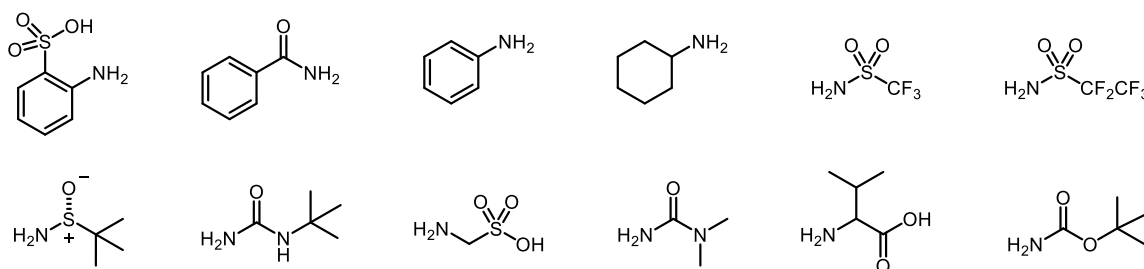

Figure 17. Current substrate limitations of the three-component olefin oxy-aminomethylation.

In addition to sulfonamides and carbamates, other classes of nitrogen nucleophiles were evaluated; however, they were found to be incompatible under the reaction conditions, resulting in either no reaction or the formation of complex product mixtures (Figure 17).

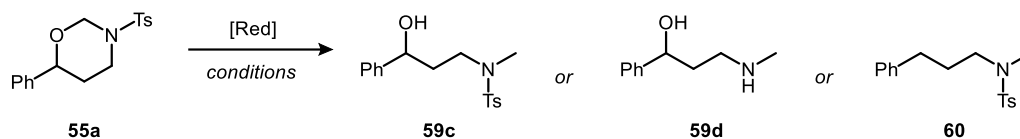### 4.1.4. Deprotection of 1,3-Oxazinanes to Access 1,3-Amino Alcohols

The synthesized oxy-aminomethylation products already display the structural framework of the target 1,3-amino alcohols, requiring only the cleavage of the *N,O*-acetal moiety and the nitrogen protecting group. Most importantly, choosing appropriate conditions enables the selective removal of these moieties, which might be particularly advantageous in complex synthetic pathways. Exemplarily, following the conditions previously reported by Zhong,[108] 1,3-oxazinane **55a** underwent a clean *N,O*-acetal ring opening by refluxing with HCl in methanol, giving access to *N*-Ts-protected amino alcohol **59a** in 89% yield (Scheme 16a). The treatment of **55a** with magnesium powder and sonication, followed by the *N,O*-acetal ring-opening procedure, resulted in the formation of the corresponding free 1,3-amino alcohol **59b** in 75% yield over the two steps (Scheme 16b).
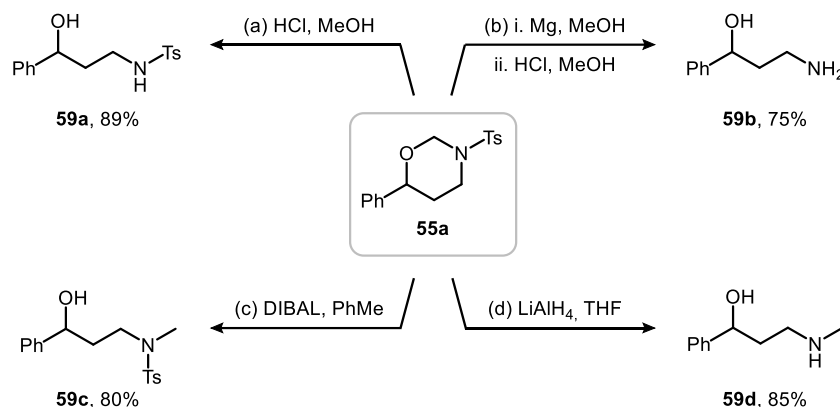
Scheme 16. Derivatization of **55a** to the corresponding 1,3-amino alcohol. Detailed reaction conditions can be found in the Experimental Section.

Next, reductive conditions for converting **55a** into its corresponding *N*-methyl derivative, a characteristic feature of several pharmaceutically-active substances such as atomoxetine, fluoxetine and nisoxetine, were investigated. As summarized in Table 4, attempts to achieve reductive ring cleavage under mild reaction conditions using NaBH$_4$ in methanol resulted in no conversion (entry 1). The use of triethylsilane in the presence of an excess of trifluoroacetic acid led to complete reduction of the benzylic alcohol, yielding the corresponding methylene unit **60** in quantitative yield (entry 2). Notably, when refluxing **55a** in toluene with 5 equivalents of diisobutylaluminum hydride (DIBAL), the heterocycle underwent clean reductive ring cleavage to produce *N*-Ts-protected amino alcohol **59c** in 80% yield (entry 3 and Scheme 16c). Attempting the reaction with LiAlH$_4$ as reducing agent in THF at 40 °C resulted in partial conversion into the *N*-methyl amino alcohol **59d** (entry 4). Importantly, subjecting

55a to LiAlH$_4$ under more vigorous conditions and prolonged reaction times led to direct conversion to **59d** in 85% yield (entry 5 and Scheme 16d).

Table 4. Screening of reducing conditions. [a]All yields were determined by ^{1}H NMR spectroscopy.

Entry	[Red] (equiv.)	Solvent	Temp (°C)	Conv. (%)	Yield (%, 59c:59d:60)[a]
1	NaBH$_4$ (2.0 equiv.)	MeOH	rt	0	0:0:0
2	Et$_3$SiH/TFA (5.0 equiv.)	DCM	40	full	0:0:quant.
3	DIBAL (5.0 equiv.)	PhMe	reflux	85%	80:0:0
4	LiAlH$_4$ (3.0 equiv.)	THF	40	30	7:22:0
5	LiAlH$_4$ (5.0 equiv.)	THF	60	full	5:85:0

4.1.5. Mechanistic Studies

4.1.5.1. NMR Monitoring Experiments

The work presented in this section was conducted in collaboration with Dr. M. Leutzsch.

To gain insight into the reaction mechanism and the reaction intermediates involved in the three-component olefin oxy-aminomethylation reaction, we initiated our investigation by conducting a ^{1}H NMR monitoring of the reaction mixture over time (Figure 18). Under optimal reaction conditions,
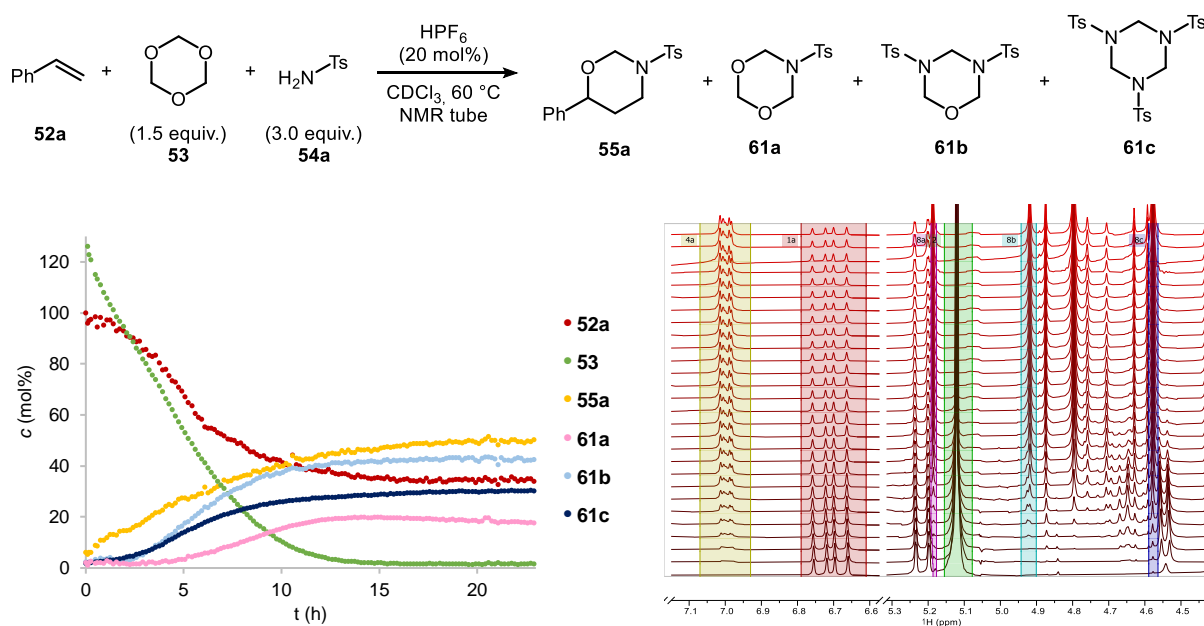

Figure 18. Left: Concentration plots obtained from ^{1}H NMR reaction monitoring during the reaction of **52a**. Right: ^{1}H NMR spectra recorded at different time points.

alongside the desired product **55a**, several byproducts resulting from the condensation of *sym*-trioxane and sulfonamide were also identified. These include 5-tosyl-1,3,5-dioxazinane (**61a**), 3,5-ditosyl-1,3,5-oxadiazinane (**61b**), and 1,3,5-tritosyl-1,3,5-triazinane (**61c**).

Intrigued by the actual nature of the electrophile, we continued our exploration by conducting several experiments in the absence of olefin. Indeed, the reaction of *sym*-trioxane and *p*-toluenesulfonamide in the presence of catalytic amounts of HPF_6 led to the formation of the previously observed condensation products **61a–c**, along with some formaldehyde monomer (Figure 19).
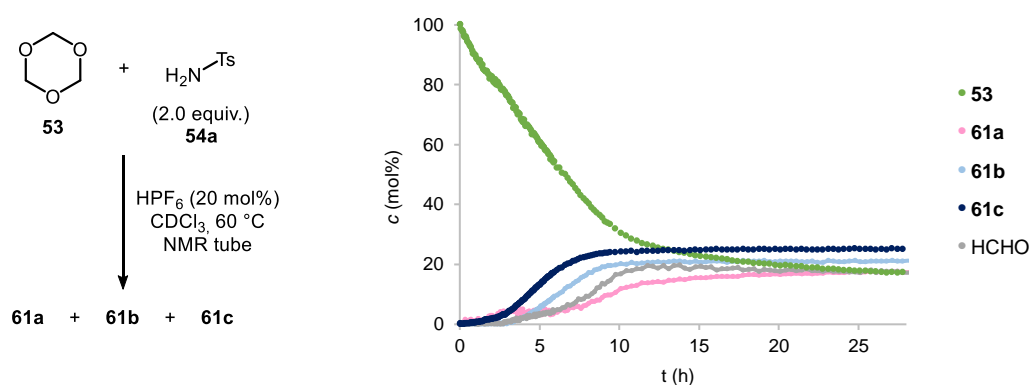
Figure 19. Concentration plots obtained from ^{1}H NMR reaction monitoring during the reaction between **53** and **54a**.

Considering the known dynamic behavior of the sulfonamide-formaldehyde condensation,[109-111] we aimed to determine whether similar interconversions occur within our system. Specifically, we sought to investigate if the formed condensation products **61a–c** could equilibrate in the presence of *sym*-trioxane. To achieve this, we conducted the following two experiments on 0.1 mmol scale (in $CDCl_3$ at 60 °C), analyzing aliquots of the reaction mixtures at certain times by ^{1}H NMR.

Reaction between 53 and 61b

The reaction of disubstituted oxadiazinane **61b** with *sym*-trioxane was studied both in the presence and absence of catalytic amounts of HPF_6. As can be seen in Figure 20, **61b** converted into dioxazinane **61a** under strong acid catalysis. No interconversion was observed in the reaction without acid catalyst.

Reaction between 53 and 61c

Similarly, trisubstituted oxadiazinane **61c** reacted with *sym*-trioxane in the presence of HPF_6 to produce **61a**, as observed in the ^{1}H NMR monitoring presented in Figure 20. As expected, no interconversion was detected in the reaction conducted without HPF_6.
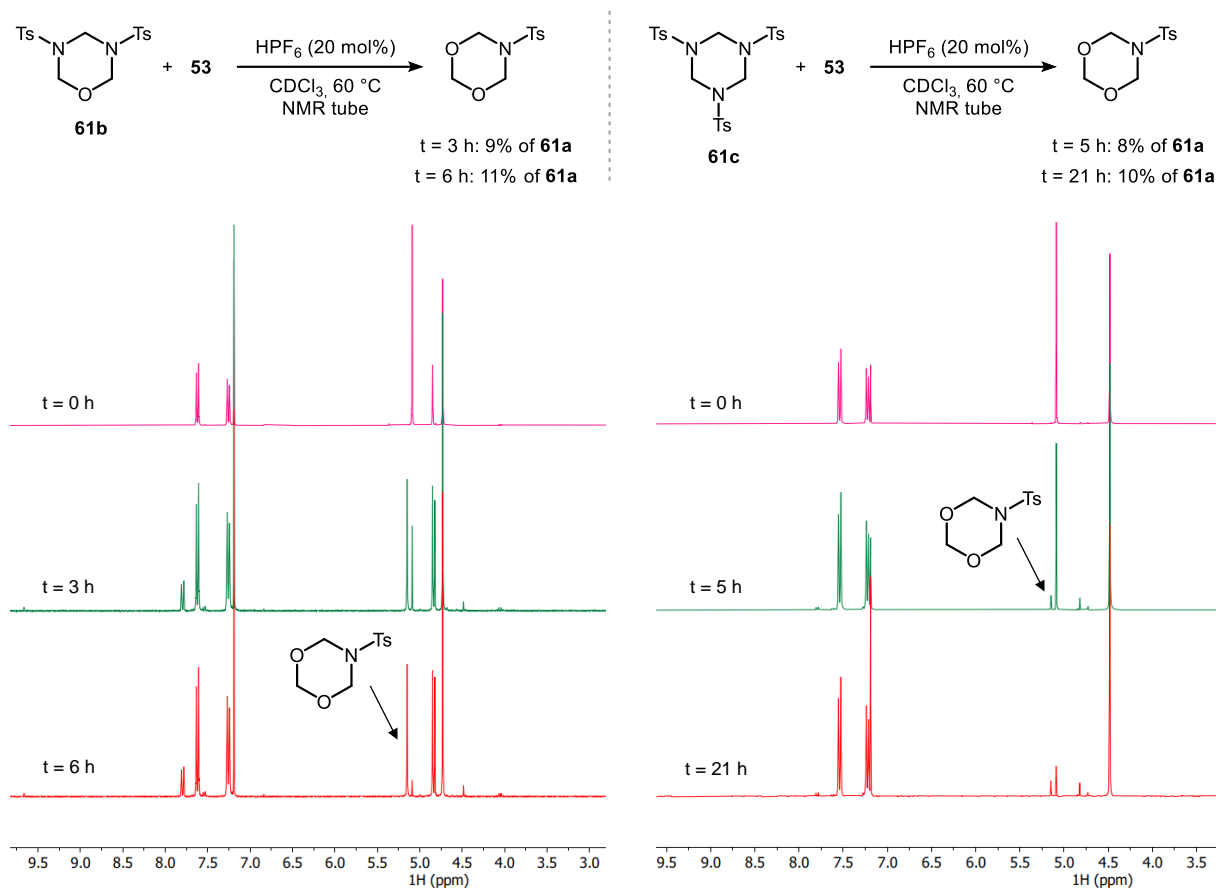
Figure 20. ^{1}H NMR monitoring of the reactions between **61b** and **53** (left) and between **61c** and **53** (right) in the presence of HPF$_6$ as catalyst.

As summarized in Scheme 17, these experiments led us to conclude that the acid-catalyzed reaction of *sym*-trioxane and sulfonamide **54a** produces sulfonamide-formaldehyde condensation products **61a–c**, which exist in a dynamic equilibrium under the reaction conditions.
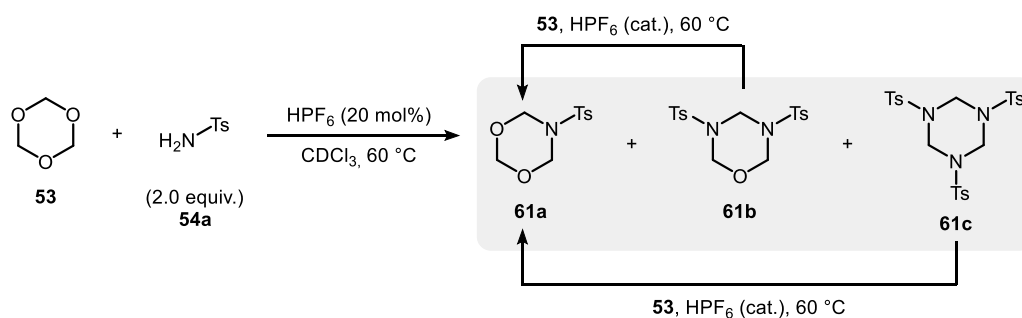
Scheme 17. Reaction between **53** and **54a** and dynamic equilibrium between condensation products **61a–c**.

Next, we further investigated the role of condensation products **61a–c** in the reaction system. When each one of these condensation products was reacted with styrene in the presence of catalytic amounts of HPF$_6$, only **61a** showed significant reactivity forming **55a** in 70% yield, thereby suggesting **61a** to be the actual reactive precursor in the annulation with styrene (Figure 21). The potential oxy-aminometylating reagents **61b** and **61c** produced only small amounts of **55a**, with yields of 10% and 5%, respectively.
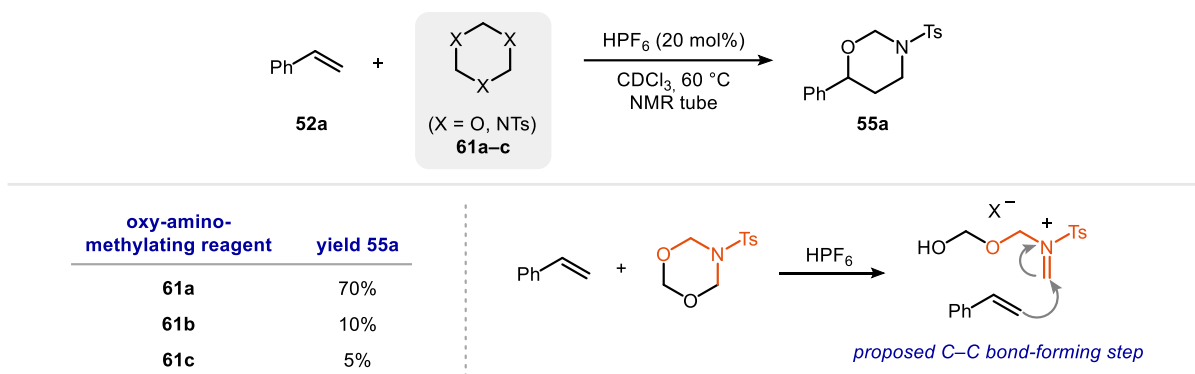
Figure 21. Sulfonamide-formaldehyde condensation products as potential electrophiles.

4.1.5.2. On the Stereospecificity: Reactions with Deuterium-Labeled Substrates

Two potential mechanisms for the acid-catalyzed oxy-aminomethylation of olefins can be proposed: a stepwise reaction pathway that involves the formation of a benzyl cation as an intermediate, or a (pseudo)-concerted pathway. To help us discern between these two possible operating mechanisms, we designed experiments using substrates exhibiting E/Z isomerism, enabling us to obtain insights into the diastereospecificity of the reaction (Figure 22).
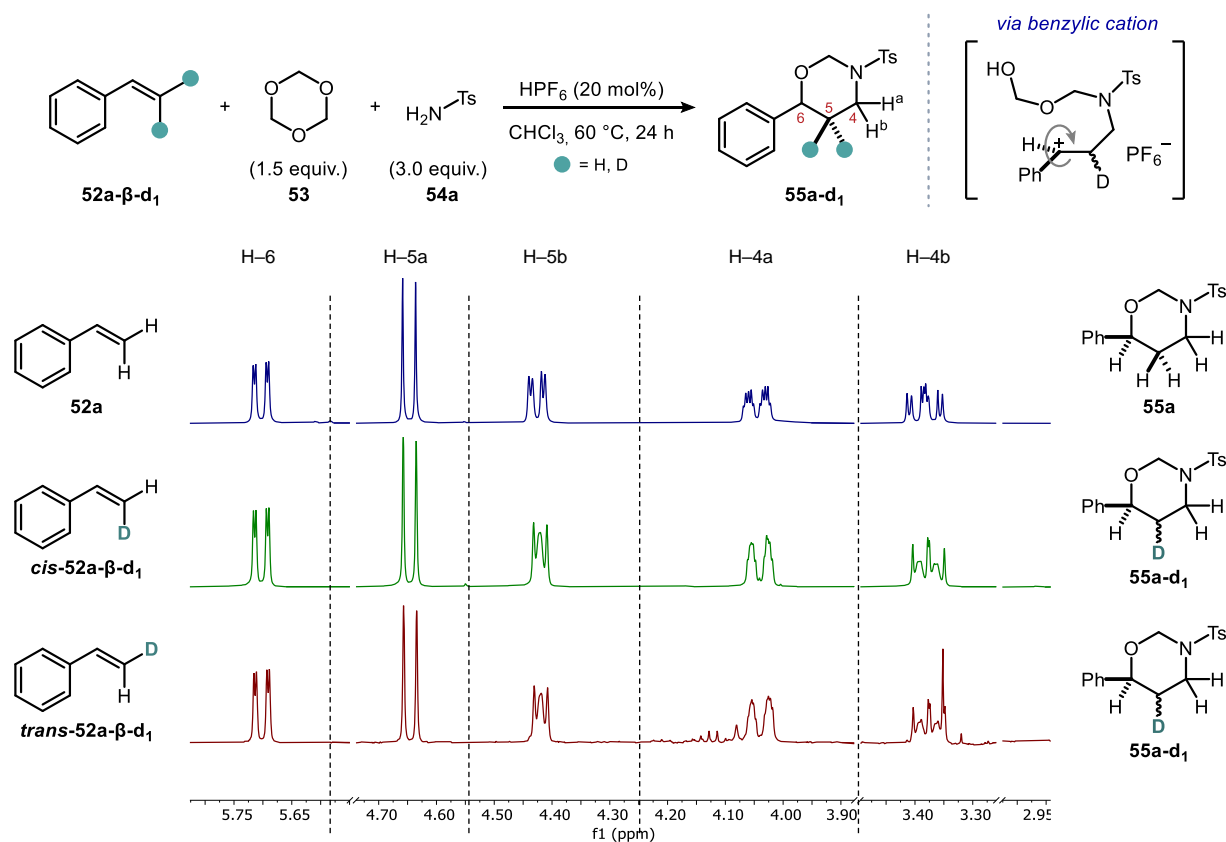
Figure 22. ^{1}H NMR analysis of the oxy-aminomethylation reaction of β-deuterostyrenes (**52a-β-d$_1$**) under HPF$_6$ catalysis.

We considered studying the three-component reaction using β-deuterium-labeled styrenes (***cis*-52a-β-d₁** and ***trans*-52a-β-d₁**, respectively) as substrates. As shown on the crude ¹H NMR spectra, the HPF₆-catalyzed reaction of these β-deuterostyrenes led in both cases to *cis/trans* mixtures of the corresponding 1,3-oxazinane. The loss of diastereotopic information observed in products **55a-d₁** suggests the involvement of a freely rotating benzylic cation species in the reaction mechanism (Figure 22).[53]

4.1.6.   Proposed Catalytic Cycle

Building on the mechanistic studies outlined in Section 4.1.5. we suggest the following catalytic cycle for the three-component reaction of aryl olefins, *sym*-trioxane, and sulfonamides, catalyzed by a strong Brønsted acid (Figure 23):
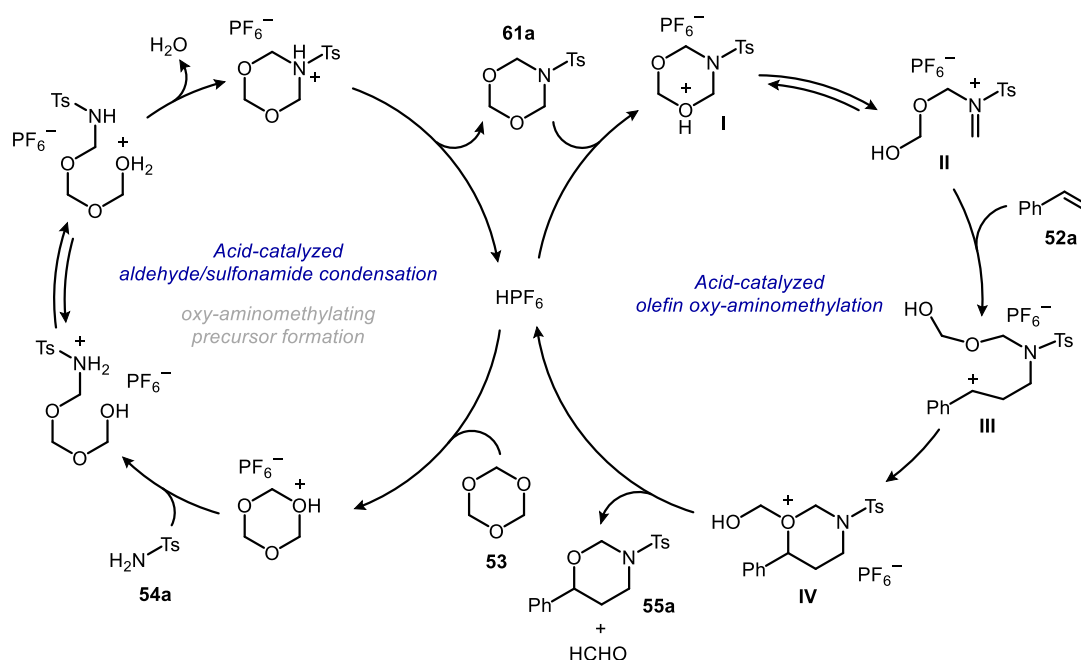

Figure 23. Proposed reaction mechanism.

The reaction is proposed to be operated by two parallel catalytic cycles. In the initial stage of the reaction, *sym*-trioxane (**53**) undergoes an acid-catalyzed condensation with *p*-toluenesulfonamide (**54a**), leading to the formation of various cyclic intermediates in dynamic equilibrium. Among these, 1,3,5-dioxazinane **61a** is proposed as the key oxy-aminomethylating precursor. In the parallel catalytic cycle, subsequent protonation of **61a** by the HPF₆ acid catalyst generates the highly reactive intermediate **I**, which can undergo ring opening to form an *N*-sulfonyl iminium ion **II**. At this stage, the nucleophilic olefin moiety of styrene (**52a**) can approach the electrophilic carbon, initiating C–C bond formation through a stepwise aza-Prins-type reaction, as indicated by the diastereomer scrambling observed in reactions with deuterium-labeled styrenes. This sequence results in the formation of the benzylic

carbocation **III**. The process concludes with ring closure to produce intermediate **IV**, which yields the desired product **55a** upon release of formaldehyde.

4.1.7.   Summary

The first chapter of the thesis dissertation presents the strong Brønsted acid-catalyzed alkene difunctionalization toward the synthesis of valuable 1,3-amino alcohol intermediates. Specifically, our methodology is based on the three-component reaction between aryl olefins, *sym*-trioxane, and ammonia surrogates such as sulfonamides or carbamates, under HPF$_6$ catalysis (Figure 24). This transformation yields a variety of 1,3-oxazinanes in moderate to good yields under mild reaction conditions, with its applicability demonstrated through several scope examples exhibiting excellent functional group tolerance. By choosing the appropriate deprotecting conditions, the obtained heterocyclic products can be readily transformed into the corresponding primary 1,3-amino alcohols or their *N*-methyl derivatives, which are highly demanded building blocks in the synthesis of biologically active compounds. Preliminary mechanistic studies suggest the intermediacy of an in situ formed 1,3,5-dioxazinane from partial aldehyde/sulfonamide condensation to be a key intermediate for the oxy-aminomethylation reaction with the olefin.
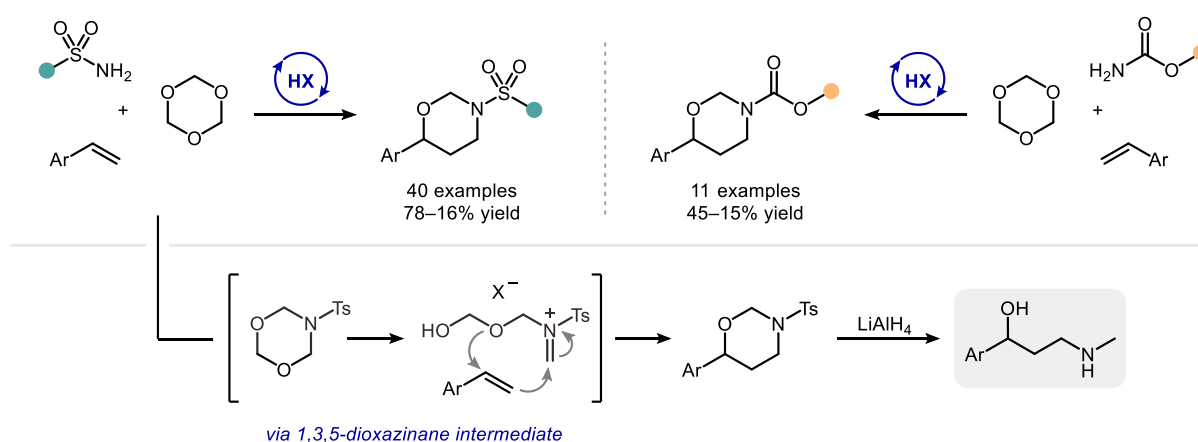

Figure 24. Brønsted acid-catalyzed oxy-aminomethylation reaction of styrenes.

4.1.8.   Outlook

After establishing the catalytic oxy-aminomethylation of aryl olefins, we sought to expand the substrate scope of this transformation. As discussed in Section 4.1.3., terminal alkyl olefins presented greater challenges due to their lower nucleophilicity, and further catalyst optimization will be required. On the nitrogen functionality, employing protecting groups that require milder deprotection conditions would also be beneficial.

Furthermore, the development of an asymmetric variant of this transformation remains highly desirable. As outlined in Section 2.3., enantioenriched 1,3-amino alcohols are prevalent structural motifs in natural products and active pharmaceutical ingredients, making the advancement of catalytic strategies for their synthesis critically important. With this goal in mind, we conducted preliminary screenings on the oxy-aminomethylation reaction of styrene with *sym*-trioxane and *p*-toluenesulfonamide using chiral Brønsted acid catalysts (Table 5).
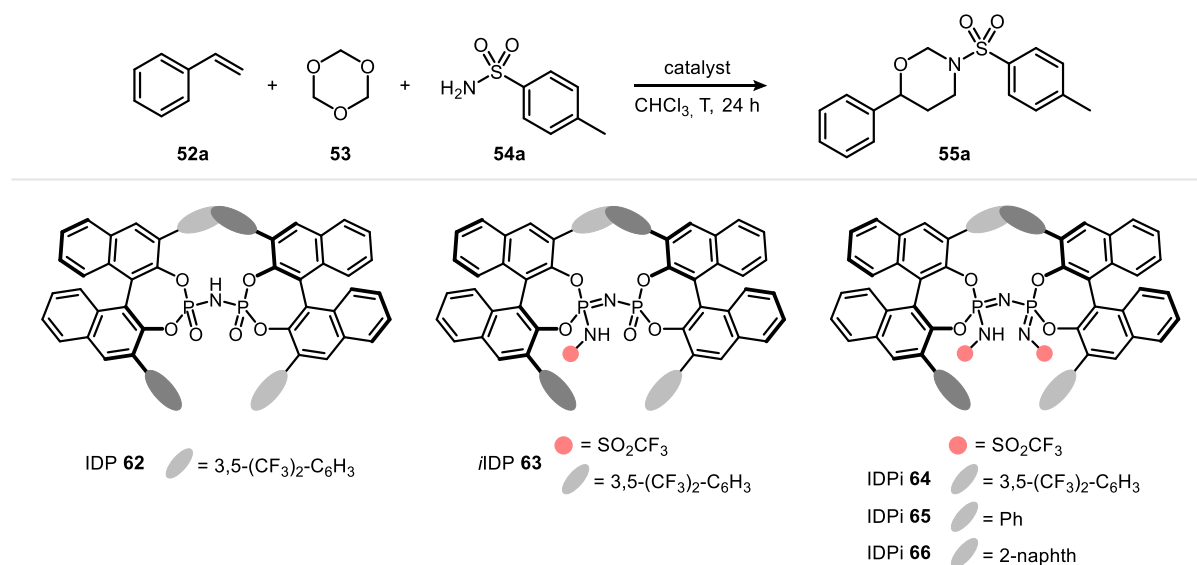
Entry	Catalyst (5.0 mol%)	Temp (°C)	Yield (%)[a]	e.r.
1	TRIP	60	0	–
2	62	60	0	–
3	63	60	0	–
4	64	rt	7	not determined
5[b]	64	60	33	51:49
6	65	rt	0	–
7[b]	65	60	8	not determined
8[b]	66	60	13	59:41

Table 5. Screening of chiral Brønsted acid catalysts. [a]All yields were determined by ^{1}H NMR spectroscopy. [b]Catalyst decomposition was detected through TLC-MS and ^{31}P NMR spectroscopy.

The moderately acidic TRIP, IDP **62**, and *i*IDP **63** catalysts failed to give any reaction product (entries 1–3). When employing the more acidic IDPi catalyst **64** at room temperature, a promising 7% of product formation could be observed (entry 4). Upon increasing the reaction temperature, the reactivity improved significantly, achieving 60% conversion and resulting in 33% yield of product **55a** and an enantiomeric ratio of 51:49. Additionally, 25% of the reaction mixture consisted of the Prins product formed between olefin and formaldehyde. However, under these conditions, catalyst decomposition was observed (entry 5). Our group has previously reported that IDPi catalysts can undergo inner core cleavage in the presence of formaldehyde, leading to catalyst deactivation (Scheme 18).[112] This process can

be further accelerated at elevated reaction temperatures. The studies suggest that the catalyst degradation could arise from the stepwise exchange of the triflyl core groups by oxygen atoms, leading to the sequential formation of the corresponding *i*IDP and IDP catalyst structures. The same study also showed that arylsulfonylimino core groups are particularly prone to cleavage under these conditions. Based on our preliminary screenings, the IDP and *i*IDP catalytic motifs lack the necessary acidity to catalyze the desired transformation. The reaction catalyzed by IDPi **65** resulted in negligible or no product formation at both room temperature and 60 ºC (entries 6–7). 2-Naphthyl-substituted IDPi **66** afforded product **55a** in 13% yield with low enantioselectivity, together with 38% of the Prins product. Catalyst decomposition was also observed in this case (entry 8).
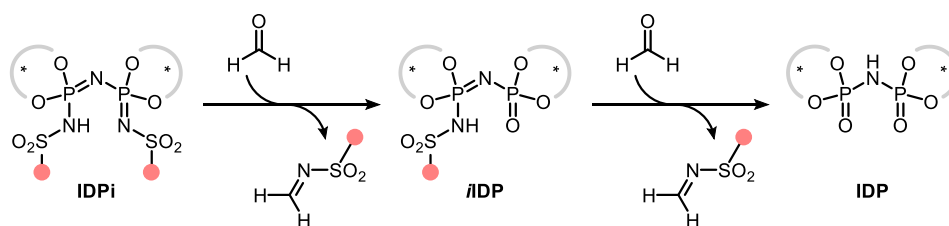

Scheme 18. Catalyst core cleavage in the presence of formaldehyde.

The key conclusions from these experiments are as follows: (a) the current reaction system necessitates a highly acidic catalyst and elevated temperatures for effective substrate activation, and (b) under IDPi catalysis, the presence of formaldehyde can lead to catalyst decomposition. These findings emphasize the need to refine our approach to mitigate these issues, as the degradation of the catalyst not only impacts the overall efficiency of the reaction but may also compromise the reproducibility and reliability of the results. Consequently, alternative methodologies that could effectively address these challenges while facilitating the asymmetric oxy-aminomethylation reaction of olefins were explored, which will be discussed in the next chapter.

4.2. Catalytic Asymmetric Cycloaddition of Olefins with In Situ Generated *N*-Boc-Formaldimine

Enantiomerically enriched 1,3-amino alcohols are essential organic compounds that have garnered significant interest in both academic and industrial research due to their versatile reactivity and wide-ranging applications. They serve as crucial building blocks in the synthesis of various biologically active molecules, including natural products, agrochemicals, and some of the world's best-selling pharmaceuticals.

In the previous chapter, we reported a method for the synthesis of 1,3-oxazinanes via the three-component reaction involving olefins, formaldehyde, and sulfonamides or carbamates. While this approach demonstrated significant potential, it also highlighted critical challenges, particularly regarding the relatively harsh deprotection conditions required for accessing the 1,3-amino alcohol functionality, the necessity of highly acidic conditions, and the risk of catalyst degradation due to the presence of formaldehyde at elevated temperatures. To tackle these challenges, we envisioned an alternative strategy that involves the use of a preformed and more reactive oxy-aminomethylating reagent that remains stable in solution and does not hydrolyze to formaldehyde. Drawing inspiration from the groundbreaking studies by Schmidt on the IEDDA reactions of *N*-acyliminium ions with alkenes,[67] as well as Hossain and Ishihara's work on the cycloaddition transformation of benzaldimines,[72-73] we envisioned that a catalytic asymmetric [4 + 2]-cycloaddition of olefins with in situ generated *N*-Boc-formaldimine could provide a valuable approach within this underexplored area (Scheme 19).
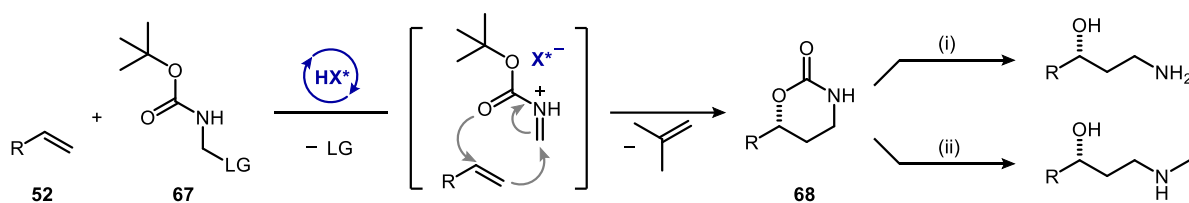
Scheme 19. Reaction design: catalytic asymmetric IEDDA reaction of olefins toward 1,3-amino alcohols. (i) KOH (2 equiv.), *i*PrOH/H$_2$O (1:1 *v/v*), reflux. (ii) LiAlH$_4$, THF, reflux.

We hypothesized that in the presence of our acidic catalysts, the electrophile **67** would be activated to produce a highly electrophilic iminium species, making it particularly susceptible to nucleophilic attack by olefins. The increased electrophilicity of such formaldiminium ions with respect to the oxy-aminomethylating reagent **61a** would permit the reaction to be carried out under lower temperatures, thus avoiding the potential catalyst decomposition. Moreover, this reaction would yield oxazinanones, which are valuable precursors for 1,3-amino alcohols and frequently function as essential structural elements in various bioactive compounds. Notable examples of bioactive compounds containing oxazinanone structures include the anti-HIV medication Efavirenz, the anticancer compound Maytansine, and the antidiabetic agent BI 135585, a selective inhibitor of 11β-HSD1.[113-116] Furthermore, it has been

established that the oxazinanone reaction products require mild deprotection conditions for the synthesis of primary or *N*-methyl amino alcohol derivatives, with no loss of enantiopurity.[117]

Building on our ongoing research into the chemical transformations of simple alkenes, our objective is to develop a highly enantioselective, Brønsted acid-catalyzed inverse-electron-demand hetero-Diels–Alder reaction of olefins with *N*-Boc-formaldimine. This approach aims to deliver a cost-effective, scalable, and straightforward method for synthesizing valuable pharmaceuticals, including (*R*)-fluoxetine, from unmodified and available olefins.

4.2.1.   Reaction Design and Optimization Studies

Our study on the catalytic asymmetric hetero-[4 + 2] cycloaddition reaction of olefins was initiated using *tert*-butyl(hydroxymethyl)carbamate (**67a**) as the *N*-Boc-formaldimine precursor in the reaction with styrene (**52a**, 20 equiv.) in the presence of various chiral Brønsted acids catalysts to afford oxazinanone **68a** (Figure 25). CPA **69**, along with the more confined IDP **62**, exhibited no conversion or only traces of product formation after 2 days at room temperature. This lack of activity can probably be attributed to their insufficient acidity, which does not adequately activate substrate **67a** for the subsequent reaction with styrene. In contrast, the more acidic DSI catalyst **70** provided product **68a** in 30% yield and moderate enantiomeric ratio. The use of a more acidic and confined *i*IDP catalyst **63** resulted
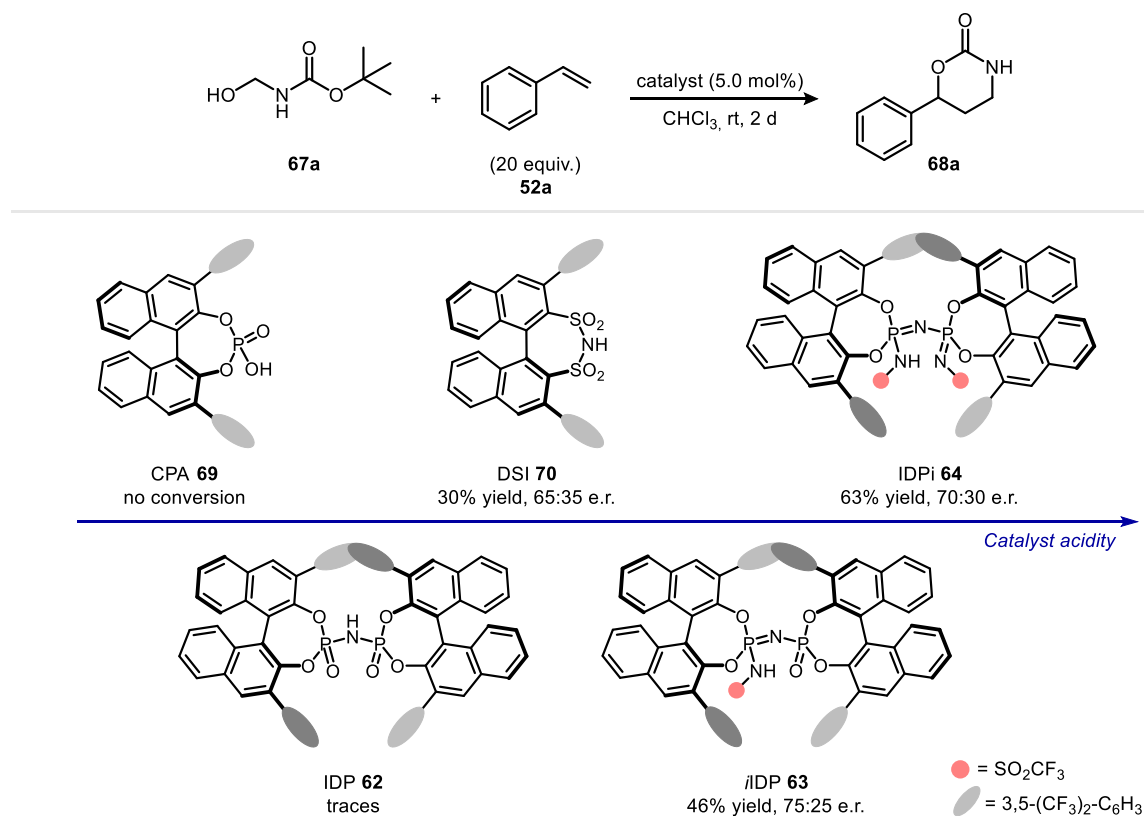

Figure 25. Initial catalyst screening for the asymmetric hetero-[4 + 2] cycloaddition reaction of styrene. All yields were determined by ^{1}H NMR spectroscopy.

in an increased reactivity and enantioselectivity. Notably, the strong and confined IDPi acid catalyst **64** provided higher yields and enantioinduction, resulting in 63% yield of product **68a** and an enantiomeric ratio of 70:30. Gratifyingly, no catalyst decomposition was observed in the reactions employing electrophile **67a**.

Next, we turned our attention into synthesizing and screening other IDPi catalysts in the transformation (Table 6). Phenyl-substituted IDPi **71a** performed better than the previously mentioned IDPi catalyst **64**, affording oxazinanone **68a** in 77% yield and 68:32 enantiomeric ratio (entries 1–2). Installation of the *p-tert*-butyl group on the 3,3'-aryl substituents of the catalyst BINOL backbone led to the formation of product **68a** in 56% yield and promising enantioselectivity (catalyst **72a**, entry 3). Excellent enantiocontrol was achieved when exchanging the IDPi triflyl core to perfluorophenylsulfonyl groups in catalyst **72b** (93:7 e.r., entry 4). We continued screening by incorporating sterically demanding substituents at the *para*-position of the catalyst's 3,3'-aryl groups. For instance, catalyst **73b** provided product **68a** in 64% yield and 72:28 enantiomeric ratio. Introducing the larger adamantyl substituent on the catalyst structure did not result in an improvement in stereoselectivity (entries 5–6). Ultimately, we decided to continue the optimization of other reaction parameters with IDPi **72b**.
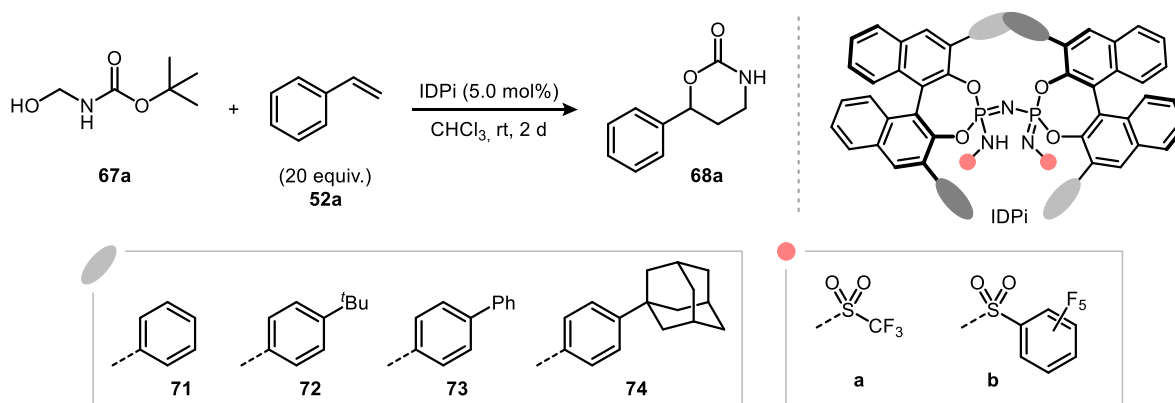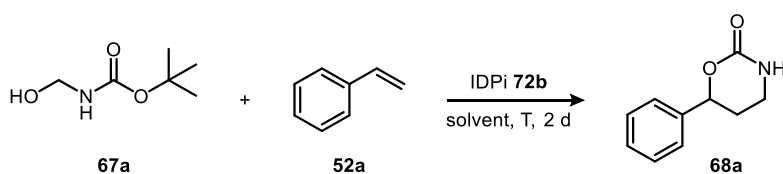

Entry	Catalyst	Yield (%)[a]	e.r.
1	**64**	63	70:30
2	**71a**	77	68:32
3	**72a**	56	82:18
4	**72b**	50	93:7
5	**73b**	64	72:28
6	**74b**	41	88:12

Table 6. IDPi catalyst screening. [a]All yields were determined by ^{1}H NMR spectroscopy.

As described in Table 7, using styrene as the limiting reagent alongside five equivalents of the electrophile led to a reduced yield and a slight drop in enantioselectivity, accompanied by the formation of a complex mixture of side products. Increasing the reaction concentration did not significantly improve the outcome (entries 1–2). Changes in the reaction solvent resulted in only slight variations in

enantioselectivity. However, the best results were achieved when the reaction was performed in chloroform or THF (entries 3–7). Screening various temperatures revealed that conducting the reaction in chloroform at –25 ºC provided high yields and excellent enantioselectivities. Decreasing the reaction temperature further resulted in diminished reactivity (entries 8–12). Importantly, reducing the amount of styrene to ten equivalents and the catalyst loading to 1.0 mol% had no adverse effect on yield or stereoselectivity (entries 13–14). Lowering the amount of styrene to five equivalents resulted in reduced yield and increased side product formation (entry 15). Nonetheless, the catalyst loading was successfully reduced to 0.5 mol% on a larger scale reaction (5.0 mmol of **67a**) without compromising the stereoselectivity, providing 0.46 g of **68a** in 62% isolated yield (entry 16). Satisfactorily, the unreacted styrene was recovered almost quantitatively (94%) by simple distillation from the crude reaction mixture, along with a 72% recovery of the IDPi catalyst (see the Experimental Section for details). Having identified these conditions, our search for the optimal reaction system for the hetero-[4 + 2] cycloaddition between **67a** and **52a** was completed.

Entry	2a equiv.	Catalyst	Solvent (conc.)	Temp (°C)	Yield (%)^a	e.r.
1^b	1	**72b** (5.0 mol%)	CHCl$_3$ (0.2 M)	rt	28	92:8
2^b	1	**72b** (5.0 mol%)	CHCl$_3$ (1.0 M)	rt	36	92:8
3	20	**72b** (5.0 mol%)	CyH (0.2 M)	rt	57	91:9
4	20	**72b** (5.0 mol%)	PhMe (0.2 M)	rt	46	93:7
5^b	20	**72b** (5.0 mol%)	Et$_2$O (0.2 M)	rt	38	91:9
6	20	**72b** (5.0 mol%)	DCM (0.2 M)	rt	42	92:8
7^b	20	**72b** (5.0 mol%)	THF (0.2 M)	rt	53	93:7
8^b	20	**72b** (5.0 mol%)	CHCl$_3$ (0.3 M)	10	62	93:7
9	20	**72b** (5.0 mol%)	CHCl$_3$ (0.3 M)	0	28	92.5:7.5
10	20	**72b** (5.0 mol%)	CHCl$_3$ (0.3 M)	–25	72	97:3
11	20	**72b** (5.0 mol%)	CHCl$_3$ (0.3 M)	–40	58	97:3
12	20	**72b** (5.0 mol%)	CHCl$_3$ (0.3 M)	–60	13	97:3
13	10	**72b** (5.0 mol%)	CHCl$_3$ (0.3 M)	–25	75	97:3
14	10	**72b** (1.0 mol%)	CHCl$_3$ (0.3 M)	–25	73	97:3
15	5	**72b** (5.0 mol%)	CHCl$_3$ (0.3 M)	–25	51	97:3
16	10	**72b** (0.5 mol%)	CHCl$_3$ (0.3 M)	–25	63	97:3

Table 7. IDPi catalyst screening. ^{a}All yields were determined by ^{1}H NMR spectroscopy. ^{b}Using 5 equiv. of **67a**.

After establishing the optimal catalyst and reaction conditions, we directed our attention to identifying the side products generated during the reaction. Although full conversion of the *N*-Boc-formaldimine precursor **67a** is achieved, the yields are not quantitative, raising important questions about the nature of these by- and side products.

Careful reaction monitoring by ^{1}H NMR spectroscopy revealed the expected formation of isobutene (**75**) together with several side products, including *tert*-butanol (**76**), isobutene cycloadduct **77**, and dimeric electrophile **78** (Scheme 20). The observation of compounds **77** and **78** suggests the occurrence of competing off-pathway side reactions, which could explain the need for an excess of olefin **52a** to achieve high yields in the desired transformation. It is plausible to hypothesize that the rapid conversion of a short-lived and highly reactive iminium ion intermediate **V** is responsible for the formation of side products **77** and **78**, thus leading to reduced yields. Isobutene is also a suitable olefin substrate in this transformation and competes with styrene for reaction with the electrophile. Crucially, elevating the concentration of styrene enhances its likelihood of reacting with the electrophile, thereby minimizing the formation of side products.
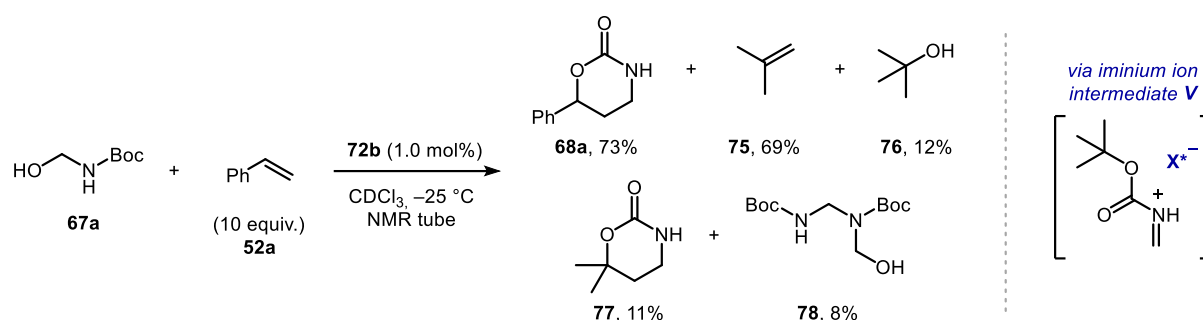
Scheme 20. Identification of products formed in the reaction.

We then considered the use of other carbamates as substrates for the asymmetric hetero-[4 + 2] cycloaddition (Figure 26). Firstly, we synthetized isopropyl(hydroxymethyl)carbamate (**79**) and ethyl(hydroxymethyl)carbamate (**80**). We anticipated that if these electrophiles engage in the reaction, the expected elimination byproducts after the cycloaddition would be propene and ethene, respectively, which are less nucleophilic than isobutene and therefore would result in a minimization of side products. Nevertheless, these substrates did not exhibit reactivity in the desired transformation; only oligomerization of the starting material was observed. Attempts to use alternative carbamate protecting groups, such as Fmoc- or Cbz-groups (**81** and **82**, respectively), resulted in no product formation.

We further investigated the use of different leaving groups on the *N*-Boc-formaldimine precursor to assess their impact on reactivity enhancement (Figure 26). Exemplarily, we synthesized electrophiles bearing an acetate leaving group and various alkoxy leaving groups (**67b–e**). The modified electrophiles led to the formation of desired product **68a** in low to moderate yields, which were diminished compared to those obtained with the original electrophile. Nevertheless, the enantiomeric ratios remained

consistent with those previously observed with electrophile **67a**, suggesting the involvement of a common iminium ion intermediate **V** in the [4 + 2]-cycloaddition. Ultimately, we chose to proceed with our investigations using *tert*-butyl(hydroxymethyl)carbamate (**67a**) as *N*-Boc-formaldimine precursor in the asymmetric cycloaddition reaction.
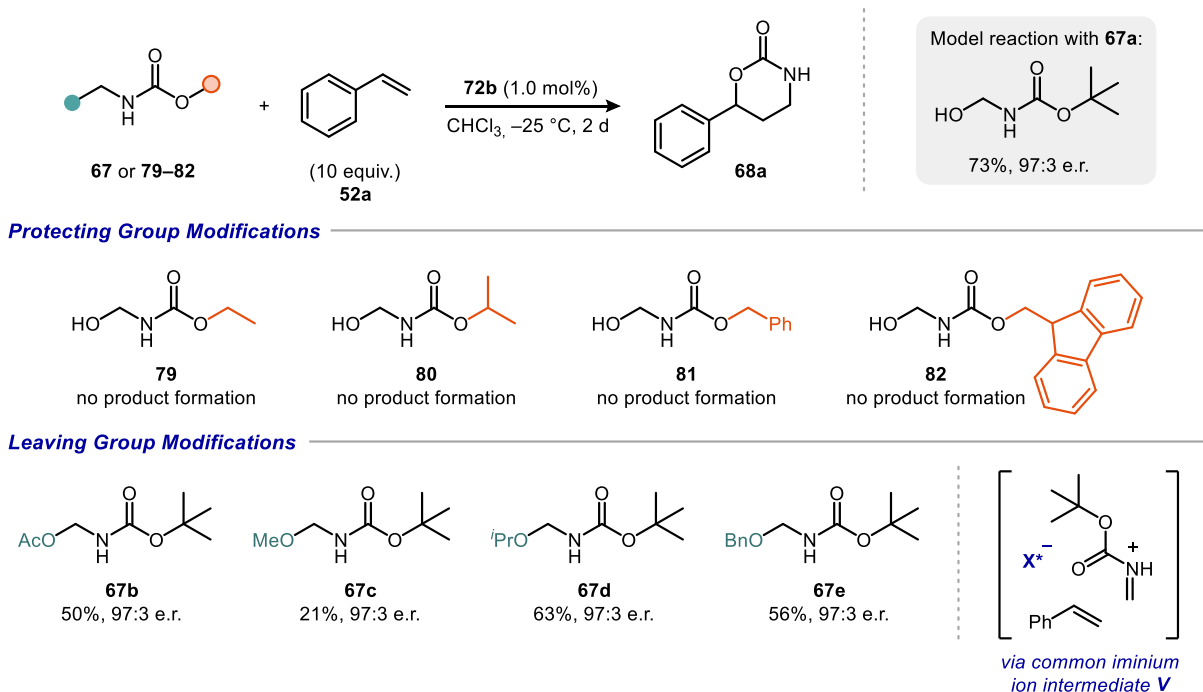

Figure 26. Modifications on the electrophile for the hetero-[4 + 2] cycloaddition.

4.2.2. Reaction Scope

The scope of the reaction was subsequently explored under the optimized conditions, evaluating a diverse array of styrene derivatives with varying electronic properties and substituents at different positions on the aromatic ring (Figure 27). Terminal styrenes with weakly electron-withdrawing groups (CH₂Cl, F, Cl, Br), could be transformed to the corresponding 1,3-oxazinan-2-ones **68b–e** with moderate to good yields and up to 99:1 enantiomeric ratios. In general, aryl olefins bearing weakly electron-donating groups on the aromatic ring, like to *p*-alkyl- or *p*-acetoxy-substituted olefins, demonstrated high reactivity; however, these reactions exhibited lower enantioselectivity compared to the parent styrene. The use of these substrates required reoptimization of both solvent and temperature to achieve excellent enantioselectivities (**68f–h**). The presence of the strongly activating methoxy group in the *para*-position resulted in high yields of 1,3-oxazinan-2-one **68i**, although with lower enantioinduction.

Additionally, styrenes with *meta*- or *ortho*-substituents were also suitable substrates, providing products **68j–m** in good yields and excellent enantiocontrol. For example, the substrate with a strong electron-donating methoxy group demonstrated good reactivity and high enantioselectivities when located in the *meta*-position (**68j**). This behavior can be attributed to the fact that, in this substitution

pattern, the resonance effect does not stabilize the benzylic cationic species, allowing the inductive effect to dominate. Naphthalene-derived olefin also proved to be a suitable substrate, yielding product **68n** in 54% yield and 97:3 ratio. Markedly, 1,4-divinylbenzene afforded the mono-functionalized product **68o** in 42% yield with an enantiomeric ratio of 95.5:4.5. From the preliminary testing of these substrates, two main trends can be identified: (a) the presence of electron-withdrawing groups results in decreased reactivity while simultaneously enhancing the enantioinduction process, and (b) the presence of strong electron-donating groups in the *para*-position leads to over-reactivity, which hinders enantioinduction.
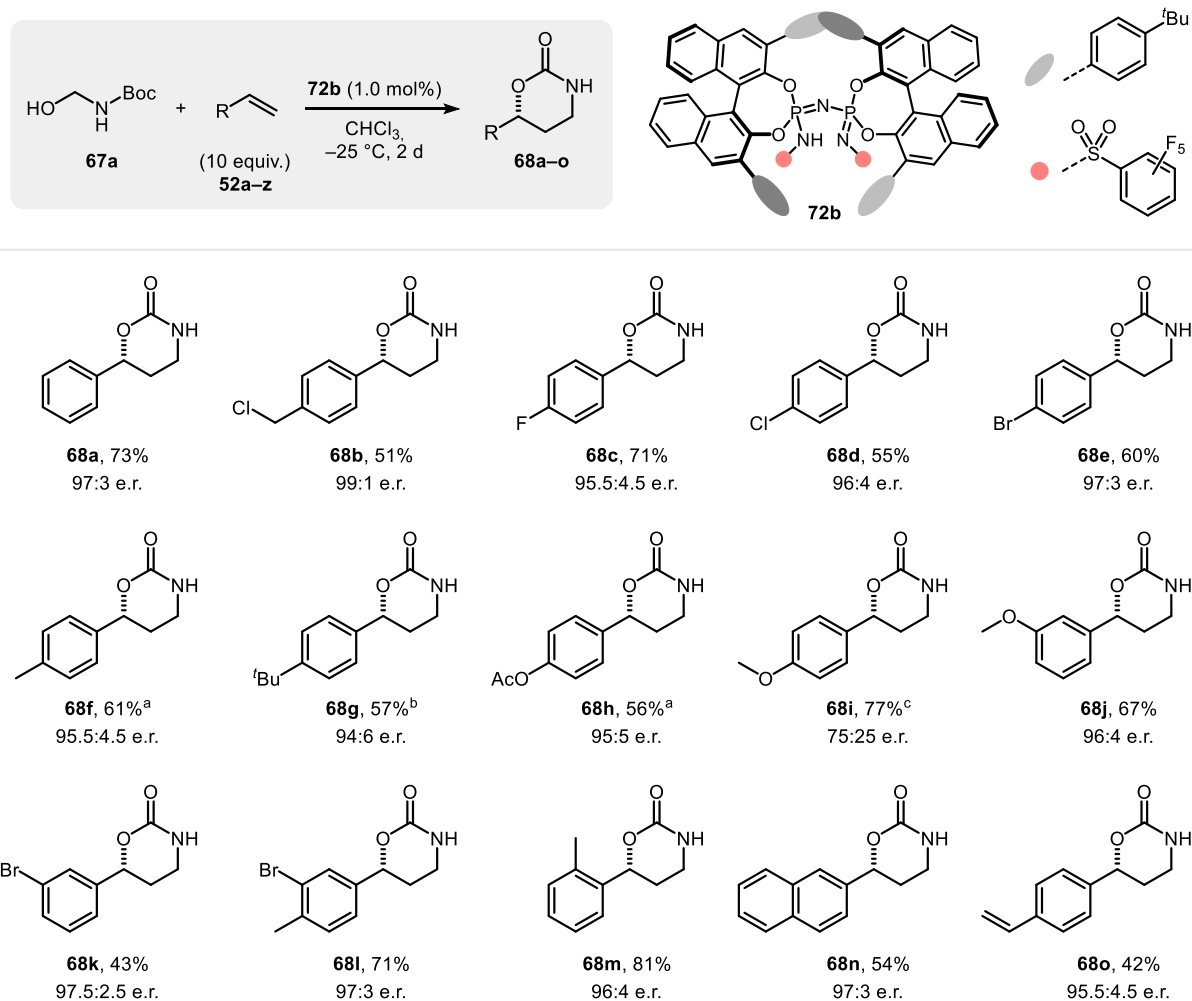
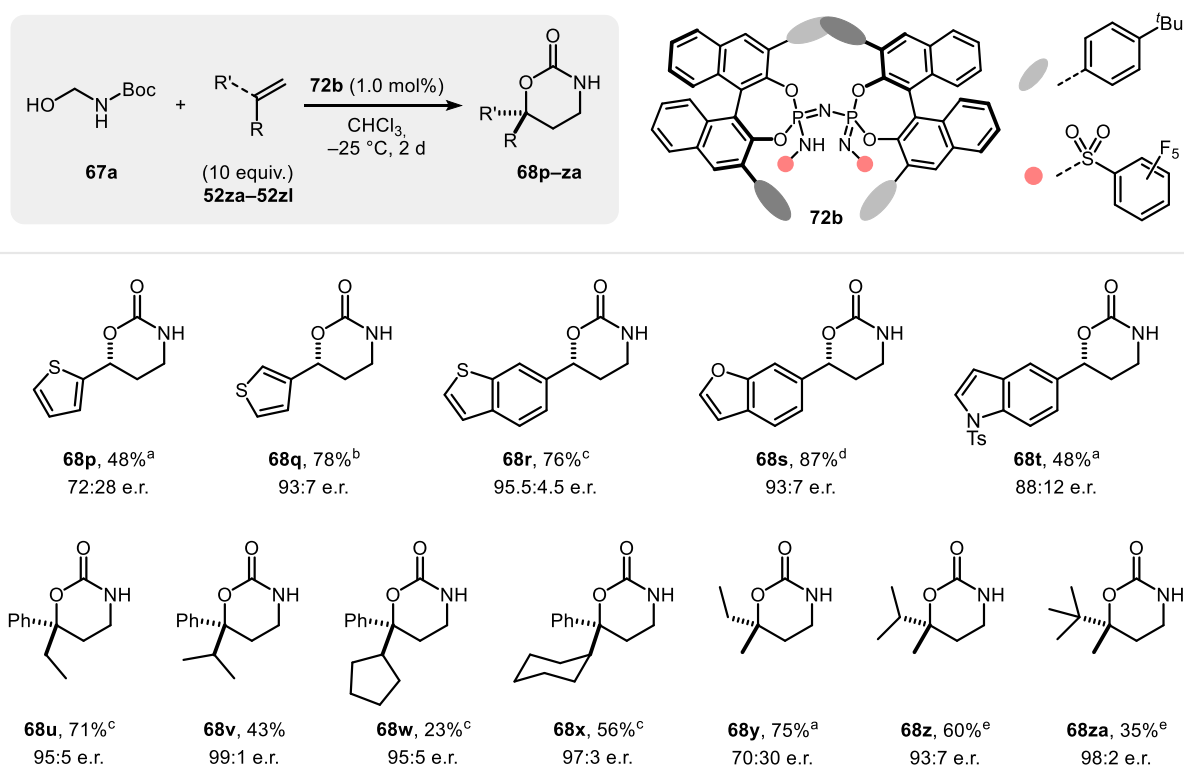Figure 27. Aryl olefin scope in the hetero-[4 + 2] cycloaddition. Isolated yields after chromatographic purification. [a]Reaction in $Et_2O/CHCl_3$ (3:1 *v/v*) at −30 °C. [b]Reaction in $Et_2O/CHCl_3$ (3:1 *v/v*) at −40 °C. [c]Yield determined by ^{1}H NMR spectroscopy.

Remarkably, the methodology was applicable to heteroaryl olefins (Figure 28). The use of the highly activated substrate 2-vinylthiophene yielded product **68p** in 48% yield with only moderate enantioselectivity, along with a complex mixture of side products. In contrast, 3-vinylthiophene afforded product **68q** in excellent yield with a 93:7 enantiomeric ratio. In addition, benzofuran-, benzothiophene-, and *N*-tosyl indole-derived olefins provided the respective cycloadducts in moderate to good yields and high enantioselectivities (**68r–t**). Furthermore, catalyst **72b** was also effective in reactions

involving α-alkyl-substituted styrenes, leading to the formation of products containing a tertiary carbamate. These reactions proceeded with reasonable to good yields and high enantiomeric ratios for products **68u–x**. After establishing a scope of amenable aromatic olefins, we subsequently turned our attention to purely aliphatic α,α-dialkyl olefins. The superior enantioinduction of the IDPi catalyst **72b** was demonstrated by affording products **68z** and **68za** in moderate to good yields and exceptional enantioselectivities. The small olefin 2-methyl-1-butene demonstrated promising reactivity and enantioselectivity under standard reaction conditions (**68x**). It is noteworthy that the excess unreacted olefin could be recovered through column chromatography in all examples of the substrate scope. Optimization of the methodology using alternative catalysts for substrates with lower enantiomeric ratios is currently ongoing in our laboratory.

Figure 28. Heteroaryl and α-substituted olefin scope in the hetero-[4 + 2] cycloaddition. Isolated yields after chromatographic purification. [a]Yield determined by ^{1}H NMR spectroscopy. [b]Reaction in MTBE at –25 °C. [c]Reaction in Et$_2$O/CHCl$_3$ (3:1 v/v) at –30 °C. [d]Reaction in Et$_2$O/CHCl$_3$ (3:1 v/v) at –40 °C. [e]Reaction in Et$_2$O/CHCl$_3$ (3:1 v/v) at –10 °C.

4.2.3.   Current Scope Limitations

A similar trend to that observed in the previous Section 4.1.3. was noted in the asymmetric reaction system (Figure 29). As mentioned earlier, highly electron-rich styrenes, including those with *para*-methoxy substituent (**52q**) and 2-vinyl-substituted heteroaryl olefins (**52za** and **52zm**), produced complex mixtures of reaction products with poor enantioselectivity, attributable to their excessive reactivity. In

contrast, styrenes featuring strong electron-withdrawing substituents at the *para*-position, or β-substituted styrenes, exhibited very low reactivity, yielding only trace amounts of the desired product. Additionally, terminal alkyl olefins, which possess significantly reduced nucleophilicity, showed no reactivity under catalysis with **72b**.
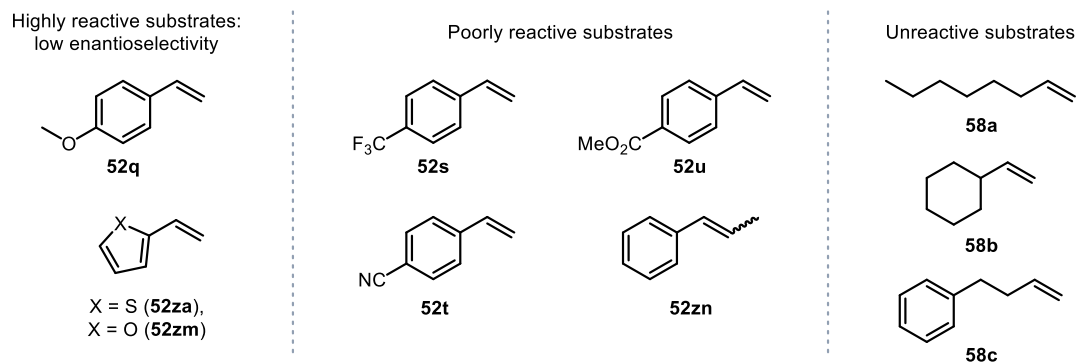

Figure 29. Current substrate limitations of the hetero-[4 + 2] cycloaddition reaction.
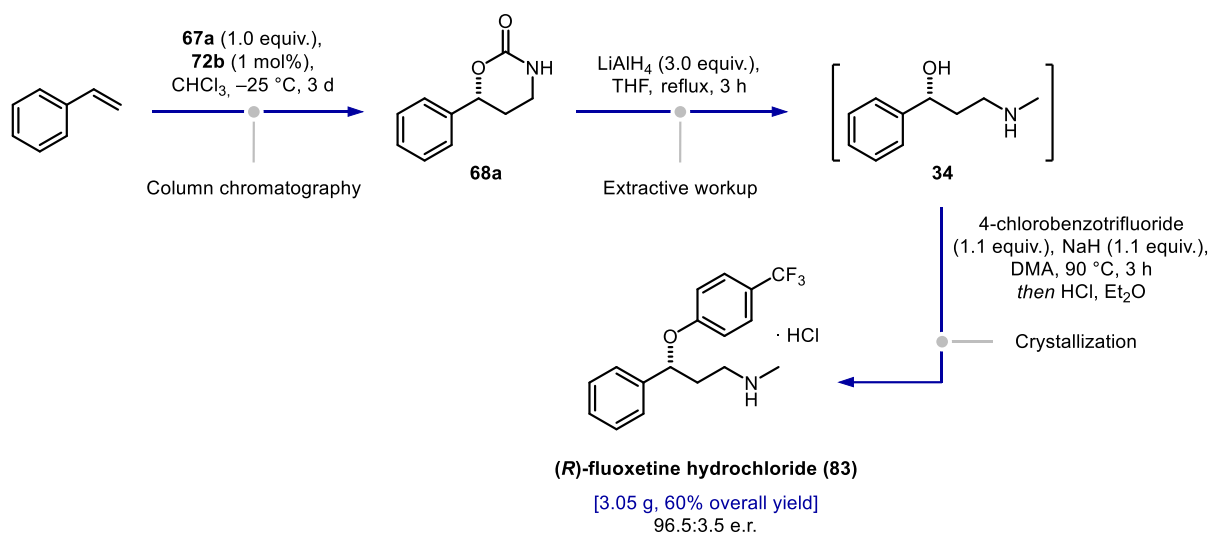
4.2.4. Three-Step Synthesis of (*R*)-Fluoxetine Hydrochloride

Depression, currently the third leading global health concern, is expected to become the second most significant health challenge worldwide by 2030.[118] Affecting 10–15% of the global population, major depression poses a substantial medical, societal, and economic burden. It is the leading cause of years lost due to disability and incurs annual costs exceeding €120 billion in Europe and over US$83 billion in North America.[119]

Selective serotonin reuptake inhibitors antidepressants are the most commonly prescribed medications for treating depression, helping to improve the quality of life for approximately 50–60% of individuals who take them. Although the precise mechanism by which SSRIs relieve depression is not fully confirmed, the most widely accepted theory involves the inhibition of serotonin reuptake in presynaptic neurons. This effect is achieved by blocking the reuptake transporter protein, increasing the availability of serotonin in the brain and ultimately contributing to mood stabilization.

Fluoxetine, commonly marketed under the brand name Prozac, is a selective serotonin reuptake inhibitor antidepressant. It is widely prescribed for the treatment of major depressive disorder, obsessive-compulsive disorder, anxiety disorders, bulimia nervosa, panic disorder, and premenstrual dysphoric disorder.[120] Currently, fluoxetine is marketed in its racemic form, even though its enantiomers are known to exhibit distinct pharmacological activities and metabolic rates.[121-123] Given its therapeutic importance and the differences in the behavior of its individual enantiomers, there has been growing interest in recent years in developing new methods to synthesize optically pure fluoxetine. As outlined in the introduction, various strategies have been explored for synthesizing the pure enantiomeric form

of this antidepressant, with most relying on the asymmetric reduction of amino ketones or chiral resolution.[83, 124]

After identifying the scope of suitable substrates, including aryl, heteroaryl, and branched α-olefins, we were keen to apply the methodology in a more practical context. To demonstrate the synthetic utility of the obtained cycloaddition products, we aimed to access the potent and selective serotonin reuptake inhibitor (R)-fluoxetine hydrochloride via a concise, multigram-scale synthesis. Our goal was to introduce a catalytic asymmetric approach starting from simple and readily available styrene, which —to the best of our knowledge— offers the shortest route to (R)-fluoxetine hydrochloride. The reaction of 2.50 g of electrophile **67a** and ten equivalents of styrene provided 2.20 g of product **68a** after chromatographic purification. As mentioned in Section 4.2.1., the catalyst and unreacted styrene can be easily recovered. Treatment of **68a** with LiAlH₄ resulted in the formation of (R)-3-(methylamino)-1-phenylpropan-1-ol (**34**), a common intermediate utilized in the synthesis of the antidepressants (R)-atomoxetine, (R)-nisoxetine, and (R)-fluoxetine. After simple extractive workup, the base-mediated nucleophilic aromatic substitution of 4-fluorobenzotrifluoride with amino alcohol **34**, followed by HCl acidification, yielded 3.05 g (96.5:3.5 e.r.) of (R)-fluoxetine hydrochloride salt (**83**), in 60% overall yield over the three-step synthesis, with only one chromatographic purification needed (Scheme 21).

Scheme 21. Synthesis of (R)-fluoxetine hydrochloride (**83**) from styrene. See the Experimental Section for detailed reaction conditions.

4.2.5. Mechanistic Studies

4.2.5.1. On the Stereospecificity: Reactions with Deuterium-Labeled Substrates

In order to deepen our understanding of the reaction system, we focused on determining whether our catalytic, enantioselective methodology proceeds through a stepwise pathway involving a benzylic carbocation, as suggested in earlier studies on the oxy-aminomethylation of styrene, or if it follows a

concerted, possibly asynchronous [4 + 2]-cycloaddition pathway between styrene and intermediate **V** (Figure 30).
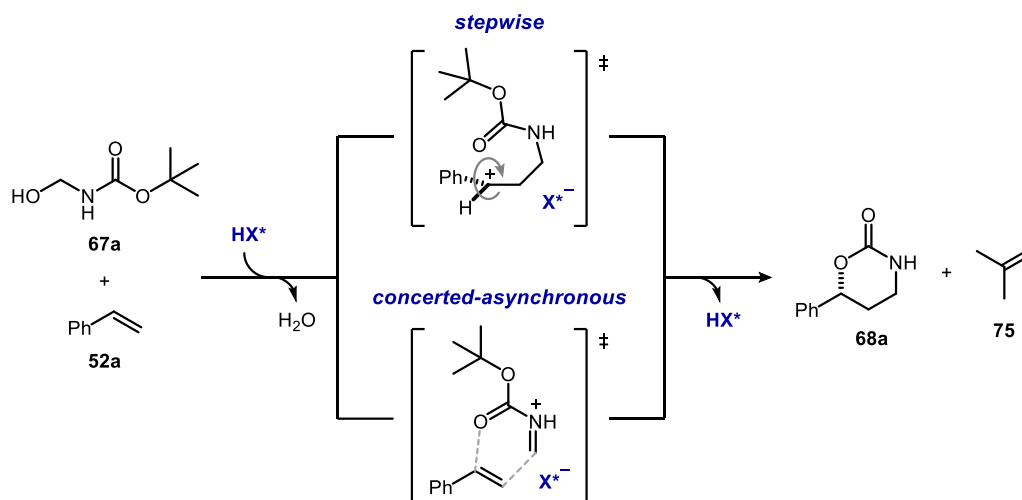

Figure 30. Possible reaction pathways of the hetero-[4 + 2] cycloaddition.

With the aim of elucidating the reaction mechanism, a series of isotope labeling and spectroscopic studies were performed. Following a procedure similar to that in the previous chapter, the stereospecific nature of the reaction was established by employing β-deuterium-labeled styrenes (*cis*-**52a-β-d₁** and
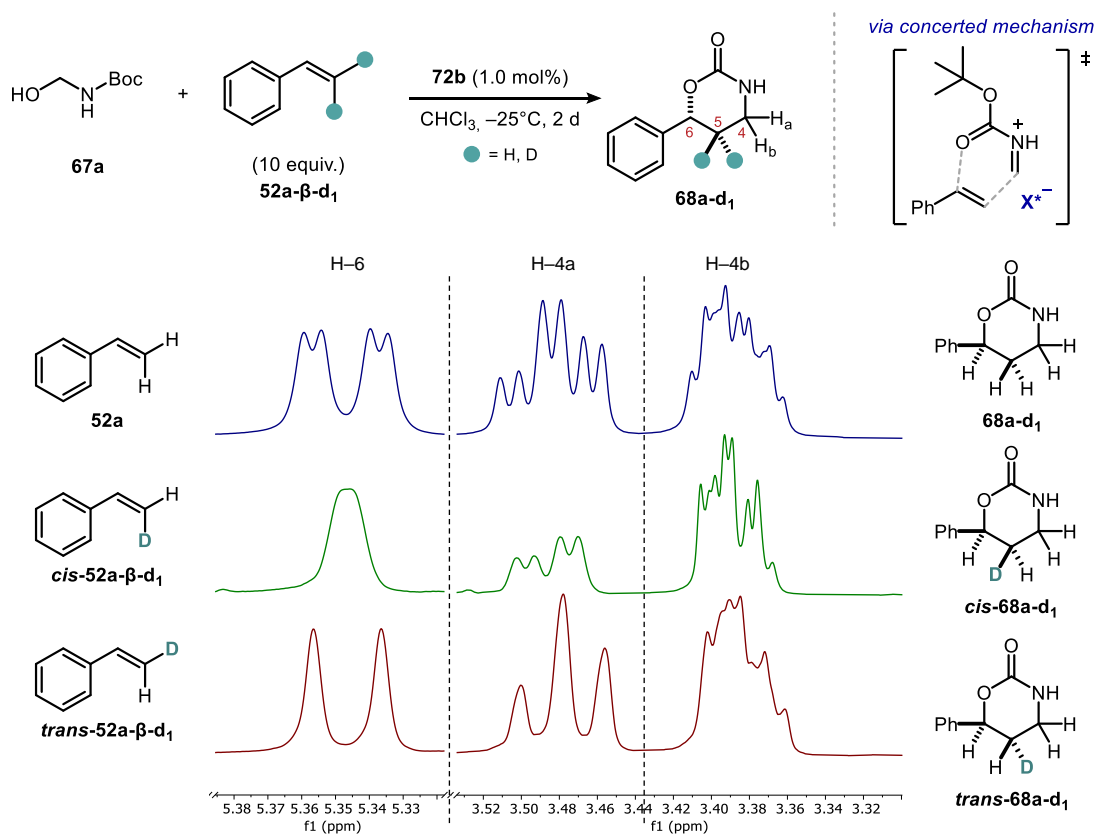

Figure 31. ^{1}H NMR analysis of [4 + 2]-cycloaddition reaction of β-deuterostyrenes (**52a-β-d₁**) under **72b** catalysis.

***trans*-52a-β-d₁**) as substrates. If a stepwise mechanism were occurring, *cis/trans* scrambling would manifest at the benzylic position of products **68a-d₁**. Examination of the ^{1}H NMR spectra of the reaction crude under optimized reaction conditions (Figure 31) revealed that the stereochemistry of the starting olefin was translated into the cycloadducts **68a-d₁**. The observed outcomes indicate that the reaction catalyzed by IDPi **72b** is likely to follow a concerted, possibly asynchronous, [4 + 2]-type cycloaddition pathway, where such benzylic freely rotating species is either not formed or, if it is formed, is rather short-lived.

4.2.5.2. ^{18}O-Labeling Reaction: Isotope Shift Effect

The work presented in this section was conducted in collaboration with Dr. M. Leutzsch.

Following our mechanistic studies on the cycloaddition reaction, we sought to determine the predominant geometry of the transition state in the proposed concerted mechanism. Specifically, we aimed to understand which oxygen atom of substrate **67a** is responsible for attacking the benzylic position during the cycloaddition.
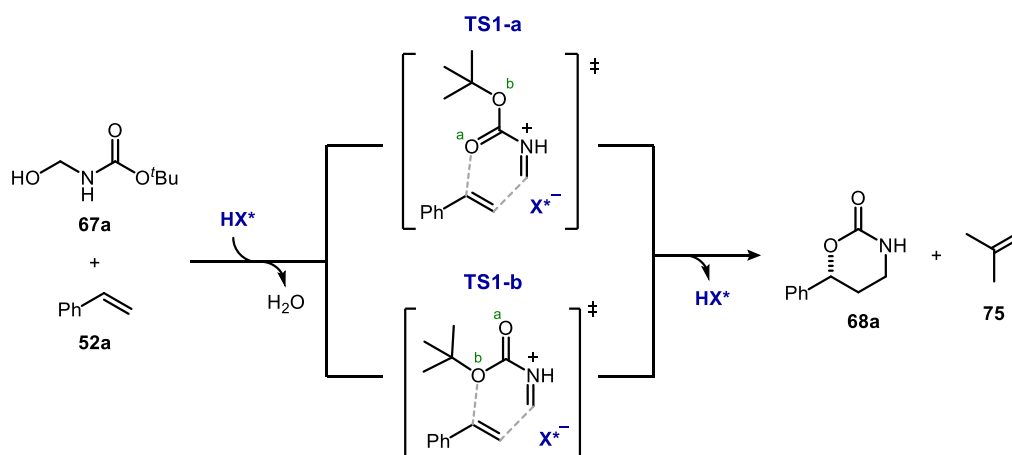
Figure 32. Possible conformations of the iminium ion **V** during the cycloaddition reaction.

As summarized in Figure 32, subsequent to the activation of the electrophile **67a**, two different transition state conformations between styrene and iminium ion **V** can be envisioned, referred to as **TS1-a** and **TS1-b**. To estimate the geometry of the transition state in the cycloaddition, selective ^{18}O-labeling of the alkoxy oxygen in substrate **67a** was undertaken, enabling differentiation between the carbonyl oxygen (O_a) and the alkoxy oxygen (O_b) without affecting the substrate's inherent reactivity.

In this way, *tert*-butyl (hydroxymethyl)carbamate-^{18}O (**67a-^{18}O**) was prepared following the synthetic route shown in Scheme 22. Firstly, ^{18}O-Labeled *tert*-butanol **84** was prepared by an S_N1 reaction between *tert*-butyl bromide with ^{18}OH$_2$ in the presence of K$_2$CO$_3$ at 60 °C.[125] After 24 hours, analysis of the reaction mixture with ^{1}H NMR spectroscopy confirmed that the reaction had achieved over 95% conversion. The mixture was dried over Na$_2$SO$_4$ to eliminate excess water, and after filtering out the

salts, compound **84** was isolated as a colorless oil. Subsequently, *tert*-butyl carbamate-[18]O (**85**) was synthesized using the carbamate preparation method developed by Kormendy and Loev.[126] The reaction was carried out by stirring *tert*-butanol-^{18}O with sodium cyanate and trifluoroacetic acid in benzene at room temperature. After a simple workup, product **85** was obtained with a 30% yield and 82.8% of ^{18}O-incorporation. The last step involved the condensation of *tert*-butyl carbamate-^{18}O with paraformalde-hyde in water, yielding **67a-[18]O** with a 22% yield and 81.7% ^{18}O-incorporation.
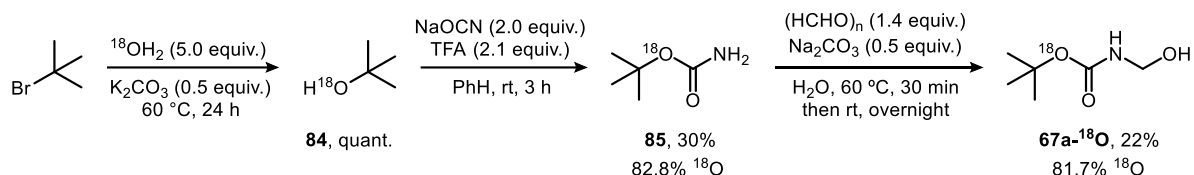
Scheme 22. Synthesis of *tert*-butyl (hydroxymethyl)carbamate-[18]O (**67a-[18]O**).

Isotopic substitution frequently causes a measurable change in the NMR chemical shift of neighboring nuclei. In the case of heavy isotopes like ^{18}O, these shifts occur due to differences in mass and bonding vibrational frequencies compared to the more common lighter isotopes, which subtly alter the electronic environment around the neighboring carbon atoms. In ^{13}C NMR, the detection of such shifts enables direct observation of the position and degree of [18]O labeling in the molecule.[127] This makes it a powerful tool for confirming isotopic incorporation, as even small changes in the ^{13}C chemical shifts can reveal the precise location of the [18]O atom within the structure, offering valuable insights into reaction mechanisms and labeling efficiency.
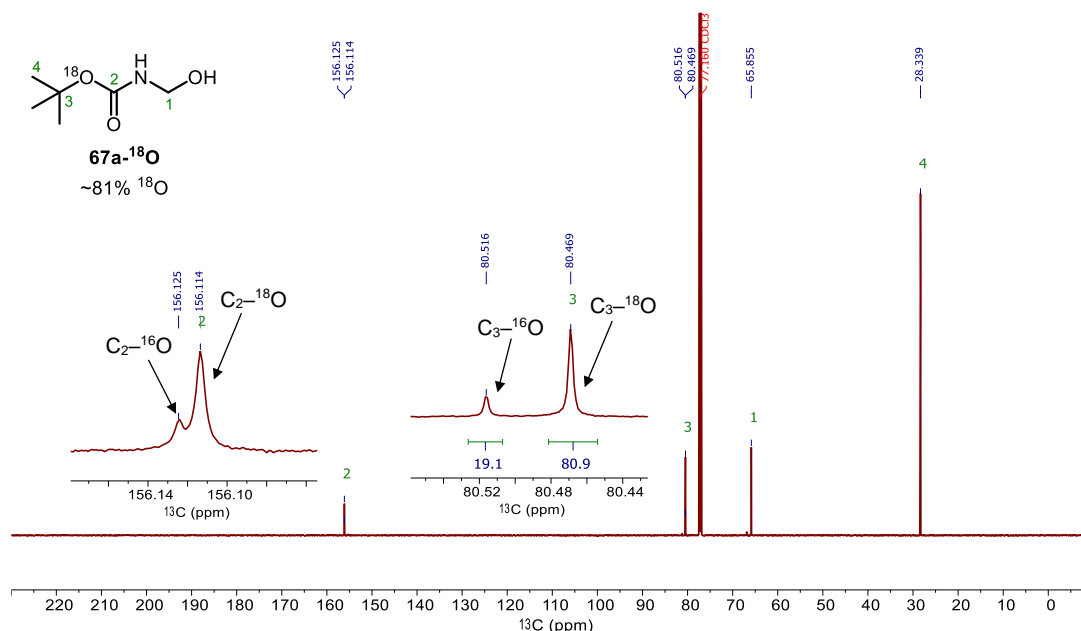
Figure 33. ^{13}C NMR analysis of substrate **67a-[18]O** at 253 K.

Figure 33 shows the ^{13}C NMR spectrum of the substrate **67a-^{18}O** at –20 °C, revealing two distinct NMR signals corresponding to the C_2 and C_3 positions. The signal exhibiting the higher chemical shift can be assigned to the ^{16}O-^{13}C isotopomer, while the lower chemical shift corresponds to the ^{18}O-^{13}C derivative, as determined by comparison with a reference sample.[II]

Subsequently, ^{18}O-enriched substrate **67a-^{18}O** was subjected to the optimized reaction conditions using IDPi **72b**, which furnished product **68a-^{18}O** in 60% yield. Analysis of ^{13}C NMR spectrum at 25 °C indicated complete incorporation of the labeled oxygen into the carbonyl C=^{18}O position of product **68a-^{18}O** (Figure 34). An isotope shift at position C_3 was not observed. The absence of oxygen isotope scrambling at positions C_3 and C_8 suggests that the nucleophilic attack of the olefin on iminium ion **V** occurs exclusively through the **TS1-a** conformation.
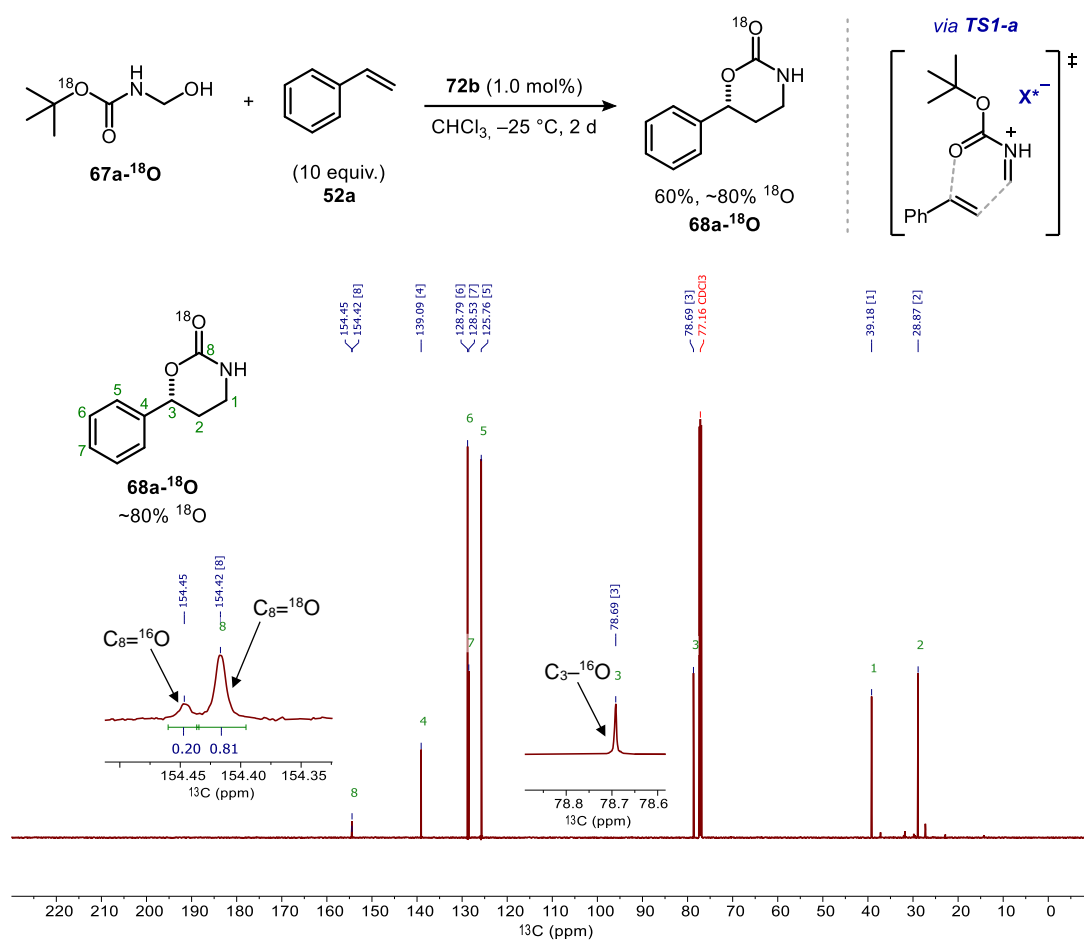
Figure 34. ^{13}C NMR analysis of product **3a-^{18}O** at 298 K.

[II] Enrichment could not be assigned at 25 °C due to line broadening caused by rotamer exchange of the ^{13}C signals of interest.

4.2.5.3. NMR Kinetic Studies

The work presented in this section was conducted in collaboration with Dr. M. Leutzsch.

During our examination of the reaction, we became increasingly intrigued by its mechanistic details, which spurred us on to investigate ways to enhance our understanding and improve the transformation. As mentioned in the previous Section 4.2.2., we initiated our investigation by conducting a ^{1}H NMR monitoring of the reaction mixture over time.
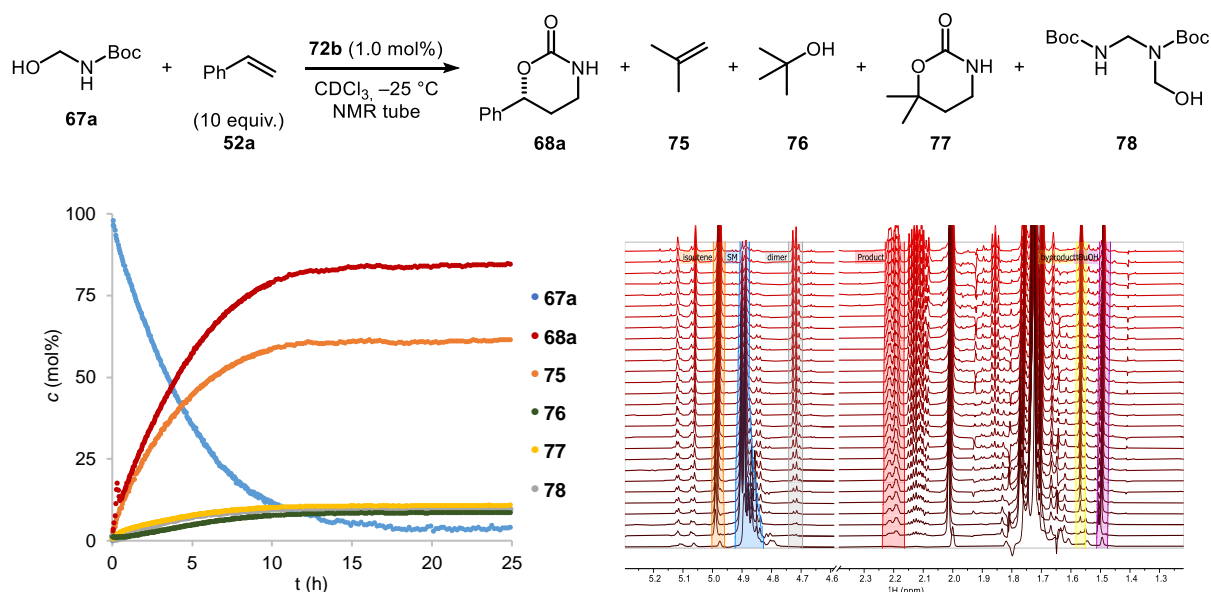
Figure 35. Left: Concentration plots obtained from ^{1}H NMR monitoring during the reaction of **67a** and styrene with 1.0 mol% of catalyst **72b** at 248 K. Right: ^{1}H NMR spectra recorded at different time points (every 30 min from t = 0).

Figure 35 presents the ^{1}H NMR spectra collected at different time intervals during the reaction at –25 °C with IDPi **75b**. The conversion rate of substrate **67a** decreases non-linearly as the reaction progresses. Additionally, the experiment confirmed the formation of isobutene (**75**), *tert*-butanol (**76**), 6,6-dimethyl-1,3-oxazinan-2-one (**77**), and the dimeric electrophile **78**.
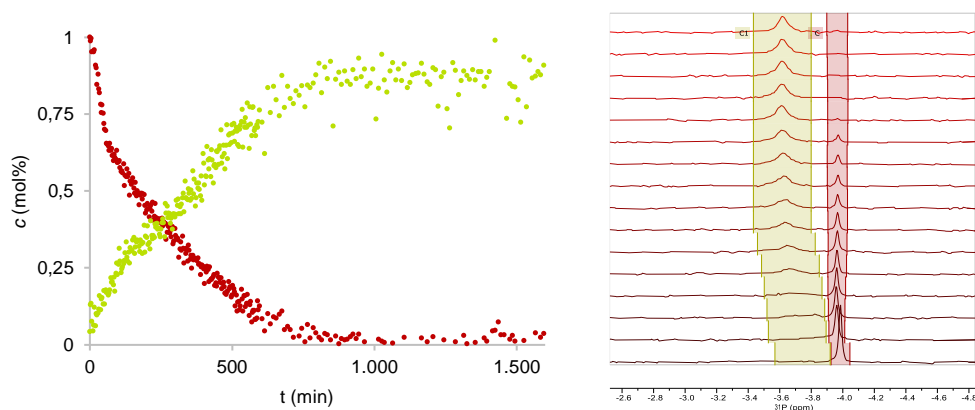
Figure 36. Left: Concentration plots obtained from the integration of the ^{31}P NMR signals during the reaction. Right: ^{31}P NMR spectra recorded at different time points (every 30 min from t = 0).

Interestingly, analysis of the ^{31}P NMR profile revealed the presence of two distinct signals, triggering us to uncover the different catalytic species present in the reaction (Figure 36). To elucidate the nature of these species, we conducted detailed NMR studies to explore the interactions between the various substrates and IDPi **72b**.

Interaction between catalyst 72b with substrate 52a

To study the nature of the different catalytic species, we first measured the ^{1}H and ^{31}P NMR of catalyst **72b** in the presence of styrene **52a** and solvent. It is worth mentioning that due to the excess of styrene present in the reaction, this reactant should also be considered as a co-solvent in the reaction system. The catalyst's ^{31}P NMR signal appears as a broad singlet at –4.1 ppm (Figure 37a).

Interaction between catalyst 72b with substrates 67a and 52a

Subsequent analysis revealed that addition of the substrate **67a** to the previous mixture shifted the ^{31}P NMR signal by approximately 0.2 ppm toward higher frequencies, together with a change on the signal shape (sharp peak at –3.9 ppm, Figure 37b).

It has been previously shown by our group that the IDPi catalyst in an ion pair can form such sharp signals due to the high symmetry in its anionic form.[128] Upon the progression of the reaction, the sharp peak decays and a second ^{31}P signal arises below and shifts toward higher frequencies upon advancement of the reaction (–3.5 ppm at the end of the reaction, Figure 37c to f). This broad peak can be assigned to the acidic form of the IDPi catalyst, which interacts weakly with other components in the reaction mixture. The chemical shift change can be attributed to changes in the composition of the reaction mixture.

Interaction between catalyst 72b with substrate 52a and reaction product 68a

In this independent experiment, the interaction between catalyst **72b** in the presence of styrene and reaction product **68a** was studied. The catalyst ^{31}P peak appears as a broad singlet at –3.4 ppm (Figure 37g). No further signal shifting was observed. This experiment allowed us to assign the broad peak appearing at –3.8 ppm, which shifted toward higher frequencies in the previous experiment, to the catalyst weakly interacting with various reaction products and side products.
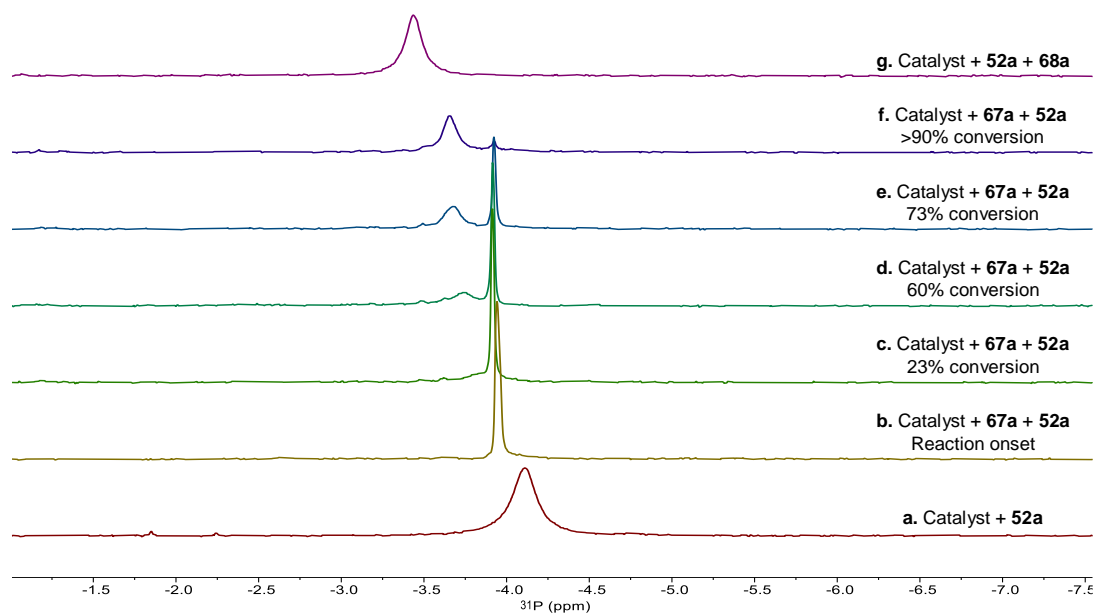
Figure 37. ^{31}P NMR catalyst **72b** signals during the course of the reaction.

Intrigued by the finding of the long-lived ionic intermediate, we carefully analyzed the ^{1}H NMR spectra in the initial minutes of the reaction. The appearance of a characteristic peak at 10.1 ppm that decayed over time led us to hypothesize the detection of an iminium ion intermediate on the NMR time scale (Figure 38). To our surprise, additional experiments with higher catalyst loadings and lower temperatures revealed the formation of ionic intermediate **VI**, which was assigned by advanced 1D and 2D NMR methods and HRMS (see the Experimental Section for details). According to the ^{1}H and ^{31}P NMR data, the continual transformation of intermediate **VI** successfully regenerated catalyst **72b** and produced the desired product **68a**.
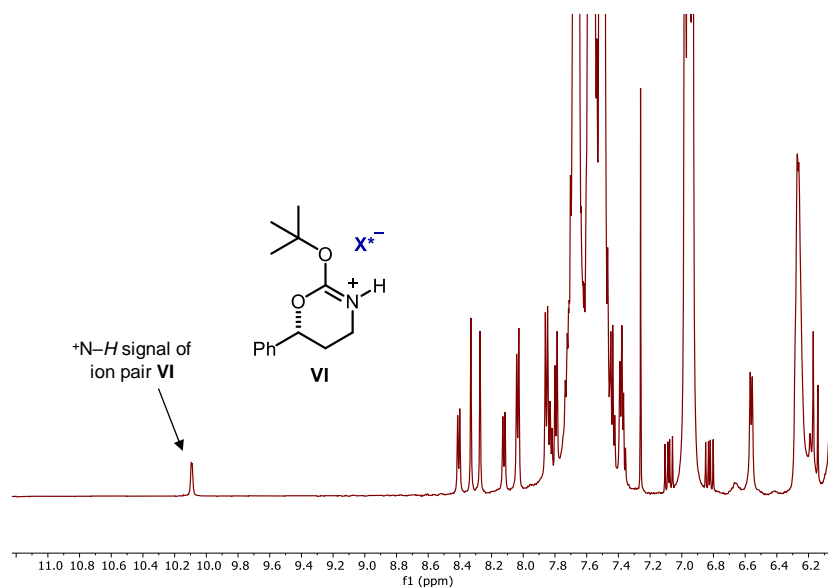
Figure 38. Identification of reaction ion pair intermediate **VI** by ^{1}H NMR at the beginning of the reaction.

No direct evidence for the formation of the iminium ion intermediate **V**, which was long-lived enough to be spectroscopically characterized by NMR, could be collected. However, it is conceivable to hypothesize that the rapid conversion of the short-lived cationic intermediate **V** leads to the formation of product **68a**. Moreover, as mentioned earlier, competing off-pathway side reactions of ion pair **V** with isobutene (**75**) or starting material **67a** would form the abovementioned side products **77** and **78**, respectively. These observations suggest that the product formation from the stable ionic intermediate **VI** via the generation of isobutene, which plausibly occurs after the stereochemical information is established, is the turnover-limiting step of the reaction.[129] The release of the catalyst from the long-lived ionic form enables the restart of the catalytic cycle.

NMR Characterization of Ion Pair VI

During the course of the reaction, a characteristic signal at 10.1 ppm was consistently observed. Initially, based on the comparable magnitude of the chemical shifts of iminium ion pairs reported by Mayr,[130] we presumed that the signal at 10.1 ppm corresponded to the $^+$N=CH_2 protons of the transient intermediate **V**. Conversely, 1D selective TOCSY spectrum obtained after selective excitation of the characteristic signal (see Experimental Section for details) was in line with the above-suggested reaction intermediate **VI**.
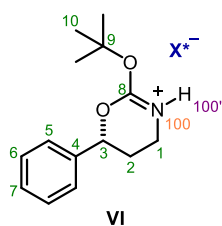
Atom	δ (ppm)	J (Hz)	COSY	HSQC	HMBC	ROESY
1 C	38.28			1', 1"		
H'	2.23		1", 100'	1		1", 100'
H"	4.34		1', 2'	1		1', 100'
2 C	27.95			2'		
H'	2.53		1", 2"	2		
H"	1.78		2', 3			
3 C	85.83			3		
H	6.18		2"	3		
4 C						
5 C						
H						
6 C						
H						
7 C						
H						
8 C						
9 C	91.55				10	
10 C	28.13			10	10	
H3	1.52			10	9, 10	100'
100 N	-273.91	94.00 (100')				
100' H	10.09	94.00 (100N)	1'			1', 1", 10

Table 8. Chemical shifts and cross peaks of intermediate **VI** at 233 K.

The connectivity to the nitrogen was further confirmed by a ^{1}H–^{15}N HMBC optimized to a $^1J_{NH}$ coupling constant of 80 Hz where a signal at –273.9 ppm was observed ($^1J_{NH} \sim 94$ Hz). The adjacent carbon chemical shifts of the assignable protons were extracted from an edited HSQC and/or HMBC measurements. The signal of H_{10} was assigned based on the relative integral from the ^{1}H NMR and the cross peaks in the ^{13}C HMBC. Table 8 shows all the chemical shifts extracted for this intermediate. Interestingly, the ^{13}C chemical shift of C_9 is rather high (91.6 ppm) for a *tert*-butyl group (e.g. δ C_q(MTBE) = 72.8 ppm) and would be in line with a slight positive charge on the carbon which renders it a good leaving group. All intermediate signals decay over time, and the ^{1}H NMR data aligns with the observation of two distinct catalytic species in the ^{31}P NMR during the reaction.

Formation of *tert*-Butanol

In another aspect, as summarized in Figure 39, four different pathways for the formation of *tert*-butanol are conceivable: through H_2O attacking on C_8 of intermediate **VI**, H_2O attacking C_9 of the same intermediate, or via H_2O attack to *tert*-butyl cation (which is formed through different routes). Subsequently, the viability of these options will be discussed.
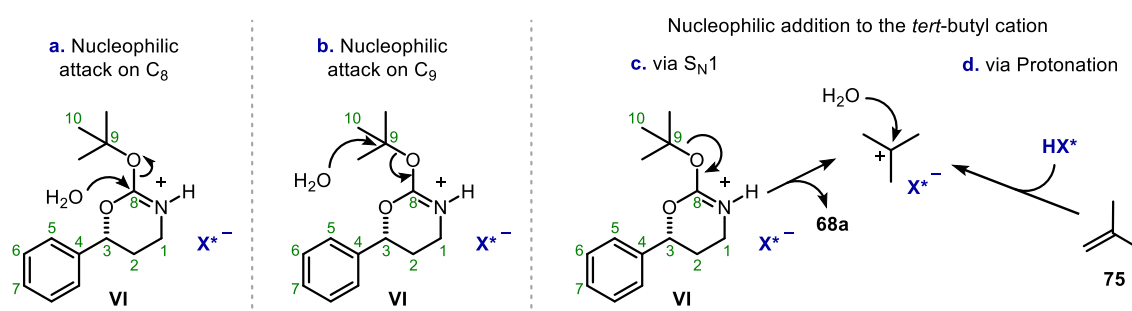
Figure 39. Potential pathways for the formation of *tert*-butanol (**76**).

Since an isotopic scrambling was not observed at position C_8 of intermediate **VI** in the previous experiment with ^{18}O-labeled substrate (see Section 4.2.5.2), the first option a. can be disregarded.

Option b. would involve the S_N2'-like reaction of water with intermediate **VI**, to yield product **68a**. The ^{13}C NMR chemical shift of C_9 is notably deshielded for a typical *tert*-butyl group (see Table 8 for further details), suggesting a partial positive charge on the quaternary carbon, thereby enhancing its leaving group capability.

Options c. and d. entail the nucleophilic addition over the *tert*-butyl cation previously formed upon cleavage of the reaction product from ion pair **VI** (c.), or via protonation of isobutene by the IDPi catalyst (d.). The latter option d. also seems not viable: ^{1}H NMR monitoring reveals no *tert*-butanol formation upon completion of the reaction. As shown in the previous Figure 35, *tert*-butanol production reaches a plateau after the starting material **67a** is consumed (t = 13 h) whilst isobutene, water, and catalyst are still present in the solution.

In conclusion, options b. and c. appear to be the most feasible under the reaction conditions, and their implications will be discussed in the following sections.

Catalyst Order Determination

Keen to understand the role of the catalyst, the reaction order of IDPi **72b** was investigated using variable time normalization analysis (VTNA) developed by Burés.[131] This analysis method uses a variable normalization of the time scale to enable the visual comparison of entire concentration reaction profiles. As a result, the order in catalyst can be determined with a few experiments using a simple mathematical data treatment. We followed the concentration profile of the consumption of **67a** and the formation of **68a** at –25 °C, varying the concentrations of IDPi **72b** (0.52 mol%, 1.1 mol%, 2.0 mol%, and 3.5 mol%). The catalyst concentration was extracted as an average from the ^{1}H NMR data over the entire reaction time. Figure 40 shows an overview of different reaction profiles with time scales normalized to different catalyst orders. Surprisingly, the best overlap was found when the reaction profiles were normalized to a 1.4 order dependence in catalyst concentration.
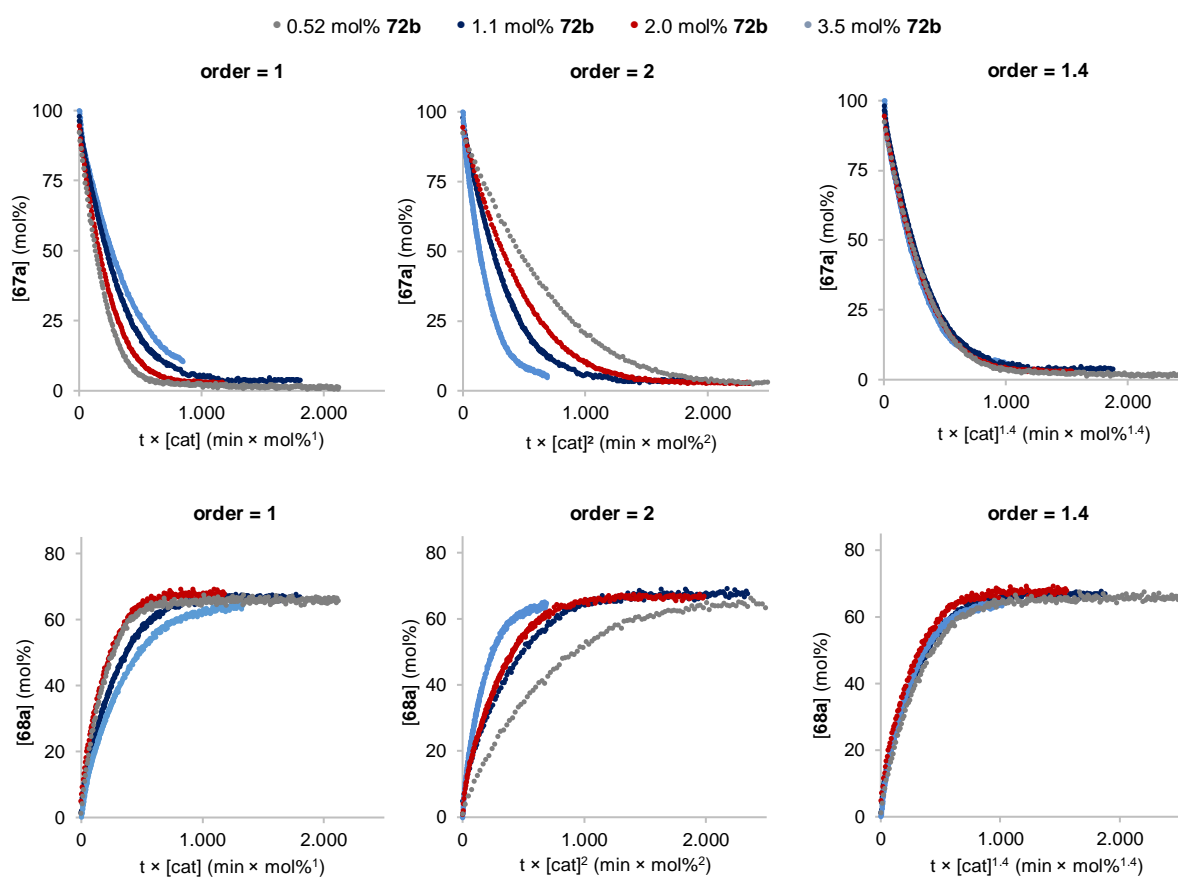
Figure 40. ^{1}H NMR concentrations profiles of **67a** (first row) and **68a** (2nd row), in CDCl$_3$ at 248 K in the presence of 0.52 mol%, 1.1 mol%, 2.0 mol%, and 3.5 mol% of **72b**, with time scales normalized to a 1st (left), 2nd (middle), and 1.4th (right) order in catalyst concentration.

The following Figure 41 shows concentration profiles of intermediate **VI** in the presence of different amounts of catalyst **72b**. At high catalyst concentrations, the intermediate decays rather quickly, whereas at low concentrations a steady state concentration seems reached. Additionally, two decay regimes seem to be present for higher catalyst concentrations.
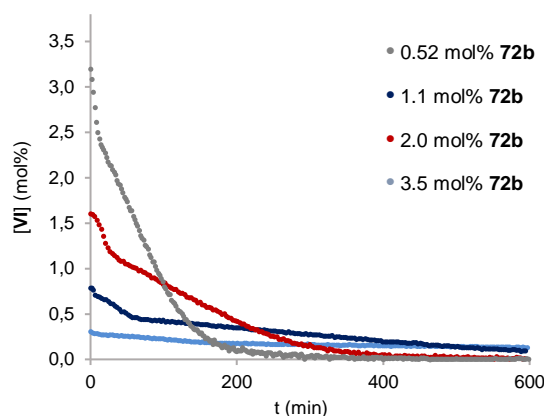
Figure 41. Concentration plots obtained from ^{1}H NMR reaction monitoring of intermediate **VI** in the presence of 0.52 mol%, 1.1 mol%, 2.0 mol%, and 3.5 mol% of IDPi **72b** during the course of the reaction.

This unexpected result led us to hypothesize that due to the high stability of the ionic intermediate **VI**, a second catalyst molecule could facilitate the isobutene elimination in the rate-limiting step and restore the catalytic cycle. Building on previous findings of a catalyst order greater than one, we hypothesized that the involvement of multiple catalyst molecules in the enantiodetermining step of the reaction could lead to nonlinear effects (NLE). To verify this hypothesis, NLE experiments were set up according to the general procedure using scalemic mixtures of catalyst **72b**. Subsequently, the resulting enantiomeric excess of the product was measured.

Nonlinear Effects Studies

As depicted in Figure 42, the enantioselectivity of product **68a** was found to exhibit a linear relationship with the enantiopurity of the catalyst used in the reaction, thereby ruling out the presence of NLE. This result is consistent with only a single catalyst molecule involved in the enantiodetermining step of the reaction. However, it does not exclude the possibility of multiple catalyst molecules being involved in other turnover-limiting steps. Based on this observation and the previous experiments, we can hypothesize that a second catalyst molecule could assist in the isobutene elimination of intermediate **VI**. Since this step occurs subsequent to the enantiodetermining step, the presence of more than one catalyst does not affect the enantiomeric excess of the product.
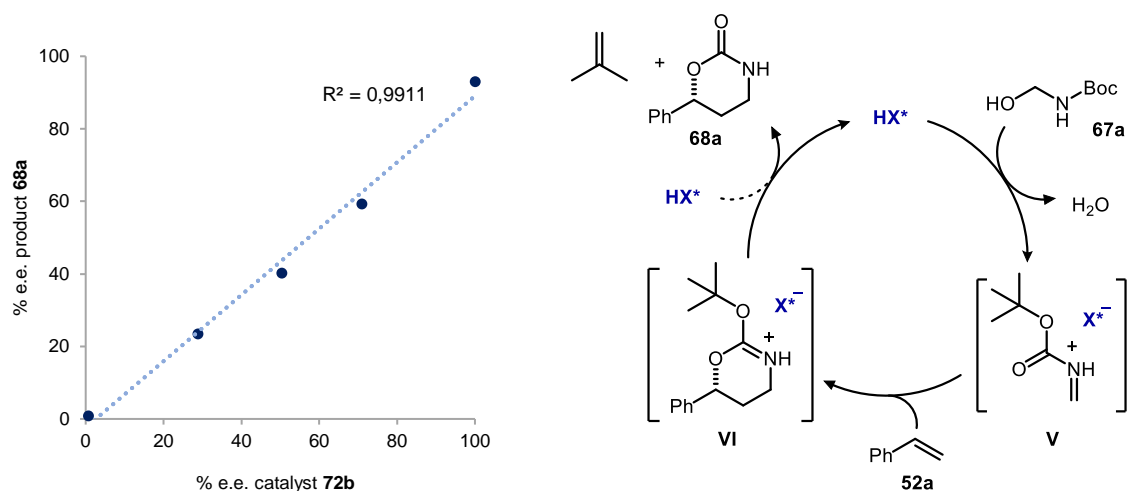
Figure 42. Left: plot of % e.e. of the product **68a** versus % e.e. of catalyst **72b**. Right: plausible catalytic cycle involving multiple catalyst molecules.

Experiments with Racemic Catalyst

To further explore the unexpected findings of our study, we analyzed the reaction rates of both racemic and enantiopure catalysts under identical conditions. As illustrated in Figure 43, we observed an intriguing kinetic trend: the racemic form of the catalyst demonstrated significantly higher reaction rates compared to its enantiopure counterparts, with the reaction using *rac*-**72b** showing a rate enhancement by a factor of 1.4. This suggests that the presence of heterochiral catalyst mixtures can lead to a faster decay of the reaction intermediate **VI**, thereby accelerating the overall reaction. The result is therefore consistent with the hypothesis positing the presence of more than one catalyst molecule assisting in the intermediate **VI** consumption step.
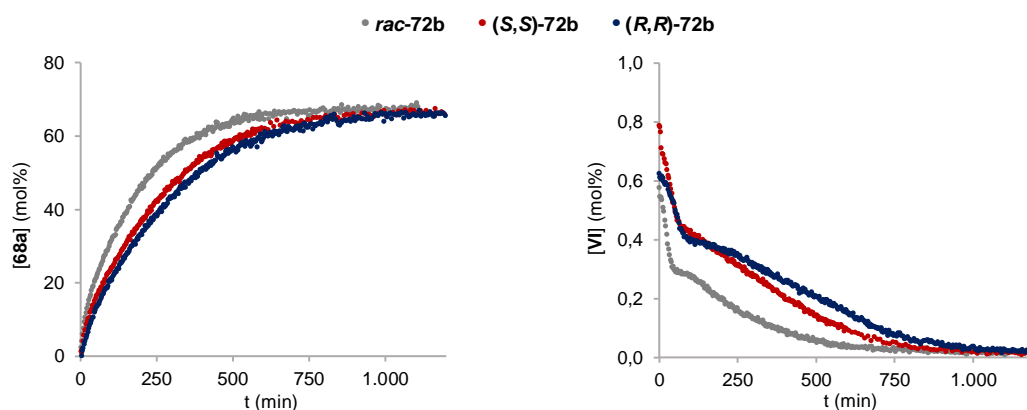
Figure 43. Concentration plots obtained from ^{1}H NMR reaction monitoring of **68a** (left) and **VI** (right) when 1.0 mol% of racemic IDPi *rac*-**72b** is used (grey); reaction with 1.0 mol% of (*S,S*)-**72b** (red); reaction with 1.0 mol% of (*R,R*)-**72b** (blue).

The reaction order with respect to the racemic catalyst was further assessed using VTNA. The consumption of **67a** was monitored at four different concentrations of *rac*-**72b** (0.48 mol%, 1.0 mol%, and 2.1 mol%). The average catalyst concentration was derived from the ^{1}H NMR data collected over

the entire reaction period. Figure 44 provides an overview of the various reaction profiles, with time scales normalized to different orders of catalyst dependence. Notably, the best overlap of the profiles was observed when normalized to a 1.5 order dependence on catalyst concentration.
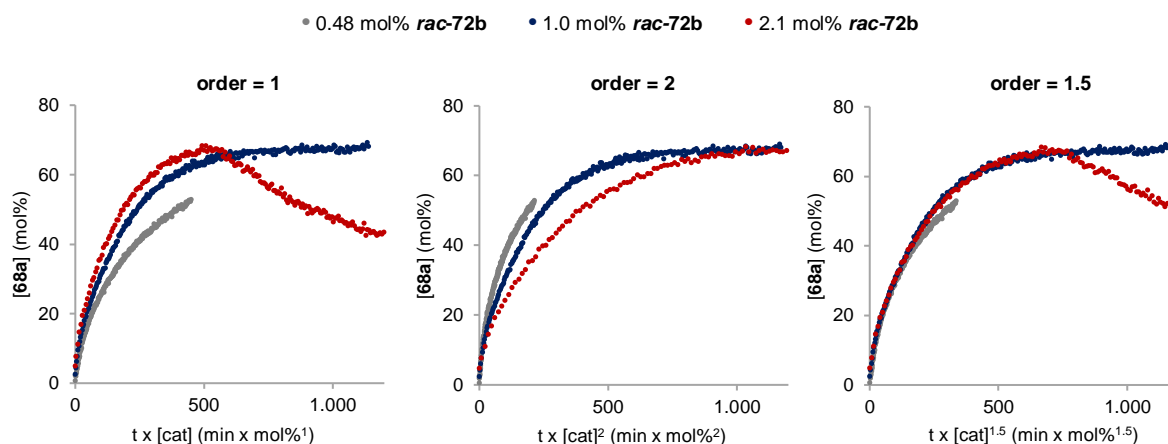
Figure 44. ^{1}H NMR concentrations profiles in CDCl$_3$ at 248 K in the presence of 0.48 mol%, 1.0 mol%, and 2.1 mol% *rac*-72b of 68a with time scales normalized to a 1st (left), 2nd (middle), and 1.5th (right) order in catalyst concentration.

Inhibition Experiments and Contribution of Water to the Reaction

Another plausible explanation for the observed catalyst order higher than one is that a water molecule would attack the electrophilic *tert*-butyl group of intermediate VI in a parallel reaction pathway (as depicted in Figure 39), leading to the formation of *tert*-butanol and 68a. A situation where a byproduct from one step in the cycle serves as a reactant in a subsequent catalytic step has been discussed by Burés in recent years and can result in catalysts orders higher than one, although only one catalyst molecule is involved in the rate-limiting step.[132] As two different byproducts (isobutene and *tert*-butanol) are formed, a scenario where a catalyst order between one and two is observed is therefore not unreasonable (Figure 45).
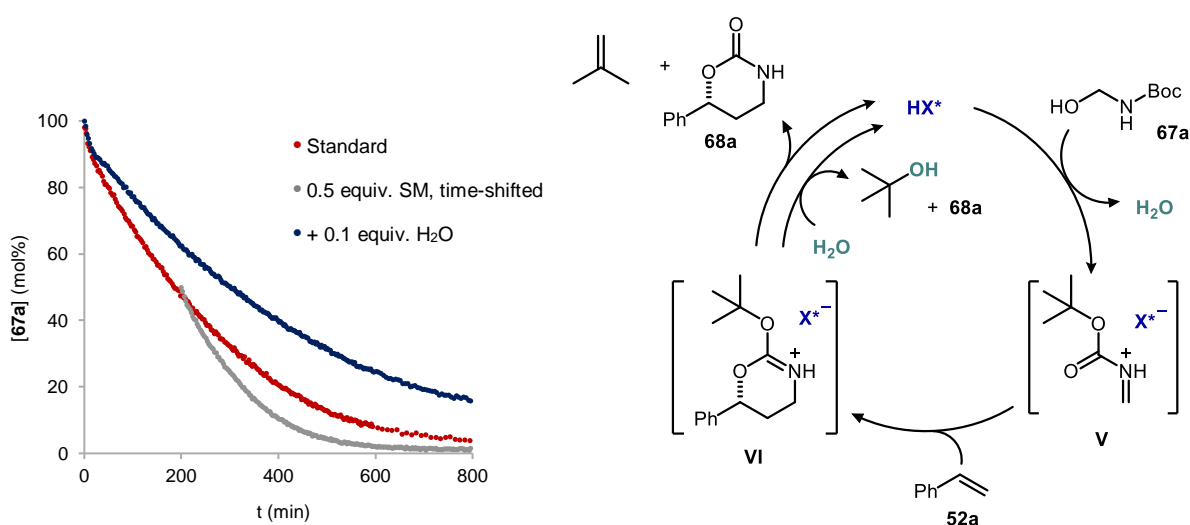
Figure 45. Left: concentration plots obtained from ^{1}H NMR reaction monitoring of 67a. Right: plausible catalytic cycle resulting in an apparent catalyst order greater than one.

To examine the influence of the different side products on the conversion rate of substrate **67a**, five independent experiments were conducted and compared against the standard conditions. In the first experiment, the reaction was monitored at a lower initial concentration of **67a** (0.15 M) and the time scale was shifted to match the same **67a** concentration of the standard condition following a procedure by Blackmond et. al.[133] In the absence of catalyst inhibition, an overlap between the standard and the shifted concentration profiles is expected. As seen in Figure 45, the "time-adjusted" profile does not overlay with that of the reaction from the marked time point onward, suggesting that some product formed during the reaction is resulting in catalyst inhibition.

Intrigued by the role of water in our system, we studied the contribution of additional water to the reaction. The outcome depicted in Figure 45 indicates that introducing 0.1 equivalents of additional water led to a reduced reaction rate. This result was surprising since we expected that the addition of water could accelerate the consumption of intermediate **VI** yielding *tert*-butanol and **68a**. However, as shown in the next Figure 46, the addition water instead resulted in a decrease in both isobutene and *tert*-butanol production. These findings may suggest that the addition of external water inhibits the overall reaction. However, it cannot be excluded that the water originating from the activation of substrate **67a**, which is likely enclosed in the catalyst pocket, could potentially react with intermediate **VI** in the turn-over-limiting step to yield **68a** and *tert*-butanol.
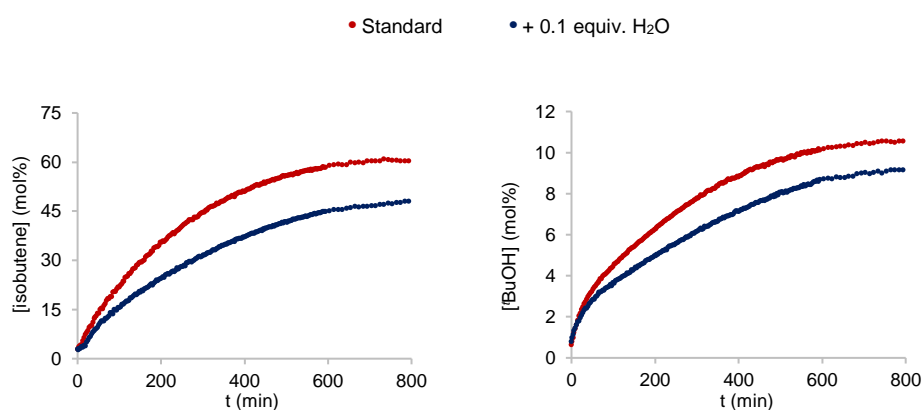
Figure 46. Left: concentration plots obtained from ^{1}H NMR reaction monitoring of isobutene (left) or *tert*-butanol (right).

We furthermore attempted the reaction with common drying agents as additives. As shown in Table 9, the reactions carried out in the presence of molecular sieves were slower and ultimately resulted in slightly reduced yields compared to those conducted without the additives (entries 1–2). Adding anhydrous sodium sulfate to the reaction mixture also resulted in a diminished yield (entry 3). NMR monitoring of the reaction with drying agents was impractical due to diffusion restrictions from the absence of stirring, leading to non-uniform concentrations within the additives that complicate data interpretation and hinder accurate assessment of reaction progress.

72b (1.0 mol%),
additive

CHCl₃, −25 °C, 2 d

67a + (10 equiv.) **52a** → **68a**
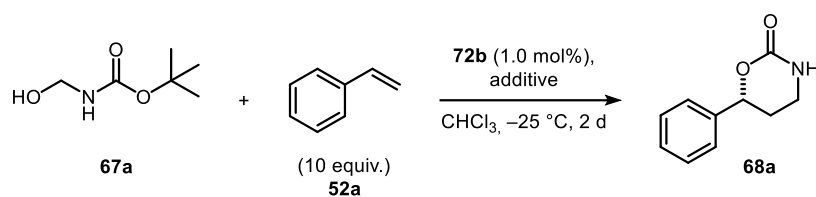
Entry	Additive	Amount	Yield (%)[a]	e.r.
1	–	–	73	97:3
2	4Å MS	200 mg/mmol	63	97:3
3	5Å MS	200 mg/mmol	56	97:3
4	Na₂SO₄	1.2 equiv.	42	96.5:3.5

Table 9. Effect of common drying agents on the reaction. [a]All yields were determined by ^{1}H NMR spectroscopy.

Next, we studied the contribution of product **68a** and side products **76** and **78** as potential inhibitors in the reaction. Independent experiments were set up, in which the additive was added to the initial reaction mixture. The data presented in Figure 47 suggest that the presence of **76** and **78** can lead to catalyst inhibition, likely attributed to the polar hydroxy groups in their structures. On the other hand, the presence of **68a** seems to have little effect on the reaction rate. Due to the complexity of the reaction system, further inhibition contributions were not investigated.
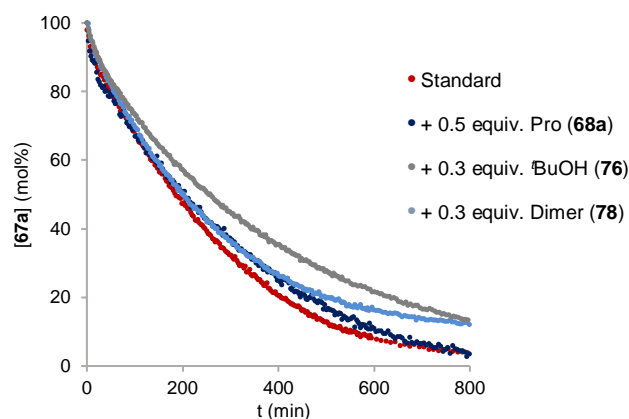
Figure 47. Concentration plots obtained from ^{1}H NMR reaction monitoring of **67a**.

4.2.6. Proposed Catalytic Cycle

Based on the experimental findings described in this work, the following reaction mechanism is proposed (Figure 48). The catalytic cycle begins with the protonation of substrate **67a** by the strong Brønsted acid **72b**. Upon release of water, the highly electrophilic *N*-Boc-formaldiminium ion **V** is generated. At this stage, competing side reactions can occur between **V** and other nucleophilic species present in the solution, as evidenced by the formation of side products **77** and **78**. The enantiodetermining step between the nucleophilic olefin moiety of styrene (**52a**) and intermediate **V** is believed to proceed in a concerted manner and via **TS1-a**, with the carbonyl oxygen of the formaldiminium ion **V** attacking

the benzylic position of styrene. The [4 + 2]-cycloaddition leads to the formation of a second oxazinium intermediate **VI**. Based on our mechanistic findings, which suggest a catalyst order greater than one, we propose two plausible pathways to complete the catalytic cycle: (a) the successive elimination of isobutene from **VI**, which can be possibly facilitated by a second catalyst molecule, resulting in the formation of oxazinanone **68a**, or (b) the water-promoted elimination of *tert*-butanol from intermediate **VI**, yielding the desired product. Further investigations into this intriguing mechanism are currently underway in our laboratory.
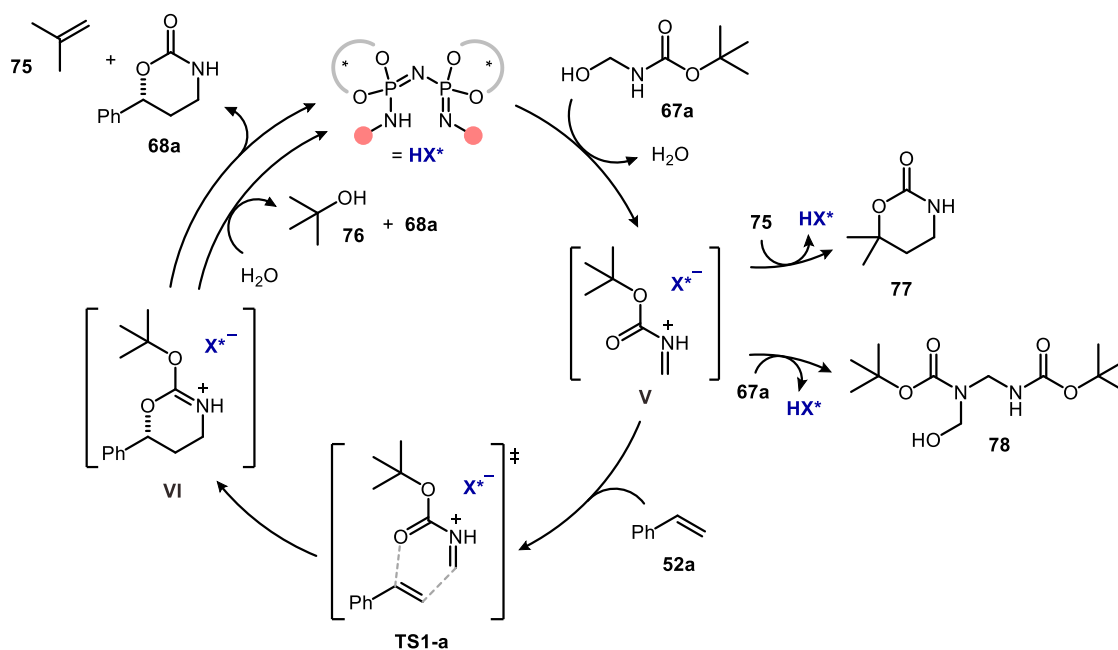
Figure 48. Proposed reaction mechanism for the IDPi-catalyzed hetero-Diels–Alder reaction of in situ generated *N*-Boc-formaldimine with olefins.

4.2.7.   Summary

Common approaches for the synthesis of enantiomerically enriched 1,3-amino alcohols include the transition metal-catalyzed asymmetric hydrogenation of aldehydes or ketones,[82-83] Mannich reactions,[88] intermolecular C–H amination of prefunctionalized substrates,[90] and hydroamination of allylic alcohols.[92-93] Despite their considerable potential, the catalytic asymmetric synthesis of 1,3-amino alcohols via alkene functionalization remains notably underexplored.[70, 72] The second chapter of this thesis dissertation discloses the highly enantioselective, inverse-electron-demand hetero-Diels–Alder reaction of olefins with in situ generated *N*-Boc-formaldimine, catalysed by strong and confined Brønsted acids (Figure 49). This transformation provides direct access to valuable 1,3-amino alcohol precursors from styrenes and 1,1-disubstituted alkenes, utilizing mild reaction conditions and a single IDPi catalyst. The synthetic utility of the obtained cycloaddition products was demonstrated by the three-step, multigram-scale synthesis of the antidepressant (*R*)-fluoxetine hydrochloride from styrene. Mechanistic investigations are consistent with a [4 + 2]-type cycloaddition proceeding via a concerted pathway and with the

intermediacy of an unusual oxazinium intermediate. Moreover, thorough kinetic analysis suggests the possibility of a second catalyst molecule contributing to restoring the catalytic cycle.
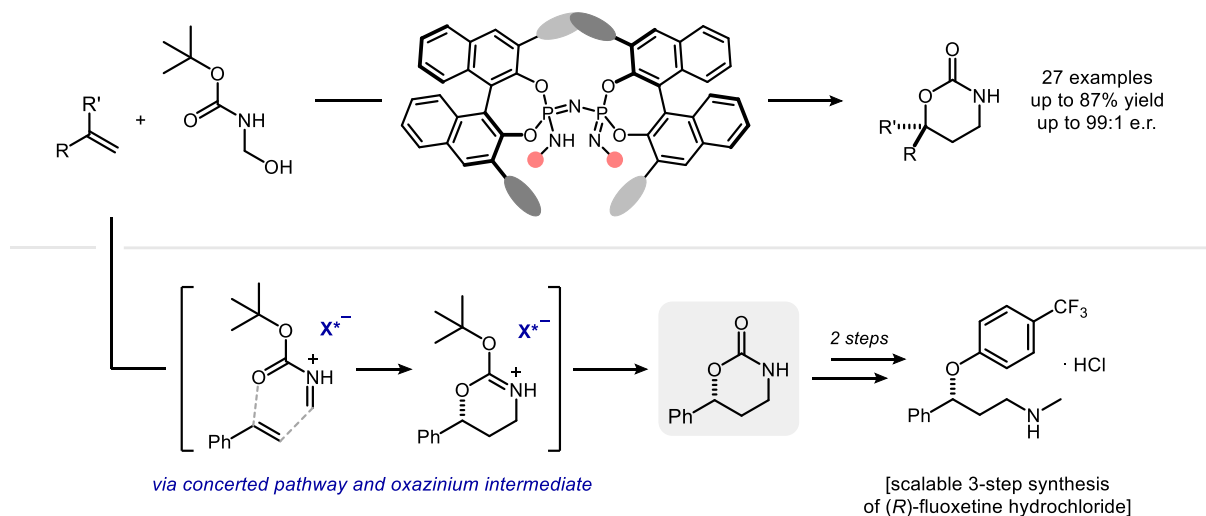

Figure 49. IDPi-catalyzed hetero-Diels–Alder reaction of olefins with in situ generated *N*-Boc-formaldimine.

4.2.8. Outlook

Following the establishment of the asymmetric hetero-[4 + 2] cycloaddition between olefins and in situ generated *N*-Boc-formaldimine, we envisioned to broaden the substrate scope of this transformation. As outlined in Section 4.2.4., terminal alkyl olefins presented additional challenges due to their reduced nucleophilicity, which necessitates the use of a more acidic catalyst for a successful transformation. In contrast, highly electron-rich styrenes, such as those with *p*-methoxy substituents and 2-vinyl-substituted heteroaryl olefins, yielded complex product mixtures with poor enantioselectivity, which can be attributed to their excessive reactivity in this catalytic system. The optimization of a suitable catalyst motif for the substrate 2-vinylthiophene (**52za**) is highly desirable, as it would facilitate the direct access to 3-(methylamino)-1-(thiophen-2-yl)propan-1-ol, the precursor of (*R*)-duloxetine (Scheme 23).
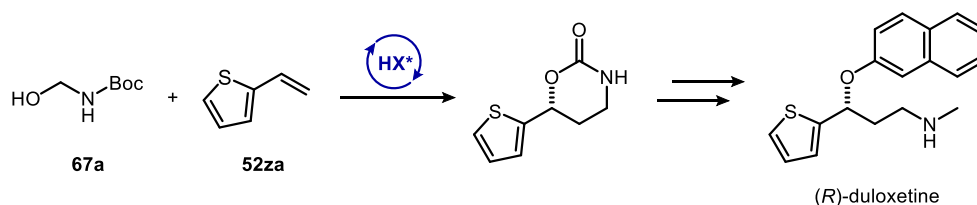
Scheme 23. Synthetic route toward (*R*)-duloxetine from 2-vinylthiophene (**52za**).

On the electrophile side, it has been discussed that previous research on the asymmetric [4 + 2]-cycloaddition of olefins and *N*-acyliminium ions predominantly involved the use of benzaldehyde-derived acylimines.[70, 72] In contrast, this study developed an unprecedented methodology utilizing formaldimines as azadienes in the enantioselective cycloaddition. Expanding this method to other

aldimines would be beneficial, as it could enable the production of 1,3-amino alcohol derivatives featuring 1,3-stereogenic centers. Particularly, the use of α-imino esters could provide a valuable platform for the synthesis of γ-hydroxy-α-amino acids derivatives.

A limitation of this methodology is the relatively large quantity of olefins needed to achieve high yields of the desired product, which may render large-scale synthesis impractical, especially when the olefin is either not commercially available or costly. As discussed in Section 4.2.1., the excess olefin in the reaction remained unreacted and could be recovered via chromatographic purification in all examples tested within the reaction scope. Additionally, when volatile olefins are used, effective recovery through bulb-to-bulb distillation is possible (see the Experimental Section for details). However, the development of a more selective catalytic system that reduces the amount of olefin required would be advantageous.

Flow chemistry and continuous processing have garnered significant interest and now represent promising alternatives to traditional batch manufacturing in chemical synthesis. Continuous-flow systems offer notable savings in space, time, and energy, making processes more efficient and improving overall safety.[134] Moreover, due to enhanced mass and heat transfer, precise modulation of the catalyst-to-substrate ratio, and the continuous removal of products, continuous-flow conditions often lead to unique reactivities and improved yields and selectivities.[135] We envision that implementing a flow setup for this reaction with heterogeneous or polymer-supported catalysts—allowing for simplified catalyst recycling—could offer a practical approach for efficient solvent and reagent recovery and recirculation, thereby enhancing both the process efficiency and economic viability.

5. Experimental Section

Unless otherwise stated, all reactions were magnetically stirred and conducted in oven-dried (90 °C) or flame-dried glassware in anhydrous solvents under argon, applying standard Schlenk techniques. Solvents and liquid reagents, as well as solutions of solid or liquid reagents were added via syringes, stainless steel or polyethylene cannulas through rubber septa or through a weak argon counter-flow. Solid reagents were added through a weak argon counter-flow. Reactions at lower temperatures (T < rt) were cooled to the specified temperature using appropriate cooling baths or cryostats, respectively. Cooling baths were prepared in Dewar vessels, filled with ice/water (0 °C), cooled acetone (< −78 °C) or dry ice/acetone (−78 °C). Alternatively, the reaction vessel was placed in an aluminum block inside a cryostat set to the desired temperature. Heated oil baths were used for reactions requiring elevated temperatures. Solvents were removed under reduced pressure at 40 °C using a rotary evaporator, and unless otherwise stated, the remaining compound was dried in high vacuum (10^{-3} mbar) at rt. All given yields are isolated yields of chromatographically and NMR-spectroscopically pure materials, unless otherwise stated.

Chemicals were purchased from commercial suppliers (including abcr, Acros Organics, Alfa Aesar, Fluorochem, Sigma-Aldrich, and TCI) and used without further purification unless otherwise stated.

Solvents (CyH, DCM, Et$_2$O, THF, toluene) were dried by distillation from an appropriate drying agent in the technical department of the Max-Planck-Institut für Kohlenforschung and received in Schlenk flasks under argon.[136] Other anhydrous solvents were purchased from commercial suppliers and used as received.

Reactions were monitored by thin layer chromatography (TLC) on silica gel pre-coated plastic sheets (0.2 mm, Macherey-Nagel). Visualization was accomplished by irradiation with UV light (254 nm and 366 nm) and/or phosphomolybdic acid (PMA) stain and/or Cerium Ammonium Molybdate (CAM) stain and/or permanganate stain.

Column chromatography was carried out using Merck silica gel (60 Å, 230−400 mesh, particle size 0.040−0.063 mm) using technical grade solvents. Elution was accelerated using compressed air. Automated column chromatography was conducted on a Biotage® Isolera™ ISO-4SW instrument, using SNAP Ultra HP-Sphere™ 25 µm chromatography cartridges. All fractions containing a desired substance were combined and concentrated in vacuo, then redissolved in an appropriate solvent and filtered through cotton to remove silica residues.

^{1}H, ^{13}C, ^{19}F, ^{31}P nuclear magnetic resonance (NMR) spectra were recorded on a Bruker AVIII-500 MHz or Bruker NEO 600 MHz (equipped with a BBO CryoProbe) spectrometer in a suitable deuterated solvent. The solvent employed and respective measuring frequency are indicated for each experiment. Chemical shifts are reported in ppm (δ) relative to tetramethylsilane (TMS) with the residual solvent

resonance serving as the internal reference (δ 7.26 ppm for CDCl$_3$; δ 5.32 ppm for CD$_2$Cl$_2$). The resonance multiplicity is described as s (singlet), d (doublet), t (triplet), q (quadruplet), p (pentet), hept (heptet), m (multiplet), and b (broad). All spectra were recorded at 298 K unless otherwise noted, processed with the program MestReNova 15.0.0, and coupling constants are reported as observed. Data are provided as follows: chemical shift in ppm, resonance multiplicity, coupling constant J in Hz, and number of protons. All spectra are broadband decoupled unless otherwise noted.

Electron impact (EI) mass spectrometry (MS) was performed on a Finnigan MAT 8200 (70 eV) or MAT 8400 (70 eV) spectrometer. Electrospray ionization (ESI) mass spectrometry was conducted on a Bruker ESQ 3000 spectrometer. High-resolution mass spectrometry (HRMS) was performed on a Finnigan MAT 95 (EI) or Bruker APEX III FTMS (7T magnet, ESI). The ionization method and mode of detection employed are indicated for the respective experiment and all masses are reported in atomic units per elementary charge (m/z) with an intensity normalized to the most intense peak.

Specific rotations $[a]_T^D$ were measured with a Rudolph RA Autopol IV Automatic Polarimeter at the indicated temperature (T) with a sodium lamp (sodium D line, λ = 589 nm). Measurements were performed in an acid-resistant 1 mL cell (50 mm length) with concentrations (g/100 mL) reported in the corresponding solvent.

High-performance liquid chromatography (HPLC) was performed on Shimadzu LC-20AD liquid chromatograph (SIL-20AC auto sampler, CMB-20A communication bus module, DGU-20A5 degasser, CTO-20AC column oven, SPD-M20A diode array detector), Shimadzu LC-20AB liquid chromatograph (SIL-20ACHT auto sampler, DGU-20A5 degasser, CTO-20AC column oven, SPD-M20A diode array detector), or Shimadzu LC-20AB liquid chromatograph (reversed phase, SIL-20ACHT auto sampler, CTO-20AC column oven, SPD-M20A diode array detector) using Daicel columns with chiral stationary phases. All solvents used were HPLC-grade solvents, purchased from Merck. The column employed and the respective solvent mixture are indicated for each experiment.

Liquid Chromatography-Mass Spectrometry Liquid chromatography-mass spectrometry (LC-MS) was performed on a Shimadzu LC-MS 2020 liquid chromatograph. All solvents used were HPLC-grade solvents purchased from Sigma-Aldrich. The column employed, the respective solvent mixture, and the MS parameters are indicated for each experiment.

Gas chromatography (GC) analyses on a chiral stationary phase were performed on HP 6890 and 5890 series instruments (split-mode capillary injection system, flame ionization detector (FID), hydrogen carrier gas). All of these analyses were conducted in the GC department of the Max-Planck-Institut für Kohlenforschung. The conditions employed are described in detail for the individual experiments.

5.1. Substrate Synthesis

5.1.1. Synthesis of Olefins

General Procedure A: Wittig Olefination
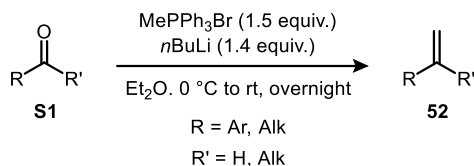
In a flame-dried double neck round-bottomed flask, methyltriphenylphosphonium bromide (2.1 g, 6.0 mmol, 1.5 equiv.) was suspended in Et$_2$O (15 mL) and cooled down to 0 °C. n-BuLi (2.5 M in hexanes, 2.2 mL, 5.6 mmol, 1.4 equiv.) was added dropwise and the mixture was stirred at 0 °C for 1 h before a solution of aldehyde or ketone **S1** (4.0 mmol, 1.0 equiv.) in Et$_2$O (5 mL) was added dropwise. The mixture was further stirred at rt overnight. After checking full conversion (TLC monitoring), the mixture was diluted with Et$_2$O (10 mL) and water (20 mL). The phases were separated and the aqueous layer was extracted with Et$_2$O (3 x 20 mL). The combined organic layers were washed with brine (1 x 20 mL), dried over anhydrous Na$_2$SO$_4$, filtered, and concentrated under reduced pressure. The crude was suspended in n-pentane and filtered to remove triphenylphosphine oxide. Purification by flash column chromatography on silica gel (n-pentane/Et$_2$O mixtures) afforded the corresponding olefin **52**.

General Procedure B: Suzuki−Miyaura Cross-Coupling
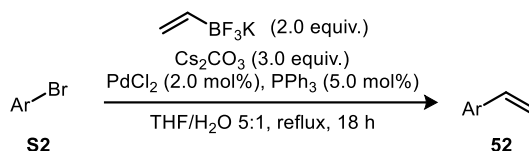
A flame-dried double neck round-bottomed flask equipped with a reflux condenser was charged with aryl bromide **S2** (3.5 mmol, 1.0 equiv.) and THF (12.5 mL). To this was added potassium vinyltrifluoroborate (938 mg, 7.0 mmol, 2.0 equiv.), PdCl$_2$ (12 mg, 0.07 mmol, 2.0 mol%), PPh$_3$ (56 mg, 0.2 mmol, 6.0 mol%), Cs$_2$CO$_3$ (3.4 g, 10.5 mmol, 3.0 equiv.), and water (2.8 mL). The mixture was stirred at rt and degassed by bubbling argon for 10 min, then heated to reflux under argon overnight. After allowing it to cool to rt and checking full conversion (TLC monitoring), the mixture was filtered through a short pad of Celite, washing with MTBE. The filtrate was washed with water (1 x 30 mL) and brine (1 x 30 mL), then dried over anhydrous Na$_2$SO$_4$, filtered, and concentrated under reduced pressure. Purification by flash column chromatography on silica gel (n-pentane/DCM mixtures) afforded the corresponding olefin **52**.

1-Allyl-4-vinylbenzene (52o)
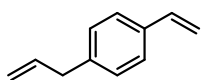
Following a reported procedure:[53] a two-necked round-bottom flask under argon atmosphere was charged with $Pd_2(dba)_3$ (4.6 mg, 5 µmol, 0.1 mol%), 4-vinylphenyl boronic acid (888 mg, 6.0 mmol, 1.2 equiv.) and 1,4-dioxane (6.5 mL). Triphenylphosphite (2.5 µL, 10 µmol, 0.2 mol%) and allyl alcohol (290 mg, 5.0 mmol, 1.0 equiv.) were added and the mixture was heated to 80 °C for 6 h. After cooling to rt, the reaction mixture was diluted with MTBE (50 mL) and washed with brine (1 x 30 mL), dried over anhydrous Na_2SO_4, filtered, and concentrated under reduced pressure. Purification by flash column chromatography on silica gel (*n*-pentane) afforded the corresponding olefin **52o** as a colorless liquid (480 mg, 67%). Spectroscopic data was consistent with the values reported in the literature.[53]

^{1}H NMR (501 MHz, CD_2Cl_2): δ 7.35 (d, *J* = 8.1 Hz, 2H), 7.16 (d, *J* = 8.2 Hz, 2H), 6.71 (dd, *J* = 17.6, 10.9 Hz, 1H), 5.97 (ddt, *J* = 16.9, 10.1, 6.7 Hz, 1H), 5.72 (dd, *J* = 17.6, 1.0 Hz, 1H), 5.20 (dd, *J* = 10.9, 1.0 Hz, 1H), 5.13 – 5.03 (m, 2H), 3.38 (d, *J* = 6.8 Hz, 2H).

^{13}C NMR (126 MHz, CD2Cl2): δ 140.4 (C), 137.9 (CH), 137.0 (CH), 135.9 (C), 129.1 (CH), 126.6 (CH), 115.9 (CH_2), 113.3 (CH_2), 40.3 (CH_2).
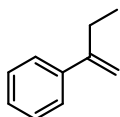
2-Bromo-1-methyl-4-vinylbenzene (52y)
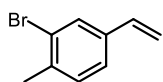
Following *General Procedure A,* employing 3-bromo-4-methylbenzaldehyde (497 mg, 2.5 mmol) as starting material. The crude product was purified by silica gel column chromatography using *n*-pentane/Et_2O (9.5:0.5 *v/v*) as eluent to give **52y** as a colorless liquid (396 mg, 80%). Spectroscopic data was consistent with the values reported in the literature.[53]

^{1}H NMR (501 MHz, $CDCl_3$) δ 7.62 (d, *J* = 1.8 Hz, 1H), 7.30 – 7.24 (m, 1H), 7.20 (d, *J* = 7.8 Hz, 1H), 6.65 (ddd, *J* = 17.6, 10.9, 1.3 Hz, 1H), 5.74 (dd, *J* = 17.5, 1.5 Hz, 1H), 5.27 (dd, *J* = 10.9, 1.6 Hz, 1H), 2.42 (s, 3H).

^{13}C NMR (126 MHz, $CDCl_3$) δ 137.4, 137.3, 135.5, 130.9, 130.1, 125.3, 125.2, 114.5, 22.8.

1,4-Divinylbenzene (52z)
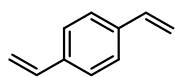
Following *General Procedure A,* employing terephthaladehyde (1.61 g, 12.0 mmol) as starting material, 2.05 equiv. of methyltriphenylphosphonium bromide (8.79 g, 24.6 mmol), and 2.2 equiv. of potassium *tert*-butoxide (2.96 g, 26.4 mmol) as base. The crude product was purified by silica gel column chromatography using *n*-pentane as eluent to give **52z** as a white solid (1.07 g, 68%). Spectroscopic data was consistent with the values reported in the literature.[137]

^{1}H NMR (501 MHz, $CDCl_3$) δ 7.40 (s, 4H), 6.73 (dd, *J* = 17.6, 10.9 Hz, 2H), 5.78 (dd, *J* = 17.6, 0.9 Hz, 2H), 5.27 (dd, *J* = 10.9, 0.9 Hz, 2H).

^{13}C NMR (126 MHz, $CDCl_3$) δ 137.1, 136.5, 126.4, 113.8.

6-Vinylbenzo[*b*]thiophene (52zc)
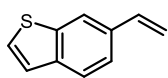
Following *General Procedure B,* employing 6-bromobenzo[*b*]thiophene (448 mg, 2.1 mmol) as starting material. The crude product was purified by silica gel column chromatography using *n*-pentane/DCM (95:5 *v/v*) as eluent to give **52zc** as a white solid (269 mg, 80%).

^{1}H NMR (501 MHz, CDCl$_3$) δ 7.88 (s, 1H), 7.77 (d, *J* = 8.3 Hz, 1H), 7.48 (dd, *J* = 8.2, 1.6 Hz, 1H), 7.43 (d, *J* = 5.2 Hz, 1H), 7.31 (dd, *J* = 5.4, 0.9 Hz, 1H), 6.84 (dd, *J* = 17.6, 10.9 Hz, 1H), 5.83 (dd, *J* = 17.5, 0.9 Hz, 1H), 5.30 (dd, *J* = 10.8, 0.8 Hz, 1H).

^{13}C NMR (126 MHz, CDCl$_3$) δ 140.4, 139.4, 136.9, 134.2, 126.9, 123.8, 123.6, 122.5, 120.6, 113.9.

6-Vinylbenzofuran (52zd)
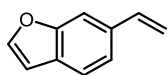
Following *General Procedure B,* employing 6-bromobenzofuran (690 mg, 3.5 mmol) as starting material. The crude product was purified by silica gel column chromatography using *n*-pentane/DCM (95:5 *v/v*) as eluent to give **52zd** as a colorless liquid (362 mg, 72%).

^{1}H NMR (501 MHz, CDCl$_3$) δ 7.62 (d, *J* = 2.1 Hz, 1H), 7.54 (d, *J* = 7.9 Hz, 2H), 7.34 (dd, *J* = 7.9, 1.5 Hz, 1H), 6.82 (dd, *J* = 17.5, 10.9 Hz, 1H), 6.75 (dd, *J* = 2.2, 1.0 Hz, 1H), 5.79 (d, *J* = 17.5 Hz, 1H), 5.26 (dd, *J* = 10.9, 0.8 Hz, 1H).

^{13}C NMR (126 MHz, CDCl$_3$) δ 155.6, 145.7, 137.1, 134.6, 127.3, 121.5, 121.1, 113.5, 109.1, 106.7.

But-1-en-2-ylbenzene (52zf)

Following *General Procedure A,* employing propiophenone (1.61 g, 12.0 mmol) as starting material. The crude product was purified by silica gel column chromatography using *n*-pentane as eluent to give **52zf** as a colorless liquid (1.15 g, 73%). Spectroscopic data was consistent with the values reported in the literature.[138]

^{1}H NMR (501 MHz, CD$_2$Cl$_2$) δ 7.45 – 7.39 (m, 2H), 7.36 – 7.29 (m, 2H), 7.28 – 7.23 (m, 1H), 5.30 – 5.25 (m, 1H), 5.07 (d, *J* = 1.5 Hz, 1H), 2.56 – 2.48 (m, 2H), 1.10 (t, *J* = 7.4 Hz, 3H).

^{13}C NMR (126 MHz, CD$_2$Cl$_2$) δ 150.6, 141.9, 128.6, 127.7, 126.4, 111.1, 28.4, 13.2.

(3-Methylbut-1-en-2-yl)benzene (52zg)
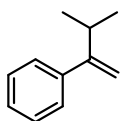
Following *General Procedure A,* employing isobutyrophenone (1.78 g, 12.0 mmol) as starting material. The crude product was purified by silica gel column chromatography using *n*-pentane as eluent to give **52zg** as a colorless liquid (1.33 g, 76%). Spectroscopic data was consistent with the values reported in the literature.[139]

^{1}H NMR (501 MHz, CDCl$_3$) δ 7.45 – 7.35 (m, 4H), 7.35 – 7.29 (m, 1H), 5.22 (t, *J* = 1.7 Hz, 1H), 5.11 (p, *J* = 1.2 Hz, 1H), 2.96 – 2.85 (m, 1H), 1.18 (dt, *J* = 6.8, 1.3 Hz, 6H).

^{13}C NMR (126 MHz, CDCl$_3$) δ 155.9, 142.9, 128.2, 127.1, 126.7, 110.0, 32.4, 22.1.
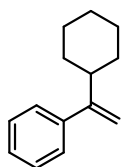
(1-Cyclopentylvinyl)benzene (52zh)
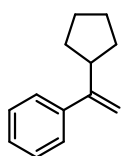
Following *General Procedure A,* employing cyclopentyl(phenyl)methanone (697 mg, 4.0 mmol) as starting material. The crude product was purified by silica gel column chromatography using *n*-pentane as eluent to give **52zh** as a colorless liquid (525 mg, 76%). Spectroscopic data was consistent with the values reported in the literature.[140]

^{1}H NMR (501 MHz, CDCl$_3$) δ 7.36 (dt, *J* = 8.1, 1.8 Hz, 2H), 7.29 (ddt, *J* = 8.0, 6.3, 1.5 Hz, 2H), 7.26 – 7.21 (m, 1H), 5.16 (d, *J* = 0.9 Hz, 1H), 5.06 (q, *J* = 1.2 Hz, 1H), 2.94 (ddt, *J* = 13.3, 8.2, 4.2 Hz, 1H), 1.93 – 1.81 (m, 2H), 1.77 – 1.52 (m, 4H), 1.52 – 1.36 (m, 2H).

^{13}C NMR (126 MHz, CDCl$_3$) δ 153.1, 143.4, 128.2, 127.1, 126.7, 110.2, 44.7, 32.3, 25.0

(1-Cyclohexylvinyl)benzene (52zi)

Following *General Procedure A,* employing cyclohexyl(phenyl)methanone (1.73 g, 9.2 mmol) as starting material. The crude product was purified by silica gel column chromatography using *n*-pentane as eluent to give **52zi** as a colorless liquid (1.62 g, 95%). Spectroscopic data was consistent with the values reported in the literature.[141]

^{1}H NMR (501 MHz, CDCl$_3$) δ 7.44 – 7.35 (m, 4H), 7.35 – 7.30 (m, 1H), 5.21 (d, *J* = 1.4 Hz, 1H), 5.08 (t, *J* = 1.4 Hz, 1H), 2.50 (tdd, *J* = 11.6, 4.0, 2.0 Hz, 1H), 1.97 – 1.72 (m, 5H), 1.45 – 1.33 (m, 2H), 1.32 – 1.19 (m, 3H).

^{13}C NMR (126 MHz, CDCl$_3$) δ 155.1, 143.0, 128.1, 126.9, 126.6, 110.3, 42.6, 32.7, 26.8, 26.4.

cis-Styrene-(β)-d$_1$ (*cis*-52a-β-d$_1$)
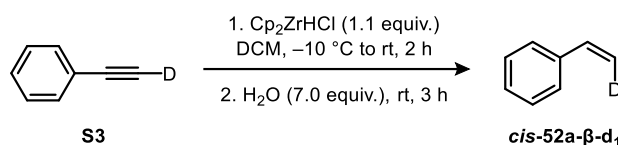
Following a reported procedure:[53] a Schlenk flask under argon atmosphere was charged with phenylacetylene-d$_1$ (245 mg, 2.4 mmol, 1.0 equiv.)[142] and dry DCM (7.5 mL). The flask was covered with aluminum foil and the mixture was cooled down to 0 °C. Schwartz's Reagent (680 mg, 2.6 mmol, 1.1 equiv.) was then added in two equal portions in rapid succession (over 2 min). The mixture was allowed to stir at 0 °C for 15 min, then the cold bath was removed and the stirring was continued at rt in the dark for 2 h. The flask was cooled to 0 °C, and the mixture was quenched with water (0.30 mL, 16.8 mmol, 7.0 equiv.) and stirred vigorously at rt for 3 h. The mixture was diluted with DCM (3 mL), followed by the addition of anhydrous Na$_2$SO$_4$ and filtration. The filtrate was concentrated under reduced pressure (400 mbar, water bath of rotavap at 25 °C) until 1 mL remained. *n*-Pentane (2 mL) was added and the

mixture was filtered over a Celite pad to remove the white precipitate; the filter cake was rinsed with *n*-pentane and the filtrate was again concentrated under reduced pressure (400 mbar, 25 °C). Purification by silica gel column chromatography using *n*-pentane as eluent afforded the corresponding olefin ***cis*-52a-β-d₁** a colorless liquid (75 mg, 30% yield, approx. 99% D-incorporation). Spectroscopic data was consistent with the values reported in the literature.[53]

^{1}H NMR (501 MHz, CDCl$_3$) δ 7.45 – 7.40 (m, 2H), 7.37 – 7.31 (m, 2H), 7.26 (tt, *J* = 7.3, 1.3 Hz, 1H), 6.72 (dt, *J* = 10.9, 2.6 Hz, 1H), 5.23 (d, *J* = 10.9 Hz, 1H).

trans-Styrene-(β)-d₁ (*trans*-52a-β-d₁)
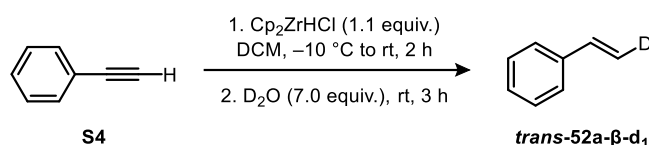
Following a reported procedure:[53] a Schlenk flask under argon atmosphere was charged with phenylacetylene (306 mg, 3.0 mmol, 1.0 equiv.) and dry DCM (7.5 mL). The flask was covered with aluminum foil and the mixture was cooled down to 0 °C. Schwartz's Reagent (850 mg, 3.3 mmol, 1.1 equiv.) was then added in two equal portions in rapid succession (over 2 min). The mixture was allowed to stir at 0 °C for 15 min, then the cold bath was removed and the stirring was continued at rt in the dark for 2 h. The flask was cooled to 0 °C, and the mixture was quenched with D$_2$O (0.38 mL, 99.9% D, 21 mmol, 7.0 equiv.) and stirred vigorously at rt for 3 h. The mixture was diluted with DCM (3 mL), followed by the addition of anhydrous Na$_2$SO$_4$ and filtration. The filtrate was concentrated under reduced pressure (400 mbar, water bath of rotavap at 25 °C) until 1 mL remained. *n*-Pentane (2 mL) was added and the mixture was filtered over a Celite pad to remove the white precipitate; the filter cake was rinsed with *n*-pentane and the filtrate was again concentrated under reduced pressure (400 mbar, 25 °C). Purification by silica gel column chromatography using *n*-pentane as eluent afforded the corresponding olefin ***trans*-52a-β-d₁** as a colorless liquid (95 mg, 30% yield, approx. 91% D-incorporation). Spectroscopic data was consistent with the values reported in the literature.[53]

^{1}H NMR (501 MHz, CDCl$_3$) δ 7.45 – 7.40 (m, 2H), 7.37 – 7.31 (m, 2H), 7.26 (tt, *J* = 7.3, 1.3 Hz, 1H), 6.72 (dt, *J* = 17.5, 1.5 Hz, 1H), 5.75 (d, *J* = 17.7 Hz, 1H).

5.1.2. Synthesis of Electrophiles

5-tosyl-1,3,5-dioxazinane (61a)
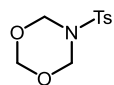
Following a reported procedure:[143] to a stirred solution of *sym*-trioxane (1.80 g, 20 mmol, 2.0 equiv.) in acetic acid (5 mL), *p*-toluenesulfonamide (1.71 g, 10 mmol, 1.0 equiv.) was added at rt. After 5 min, methanesulfonic acid (10 ml) was added dropwise over 2 min and the stirring was continued at 35 °C for 15 min. The mixture was cooled down to 0 °C, then diluted with CHCl₃ (100 mL), washed with ice-water (2 x 50 mL) and aq. 5% NaHCO₃ (2 x 50 mL). Collected organic phases were dried over anhydrous Na₂SO₄ and evaporated to afford product **61a** as a white solid (2.1 g, 86%). Spectroscopic data was consistent with the values reported in the literature.[143]

^{1}H NMR (300 MHz, CDCl₃) δ 7.92 – 7.81 (m, 2H), 7.38 – 7.23 (m, 2H), 5.21 (s, 4H), 4.89 (s, 2H), 2.44 (s, 3H).

^{13}C NMR (75 MHz, CDCl₃) δ 143.5, 136.7, 129.1, 127.7, 93.6, 77.0, 21.1.

EI-HRMS: *m/z* calculated for $C_{10}H_{13}NO_4S^+$ ([M]$^+$): 243.0560; found: 243.0560.

3,5-ditosyl-1,3,5-oxadiazinane (61b)
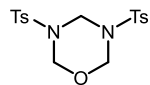
Following a reported procedure:[143] *p*-toluenesulfonamide (1.71 g, 10 mmol, 2.0 equiv.) and *sym*-trioxane (450 mg, 5.0 mmol, 1.0 equiv.) in trifluoroacetic acid (10 ml) were stirred for 2 h at 35 °C. The mixture was then cooled down to 0 °C and CHCl₃ (50 ml) was added, followed by 25 mL of ice-water. The organic phase was separated, washed with ice-water (25 mL) and aq. 5% NaHCO₃ (2 x 25 mL), dried over anhydrous Na₂SO₄ and evaporated. The residue was purified by column chromatography on silica gel (*n*-hexane/MTBE mixtures from 9:1 to 2:1 *v/v*) to afford **61b** as a white solid (169 mg, 9%). Spectroscopic data was consistent with the values reported in the literature.[143]

^{1}H NMR (501 MHz, CDCl₃) δ 7.71 (d, *J* = 8.3 Hz, 4H), 7.35 (d, *J* = 8.2 Hz, 4H), 4.94 (s, 2H), 4.82 (s, 4H), 2.47 (s, 6H).

^{13}C NMR (126 MHz, CDCl₃) δ 144.4, 135.5, 129.9, 127.7, 78.1, 59.9, 21.6.

ESI-HRMS: *m/z* calculated for $C_{17}H_{20}N_2O_5S_2Na^+$ ([M+Na]$^+$): 419.0709; found: 419.0709.

1,3,5-tritosyl-1,3,5-triazinane (61c)
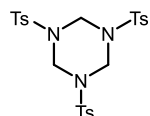
Following a reported procedure:[143] a solution of *sym*-trioxane (30 mg, 0.33 mmol, 1.0 equiv.) in acetic acid (0.25 mL), was added dropwise to a stirring solution of *p*-toluenesulfonamide (171 mg, 1.0 mmol, 3.0 equiv.) in methanesulfonic acid (1 mL). The mixture was further stirred for 15 min at rt. After cooling down to 0 °C, 10 g of crushed ice were added and the

mixture was maintained for 2 h in an ice-bath with occasional shaking. The precipitate was filtered off and washed with ice-water, aq. 5% NaHCO$_3$, and water. The dried crude was recrystallized from methanol to obtain product **61c** as a white solid (163 mg, 90%). Spectroscopic data was consistent with the values reported in the literature.[143]

^{1}H NMR (501 MHz, CDCl$_3$) δ 7.61 (d, J = 8.3 Hz, 6H), 7.32 – 7.28 (d, J = 8.2 Hz, 6H), 4.55 (s, 6H), 2.44 (s, 9H).

^{13}C NMR (126 MHz, CDCl$_3$) δ 144.6, 134.6, 129.9, 127.6, 60.0, 21.7.

EI-HRMS: *m/z* calculated for C$_{24}$H$_{27}$N$_3$O$_6$S$_3$Na$^+$ ([M+Na]$^+$): 572.0954; found: 572.0954

tert-Butyl (hydroxymethyl)carbamate (67a)
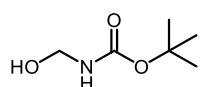
Following a reported procedure:[144] to a round-bottomed flask was added *tert*-butyl carbamate (4.6 g, 34.1 mmol, 1.0 equiv.), Na$_2$CO$_3$ (1.8 g, 17.1 mmol, 0.5 equiv.), paraformaldehyde (1.4 g, 47.8 mmol, 1.4 equiv.) and water (50 mL). The mixture was vigorously stirred and heated to 60 °C for 30 min, until a clear solution was obtained. Then, the mixture was further stirred at rt overnight. The mixture was then diluted with water (20 mL), poured into a separatory funnel and extracted with EtOAc (3 x 20 mL). The combined organic phases were washed with water (1 x 20 mL) and brine (1 x 20 mL), then dried over anhydrous Na$_2$SO$_4$, filtered, and concentrated. A viscous oily residue was obtained, which was purified by silica gel column chromatography using *n*-hexane/EtOAc (2:1 *v/v*) as eluent to afford 2.6 g (52% yield) of compound **67a** as a white solid. Spectroscopic data was consistent with the values reported in the literature.[144]

^{1}H NMR (501 MHz, CDCl$_3$) δ 5.52 (s, 1H), 4.66 (t, J = 6.6 Hz, 2H), 3.01 (s, 1H), 1.47 (s, 9H).

^{13}C NMR (126 MHz, CDCl$_3$) δ 20.2, 65.4, 80.1, 156.1.

((*tert*-Butoxycarbonyl)amino)methyl acetate (67b)
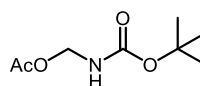
Following a reported procedure:[145] *tert*-butyl carbamate (586 mg, 5.0 mmol, 1.0 equiv.) and paraformaldehyde (165 mg, 5.5 mmol, 1.1 equiv.) were suspended in a mixture of acetic acid (4.5 mL) and acetic anhydride (13.5 mL) in a round-bottomed flask. The reaction was vigorously stirred and heated to 60 °C for 24 h. After this time, the solvent was removed under vacuum at 70 °C to give a yellow oily residue, which was purified by silica gel column chromatography using *n*-hexane/EtOAc (8:2 *v/v*) as eluent to afford 685 mg (72% yield) of product **67b** as a viscous colorless liquid. Spectroscopic data was consistent with the values reported in the literature.[145]

^{1}H NMR (501 MHz, CDCl$_3$) δ 5.70 (s, 1H), 5.14 (d, J = 7.6 Hz, 2H), 2.06 (s, 3H), 1.45 (s, 9H).

^{13}C NMR (126 MHz, CDCl$_3$) 171.8, 155.0, 80.6, 66.6, 28.2, 21.0.

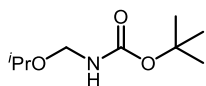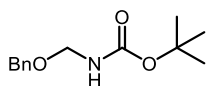### *tert*-Butyl (methoxymethyl)carbamate (67c)
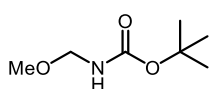
Obtained adapting a reported procedure:[146] to a round-bottomed flask was added compound **67a** (96 mg, 0.65 mmol, 1.0 equiv.), methanol (0.16 mL, 3.9 mmol, 6.0 equiv.), and 1.2 mL of MTBE. Subsequently, *p*-toluenesulfonic acid hydrate (1.3 mg, 1.0 mol%) was added and the mixture was stirred for 24 h at rt. NaHCO$_3$ (11 mg) and anhydrous Na$_2$SO$_4$ (50 mg) were added, and stirring was continued for another 2 h to remove the acid and the water formed. Subsequently, the solids were filtered and the solvents were concentrated. The crude mixture was purified by silica gel column chromatography using *n*-hexane/EtOAc (2:1 *v/v*) as eluent to afford 21 mg (20% yield) of compound **67c** as a white solid.

^{1}H NMR (501 MHz, CDCl$_3$) δ 5.33 (s, 1H), 4.55 (d, *J* = 7.2 Hz, 2H), 3.31 (s, 3H), 1.45 (s, 9H).

^{13}C NMR (126 MHz, CDCl$_3$) δ 155.8, 80.1, 73.4, 55.6, 28.4.

HRMS (ESI) calculated for C$_7$H$_{15}$NO$_3$Na ([M+Na$^+$]): 184.09441, found: 184.09436.

tert-Butyl (isopropoxymethyl)carbamate (67d)

Obtained adapting a reported procedure:[146] to a round-bottomed flask was added compound **67a** (100 mg, 0.68 mmol, 1.0 equiv.), isopropanol (0.31 mL, 4.1 mmol, 6.0 equiv.), and 1.2 mL of MTBE. Subsequently, *p*-toluenesulfonic acid hydrate (1.3 mg, 1.0 mol%) was added and the mixture was stirred for 24 h at rt. NaHCO$_3$ (11 mg) and anhydrous Na$_2$SO$_4$ (50 mg) were added, and stirring was continued for another 2 h to remove the acid and the water formed. Subsequently, the solids were filtered and the solvents were concentrated. The crude mixture was purified by silica gel column chromatography using *n*-hexane/EtOAc (2:1 *v/v*) as eluent to afford 82 mg (64% yield) of compound **67d** as a white solid.

^{1}H NMR (501 MHz, CDCl$_3$) δ 5.32 (s, 1H), 4.61 (d, *J* = 7.1 Hz, 2H), 3.76 (hept, *J* = 6.3 Hz, 1H), 1.43 (s, 9H), 1.14 (d, *J* = 6.2, 6H).

HRMS (ESI) calculated for C$_9$H$_{19}$NO$_3$Na ([M+Na$^+$]): 212.12571, found: 212.12585.

tert-Butyl ((benzyloxy)methyl)carbamate (67e)

Obtained adapting a reported procedure:[146] to a round-bottomed flask was added compound **67a** (100 mg, 0.68 mmol, 1.0 equiv.), benzyl alcohol (0.42 mL, 4.1 mmol, 6.0 equiv.), and 1.2 mL of MTBE. Subsequently, *p*-toluenesulfonic acid hydrate (1.3 mg, 1.0 mol%) was added and the mixture was stirred for 24 h at rt. NaHCO$_3$ (11 mg) and anhydrous Na$_2$SO$_4$ (50 mg) were added, and stirring was continued for another 2 h to remove the acid and the water formed. Subsequently, the solids were filtered and the solvents were concentrated. The crude mixture was purified by silica gel column chromatography using *n*-hexane/EtOAc (2:1 *v/v*) as eluent to afford 108 mg (67% yield) of compound **67e** as a white solid.

^{1}H NMR (501 MHz, CDCl$_3$) δ 7.33 – 7.12 (m, 5H), 5.35 (s, 1H), 4.62 (d, J = 7.2 Hz, 2H), 4.48 (s, 2H), 1.39 (s, 9H).

^{13}C NMR (126 MHz, CDCl$_3$) δ 155.8, 138.2, 128.5, 127.8, 80.1, 71.7, 70.2, 53.1, 28.4.

HRMS (ESI) calculated for C$_{13}$H$_{19}$NO$_3$Na ([M+Na$^+$]): 260.12571, found: 260.12598.

Ethyl (hydroxymethyl)carbamate (79)
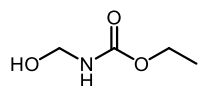
Obtained adapting a reported procedure:[144] to a round-bottomed flask was added urethane (432 mg, 4.8 mmol, 1.0 equiv.), Na$_2$CO$_3$ (257 mg, 2.4 mmol, 0.5 equiv.), paraformaldehyde (204 mg, 6.8 mmol, 1.4 equiv.) and water (7.3 mL). The mixture was vigorously stirred and heated to 60 °C for 30 min, until a clear solution was obtained. Then, the mixture was further stirred at rt overnight. The mixture was then diluted with water (5 mL), poured into a separatory funnel and extracted with EtOAc (3 x 5 mL). The combined organic phases were washed with water (1 x 5 mL) and brine (1 x 5 mL), then dried over anhydrous Na$_2$SO$_4$, filtered, and concentrated. A viscous oily residue was obtained, which was purified by silica gel column chromatography using *n*-hexane/EtOAc (2:1 *v/v*) as eluent to afford 176 mg (30% yield) of compound **79** as a white solid. Spectroscopic data was consistent with the values reported in the literature.[147]

^{1}H NMR (501 MHz, CDCl$_3$) δ 5.74 (s, 1H), 4.71 (t, J = 5.7 Hz, 2H), 4.15 (q, J = 7.0 Hz, 2H), 3.45 (s, 1H), 1.25 (t, J = 7.1 Hz, 3H).

^{13}C NMR (126 MHz, CDCl$_3$) δ 157.0, 66.3, 61.4, 14.6.

HRMS (ESI) calculated for C$_4$H$_9$NO$_2$Na ([M+Na$^+$]): 142.04746, found: 142.04725.

Isopropyl (hydroxymethyl)carbamate (80)
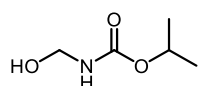
Obtained adapting a reported procedure:[144] to a round-bottomed flask was added isopropyl carbamate (500 mg, 4.8 mmol, 1.0 equiv.), Na$_2$CO$_3$ (260 mg, 2.4 mmol, 0.5 equiv.), paraformaldehyde (200 mg, 6.8 mmol, 1.4 equiv.) and water (7 mL). The mixture was vigorously stirred and heated to 60 °C for 30 min, until a clear solution was obtained. Then, the mixture was further stirred at rt overnight. The mixture was then diluted with water (5 mL), poured into a separatory funnel and extracted with EtOAc (3 x 5 mL). The combined organic phases were washed with water (1 x 5 mL) and brine (1 x 5 mL), then dried over anhydrous Na$_2$SO$_4$, filtered, and concentrated. A viscous oily residue was obtained, which was purified by silica gel column chromatography using *n*-hexane/EtOAc (2:1 *v/v*) as eluent to afford 285 mg (44% yield) of compound **80** as a white solid.

^{1}H NMR (501 MHz, CDCl$_3$) δ 5.62 (s, 1H), 4.94 (hept, J = 6.3 Hz, 1H), 4.70 (t, J = 7.1 Hz, 2H), 3.22 (d, J = 7.4 Hz, 1H), 1.24 (d, J = 6.3 Hz, 6H).

^{13}C NMR (126 MHz, CDCl$_3$) δ 156.6, 68.9, 66.3, 22.2.

HRMS (ESI) calculated for $C_5H_{11}NO_2Na$ ([M+Na$^+$]): 156.06311, found: 156.06407.

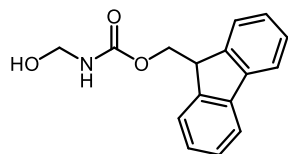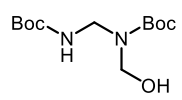## Benzyl (hydroxymethyl)carbamate (81)
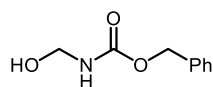
Obtained adapting a reported procedure:[144] to a round-bottomed flask was added benzyl carbamate (733 mg, 4.8 mmol, 1.0 equiv.), Na$_2$CO$_3$ (260 mg, 2.4 mmol, 0.5 equiv.), paraformaldehyde (200 mg, 6.8 mmol, 1.4 equiv.) and water (7 mL). The mixture was vigorously stirred and heated to 60 °C for 30 min, until a clear solution was obtained. Then, the mixture was further stirred at rt overnight. The mixture was then diluted with water (5 mL), poured into a separatory funnel and extracted with EtOAc (3 x 5 mL). The combined organic phases were washed with water (1 x 5 mL) and brine (1 x 5 mL), then dried over anhydrous Na$_2$SO$_4$, filtered, and concentrated. A viscous oily residue was obtained, which was purified by silica gel column chromatography using *n*-hexane/EtOAc (2:1 *v/v*) as eluent to afford 316 mg (36% yield) of compound **81** as a white solid. Spectroscopic data was consistent with the values reported in the literature.[148]

^{1}H NMR (501 MHz, CDCl$_3$) δ 7.38–7.31 (m, 5H), 5.97 (s, 1H), 5.13 (s, 2H), 4.72 (d, *J* = 6.6 Hz, 2H), 4.10 (s, 1H).

HRMS (ESI) calculated for $C_9H_{11}NO_3Na$ ([M+Na$^+$]): 204.0637, found: 204.0636.

(9*H*-Fluoren-9-yl)methyl (hydroxymethyl)carbamate (82)

Obtained adapting a reported procedure:[144] to a round-bottomed flask was added (9*H*-fluoren-9-yl)methyl carbamate (1.15 g, 4.8 mmol, 1.0 equiv.), Na$_2$CO$_3$ (260 mg, 2.4 mmol, 0.5 equiv.), paraformaldehyde (200 mg, 6.8 mmol, 1.4 equiv.) and water (7 mL). The mixture was vigorously stirred and heated to 60 °C for 30 min, until a clear solution was obtained. Then, the mixture was further stirred at rt overnight. The mixture was then diluted with water (5 mL), poured into a separatory funnel and extracted with EtOAc (3 x 5 mL). The combined organic phases were washed with water (1 x 5 mL) and brine (1 x 5 mL), dried over anhydrous Na$_2$SO$_4$, filtered, and concentrated. A viscous oily residue was obtained, which was purified by silica gel column chromatography using *n*-hexane/EtOAc (2:1 *v/v*) as eluent to afford 558 mg (43% yield) of compound **82** as a white solid. Spectroscopic data was consistent with the values reported in the literature.[149]

^{1}H NMR (501 MHz, CDCl$_3$) δ 7.77 (d, *J* = 7.5 Hz, 2H), 7.57 (d, *J* = 7.1 Hz, 2H), 7.41 (t, *J* = 7.4 Hz, 2H), 7.31 (t, *J* = 7.4, Hz, 2H), 5.56–5.71 (s, 1H), 5.19 (d, *J* = 7.9 Hz, 2H), 4.49 (d, *J* = 6.9 Hz, 2H), 4.24 (t, *J* = 6.2 Hz, 1H), 2.95 (t, *J* = 6.6 Hz, 1H).

HRMS (ESI) calculated for $C_{16}H_{15}NO_3Na$ ([M+Na$^+$]): 292.0944, found: 292.0944.

tert-Butyl (((_tert_-butoxycarbonyl)amino)methyl)(hydroxymethyl)carbamate (78)

A flame-dried Schlenk under argon atmosphere was charged with 265 mg of **67a** (1.8 mmol) and 2.2 mL of CHCl$_3$. The mixture was cooled down to –20 ºC for 15 min. After this time, a stock solution of catalyst **72b** in 0.1 mL of CHCl$_3$ (1.0 mol%) was added to the previous flask via syringe in one portion. After checking full conversion (TLC monitoring) the reaction was quenched with one equivalent of triethylamine. The mixture was warmed up to rt, suspended on Celite, and further purified by silica gel column chromatography (_n_-hexane/EtOAc mixtures from 8:2 to 6:4 _v/v_) to afford 59 mg (24% yield) of product **78**.

2 rotamers are observed in the NMR data at 233 K (–40 °C).

Major rotamer:

^{1}H NMR (600 MHz, 233K, CDCl$_3$) δ 5.86 (t, _J_ = 6.6 Hz, 1H), 4.89 (t, _J_ = 7.6 Hz, 1H), 4.80 (d, _J_ = 7.5 Hz, 2H), 4.50 (d, _J_ = 6.6 Hz, 2H), 1.47 (s, 9H), 1.43 (s, 9H).

^{13}C NMR (151 MHz, 233 K, CDCl$_3$) δ 158.0, 155.1, 81.4, 72.7, 55.2, 28.3, 28.2.

Minor rotamer:

^{1}H NMR (600 MHz, 233K, CDCl$_3$) δ 5.46 (t, _J_ = 6.7 Hz, 1H), 4.83 (d, _J_ = 7.7 Hz, 2H), 4.60 (t, _J_ = 7.7 Hz, 1H), 4.52 (d, _J_ = 6.7 Hz, 2H), 1.48 (s, 9H), 1.44 (s, 9H).
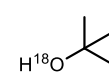
^{13}C NMR (151 MHz, 233 K CDCl$_3$) δ 157.5, 154.6, 81.6, 81.4, 72.5, 55.1, 28.4, 28.3.

HRMS (ESI) calculated for C$_{12}$H$_{24}$N$_2$O$_5$Na ([M+Na$^+$]): 299.157742, found: 299.15788.

5.1.3. Synthesis ^{18}O-Labelled Substrate Analogous
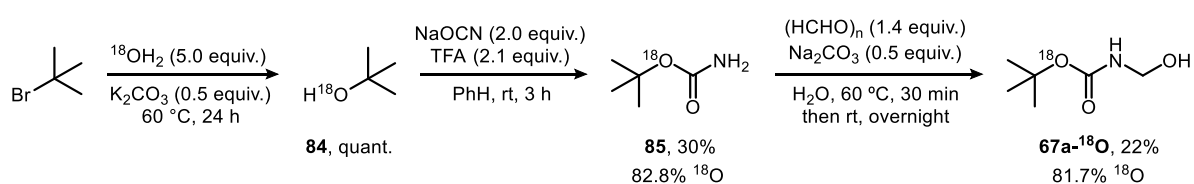
2-Methylpropan-2-ol-^{18}O (84)
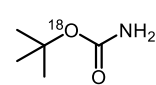
Obtained adapting a reported procedure:[125] a flame-dried Schlenk under argon atmosphere was charged with 1.37 g of _tert_-butyl bromide (10 mmol, 1.0 equiv.) and 1.0 mL of H$_2$^{18}O (97%, 5.0 equiv.). 690 mg (0.5 equiv.) of Na$_2$CO$_3$ were added slowly and the mixture was vigorously stirred at 70 °C overnight. After cooling to rt, analysis of the reaction mixture with ^{1}H NMR spectroscopy revealed that the reaction had gone to >95% conversion. The mixture was diluted with DCM and anhydrous Na$_2$SO$_4$ was added. The resulting mixture was filtered and carefully evaporated at 25 °C to obtain 2-methylpropan-2-ol-^{18}O (**84**) as a colorless oil. Spectroscopic data was consistent with the values reported in the literature.[125]

^{1}H NMR (501 MHz, CDCl$_3$) δ 1.29 (s, 9H).

^{13}C NMR (126 MHz, CDCl$_3$) δ 69.3, 31.4.

HRMS (ESI) calculated for C$_4$H$_{10}$^{18}ONa ([M+Na$^+$]): 99.06663, found: 99.06653.

tert-Butyl carbamate-^{18}O (85)
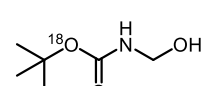
Obtained adapting a reported procedure.[126] to a round-bottomed flask was added 2-methylpropan-2-ol-^{18}O (**84**, 0.72 g, 9.5 mmol, 1.0 equiv.), sodium cyanate (1.24 g, 19 mmol, 2.0 equiv.), and 8 mL of benzene. Trifluoroacetic acid (1.5 mL, 20 mmol, 2.1 equiv.) was added dropwise under stirring at rt. The flask was closed loosely with a glass stopper and the mixture was stirred at rt overnight. Water (10 mL) was added and both phases were separated. The aqueous phase was extracted with EtOAc (3 x 5 mL). The combined organic phases were washed with water (1 x 10 mL) and brine (1 x 10 mL), dried over anhydrous Na$_2$SO$_4$ and evaporated. The obtained solid was recrystallized from *n*-hexane to obtain 336 mg (30% yield, 82.8% ^{18}O-incorporation) of compound **85** as colorless crystal needles. Spectroscopic data was consistent with the values reported in the literature.[126]

^{1}H NMR (501 MHz, CDCl$_3$) δ 4.70 (s, 1H), 1.43 (s, 4H).

^{13}C NMR (126 MHz, CDCl$_3$) δ 156.7, 79.7, 28.4.

HRMS (GC-EI) calculated for C$_5$H$_{12}$NO^{18}O ([M$^+$]): 120.090498, found: 120.090338.

tert-Butyl (hydroxymethyl)carbamate-^{18}O (67a-^{18}O)

Obtained adapting a reported procedure:[144] to a round-bottomed flask was added *tert*-butyl carbamate-^{18}O (**85**, 290 mg, 2.4 mmol, 1.0 equiv.), Na$_2$CO$_3$ (130 mg, 1.2 mmol, 0.5 equiv.), paraformaldehyde (102 mg, 3.4 mmol, 1.4 equiv.) and water (3.7 mL). The flask was closed with a septum and the mixture was vigorously stirred and heated to 60 °C for 30 min, until a clear solution was obtained. Then, the mixture was further stirred at rt overnight. The mixture was then diluted with water (2 mL), poured into a separatory funnel and extracted with EtOAc (3 x 2 mL). The combined organic phases were washed with water (1 x 2 mL) and brine (1 x 2 mL), then dried over anhydrous Na$_2$SO$_4$, filtered, and concentrated. A viscous oily residue was obtained, which was purified by silica gel column chromatography using *n*-hexane/EtOAc (2:1 *v/v*) as eluent to afford 78 mg (22% yield, 81.7% ^{18}O-incorporation) of product **67a-^{18}O** as a white solid. Spectroscopic data was consistent with the values reported in the literature.[144]

NMR at 253 K (–20 °C) shows two rotamers (ratio approx. 10:1).

Major rotamer:

^{1}H NMR (600 MHz, CDCl$_3$) δ 5.65 (t, J = 6.9 Hz, 1H), 4.67 (t, J = 7.3 Hz, 2H), 3.60 (t, J = 7.6 Hz, 1H), 1.44 (s, 9H).

^{13}C NMR (151 MHz, 253 K, CDCl$_3$) δ 156.125 (^{16}O-C2), 156.114 (^{18}O-C2), 80.516 (^{16}O-C3), 80.469 (^{18}O-C3), 65.855 (C1), 28.339 (C4).

HRMS (ESI) calculated for C$_6$H$_{13}$NO$_2$[18]ONa ([M+Na$^+$]): 172.08301, found: 172.08225.

## 5.2. Acid-Catalyzed Oxy-aminomethylation of Styrenes

General Procedure C:
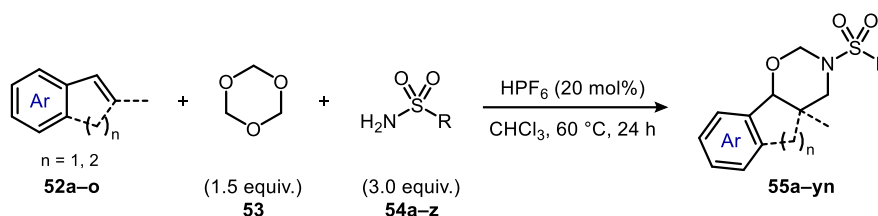
An oven-dried 10 mL glass tube (with screw cap) was charged with olefin **52** (0.2 mmol, 1.0 equiv.), *sym*-trioxane (**53**, 0.3 mmol, 1.5 equiv.), sulfonamide **54** (0.6 mmol, 3.0 equiv.) and CHCl$_3$ (2 mL). HPF$_6$ (20 mol%, 55% in water) was added in one portion. The tube was closed and the reaction mixture was stirred at 60 °C for 24 h. After the reaction was completed, the mixture was cooled to room temperature and concentrated under reduced pressure to give a crude product. This residue was further purified by silica gel column chromatography (*n*-hexane/EtOAc mixtures from 10:1 to 5:1 *v/v*) to give the desired product **55**.

General Procedure D:
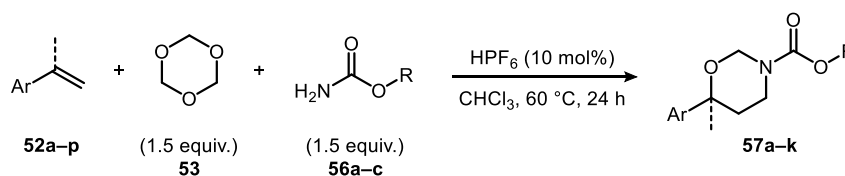
An oven-dried 10 mL glass tube (with screw cap) was charged with olefin **52** (0.5 mmol, 1.0 equiv.), *sym*-trioxane (**53**, 0.75 mmol, 1.5 equiv.), carbamate **56** (0.75 mmol, 1.5 equiv.) and CHCl$_3$ (0.5 mL). HPF$_6$ (10 mol%, 55% in water) was added in one portion. The tube was closed under argon and the reaction mixture was stirred at 60 °C for 24 h. After the reaction was completed, the mixture was cooled to room temperature and concentrated under reduced pressure to give a crude product. This residue was further purified by column chromatography (silica, *n*-hexane/MTBE mixtures from 5:1 to 2:1 *v/v*) to give the desired product **57**.

6-Phenyl-3-tosyl-1,3-oxazinane (55a)
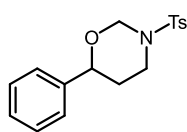
Obtained following the *General Procedure C*, as a white solid (50 mg, 78%).

^{1}H NMR (501 MHz, CDCl$_3$) δ 7.88 (d, *J* = 8.3 Hz, 2H), 7.38 (d, *J* = 8.0 Hz, 2H), 7.31 – 7.22 (m, 3H), 7.03 – 6.94 (m, 2H), 5.72 (dd, *J* = 11.2, 2.2 Hz, 1H), 4.66 (d, *J* = 11.2 Hz, 1H), 4.44 (dd, *J* = 10.9, 3.2 Hz, 1H), 4.06 (ddt, *J* = 14.5, 4.6, 2.2 Hz, 1H), 3.40 (ddd, *J* = 14.5, 12.3, 3.9 Hz, 1H), 2.48 (s, 3H), 1.49 – 1.35 (m, 2H).

^{13}C NMR (126 MHz, CDCl$_3$) δ 143.8 (C), 141.0 (C), 137.8 (C), 129.9 (CH), 128.5 (CH), 128.1 (CH), 128.0 (CH), 125.8 (CH), 79. (CH), 78.5 (CH$_2$), 44.9 (CH$_2$), 30.9 (CH$_2$), 21.7 (CH$_3$).

ESI-HRMS: *m/z* calculated for C$_{17}$H$_{19}$NO$_3$SNa$^+$ ([M+Na]$^+$): 340.0978; found: 340.0976.

6-(4-(Chloromethyl)phenyl)-3-tosyl-1,3-oxazinane (55b)
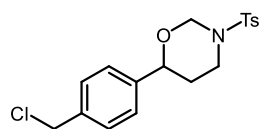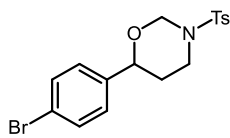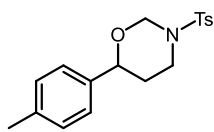
Obtained following the *General Procedure C*, as a white solid (45 mg, 62%).

^{1}H NMR (501 MHz, CDCl$_3$) δ 7.86 (d, *J* = 8.4 Hz, 2H), 7.36 (d, *J* = 8.0 Hz, 2H), 7.28 (d, *J* = 8.2 Hz, 2H), 6.97 (d, *J* = 8.2 Hz, 2H), 5.70 (dd, *J* = 11.2, 2.2 Hz, 1H), 4.64 (d, *J* = 11.3 Hz, 1H), 4.54 (s, 2H), 4.43 (dd, *J* = 11.2, 2.8 Hz, 1H), 4.04 (ddt, *J* = 14.5, 4.5, 2.1 Hz, 1H), 3.38 (ddd, *J* = 14.5, 12.6, 3.5 Hz, 1H), 2.47 (s, 3H), 1.47 – 1.31 (m, 2H).

^{13}C NMR (126 MHz, CDCl$_3$) δ 143.9 (C), 141.3 (C), 137.8 (C), 137.3 (C), 129.9 (CH), 128.8 (CH), 128.1 (CH), 126.2 (CH), 79.3 (CH), 78.5 (CH$_2$), 46.0 (CH$_2$), 44.8 (CH$_2$), 31.0 (CH$_2$), 21.7 (CH$_3$).

ESI-HRMS: *m/z* calculated for C$_{18}$H$_{20}$ClNO$_3$SNa$^+$ ([M+Na]$^+$): 388.0745; found: 388.0743.

6-(4-Fluorophenyl)-3-tosyl-1,3-oxazinane (55c)
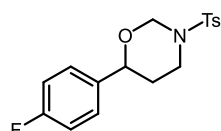
Obtained following the *General Procedure C*, as a white solid (32 mg, 48%).

^{1}H NMR (501 MHz, CDCl$_3$) δ 7.85 (d, *J* = 8.3 Hz, 2H), 7.36 (d, *J* = 8.1 Hz, 2H), 6.94 (d, *J* = 7.0 Hz, 4H), 5.69 (dd, *J* = 11.2, 2.3 Hz, 1H), 4.63 (d, *J* = 11.3 Hz, 1H), 4.41 (dd, *J* = 11.2, 3.0 Hz, 1H), 4.04 (ddt, *J* = 14.5, 4.5, 2.1 Hz, 1H), 3.37 (ddd, *J* = 14.5, 12.5, 3.6 Hz, 1H), 2.46 (s, 3H), 1.47 – 1.30 (m, 2H).

^{19}F NMR (471 MHz, CDCl$_3$) δ -114.16 (s, 1F).

^{13}C NMR (126 MHz, CDCl$_3$) δ 162.5 (d, *J* = 246.3 Hz, C), 143.9 (C), 137.8 (C), 136.9 (d, *J* = 3.0 Hz, C), 129.9 (CH), 128.1 (CH), 127.5 (d, *J* = 8.0 Hz, CH), 115.4 (d, *J* = 21.7 Hz, CH), 79.0 (CH), 78.5 (CH$_2$), 44.8 (CH$_2$), 31.1 (CH$_2$), 21.7 (CH$_3$).

ESI-HRMS: *m/z* calculated for C$_{17}$H$_{18}$FNO$_3$SNa$^+$ ([M+Na]$^+$): 358.0884; found: 358.0880.

6-(4-Chlorophenyl)-3-tosyl-1,3-oxazinane (55d)
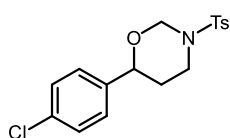
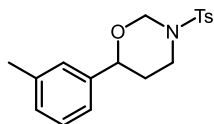Obtained following the *General Procedure C*, as a white solid (43 mg, 68%).

^{1}H NMR (501 MHz, CDCl$_3$) δ 7.85 (d, *J* = 8.3 Hz, 2H), 7.36 (d, *J* = 8.0 Hz, 2H), 7.22 (d, *J* = 8.5 Hz, 2H), 6.90 (d, *J* = 8.4 Hz, 2H), 5.69 (dd, *J* = 11.2, 2.2 Hz, 1H), 4.63 (d, *J* = 11.3 Hz, 1H), 4.41 (dd, *J* = 11.3, 2.8 Hz, 1H), 4.04 (ddt, *J* = 14.5, 4.5, 2.1 Hz, 1H), 3.37 (ddd, *J* = 14.5, 12.7, 3.4 Hz, 1H), 2.46 (s, 3H), 1.43 (dq, *J* = 13.5, 2.7 Hz, 1H), 1.33 (dddd, *J* = 13.7, 12.8, 11.3, 4.9 Hz, 1H).

^{13}C NMR (126 MHz, CDCl$_3$) δ 143.9 (C), 139.6 (C), 137.8 (C), 133.8 (C), 129.9 (CH), 128.7 (CH), 128.1 (CH), 127.2 (CH), 78.9 (CH), 78.4 (CH$_2$), 44.8 (CH$_2$), 31.0 (CH$_2$), 21.7 (CH$_3$).

ESI-HRMS: *m/z* calculated for C$_{17}$H$_{18}$ClNO$_3$SNa$^+$ ([M+Na]$^+$): 374.0588; found: 374.0589.

6-(4-Bromophenyl)-3-tosyl-1,3-oxazinane (55e)

Obtained following the *General Procedure C*, as a white solid (32 mg, 40%).

^{1}H NMR (501 MHz, CDCl$_3$) δ 7.85 (d, *J* = 8.4 Hz, 2H), 7.37 (d, *J* = 8.5 Hz, 2H), 7.35 (d, *J* = 8.0 Hz, 2H), 6.84 (d, *J* = 8.4 Hz, 2H), 5.69 (dd, *J* = 11.2, 2.2 Hz, 1H), 4.62 (d, *J* = 11.2 Hz, 1H), 4.39 (dd, *J* = 11.4, 2.7 Hz, 1H), 4.03 (ddt, *J* = 14.5, 4.5, 2.1 Hz, 1H), 3.37 (ddd, *J* = 14.5, 12.7, 3.4 Hz, 1H), 2.46 (s, 3H), 1.42 (dq, *J* = 13.8, 2.8 Hz, 1H), 1.32 (dddd, *J* = 13.7, 12.8, 11.4, 4.9 Hz, 1H).

^{13}C NMR (126 MHz, CDCl$_3$) δ 143.9 (C), 140.1 (C), 137.8 (C), 131.6 (CH), 129.9 (CH), 128.1 (CH), 127.5 (CH), 121.9 (C), 78.9 (CH), 78.4 (CH$_2$), 44.7 (CH$_2$), 31.0 (CH$_2$), 21.7 (CH$_3$).

ESI-HRMS: *m/z* calculated for C$_{17}$H$_{18}$BrNO$_3$SNa$^+$ ([M+Na]$^+$): 418.0083; found: 418.0084.

6-(*p*-Tolyl)-3-tosyl-1,3-oxazinane (55f)

Obtained following the *General Procedure C*, as a white solid (15 mg, 20%).

^{1}H NMR (501 MHz, CDCl$_3$) δ 7.86 (d, *J* = 8.3 Hz, 2H), 7.36 (d, *J* = 7.9 Hz, 2H), 7.06 (d, *J* = 7.9 Hz, 2H), 5.69 (dd, *J* = 11.2, 2.3 Hz, 1H), 4.63 (d, *J* = 11.2 Hz, 1H), 4.38 (dd, *J* = 9.8, 4.2 Hz, 1H), 4.09 – 3.99 (m, 1H), 3.42 – 3.32 (m, 1H), 2.47 (s, 3H), 2.30 (s, 3H), 1.44 – 1.32 (m, 2H).

^{13}C NMR (126 MHz, CDCl$_3$) δ 143.8 (C), 138.1 (C), 137.9 (C), 129.9 (CH), 129.2 (CH), 128.14 (C), 128.09 (CH), 125.8 (CH), 79.6 (CH), 78.5 (CH$_2$), 44.9 (CH$_2$), 30.9 (CH$_2$), 21.7 (CH$_3$), 21.2 (CH$_3$).

ESI-HRMS: *m/z* calculated for C$_{18}$H$_{21}$NO$_3$SNa$^+$ ([M+Na]$^+$): 354.1134; found: 354.1134.

6-(4-(*tert*-Butyl)phenyl)-3-tosyl-1,3-oxazinane (55g)
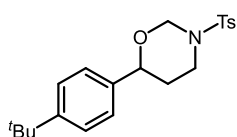
Obtained following the *General Procedure C*, as a white solid (37 mg, 50%).

^{1}H NMR (501 MHz, CDCl$_3$) δ 7.87 (d, *J* = 8.3 Hz, 2H), 7.37 (d, *J* = 7.9 Hz, 2H), 7.27 (d, *J* = 8.4 Hz, 2H), 6.90 (d, *J* = 8.3 Hz, 2H), 5.68 (dd, *J* = 11.2, 2.2 Hz, 1H), 4.63 (d, *J* = 11.2 Hz, 1H), 4.41 – 4.37 (m, 1H), 4.04 (ddt, *J* = 14.5, 4.1, 2.3 Hz, 1H), 3.40 – 3.33 (m, 1H), 2.48 (s, 3H), 1.46 – 1.40 (m, 2H), 1.28 (s, 9H).

^{13}C NMR (126 MHz, CDCl$_3$) δ 151.2 (C), 143.8 (C), 137.89 (C), 137.86 (C), 129.9 (CH), 128.1 (CH), 125.7 (CH), 125.4 (CH), 79.7 (CH), 78.6 (CH$_2$), 44.9 (CH$_2$), 34.7 (C), 31.4 (CH$_3$), 30.7 (CH$_2$), 21.7 (CH$_3$).

ESI-HRMS: *m/z* calculated for C$_{21}$H$_{27}$NO$_3$SNa$^+$ ([M+Na]$^+$): 396.1604; found: 396.1602.

6-(*m*-Tolyl)-3-tosyl-1,3-oxazinane (55h)

Obtained following the *General Procedure C*, as a white solid (40 mg, 60%).

^{1}H NMR (501 MHz, CDCl$_3$) δ 7.88 (d, *J* = 8.3 Hz, 2H), 7.37 (d, *J* = 8.1 Hz, 2H), 7.14 (t, *J* = 7.6 Hz, 1H), 7.05 (d, *J* = 7.7 Hz, 1H), 6.78 (d, *J* = 7.6 Hz, 1H), 6.73 (s, 1H), 5.70 (dd, *J* = 11.3, 2.2 Hz, 1H), 4.65 (d, *J* = 11.3 Hz, 1H), 4.39 (dd, *J* = 10.4, 3.6 Hz, 1H), 4.05 (ddt, *J* = 14.5, 4.7, 2.3 Hz, 1H), 3.44 – 3.34 (m, 1H), 2.47 (s, 3H), 2.29 (s, 3H), 1.44 – 1.30 (m, 2H).

^{13}C NMR (126 MHz, CDCl$_3$) δ 143.8 (C), 140.9 (C), 138.2 (C), 138.0 (C), 129.9 (CH), 128.9 (CH), 128.4 (CH), 128.1 (CH), 126.5 (CH), 123.0 (CH), 79.8 (CH), 78.5 (CH$_2$), 44.9 (CH$_2$), 30.9 (CH$_2$), 21.7 (CH$_3$), 21.5 (CH$_3$).

ESI-HRMS: *m/z* calculated for C$_{18}$H$_{21}$NO$_3$SNa$^+$ ([M+Na]$^+$): 354.1134; found: 354.1133.

6-(*o*-Tolyl)-3-tosyl-1,3-oxazinane (55i)
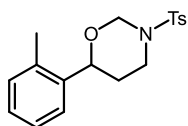
Obtained following the *General Procedure C*, as a white solid (42 mg, 63%).

^{1}H NMR (501 MHz, CDCl$_3$) δ 7.87 (d, *J* = 8.3 Hz, 2H), 7.37 (d, *J* = 8.2 Hz, 2H), 7.13 (td, *J* = 7.3, 1.6 Hz, 1H), 7.12 – 7.04 (m, 2H), 6.80 (dd, *J* = 7.7, 1.6 Hz, 1H), 5.72 (dd, *J* = 11.3, 2.2 Hz, 1H), 4.67 (d, *J* = 11.2 Hz, 1H), 4.62 (dd, *J* = 11.1, 2.7 Hz, 1H), 4.07 (ddt, *J* = 14.4, 4.5, 2.1 Hz, 1H), 3.39 (ddd, *J* = 14.4, 12.6, 3.5 Hz, 1H), 2.46 (s, 3H), 2.22 (s, 3H), 1.46 – 1.38 (m, 1H), 1.34 (dddd, *J* = 13.9, 12.7, 11.1, 4.8 Hz, 1H).

^{13}C NMR (126 MHz, CDCl$_3$) δ 143.9 (C), 139.1 (C), 137.8 (C), 134.0 (C), 130.4 (CH), 129.9 (CH), 128.0 (CH), 127.8 (CH), 126.3 (CH), 125.6 (CH), 78.7 (CH$_2$), 76.5 (CH), 45.0 (CH$_2$), 29.6 (CH$_2$), 21.7 (CH$_3$), 19.0 (CH$_3$).

ESI-HRMS: *m/z* calculated for C$_{18}$H$_{21}$NO$_3$SNa$^+$ ([M+Na]$^+$): 354.1134; found: 354.1132.

6-Mesityl-3-tosyl-1,3-oxazinane (55j)
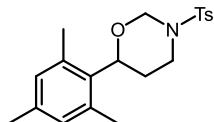
Obtained following the *General Procedure C*, as a white solid (25 mg, 35%).

^{1}H NMR (501 MHz, CDCl$_3$) δ 7.80 (d, *J* = 8.4 Hz, 2H), 7.33 (d, *J* = 8.0 Hz, 2H), 6.74 (s, 2H), 5.62 (dd, *J* = 10.9, 2.2 Hz, 1H), 4.77 (dd, *J* = 11.9, 2.4 Hz, 1H), 4.54 (d, *J* = 11.0 Hz, 1H), 4.13 (ddt, *J* = 14.2, 4.4, 1.9 Hz, 1H), 3.28 (ddd, *J* = 14.2, 12.6, 3.3 Hz, 1H), 2.45 (s, 3H), 2.19 (s, 3H), 2.06 (s, 6H), 2.01 – 1.90 (m, 1H), 1.40 – 1.32 (m, 1H).

^{13}C NMR (126 MHz, CDCl$_3$) δ 143.7 (C), 137.5 (C), 137.2 (C), 135.9 (C), 133.1 (C), 130.12 (CH), 130.06 (CH), 127.5 (CH), 78.7 (CH$_2$), 78.2 (CH), 45.3 (CH$_2$), 27.8 (CH$_2$), 21.6 (CH$_3$), 20.8 (CH$_3$), 20.6 (CH$_3$).

ESI-HRMS: *m/z* calculated for C$_{20}$H$_{26}$NO$_3$S$^+$ ([M+H]$^+$): 360.1628; found: 360.1627.

6-(Naphthalen-2-yl)-3-tosyl-1,3-oxazinane (55k)
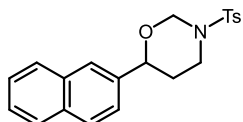
Obtained following the *General Procedure C*, as a white solid (28 mg, 38%).

^{1}H NMR (501 MHz, CDCl$_3$) δ 7.91 (d, *J* = 8.3 Hz, 2H), 7.81 – 7.77 (m, 1H), 7.76 – 7.71 (m, 2H), 7.50 – 7.43 (m, 3H), 7.40 (d, *J* = 8.1 Hz, 2H), 7.04 (dd, *J* = 8.5, 1.7 Hz, 1H), 5.76 (dd, *J* = 11.3, 2.2 Hz, 1H), 4.72 (d, *J* = 11.3 Hz, 1H), 4.60 (dd, *J* = 11.0, 3.0 Hz, 1H), 4.09 (ddt, *J* = 14.5, 4.4, 2.2 Hz, 1H), 3.44 (ddd, *J* = 14.5, 12.5, 3.7 Hz, 1H), 2.48 (s, 3H), 1.55 – 1.40 (m, 2H).

^{13}C NMR (126 MHz, CDCl$_3$) δ 143.9, 138.5, 138.0, 133.3, 133.2, 130.0, 128.3, 128.2, 128.0, 127.8, 126.4, 126.2, 124.7, 123.8, 79.7, 78.6, 44.9, 31.0, 21.8.

ESI-HRMS: *m/z* calculated for C$_{21}$H$_{21}$NO$_3$SNa$^+$ ([M+Na]$^+$): 390.1134; found: 390.1138.

(4a*R**,9b*S**)-3-Tosyl-2,3,4,4a,5,9b-hexahydroindeno[2,1-*e*][1,3]oxazine (55l)
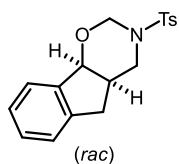
Obtained following the *General Procedure C*, as a white solid (27 mg, 41%).

^{1}H NMR (600 MHz, CDCl$_3$) δ 7.77 (d, *J* = 8.3 Hz, 2H), 7.35 (d, *J* = 7.2 Hz, 1H), 7.31 (d, *J* = 7.9 Hz, 2H), 7.29 – 7.23 (m, 2H), 7.22 (d, *J* = 7.3 Hz, 1H), 4.96 (d, *J* = 5.5 Hz, 1H), 4.91 (d, *J* = 10.2 Hz, 1H), 4.84 (dd, *J* = 10.2, 1.0 Hz, 1H), 3.55 (ddd, *J* = 13.8, 5.8, 1.0 Hz, 1H), 3.32 (dd, *J* = 13.8, 7.0 Hz, 1H), 2.79 (dd, *J* = 15.7, 7.0 Hz, 1H), 2.60 (dd, *J* = 15.7, 5.3 Hz, 1H), 2.43 (s, 3H), 2.37 (qd, *J* = 5.5, 1.5 Hz, 1H).

^{13}C NMR (151 MHz, CDCl$_3$) δ 143.7 (C), 142.7 (C), 140.0 (C), 137.0 (C), 129.9 (CH), 129.0 (CH), 127.6 (CH), 127.2 (CH), 125.7 (CH), 124.8 (CH), 80.2 (CH), 74.2 (CH$_2$), 45.4 (CH$_2$), 36.0 (CH), 33.6 (CH$_2$), 21.7 (CH$_3$).

ESI-HRMS: *m/z* calculated for C$_{18}$H$_{20}$NO$_3$S$^+$ ([M+H]$^+$): 330.1158; found: 330.1159.

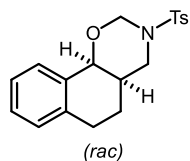**(4a*S**,10b*S**)-3-Tosyl-3,4,4a,5,6,10b-hexahydro-2*H*-naphtho[2,1-*e*][1,3]oxazine (*trans*-55m)**
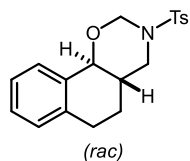
Obtained following the *General Procedure C*, as a white solid (10 mg, 16%).

^{1}H NMR (600 MHz, CDCl$_3$) δ 7.75 (d, *J* = 8.3 Hz, 2H), 7.44 – 7.39 (m, 1H), 7.25 (d, *J* = 8.2 Hz, 2H), 7.21 – 7.13 (m, 2H), 7.06 – 7.01 (m, 1H), 5.74 (dd, *J* = 10.4, 2.0 Hz, 1H), 4.63 (d, *J* = 10.4 Hz, 1H), 4.19 (d, *J* = 10.2 Hz, 1H), 3.92 (ddd, *J* = 13.4, 4.4, 2.0 Hz, 1H), 2.88 (dd, *J* = 13.4, 11.4 Hz, 1H), 2.80 – 2.75 (m, 2H), 2.38 (s, 3H), 1.68 (ddt, *J* = 13.2, 5.0, 3.0 Hz, 1H), 1.55 (tdt, *J* = 7.2, 4.3, 2.2 Hz, 1H), 1.45 – 1.35 (m, 1H).

^{13}C NMR (151 MHz, CDCl$_3$) δ 143.7 (C), 137.0 (C), 135.7 (C), 135.4 (C), 129.9 (CH), 128.7 (CH), 127.6 (CH), 127.5 (CH), 126.1 (CH), 125.0 (CH), 80.7 (CH), 78.6 (CH$_2$), 49.9 (CH$_2$), 35.9 (CH), 28.0 (CH$_2$), 24.4 (CH$_2$), 21.7 (CH$_3$).

ESI-HRMS: *m/z* calculated for C$_{19}$H$_{21}$NO$_3$SNa$^+$ ([M+Na]$^+$): 366.1134; found: 366.1138.

(4a*R**,10b*S**)-3-Tosyl-3,4,4a,5,6,10b-hexahydro-2*H*-naphtho[2,1-*e*][1,3]oxazine (*cis*-55m)

Obtained following the *General Procedure C*, as a white solid (10 mg, 16%).

^{1}H NMR (600 MHz, CDCl$_3$) δ 7.71 (d, *J* = 8.3 Hz, 2H), 7.31 (d, *J* = 7.9 Hz, 2H), 7.28 (dd, *J* = 7.5, 1.7 Hz, 1H), 7.23 (td, *J* = 7.4, 1.7 Hz, 1H), 7.21 – 7.17 (m, 1H), 7.10 (d, *J* = 7.3 Hz, 1H), 5.25 (dd, *J* = 9.6, 1.8 Hz, 1H), 4.57 (d, *J* = 9.7 Hz, 1H), 4.46 (d, *J* = 3.1 Hz, 1H), 3.73 (ddd, *J* = 13.2, 3.5, 1.8 Hz, 1H), 3.34 (dd, *J* = 13.1, 3.8 Hz, 1H), 2.81 (ddd, *J* = 17.1, 5.5, 3.7 Hz, 1H), 2.73 (ddd, *J* = 17.0, 10.9, 5.8 Hz, 1H), 2.43 (s, 3H), 1.96 (dtd, *J* = 12.9, 11.1, 5.6 Hz, 1H), 1.90 – 1.85 (m, 1H), 1.60 – 1.52 (m, 1H).

^{13}C NMR (151 MHz, CDCl$_3$) δ 143.7 (C), 137.3 (C), 136.6 (C), 134.1 (C), 130.3 (CH), 129.9 (CH), 129.1 (CH), 128.7 (CH), 127.4 (CH), 126.4 (CH), 77.3 (CH), 75.5 (CH$_2$), 48.7 (CH$_2$), 33.4 (CH), 28.5 (CH$_2$), 22.5 (CH$_2$), 21.7 (CH$_3$).

ESI-HRMS: *m/z* calculated for C$_{19}$H$_{21}$NO$_3$SNa$^+$ ([M+Na]$^+$): 366.1134; found: 366.1138.

**(5*S**,6*S**)-5-Methyl-6-phenyl-3-tosyl-1,3-oxazinane (*trans*-55n)**
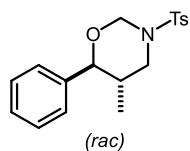
Obtained following the *General Procedure C*, as a white solid (21 mg, 31%).

^{1}H NMR (600 MHz, CDCl$_3$) δ 7.93 – 7.86 (m, 2H), 7.45 – 7.38 (m, 2H), 7.30 – 7.21 (m, 3H), 6.92 – 6.84 (m, 2H), 5.69 (dd, *J* = 11.2, 2.2 Hz, 1H), 4.60 (d, *J* = 11.2 Hz, 1H), 4.01 (ddd, *J* = 14.5, 4.8, 2.2 Hz, 1H), 3.92 (d, *J* = 10.1 Hz, 1H), 2.96 (dd, *J* = 14.5, 11.8 Hz, 1H), 2.52 (s, 3H), 1.49 (ddqd, *J* = 11.4, 10.0, 6.7, 4.7 Hz, 1H), 0.51 (d, *J* = 6.7 Hz, 3H).

^{13}C NMR (151 MHz, CDCl$_3$) δ 143.8 (C), 139.1 (C), 137.9 (C), 130.0 (CH), 128.5 (CH), 128.4 (CH), 128.1 (CH), 127.2 (CH), 86.7 (CH), 78.3 (CH$_2$), 51.5 (CH$_2$), 33.3 (CH), 21.7 (CH$_3$), 14.3 (CH$_3$).

ESI-HRMS: *m/z* calculated for C$_{18}$H$_{21}$NO$_3$SNa$^+$ ([M+Na]$^+$): 354.1134; found: 354.1136.

**(5R*,6S*)-5-Methyl-6-phenyl-3-tosyl-1,3-oxazinane (*cis*-55n)**
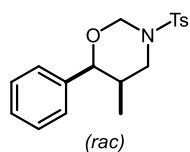
Obtained following the *General Procedure C*, as a white solid (10 mg, 16%).

^{1}H NMR (600 MHz, CDCl$_3$) δ 7.72 – 7.68 (m, 2H), 7.35 – 7.30 (m, 4H), 7.24 (ddt, *J* = 8.5, 6.7, 1.4 Hz, 1H), 7.20 (ddt, *J* = 6.9, 1.3, 0.8 Hz, 2H), 5.54 (dd, *J* = 9.1, 2.1 Hz, 1H), 4.58 (d, *J* = 2.5 Hz, 1H), 4.34 (d, *J* = 9.1 Hz, 1H), 3.79 (dt, *J* = 12.2, 2.2 Hz, 1H), 3.16 (dd, *J* = 12.2, 3.1 Hz, 1H), 2.44 (s, 3H), 1.99 (dddd, *J* = 9.7, 7.0, 4.2, 2.0 Hz, 1H), 0.73 (d, *J* = 6.9 Hz, 1H).

^{13}C NMR (151 MHz, CDCl$_3$) δ 143.7 (C), 139.8 (C), 136.2 (C), 129.9 (CH), 128.3 (CH), 127.3 (CH), 127.3 (CH), 125.3 (CH), 81.5 (CH), 79.2 (CH$_2$), 51.2 (CH$_2$), 33.8 (CH), 21.7 (CH$_3$), 11.4 (CH$_3$).

ESI-HRMS: *m/z* calculated for C$_{18}$H$_{21}$NO$_3$SNa$^+$ ([M+Na]$^+$): 354.1134; found: 354.1136.

6-(4-Allylphenyl)-3-tosyl-1,3-oxazinane (55o)
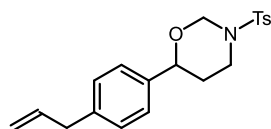
Obtained following the *General Procedure C*, as a white solid (38 mg, 53%).

^{1}H NMR (501 MHz, CDCl$_3$) δ 7.86 (d, *J* = 8.1 Hz, 2H), 7.36 (d, *J* = 8.0 Hz, 2H), 7.08 (d, *J* = 8.0 Hz, 2H), 6.89 (d, *J* = 7.9 Hz, 2H), 5.92 (ddt, *J* = 17.5, 9.5, 6.7 Hz, 1H), 5.69 (dd, *J* = 11.2, 2.2 Hz, 1H), 5.10 – 5.01 (m, 2H), 4.64 (d, *J* = 11.2 Hz, 1H), 4.40 (dd, *J* = 10.1, 4.0 Hz, 1H), 4.04 (ddt, *J* = 14.5, 4.9, 2.5 Hz, 1H), 3.41 – 3.36 (m, 1H), 3.34 (d, *J* = 6.8 Hz, 2H), 2.47 (s, 3H), 1.45 – 1.33 (m, 2H).

^{13}C NMR (126 MHz, CDCl$_3$) δ 143.8, 140.0, 138.8, 137.8, 137.3, 129.9, 128.7, 128.1, 126.0, 116.0, 79.6, 78.5, 44.9, 40.0, 30.9, 21.7.

ESI-HRMS: *m/z* calculated for C$_{20}$H$_{23}$NO$_3$S$^+$ ([M]$^+$): 357.1393; found: 357.1399.

6-Phenyl-3-(phenylsulfonyl)-1,3-oxazinane (55p)
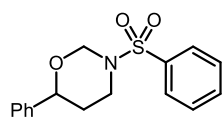
Obtained following the *General Procedure C*, as a white solid (42 mg, 69%).

^{1}H NMR (501 MHz, CDCl$_3$) δ 8.03 – 7.97 (m, 2H), 7.67 – 7.60 (m, 1H), 7.61 – 7.54 (m, 2H), 7.28 – 7.21 (m, 3H), 6.98 – 6.92 (m, 2H), 5.73 (dd, *J* = 11.3, 2.2 Hz, 1H), 4.67 (d, *J* = 11.3 Hz, 1H), 4.43 (dd, *J* = 11.3, 2.7 Hz, 1H), 4.06 (ddt, *J* = 14.6, 4.6, 2.1 Hz, 1H), 3.41 (ddd, *J* = 14.5, 12.7, 3.3 Hz, 1H), 1.45 (dq, *J* = 13.6, 2.8 Hz, 1H), 1.35 (dddd, *J* = 13.8, 12.9, 11.3, 4.9 Hz, 1H).

^{13}C NMR (126 MHz, CDCl$_3$) δ 140.9 (C), 140.8 (C), 133.0 (CH), 129.3 (CH), 128.5 (CH), 128.1 (CH), 128.0 (CH), 125.8 (CH), 79.8 (CH), 78.5 (CH$_2$), 44.9 (CH$_2$), 30.9 (CH$_2$).

ESI-HRMS: *m/z* calculated for C$_{16}$H$_{17}$NO$_3$SNa$^+$ ([M+Na]$^+$): 326.0821; found: 326.0820.

6-Phenyl-3-(*o*-tolylsulfonyl)-1,3-oxazinane (55q)
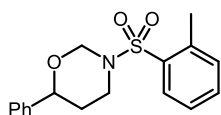
Obtained following the *General Procedure C*, as a white solid (25 mg, 40%).

^{1}H NMR (501 MHz, CDCl$_3$) δ 8.06 (dd, *J* = 7.9, 1.4 Hz, 1H), 7.48 (td, *J* = 7.5, 1.4 Hz, 1H), 7.37 – 7.24 (m, 5H), 7.16 – 7.13 (m, 2H), 5.66 (dd, *J* = 11.1, 2.2 Hz, 1H), 4.70 (d, *J* = 11.1 Hz, 1H), 4.51 (dd, *J* = 10.1, 3.9 Hz, 1H), 3.92 (ddt, *J* = 14.2, 4.5, 2.4 Hz, 1H), 3.41 – 3.34 (m, 1H), 2.72 (s, 3H), 1.66 – 1.57 (m, 2H).

^{13}C NMR (126 MHz, CDCl$_3$) δ 141.0 (C), 138.2 (C), 138.1 (C), 133.10 (CH), 133.08 (CH), 130.3 (CH), 128.6 (CH), 128.1 (CH), 126.4 (CH), 125.9 (CH), 79.8 (CH), 77.7 (CH$_2$), 44.7 (CH$_2$), 31.9 (CH$_2$), 20.7 (CH$_3$).

ESI-HRMS: *m/z* calculated for C$_{17}$H$_{19}$NO$_3$SNa$^+$ ([M+Na]$^+$): 340.0978; found: 340.0974.

3-((4-(*tert*-Butyl)phenyl)sulfonyl)-6-phenyl-1,3-oxazinane (55r)
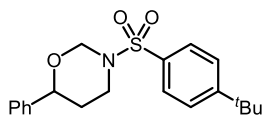
Obtained following the *General Procedure C*, as a white solid (50 mg, 70%).

^{1}H NMR (501 MHz, CDCl$_3$) δ 7.91 (d, *J* = 8.6 Hz, 2H), 7.58 (d, *J* = 8.5 Hz, 2H), 7.25 – 7.19 (m, 3H), 6.92 – 6.87 (m, 2H), 1.43 – 1.23 (m, 2H), 5.71 (dd, *J* = 11.4, 2.2 Hz, 1H), 4.67 (d, *J* = 11.4 Hz, 1H), 4.41 (dd, *J* = 11.3, 2.8 Hz, 1H), 4.09 (ddt, *J* = 14.6, 4.5, 2.1 Hz, 1H), 3.42 (ddd, *J* = 14.6, 12.7, 3.5 Hz, 1H), 1.43 – 1.23 (m, 2H), 1.38 (s, 9H).

^{13}C NMR (126 MHz, CDCl$_3$) δ 156.9 (C), 141.0 (C), 137.9 (C), 128.5 (CH), 128.2 (CH), 127.9 (CH), 126.3 (CH), 125.9 (CH), 79.9 (CH), 78.6 (CH$_2$), 45.0 (CH$_2$), 35.4 (C), 31.3 (CH$_3$), 30.8 (CH$_2$).

ESI-HRMS: *m/z* calculated for C$_{20}$H$_{25}$NO$_3$SNa$^+$ ([M+Na]$^+$): 382.1447; found: 382.1450.

3-((4-Methoxyphenyl)sulfonyl)-6-phenyl-1,3-oxazinane (55s)
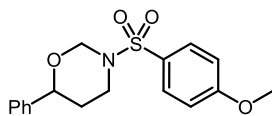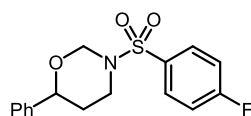
Obtained following the *General Procedure C*, as a white solid (25 mg, 37%).

^{1}H NMR (501 MHz, CDCl$_3$) δ 7.92 (d, *J* = 8.9 Hz, 2H), 7.30 – 7.23 (m, 3H), 7.04 (d, *J* = 8.9 Hz, 2H), 7.01 (dd, *J* = 7.6, 2.0 Hz, 2H), 5.71 (dd, *J* = 11.2, 2.2 Hz, 1H), 4.66 (d, *J* = 11.3 Hz, 1H), 4.45 (dd, *J* = 11.1, 2.9 Hz, 1H), 4.03 (ddt, *J* = 14.5, 4.5, 2.2 Hz, 1H), 3.90 (s, 3H), 3.40 (ddd, *J* = 14.5, 12.5, 3.6 Hz, 1H), 1.50 – 1.33 (m, 2H).

^{13}C NMR (126 MHz, CDCl$_3$) δ 163.3 (C), 141.0 (C), 132.4 (C), 130.2 (CH), 128.5 (CH), 128.1 (CH), 125.8 (CH), 114.5 (CH), 79.7 (CH), 78.5 (CH$_2$), 55.8 (CH$_3$), 44.8 (CH$_2$), 30.9 (CH$_2$).

ESI-HRMS: *m/z* calculated for C$_{17}$H$_{19}$NO$_4$SNa$^+$ ([M+Na]$^+$): 356.0927; found: 356.0927.

3-((4-Fluorophenyl)sulfonyl)-6-phenyl-1,3-oxazinane (55t)

Obtained following the *General Procedure C*, as a white solid (10 mg, 16%).

^{1}H NMR (501 MHz, CDCl$_3$) δ 8.07 – 8.01 (m, 2H), 7.35 – 7.25 (m, 5H), 7.03 (dd, *J* = 7.8, 1.8 Hz, 2H), 5.74 (dd, *J* = 11.3, 2.2 Hz, 1H), 4.72 (d, *J* = 11.3 Hz, 1H), 4.50 (dd, *J* = 11.4, 2.6 Hz, 1H), 4.08 (ddt, *J* = 14.6, 4.6, 2.1 Hz, 1H), 3.46 (ddd, *J* = 14.6, 12.8, 3.3 Hz, 1H), 1.53 (dq, *J* = 13.8, 2.7 Hz, 1H), 1.45 – 1.33 (m, 1H).

^{19}F NMR (471 MHz, CDCl$_3$) δ -104.96 (s, 1F).

^{13}C NMR (126 MHz, CDCl$_3$) δ 165.4 (d, *J* = 255.3 Hz, C), 140.7 (C), 136.9 (d, *J* = 3.2 Hz, C), 130.7 (d, *J* = 9.2 Hz, CH), 128.6 (CH), 128.2 (CH), 125.6 (CH), 116.5 (d, *J* = 22.5 Hz, CH), 79.7 (CH), 78.5 (CH$_2$), 44.9 (CH$_2$), 30.9 (CH$_2$).

ESI-HRMS: *m/z* calculated for C$_{16}$H$_{16}$FNO$_3$SNa$^+$ ([M+Na]$^+$): 344.0727; found: 344.0726.

**3-((4-Chlorophenyl)sulfonyl)-6-phenyl-1,3-oxazinane (55u)**
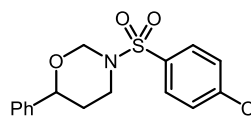
Obtained following the *General Procedure C*, as a white solid (45 mg, 67%).

^{1}H NMR (501 MHz, CDCl$_3$) δ 7.93 (d, *J* = 8.6 Hz, 2H), 7.55 (d, *J* = 8.6 Hz, 2H), 7.32 – 7.23 (m, 3H), 6.98 – 6.94 (m, 2H), 5.69 (dd, *J* = 11.3, 2.2 Hz, 1H), 4.68 (d, *J* = 11.4 Hz, 1H), 4.46 (dd, *J* = 11.3, 2.7 Hz, 1H), 4.05 (ddt, *J* = 14.6, 4.5, 2.1 Hz, 1H), 3.43 (ddd, *J* = 14.6, 12.8, 3.5 Hz, 1H), 1.49 (dq, *J* = 13.8, 3.0 Hz, 1H), 1.39 (dddd, *J* = 13.8, 12.8, 11.3, 5.0 Hz, 1H).

^{13}C NMR (126 MHz, CDCl$_3$) δ 140.7 (C), 139.6 (C), 139.5 (C), 129.6 (CH), 129.5 (CH), 128.7 (CH), 128.3 (CH), 125.7 (CH), 79.7 (CH), 78.5 (CH$_2$), 45.0 (CH$_2$), 31.0 (CH$_2$).

ESI-HRMS: *m/z* calculated for C$_{16}$H$_{16}$ClNO$_3$SNa$^+$ ([M+Na]$^+$): 360.0432; found: 360.0431.

3-((4-Bromophenyl)sulfonyl)-6-phenyl-1,3-oxazinane (55v)
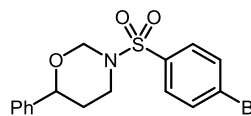
Obtained following the *General Procedure C*, as a white solid (58 mg, 76%).

^{1}H NMR (501 MHz, CDCl$_3$) δ 7.85 (d, *J* = 8.6 Hz, 2H), 7.72 (d, *J* = 8.6 Hz, 2H), 7.32 – 7.23 (m, 3H), 6.97 – 6.93 (m, 2H), 5.69 (dd, *J* = 11.3, 2.2 Hz, 1H), 4.68 (d, *J* = 11.4 Hz, 1H), 4.46 (dd, *J* = 11.3, 2.8 Hz, 1H), 4.06 (ddt, *J* = 14.6, 4.5, 2.1 Hz, 1H), 3.43 (ddd, *J* = 14.7, 12.8, 3.5 Hz, 1H), 1.51 – 1.46 (m, 1H), 1.40 (dddd, *J* = 13.7, 12.7, 11.2, 4.9 Hz, 1H).

^{13}C NMR (126 MHz, CDCl$_3$) δ 140.7 (C), 140.0 (C), 132.6 (CH), 129.6 (CH), 128.7 (CH), 128.3 (CH), 128.1 (C), 125.7 (CH), 79.7 (CH), 78.5 (CH$_2$), 45.0 (CH$_2$), 30.9 (CH$_2$).

ESI-HRMS: *m/z* calculated for C$_{16}$H$_{16}$BrNO$_3$SNa$^+$ ([M+Na]$^+$): 403.9927; found: 403.9926.

3-((4-Nitrophenyl)sulfonyl)-6-phenyl-1,3-oxazinane (55w)
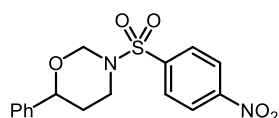
Obtained following the *General Procedure C*, as a white solid (25 mg, 36%).

^{1}H NMR (501 MHz, CDCl$_3$) δ 8.40 (d, J = 8.8 Hz, 2H), 8.18 (d, J = 8.8 Hz, 2H), 7.28 – 7.23 (m, 3H), 6.97 – 6.93 (m, 2H), 5.73 (dd, J = 11.3, 2.2 Hz, 1H), 4.74 (d, J = 11.4 Hz, 1H), 4.50 (dd, J = 11.5, 2.5 Hz, 1H), 4.08 (ddt, J = 14.5, 4.6, 2.1 Hz, 1H), 3.49 (ddd, J = 14.7, 12.9, 3.3 Hz, 1H), 1.55 (dq, J = 13.8, 2.7 Hz, 1H), 1.33 (dddd, J = 13.9, 12.9, 11.4, 4.9 Hz, 1H).

^{13}C NMR (126 MHz, CDCl$_3$) δ 150.3 (C), 146.8 (C), 140.4 (C), 129.3 (CH), 128.7 (CH), 128.4 (CH), 125.4 (CH), 124.5 (CH), 79.6 (CH), 78.5 (CH$_2$), 45.0 (CH$_2$), 31.1 (CH$_2$).

ESI-HRMS: *m/z* calculated for C$_{16}$H$_{16}$N$_2$O$_5$SNa$^+$ ([M+Na]$^+$): 371.0672; found: 371.0673.

3-((3-Chlorophenyl)sulfonyl)-6-phenyl-1,3-oxazinane (55x)
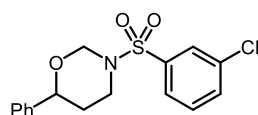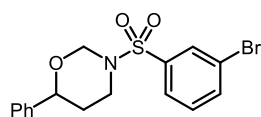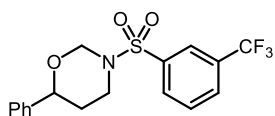
Obtained following the *General Procedure C*, as a white solid (30 mg, 44%).

^{1}H NMR (501 MHz, CDCl$_3$) δ 8.01 (t, J = 1.9 Hz, 1H), 7.88 (dt, J = 7.8, 1.5 Hz, 1H), 7.59 (ddd, J = 8.0, 2.2, 1.1 Hz, 1H), 7.50 (t, J = 7.9 Hz, 1H), 7.31 – 7.23 (m, 3H), 7.05 – 7.00 (m, 2H), 5.73 (dd, J = 11.3, 2.2 Hz, 1H), 4.70 (d, J = 11.3 Hz, 1H), 4.48 (dd, J = 11.5, 2.6 Hz, 1H), 4.03 (ddt, J = 14.7, 4.6, 2.1 Hz, 1H), 3.45 (ddd, J = 14.6, 12.9, 3.3 Hz, 1H), 1.49 (dq, J = 13.8, 2.7 Hz, 1H), 1.37 – 1.25 (m, 1H).

^{13}C NMR (126 MHz, CDCl$_3$) δ 142.6 (C), 140.8 (C), 135.6 (C), 133.1 (CH), 130.5 (CH), 128.6 (CH), 128.2 (CH), 128.1 (CH), 126.2 (CH), 125.6 (CH), 79.7 (CH), 78.5 (CH$_2$), 44.9 (CH$_2$), 31.2 (CH$_2$).

CI-HRMS: *m/z* calculated for C$_{16}$H$_{17}$ClNO$_3$S$^+$ ([M+H]$^+$): 338.0612; found: 338.0618.

3-((3-Bromophenyl)sulfonyl)-6-phenyl-1,3-oxazinane (55y)

Obtained following the *General Procedure C*, as a white solid (49 mg, 64%).

^{1}H NMR (501 MHz, CDCl$_3$) δ 8.16 (t, J = 1.8 Hz, 1H), 7.92 (ddd, J = 8.0, 1.8, 1.1 Hz, 1H), 7.75 (ddd, J = 8.0, 1.9, 1.0 Hz, 1H), 7.43 (t, J = 7.9 Hz, 1H), 7.32 – 7.23 (m, 3H), 7.06 – 7.02 (m, 2H), 5.73 (dd, J = 11.3, 2.2 Hz, 1H), 4.70 (d, J = 11.4 Hz, 1H), 4.48 (dd, J = 11.5, 2.6 Hz, 1H), 4.02 (ddt, J = 14.6, 4.6, 2.0 Hz, 1H), 3.45 (ddd, J = 14.6, 12.9, 3.3 Hz, 1H), 1.49 (dq, J = 13.9, 2.3 Hz, 1H), 1.37 – 1.23 (m, 1H).

^{13}C NMR (126 MHz, CDCl$_3$) δ 142.8 (C), 140.8 (C), 136.0 (CH), 130.9 (CH), 130.8 (CH), 128.6 (CH), 128.2 (CH), 126.6 (CH), 125.7 (CH), 123.4 (C), 79.7 (CH), 78.5 (CH$_2$), 44.9 (CH$_2$), 31.2 (CH$_2$).

CI-HRMS: *m/z* calculated for C$_{16}$H$_{17}$BrNO$_3$S$^+$ ([M+H]$^+$): 382.0107; found: 382.0110.

6-Phenyl-3-((3-(trifluoromethyl)phenyl)sulfonyl)-1,3-oxazinane (55z)

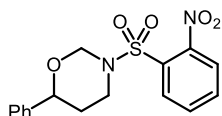Obtained following the *General Procedure C*, as a white solid (25 mg, 34%).

^{1}H NMR (501 MHz, CDCl$_3$) δ 8.27 (s, 1H), 8.19 (d, *J* = 7.9 Hz, 1H), 7.88 (d, *J* = 7.8 Hz, 1H), 7.71 (t, *J* = 7.9 Hz, 1H), 7.30 – 7.23 (m, 3H), 7.00 – 6.93 (m, 2H), 5.75 (dd, *J* = 11.3, 2.3 Hz, 1H), 4.72 (d, *J* = 11.4 Hz, 1H), 4.48 (dd, *J* = 11.4, 2.5 Hz, 1H), 4.06 (ddt, *J* = 14.7, 4.6, 2.1 Hz, 1H), 3.48 (ddd, *J* = 14.6, 12.9, 3.3 Hz, 1H), 1.51 (dq, *J* = 13.8, 2.7 Hz, 1H), 1.27 (tdd, *J* = 13.5, 11.5, 4.9 Hz, 1H).

^{19}F NMR (471 MHz, CDCl$_3$) δ -62.75 (s, 3F).

^{13}C NMR (126 MHz, CDCl$_3$) δ 142.2 (C), 140.6 (C), 132.2 (q, *J* = 33.4 Hz, C), 131.3 (CH), 130.1 (CH), 129.6 (q, *J* = 3.6 Hz, CH), 128.6 (CH), 128.2 (CH), 125.5 (CH), 125.0 (q, *J* = 3.8 Hz, CH), 123.4 (q, *J* = 273.0 Hz, C), 79.7 (CH), 78.5 (CH$_2$), 45.0 (CH$_2$), 31.1 (CH$_2$).

CI-HRMS: *m/z* calculated for C$_{17}$H$_{17}$F$_3$NO$_3$S$^+$ ([M+H]$^+$): 372.0876; found: 372.0884.

**3-((2-Nitrophenyl)sulfonyl)-6-phenyl-1,3-oxazinane (55za)**

Obtained following the *General Procedure C*, as a white solid (45 mg, 61%).

^{1}H NMR (501 MHz, CDCl$_3$) δ 8.19 – 8.15 (m, 1H), 7.76 – 7.71 (m, 2H), 7.67 – 7.61 (m, 1H), 7.34 – 7.24 (m, 3H), 7.17 – 7.12 (m, 2H), 5.66 (dd, *J* = 11.1, 2.3 Hz, 1H), 4.74 (d, *J* = 11.1 Hz, 1H), 4.56 (dd, *J* = 11.5, 2.6 Hz, 1H), 4.16 (ddt, *J* = 14.3, 4.7, 2.2 Hz, 1H), 3.44 (ddd, *J* = 14.2, 12.5, 3.2 Hz, 1H), 1.85 (dddd, *J* = 14.0, 12.6, 11.4, 4.8 Hz, 1H), 1.74 (dq, *J* = 14.0, 2.7 Hz, 1H).

^{13}C NMR (126 MHz, CDCl$_3$) δ 140.8, 133.9, 133.7, 131.9, 131.3, 128.6, 128.2, 125.8, 124.2, 79.8, 78.5, 45.3, 32.2.

ESI-HRMS: *m/z* calculated for C$_{16}$H$_{16}$N$_2$O$_5$SNa$^+$ ([M+Na]$^+$): 371.0672; found: 371.0674.

3-((3,5-Difluorophenyl)sulfonyl)-6-phenyl-1,3-oxazinane (55zb)
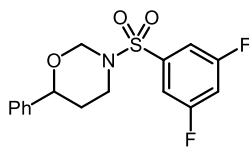
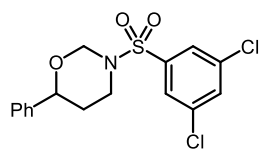Obtained following the *General Procedure C*, as a white solid (38 mg, 53%).

^{1}H NMR (501 MHz, CDCl$_3$) δ 7.57 – 7.51 (m, 2H), 7.33 – 7.25 (m, 3H), 7.10 – 7.03 (m, 3H), 5.70 (dd, *J* = 11.3, 2.3 Hz, 1H), 4.71 (d, *J* = 11.3 Hz, 1H), 4.50 (dd, *J* = 11.5, 2.6 Hz, 1H), 4.03 (ddt, *J* = 14.5, 4.6, 2.1 Hz, 1H), 3.47 (ddd, *J* = 14.6, 12.9, 3.3 Hz, 1H), 1.56 (dq, *J* = 13.9, 2.7 Hz, 1H), 1.36 (dddd, *J* = 13.9, 12.9, 11.4, 4.9 Hz, 1H).

^{19}F NMR (471 MHz, CDCl$_3$) δ -105.51 (s, 2F).

^{13}C NMR (126 MHz, CDCl$_3$) δ 163.9 (d, *J* = 11.5 Hz, C), 161.8 (d, *J* = 11.5 Hz, C), 143.8 (t, *J* = 8.2 Hz, C), 140.5 (C), 128.7 (CH), 128.2 (CH), 125.4 (CH), 111.7 (d, *J* = 7.3 Hz, CH), 111.5 (d, *J* = 7.2 Hz, CH), 108.7 (t, *J* = 24.9 Hz, CH), 79.6 (CH), 78.4 (CH$_2$), 44.9 (CH$_2$), 31.2 (CH$_2$).

CI-HRMS: *m/z* calculated for C$_{16}$H$_{16}$F$_2$NO$_3$S$^+$ ([M+H]$^+$): 340.0813; found: 340.0819.

## 3-((3,5-Dichlorophenyl)sulfonyl)-6-phenyl-1,3-oxazinane (55zc)

Obtained following the *General Procedure C*, as a white solid (31 mg, 39%).

^{1}H NMR (501 MHz, CDCl$_3$) δ 7.89 (d, *J* = 1.9 Hz, 2H), 7.59 (t, *J* = 1.9 Hz, 1H), 7.35 – 7.24 (m, 3H), 7.13 – 7.04 (m, 2H), 5.73 (dd, *J* = 11.4, 2.3 Hz, 1H), 4.72 (d, *J* = 11.4 Hz, 1H), 4.52 (dd, *J* = 11.5, 2.6 Hz, 1H), 4.00 (ddt, *J* = 14.7, 4.8, 2.3 Hz, 1H), 3.48 (ddd, *J* = 14.8, 13.0, 3.3 Hz, 1H), 1.54 (dq, *J* = 14.0, 2.7 Hz, 1H), 1.36 – 1.24 (m, 1H).

^{13}C NMR (126 MHz, CDCl$_3$) δ 143.8 (C), 140.7 (C), 136.3 (C), 133.0 (CH), 128.7 (CH), 128.3 (CH), 126.5 (CH), 125.5 (CH), 79.7 (CH), 78.5 (CH$_2$), 44.9 (CH$_2$), 31.4 (CH$_2$).

ESI-HRMS: *m/z* calculated for C$_{16}$H$_{15}$Cl$_2$NO$_3$SNa$^+$ ([M+Na]$^+$): 394.0042; found: 394.0045.

6-Phenyl-3-((3,4,5-trifluorophenyl)sulfonyl)-1,3-oxazinane (55zd)
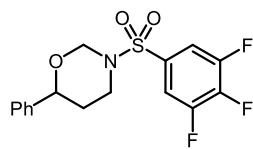
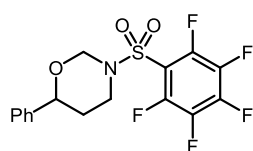Obtained following the *General Procedure C*, as a white solid (40 mg, 56%).

^{1}H NMR (501 MHz, CDCl$_3$) δ 7.67 (t, *J* = 6.2 Hz, 2H), 7.37 – 7.25 (m, 3H), 7.12 – 7.05 (m, 2H), 5.69 (dd, *J* = 11.3, 2.3 Hz, 1H), 4.72 (d, *J* = 11.4 Hz, 1H), 4.53 (dd, *J* = 11.4, 2.6 Hz, 1H), 4.01 (ddt, *J* = 14.6, 4.6, 2.1 Hz, 1H), 3.48 (ddd, *J* = 14.6, 12.9, 3.3 Hz, 1H), 1.59 (dq, *J* = 13.9, 2.7 Hz, 1H), 1.41 – 1.31 (m, 1H).

^{19}F NMR (471 MHz, CDCl$_3$) δ -129.56 (d, *J* = 20.1 Hz, 2F), -151.52 (t, *J* = 20.0 Hz, 1F).

^{13}C NMR (126 MHz, CDCl$_3$) δ 140.5, 128.8, 128.3, 125.4, 113.3 (d, *J* = 6.2 Hz), 113.1 (d, *J* = 6.2 Hz), 79.6, 78.5, 45.0, 31.3. *(Other aromatic carbons could not be observed)*

CI-HRMS: *m/z* calculated for C$_{16}$H$_{15}$F$_3$NO$_3$SNa$^+$ ([M+H]$^+$): 358.0719; found: 358.0727.

3-((Perfluorophenyl)sulfonyl)-6-phenyl-1,3-oxazinane (55ze)

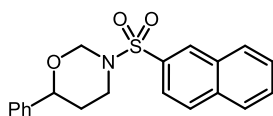Obtained following the *General Procedure C*, as a white solid (40 mg, 51%).

^{1}H NMR (501 MHz, CDCl$_3$) δ 7.35 – 7.27 (m, 3H), 7.13 – 7.09 (m, 2H), 5.71 (dd, *J* = 11.2, 2.3 Hz, 1H), 4.77 (d, *J* = 11.2 Hz, 1H), 4.57 (dd, *J* = 11.4, 2.6 Hz, 1H), 4.25 (ddt, *J* = 14.3, 4.6, 2.1 Hz, 1H), 3.54 (ddd, *J* = 14.3, 12.8, 3.3 Hz, 1H), 1.79 (dq, *J* = 14.0, 2.7 Hz, 1H), 1.64 (tdd, *J* = 13.5, 11.4, 5.0 Hz, 1H).

^{19}F NMR (471 MHz, CDCl$_3$) δ -134.60 (dt, *J* = 20.8, 6.0 Hz, 2F), -145.53 (tt, *J* = 20.9, 6.5 Hz, 1F), -157.93 – -158.85 (m, 2F).

^{13}C NMR (126 MHz, CDCl$_3$) δ 140.4 (C), 128.8 (CH), 128.3 (CH), 125.2 (CH), 79.2 (CH), 78.2 (CH$_2$), 45.3 (CH$_2$), 31.8 (CH$_2$). *(Carbon atoms from the C$_6$F$_5$ unit were not visible)*

CI-HRMS: *m/z* calculated for $C_{16}H_{13}F_5NO_3S^+$ ([M+H]$^+$): 394.0531; found: 394.0530.

**3-(Naphthalen-2-ylsulfonyl)-6-phenyl-1,3-oxazinane (55zf)**

Obtained following the *General Procedure C*, as a white solid (35 mg, 48%).

^{1}H NMR (501 MHz, CDCl$_3$) δ 8.55 (d, *J* = 1.8 Hz, 1H), 8.16 – 7.84 (m, 4H), 7.66 (dddd, *J* = 20.4, 8.2, 6.9, 1.3 Hz, 2H), 7.23 – 7.05 (m, 3H), 6.89 – 6.76 (m, 2H), 5.81 (dd, *J* = 11.2, 2.2 Hz, 1H), 4.71 (d, *J* = 11.2 Hz, 1H), 4.42 (dd, *J* = 11.3, 2.7 Hz, 1H), 4.11 (ddt, *J* = 14.5, 4.5, 2.1 Hz, 1H), 3.43 (ddd, *J* = 14.5, 12.7, 3.4 Hz, 1H), 1.45 – 1.24 (m, 2H).

^{13}C NMR (126 MHz, CDCl$_3$) δ 140.8 (C), 137.7 (C), 135.1 (C), 132.5 (C), 129.51 (CH), 129.46 (CH), 129.3 (CH), 129.1 (CH), 128.5 (CH), 128.1 (CH), 128.0 (CH), 127.8 (CH), 125.7 (CH), 123.4 (CH), 79.7 (CH), 78.5 (CH$_2$), 44.9 (CH$_2$), 31.1 (CH$_2$).

ESI-HRMS: *m/z* calculated for $C_{20}H_{19}NO_3SNa^+$ ([M+Na]$^+$): 376.0978; found: 376.0977.


3-(Methylsulfonyl)-6-phenyl-1,3-oxazinane (55zg)
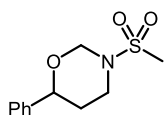
Obtained following the *General Procedure C*, as a white solid (26 mg, 54%).

^{1}H NMR (501 MHz, CDCl$_3$) δ 7.37 (ddt, *J* = 7.8, 5.5, 1.3 Hz, 2H), 7.34 – 7.29 (m, 3H), 5.53 (dd, *J* = 11.6, 2.3 Hz, 1H), 4.74 (d, *J* = 11.6 Hz, 1H), 4.64 (dd, *J* = 11.3, 2.7 Hz, 1H), 4.14 (ddt, *J* = 14.8, 4.7, 2.0 Hz, 1H), 3.53 (ddd, *J* = 14.8, 12.9, 3.5 Hz, 1H), 3.10 (s, 3H), 1.96 (dddd, *J* = 14.0, 12.9, 11.4, 5.0 Hz, 1H), 1.87 – 1.80 (m, 1H).

^{13}C NMR (126 MHz, CDCl$_3$) δ 140.9 (C), 128.8 (CH), 128.3 (CH), 125.6 (CH), 79.7 (CH), 78.2 (CH$_2$), 44.9 (CH$_2$), 42.0 (CH$_3$), 31.9 (CH$_2$).

CI-HRMS: *m/z* calculated for $C_{11}H_{16}NO_3S^+$ ([M+H]$^+$): 242.0845; found: 242.0850.

3-(Isopropylsulfonyl)-6-phenyl-1,3-oxazinane (55zh)
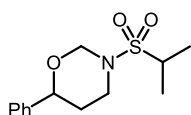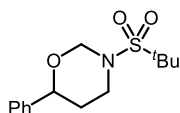
Obtained following the *General Procedure C*, as a white solid (39 mg, 71%).

^{1}H NMR (501 MHz, CDCl$_3$) δ 7.55 – 7.23 (m, 5H), 5.41 (dd, *J* = 11.0, 2.2 Hz, 1H), 4.69 (d, *J* = 10.9 Hz, 1H), 4.58 (dd, *J* = 11.4, 2.5 Hz, 1H), 4.01 (ddt, *J* = 14.2, 4.7, 2.2 Hz, 1H), 3.44 (ddd, *J* = 14.3, 12.5, 3.1 Hz, 1H), 3.19 (hept, *J* = 6.9 Hz, 1H), 1.98 (dddd, *J* = 13.7, 12.5, 11.4, 4.9 Hz, 1H), 1.83 (dq, *J* = 13.6, 2.6 Hz, 1H), 1.44 (dd, *J* = 21.2, 6.8 Hz, 6H).

^{13}C NMR (126 MHz, CDCl$_3$) δ 141.1 (C), 128.7 (CH), 128.2 (CH), 125.9 (CH), 79.7 (CH), 78.2 (CH$_2$), 54.5 (CH), 45.3 (CH$_2$), 33.3 (CH$_2$), 17.0 (CH$_3$), 16.6 (CH$_3$).

CI-HRMS: *m/z* calculated for $C_{13}H_{20}NO_3S^+$ ([M+H]$^+$): 270.1158; found: 270.1157.

### 3-(*tert*-Butylsulfonyl)-6-phenyl-1,3-oxazinane (55zi)

Obtained following the *General Procedure C*, as a white solid (30 mg, 53%).

^{1}H NMR (501 MHz, CDCl$_3$) δ 7.36 (d, *J* = 4.4 Hz, 4H), 7.30 (ddd, *J* = 8.8, 5.0, 3.8 Hz, 1H), 5.37 (dd, *J* = 10.7, 2.3 Hz, 1H), 4.69 (d, *J* = 10.6 Hz, 1H), 4.57 (dd, *J* = 11.4, 2.6 Hz, 1H), 4.03 (ddt, *J* = 13.9, 4.7, 2.2 Hz, 1H), 3.43 (ddd, *J* = 13.8, 12.4, 2.9 Hz, 1H), 2.04 (dddd, *J* = 13.7, 12.4, 11.4, 4.8 Hz, 1H), 1.82 (dq, *J* = 13.6, 2.5 Hz, 1H), 1.42 (s, 9H).

^{13}C NMR (126 MHz, CDCl$_3$) δ 141.2 (C), 128.7 (CH), 128.1 (CH), 126.0 (CH), 79.7 (CH), 79.0 (CH$_2$), 61.1 (C), 46.6 (CH$_2$), 33.7 (CH$_2$), 24.4 (CH$_3$).

CI-HRMS: *m/z* calculated for C$_{14}$H$_{22}$NO$_3$S$^+$ ([M+H]$^+$): 284.1315; found: 284.1313.

### 3-(Cyclopropylsulfonyl)-6-phenyl-1,3-oxazinane (55zj)
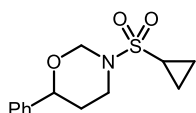
Obtained following the *General Procedure C*, as a white solid (35 mg, 65%).

^{1}H NMR (501 MHz, CDCl$_3$) δ 7.40 – 7.34 (m, 2H), 7.34 – 7.29 (m, 3H), 5.52 (dd, *J* = 11.5, 2.2 Hz, 1H), 4.73 (d, *J* = 11.5 Hz, 1H), 4.63 (dd, *J* = 11.4, 2.6 Hz, 1H), 4.08 (ddt, *J* = 14.7, 4.5, 2.0 Hz, 1H), 3.52 (ddd, *J* = 14.7, 12.9, 3.2 Hz, 1H), 2.56 (tt, *J* = 7.9, 4.9 Hz, 1H), 2.09 (dddd, *J* = 13.7, 12.9, 11.4, 4.9 Hz, 1H), 1.82 (dq, *J* = 13.8, 2.7 Hz, 1H), 1.37 – 1.23 (m, 2H), 1.16 – 1.03 (m, 2H).

^{13}C NMR (126 MHz, CDCl$_3$) δ 141.2 (C), 128.8 (CH), 128.2 (CH), 125.7 (CH), 79.6 (CH), 78.5 (CH$_2$), 45.2 (CH$_2$), 32.5 (CH$_2$), 31.5 (CH), 6.5 (CH$_2$), 6.0 (CH$_2$).

CI-HRMS: *m/z* calculated for C$_{13}$H$_{18}$NO$_3$S$^+$ ([M+H]$^+$): 268.1002; found: 268.1006.

3-((Fluoromethyl)sulfonyl)-6-phenyl-1,3-oxazinane (55zk)
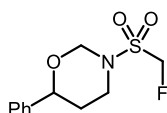
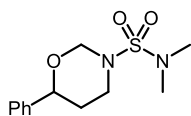Obtained following the *General Procedure C*, as a white solid (11 mg, 21%).

^{1}H NMR (501 MHz, CDCl$_3$) δ 7.44 – 7.30 (m, 5H), 5.44 (dd, *J* = 11.4, 2.3 Hz, 1H), 5.35 (d, *J* = 10.0 Hz, 1H), 5.27 – 5.23 (m, 1H), 5.15 (d, *J* = 10.0 Hz, 1H), 4.77 (d, *J* = 11.5 Hz, 1H), 4.62 (d, *J* = 10.8 Hz, 1H), 4.16 (ddt, *J* = 14.5, 4.7, 2.1 Hz, 1H), 3.55 (ddd, *J* = 14.4, 12.8, 3.3 Hz, 1H), 2.14 – 2.04 (m, 1H), 1.83 (dq, *J* = 14.0, 2.7 Hz, 1H).

^{19}F NMR (471 MHz, CDCl$_3$) δ -211.07 (s, 1F).

^{13}C NMR (126 MHz, CDCl$_3$) δ 140.6 (C), 128.8 (CH), 128.4 (CH), 125.9 (CH), 89.7 (d, *J* = 215.1 Hz, CH$_2$), 80.0 (CH), 78.1 (CH$_2$), 45.5 (CH$_2$), 32.5 (d, *J* = 2.9 Hz, CH$_2$).

ESI-HRMS: *m/z* calculated for C$_{11}$H$_{14}$FNO$_3$SNa$^+$ ([M+Na]$^+$): 282.0571; found: 282.0572.

**N,N-Dimethyl-6-phenyl-1,3-oxazinane-3-sulfonamide (55zl)**

Obtained following the *General Procedure C*, as a white solid (21 mg, 39%).

^{1}H NMR (501 MHz, CDCl$_3$) δ 7.40 – 7.29 (m, 5H), 5.43 (dd, *J* = 11.1, 2.3 Hz, 1H), 4.67 (d, *J* = 11.1 Hz, 1H), 4.58 (dd, *J* = 11.5, 2.5 Hz, 1H), 3.91 (ddt, *J* = 14.3, 4.6, 2.1 Hz, 1H), 3.40 (ddd, *J* = 14.3, 12.7, 3.1 Hz, 1H), 2.88 (s, 6H), 2.04 (dddd, *J* = 13.7, 12.6, 11.4, 4.8 Hz, 1H), 1.77 (dq, *J* = 13.7, 2.6 Hz, 1H).

^{13}C NMR (126 MHz, CDCl$_3$) δ 141.1, 128.7, 128.1, 125.8, 79.7, 78.7, 45.2, 38.3, 32.2.

ESI-HRMS: *m/z* calculated for C$_{12}$H$_{18}$N$_2$O$_3$SNa$^+$ ([M+Na]$^+$): 293.0930; found: 293.0929.

(1*S*,4*R*)-7,7-Dimethyl-1-((6-phenyl-1,3-oxazinan-3-yl)sulfonyl)bicyclo[2.2.1]heptan-2-one (55zm)
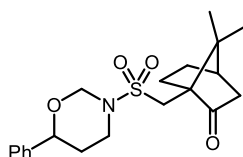
Obtained following the *General Procedure C*, as a mixture of two diastereomers in almost equal amounts (d.r. = 1.3:1), as a white solid (20 mg, 29% global yield).

Major diastereomer:

^{1}H NMR (600 MHz, CDCl$_3$) δ 7.39 – 7.28 (m, 5H), 5.54 (dd, *J* = 11.3, 2.2 Hz, 1H), 4.72 (d, *J* = 11.3 Hz, 1H), 4.61 (d, *J* = 11.5, 1H), 4.13 (ddt, *J* = 14.3, 4.7, 2.1 Hz, 1H), 3.72 (d, *J* = 14.6 Hz, 1H), 3.47 (ddd, *J* = 14.4, 12.8, 3.2 Hz, 1H), 2.93 (d, *J* = 14.3 Hz, 1H), 2.61 – 2.53 (m, 1H), 2.43 – 2.37 (m, 1H), 2.15 – 2.00 (m, 3H), 1.97 (d, *J* = 18.4 Hz, 1H), 1.85 – 1.80 (m, 1H), 1.70 – 1.65 (m, 1H), 1.47 – 1.42 (m, 1H), 1.17 (s, 3H), 0.92 (s, 3H).

^{13}C NMR (125 MHz, CDCl$_3$) δ 215.2, 141.1, 128.8, 128.2, 125.9, 79.8, 77.9, 58.9, 51.2, 47.9, 44.9, 43.1, 42.7, 32.7, 27.0, 25.2, 20.2, 19.9.

ESI-HRMS: *m/z* calculated for C$_{20}$H$_{27}$NO$_4$SNa$^+$ ([M+Na]$^+$): 400.1553; found: 400.1554.

Minor diastereomer:

^{1}H NMR (600 MHz, CDCl$_3$) δ 7.39 – 7.28 (m, 5H), 5.51 (dd, *J* = 11.3, 2.2 Hz, 1H), 4.70 (d, *J* = 11.3 Hz, 1H), 4.60 (d, *J* = 11.5 Hz, 1H), 4.17 (ddt, *J* = 14.7, 4.8, 2.1 Hz, 1H), 3.56 (d, *J* = 14.7 Hz, 1H), 3.52 (ddd, *J* = 14.7, 4.7, 2.1 Hz, 1H), 3.08 (d, *J* = 14.6 Hz, 1H), 2.61 – 2.53 (m, 1H), 2.43 – 2.37 (m, 1H), 2.15 – 2.00 (m, 3H), 1.97 (d, *J* = 18.4 Hz, 1H), 1.85 – 1.80 (m, 1H), 1.70 – 1.65 (m, 1H), 1.47 – 1.42 (m, 1H), 1.17 (s, 3H), 0.92 (s, 3H).

^{13}C NMR (125 MHz, CDCl$_3$) δ 215.2, 141.0, 128.8, 128.2, 125.9, 79.9, 78.0, 58.8, 50.9, 48.1, 44.8, 42.9, 42.7, 32.2, 27.1, 25.2, 20.2, 19.9.

ESI-HRMS: *m/z* calculated for C$_{20}$H$_{27}$NO$_4$SNa$^+$ ([M+Na]$^+$): 400.1553; found: 400.1554.

3-((((6-Phenyl-1,3-oxazinan-3-yl)sulfonyl)methyl)benzo[*d*]isoxazole (55zn)
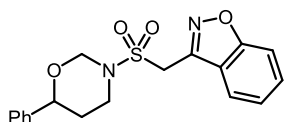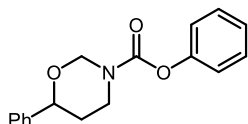
Obtained following the *General Procedure C*, as a white solid (50 mg, 70%).

^{1}H NMR (501 MHz, CDCl$_3$) δ 7.98 (dt, *J* = 8.0, 1.0 Hz, 1H), 7.64 – 7.58 (m, 2H), 7.42 – 7.28 (m, 6H), 5.29 (dd, *J* = 10.9, 2.2 Hz, 1H), 4.79 (d, *J* = 1.9 Hz, 2H), 4.59 (d, *J* = 10.9 Hz, 1H), 4.52 (dd, *J* = 11.4, 2.5 Hz, 1H), 3.96 (ddt, *J* = 14.1, 4.7, 2.1 Hz, 1H), 3.42 (ddd, *J* = 14.0, 12.7, 3.1 Hz, 1H), 2.02 (dddd, *J* = 13.8, 12.7, 11.4, 5.0 Hz, 1H), 1.77 (dq, *J* = 13.8, 2.6 Hz, 1H).

^{13}C NMR (126 MHz, CDCl$_3$) δ 164.0 (C), 149.5 (C), 140.6 (C), 130.7 (CH), 128.7 (CH), 128.3 (CH), 126.0 (CH), 124.5 (CH), 122.8 (CH), 120.8 (C), 110.1 (CH), 80.0 (CH), 78.1 (CH$_2$), 50.6 (CH$_2$), 45.2 (CH$_2$), 32.6 (CH$_2$).

ESI-HRMS: *m/z* calculated for C$_{18}$H$_{18}$N$_2$O$_4$SNa$^+$ ([M+Na]$^+$): 381.0879; found: 381.0879.

Phenyl 6-phenyl-1,3-oxazinane-3-carboxylate (57a)

Obtained by adapting the *General Procedure D*, using 3.0 equiv. of phenyl carbamate, 20 mol% of HPF$_6$, and 2 mL of CHCl$_3$ as a white solid (19 mg, 34%).

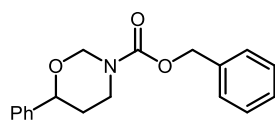NMR at room temperature (298 K): broad bands, rotameric mixture.

NMR at 233 K (–40 °C) shows two main rotamers (ratio approx. 65:35).

^{1}H NMR (600 MHz, CDCl$_3$, 233 K) δ 7.44 – 7.37 (m, 6H), 7.37 – 7.32 (m, 1H), 7.27 – 7.23 (m, 1H), 7.17 – 7.12 (m, 2H), 5.92 (dd, *J* = 10.6, 2.1 Hz, 0.65H, *major*), 5.87 (dd, *J* = 10.2, 2.1 Hz, 0.37H, *minor*), 4.75 (d, *J* = 10.6 Hz, 0.66H, *major*), 4.66 (dd, *J* = 11.6, 2.2 Hz, 1H), 4.59 (d, *J* = 10.3 Hz, 0.36H, *minor*), 4.53 (ddt, *J* = 13.7, 4.5, 2.1 Hz, 0.39H, *minor*), 4.46 (ddt, *J* = 13.5, 4.5, 2.0 Hz, 0.67H, *major*), 3.47 (ddd, *J* = 13.7, 12.5, 3.1 Hz, 0.39H, *minor*), 3.30 (ddd, *J* = 13.5, 12.5, 3.1 Hz, 0.66H, *major*), 2.02 (tddd, *J* = 21.2, 12.5, 11.3, 4.8 Hz, 1H), 1.89 (ddq, *J* = 13.3, 9.9, 2.6 Hz, 1H).

^{13}C NMR (151 MHz, CDCl$_3$, 233 K) δ 153.3 (C, *minor*), 153.1 (C, *major*), 150.74 (C, *major*), 150.71 (C, *minor*), 141.0 (C, *minor*), 140.7 (C, *major*), 129.5 (CH), 128.73 (CH, *major*), 128.65 (CH, *minor*), 128.3 (CH, *major*), 128.1 (CH, *minor*), 126.0 (CH, *major*), 125.84 (CH, *minor*), 125.80 (CH, *major*), 125.78 (CH, *minor*), 121.9 (CH, *major*), 121.8 (CH, *minor*), 79.9 (CH, *major*), 79.7 (CH, *minor*), 76.8 (CH$_2$, *major*), 76.5 (CH$_2$, *minor*), 43.7 (CH$_2$, *minor*), 43.1 (CH$_2$, *major*), 33.5 (CH$_2$, *minor*), 32.7 (CH$_2$, *major*).

CI-HRMS: *m/z* calculated for C$_{17}$H$_{18}$NO$_3$$^+$ ([M+H]$^+$): 284.1281; found: 284.1281

Benzyl 6-phenyl-1,3-oxazinane-3-carboxylate (57b)

Obtained by adapting the *General Procedure D*, using 3.0 equiv. of benzyl carbamate, 20 mol% of HPF$_6$, and 2 mL of CHCl$_3$ as a white solid (30 mg, 23%).

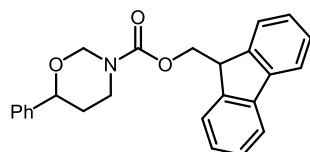NMR at room temperature (298 K): broad bands, rotameric mixture.

NMR at 233 K (–40 °C) shows two main rotamers (ratio approx. 65:35).

^{1}H NMR (600 MHz, CDCl$_3$, 233K) δ 7.42 – 7.29 (m, 10H), 5.84 (dd, J = 10.3, 2.0 Hz, 0.37H), 5.73 (dd, J = 10.5, 2.1 Hz, 0.62H), 5.23 (d, J = 12.2 Hz, 0.60H), 5.20 (d, J = 12.2 Hz, 0.40H), 5.14 (d, J = 4.6 Hz, 0.60H), 5.12 (d, J = 4.6 Hz, 0.40H), 4.59 (dd, J = 11.4, 2.4 Hz, 1H), 4.58 (d, J = 10.6 Hz, 0.62H), 4.50 (d, J = 10.3 Hz, 0.38H), 4.41 (ddt, J = 13.5, 4.5, 2.0 Hz, 0.64H), 4.32 (ddt, J = 13.7, 4.5, 2.1 Hz, 0.39H), 3.29 (ddd, J = 13.7, 12.4, 3.1 Hz, 0.37H), 3.20 (td, J = 13.0, 3.0 Hz, 0.62H), 1.97 – 1.89 (m, 0.62H), 1.88 – 1.73 (m, 1.40H).

^{13}C NMR (151 MHz, CDCl$_3$, 233K) δ 154.8 (C, *minor*), 154.6 (C, *major*), 141.1 (C, *minor*), 140.9 (C, *major*), 136.04 (C, *minor*), 136.02 (C, *major*), 128.65 (CH, *major*), 128.64 (CH, *minor*), 128.61 (CH, *major*), 128.60 (CH, *minor*), 128.3 (CH), 128.3 (CH), 128.2 (CH), 128.2 (CH), 128.1 (CH), 128.0 (CH), 126.0 (CH, *major*), 125.9 (CH, *minor*), 79.9 (CH, *major*), 79.7 (CH, *minor*), 76.5 (CH$_2$, *major*), 76.4 (CH$_2$, *minor*), 67.52 (CH$_2$, *major*), 67.49 (CH$_2$, *minor*), 43.2 (CH$_2$, *minor*), 43.0 (CH$_2$, *major*), 33.4 (CH$_2$, *minor*), 32.8 (CH$_2$, *major*).

ESI-HRMS: *m/z* calculated for C$_{18}$H$_{19}$NO$_3$Na$^+$ ([M+Na]$^+$): 320.1257; found: 320.1255.

(9*H*-Fluoren-9-yl)methyl 6-phenyl-1,3-oxazinane-3-carboxylate (57c)

Obtained by adapting the *General Procedure D*, using 1.0 mmol (1.0 equiv.) of styrene and 3.0 equiv. of (9*H*-fluoren-9-yl)methyl carbamate, as a white solid (136 mg, 37%)
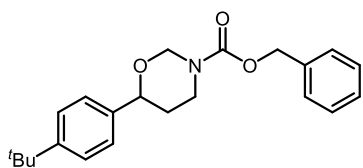
NMR at room temperature (298 K): broad bands, rotameric mixture.

^{1}H NMR (501 MHz, CDCl$_3$) δ 7.78 (d, J = 7.5 Hz, 2H), 7.69 – 7.57 (m, 2H), 7.45 – 7.28 (m, 9H), 5.77 (br d, J = 12.2 Hz, 1H), 4.70 – 4.14 (m, 6 H), 3.32 – 3.17 (m, 1H), 1.83 (m, 2H).

^{13}C NMR (126 MHz, CDCl$_3$) δ 154.8 (C), 144.1 (C), 144.0 (C), 141.5 (C), 141.4 (CH), 128.6 (CH), 128.0 (CH), 127.9 (CH), 127.3 (CH), 127.2 (CH), 126.0 (CH), 125.2 (CH), 120.2 (CH), 120.1 (CH), 80.0 (CH), 76.8 (CH$_2$), 67.9 (CH$_2$), 47.4 (CH), 43.5 (CH$_2$), 33.2 (CH$_2$).

ESI-HRMS: *m/z* calculated for C$_{25}$H$_{23}$NO$_3$Na$^+$ ([M+Na]$^+$): 408.1570; found: 408.1570.

Benzyl 6-phenyl-1,3-oxazinane-3-carboxylate (57d)

Obtained by adapting the *General Procedure D*, using 1.0 mmol (1.0 equiv.) of *p-tert*-butylstyrene and 3.0 equiv. of benzyl carbamate, as a colorless oil (130 mg, 39%).
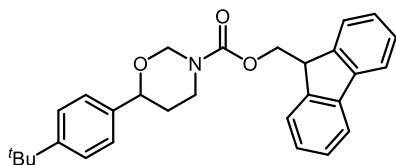
NMR at room temperature (298 K): broad bands, rotameric mixture.

^{1}H NMR (501 MHz, CDCl$_3$) δ 7.46 – 7.17 (m, 10H), 5.77 (m, 0.6H), 5.36 – 4.99 (m, 2.6H), 4.53 (dd, *J* = 11.3, 2.5 Hz, 1H), 4.51 – 4.25 (m, 1H), 3.41 – 3.06 (m, 0.7H), 2.04 – 1.69 (m, 1.8H), 1.31 (s, 9H).

^{13}C NMR (126 MHz, CDCl$_3$) δ 155.3 (C), 154.8 (C), 150.9 (C), 150.3 (C), 138.3 (C), 136.6 (C), 128.6 (CH), 128.5 (CH), 128.2 (CH), 128.1 (CH), 127.8 (CH), 125.8 (CH), 125.8 (CH), 125.6 (CH), 125.5 (CH), 79.65 (CH), 76.8 (CH$_2$), 67.5 (CH$_2$), 66.7 (C), 43.3 (CH$_2$), 34.6 (C), 31.4 (CH$_3$).

ESI-HRMS: *m/z* calculated for C$_{22}$H$_{27}$NO$_3$Na$^+$ ([M+Na]$^+$): 376.1883; found: 376.1882.

(9*H*-Fluoren-9-yl)methyl 6-phenyl-1,3-oxazinane-3-carboxylate (57e)

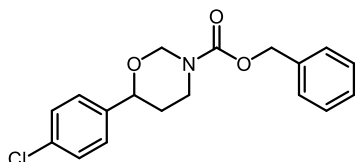Obtained following the *General Procedure D*, as a white solid (75 mg, 35%).

NMR at room temperature (298 K): broad bands, rotameric mixture.

^{1}H NMR (501 MHz, CDCl$_3$) δ 7.78 (d, *J* = 7.5 Hz, 2H), 7.62 (m, 2H), 7.44 – 7.36 (m, 4H), 7.36 – 7.27 (m, 4H), 5.75 (m, 1H), 4.71 – 4.46 (m, 3.6H), 4.44 – 4.34 (m, 1.3H), 4.33 – 4.27 (m, 1.2H), 4.25 – 4.14 (m, 0.4H), 3.31 – 3.11 (m, 1H), 1.96 (m, 0.7H), 1.85 – 1.74 (m, 1.5H), 1.33 (s, 9H).

^{13}C NMR (126 MHz, CDCl$_3$) δ 154.9 (C), 151.1 (C), 144.1 (C), 144.0 (C), 141.5 (C), 138.3 (C), 127.9 (CH), 127.3 (CH), 125.9 (CH), 125.6 (CH), 125.2 (CH), 120.2 (CH), 79.9 (CH), 76.8 (CH$_2$), 67.9 (CH$_2$), 47.4 (CH), 43.5 (CH$_2$), 34.7 (C), 31.5 (CH$_3$).

ESI-HRMS: *m/z* calculated for C$_{29}$H$_{31}$NO$_3$Na$^+$ ([M+Na]$^+$): 464.2196; found: 464.2196.

Benzyl 6-phenyl-1,3-oxazinane-3-carboxylate (57f)

Obtained by adapting the *General Procedure D*, using 1.0 mmol (1.0 equiv.) of *p*-chlorostyrene, as a white solid (50 mg, 15%).
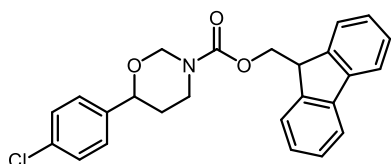
NMR at room temperature (298 K): broad bands, rotameric mixture.

^{1}H NMR (501 MHz, CDCl$_3$) δ 7.41 – 7.33 (m, 4H), 7.34 – 7.28 (m, 3H), 7.26 (d, *J* = 8.2 Hz, 2H), 5.77 (m, 1H), 5.25 – 5.11 (m, 2H), 4.54 (dd, *J* = 10.7, 3.2 Hz, 1H), 4.52 – 4.43 (m, 0.5H), 4.42 – 4.23 (m, 1.5H), 3.30 – 3.10 (m, 0.6H), 1.90 – 1.70 (m, 2.1H).

^{13}C NMR (126 MHz, CDCl$_3$) δ 154.8 (C), 139.9 (C), 136.5 (C), 133.7 (CH), 128.8 (CH), 128.7 (CH), 128.3 (CH), 128.2 (CH), 128.2 (CH), 127.3 (CH), 79.1 (CH), 76.8 (CH$_2$), 67.7 (CH$_2$), 43.3 (CH$_2$).

ESI-HRMS: *m/z* calculated for C$_{18}$H$_{18}$NO$_3$ClNa$^+$ ([M+Na]$^+$): 354.0867; found: 354.0867.

(9*H*-Fluoren-9-yl)methyl 6-phenyl-1,3-oxazinane-3-carboxylate (57g)

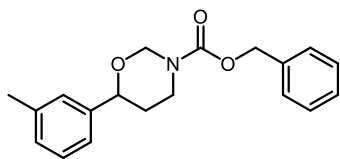Obtained following the *General Procedure D*, as a white solid (38 mg, 45%).

NMR at room temperature (298 K): broad bands, rotameric mixture.

^{1}H NMR (501 MHz, CDCl$_3$) δ 7.77 (d, J = 7.6 Hz, 2H), 7.61 (s, 2H), 7.41 (t, J = 7.4 Hz, 2H), 7.37 – 7.24 (m, 6H), 5.84 – 5.68 (m, 1H), 4.65 – 4.45 (m, 3H), 4.47 – 4.34 (m, 1.4H), 4.33 – 4.23 (s, 1.1H), 4.20 – 4.09 (s, 0.4H), 3.30 – 3.14 (m, 1H), 1.91 – 1.57 (m, 2.1H).

^{13}C NMR (126 MHz, CDCl$_3$) δ 143.9, 141.5, 139.9, 128.8, 127.9, 127.3, 127.3, 125.2, 120.2, 76.7, 47.4, 43.4.

ESI-HRMS: *m/z* calculated for C$_{25}$H$_{22}$NO$_3$ClNa$^+$ ([M+Na]$^+$): 442.1180; found: 442.1183.

Benzyl 6-phenyl-1,3-oxazinane-3-carboxylate (57h)

Obtained by adapting the *General Procedure D* using 1.0 mmol (1.0 equiv.) of *m*-methylstyrene, as a white solid (83 mg, 27%).
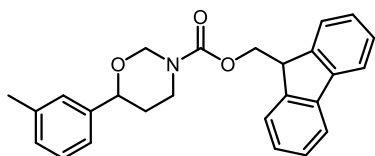
NMR at room temperature (298 K): broad bands, rotameric mixture.

^{1}H NMR (501 MHz, CDCl$_3$) δ 7.40 – 7.27 (m, 5H), 7.22 (t, *J* = 7.6 Hz, 1H), 7.16 (s, 1H), 7.10 (t, *J* = 8.2 Hz, 2H), 5.92 – 5.58 (m, 1H), 5.24 – 5.12 (m, 2H), 4.57 – 4.43 (m, 2H), 4.42 – 4.25 (m, 1H), 3.32 – 3.04 (m, 1H), 2.34 (s, 3H), 1.98 – 1.81 (m, 1H), 1.81 – 1.69 (m, 1H).

^{13}C NMR (126 MHz, CDCl$_3$) δ 154.9 (C), 141.4 (C), 138.3 (C), 136.6 (C), 128.8 (CH), 128.7 (CH), 128.5 (CH), 128.3 (CH), 128.2 (CH), 126.7 (CH), 123.1 (CH), 79.9 (CH), 76.8 (CH$_2$), 67.6 (CH$_2$), 43.4 (CH$_2$), 33.5 (CH$_2$), 33.1 (CH$_2$), 21.7 (CH$_3$).

ESI-HRMS: *m/z* calculated for C$_{19}$H$_{21}$NO$_3$Na$^+$ ([M+Na]$^+$): 334.1414; found: 334.1413.

(9*H*-Fluoren-9-yl)methyl 6-phenyl-1,3-oxazinane-3-carboxylate (57i)

Obtained following the *General Procedure D*, as a white solid (54 mg, 28%).

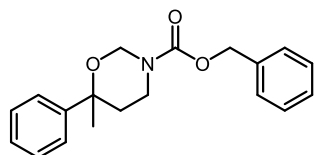NMR at room temperature (298 K): broad bands, rotameric mixture.

^{1}H NMR (501 MHz, CDCl$_3$) δ 7.77 (d, *J* = 7.5 Hz, 2H), 7.67 – 7.55 (m, 3H), 7.48 – 7.29 (m, 4H), 7.29 – 7.21 (m, 1H), 7.21 – 7.01 (m, 3H), 5.83 – 5.71 (m, 1H), 4.65 – 4.46 (m, 4H), 4.45 – 4.34 (m, 1.3H),

4.34 – 4.23 (m, 1.2H), 4.24 – 4.11 (m, 0.5H), 3.29 – 3.13 (m, 1H), 2.36 (s, 3H), 1.99 – 1.85 (m, 0.6H), 1.85 – 1.69 (m, 1.4H).

^{13}C NMR (126 MHz, CDCl$_3$) δ 154.8, 144.0, 141.5, 141.3, 138.3, 128.8, 128.5, 127.9, 127.3, 127.2, 126.7, 125.2, 123.1, 120.2, 120.1, 80.1, 76.8, 67.9, 47.4, 43.5, 33.2, 21.6.

ESI-HRMS: *m/z* calculated for C$_{26}$H$_{25}$NO$_3$Na$^+$ ([M+Na]$^+$): 422.1727; found: 422.1726.

Benzyl 6-phenyl-1,3-oxazinane-3-carboxylate (57j)

Obtained by adapting the *General Procedure D* using 0.7 mmol (1.0 equiv.) of α-methylstyrene and 0.65 mL CHCl$_3$, as a colorless oil (75 mg, 34%).
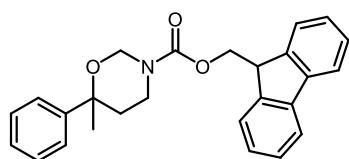
NMR at room temperature (298 K): broad bands, rotameric mixture.

^{1}H NMR (500 MHz, CDCl$_3$) δ 7.40 – 7.38 (m, 4H), 7.37 – 7.35 (m, 4H), 7.34 – 7.29 (m, 3H), 7.29 – 7.26 (m, 1H), 5.30 (d, *J* = 10.5 Hz, 1H), 5.18 (d, *J* = 5.7 Hz, 2H), 4.59 (d, *J* = 10.5 Hz, 1H), 4.01 – 3.92 (m, 1H), 3.26 (t, *J* = 11.4 Hz, 1H), 2.31 (d, *J* = 14.0 Hz, 1H), 2.01 (ddd, *J* = 14.7, 10.3, 3.8 Hz, 1H), 1.46 (s, 3H).

^{13}C NMR (151 MHz, CDCl$_3$) δ 155.0 (C), 143.6 (C), 136.6 (C), 128.9 (CH), 128.6 (CH), 128.5 (CH), 128.2 (CH), 128.1 (CH), 128.0 (CH), 127.3 (CH), 125.9 (CH), 124.9 (CH), 76.7 (C), 71.3 (CH$_2$), 67.4 (CH$_2$), 40.1 (CH$_2$), 33.8 (CH$_2$), 32.2 (CH$_3$).

ESI-HRMS: *m/z* calculated for C$_{19}$H$_{21}$NO$_3$Na$^+$ ([M+Na]$^+$): 334.1414; found: 334.1415.

(9*H*-Fluoren-9-yl)methyl 6-phenyl-1,3-oxazinane-3-carboxylate (57k)

Obtained by adapting the *General Procedure D* using 0.75 mL CHCl$_3$, as a white solid (56.1 mg, 27%).

NMR at room temperature (298 K): broad bands, rotameric mixture.

^{1}H NMR (501 MHz, CDCl$_3$) δ 7.78 (d, *J* = 7.5 Hz, 2H), 7.62 (m, *J* = 7.7 Hz, 2H), 7.48 – 7.38 (m, 6H), 7.32 (m, *J* = 7.4, 5.5, 1.1 Hz, 3H), 5.34 (d, *J* = 10.5 Hz, 1H), 4.63 (d, *J* = 10.7 Hz, 0.5H), 4.54 – 4.37 (m, 2.5H), 4.33 – 4.26 (m, 1H), 4.19 – 4.13 (m, 0.1H), 4.04 (d, *J* = 13.7 Hz, 0.5H), 3.83 (d, *J* = 13.3 Hz, 0.3H), 3.72 (s, 0.5H), 3.23 (ddd, *J* = 13.9, 11.3, 3.1 Hz, 1H), 2.57 (s, 0.1H), 2.40 – 2.32 (m, 0.6H), 2.26 (d, *J* = 13.9 Hz, 0.3H), 2.11 – 1.98 (m, 0.6H), 1.87 (p, *J* = 7.5 Hz, 0.4H), 1.46 (d, *J* = 22.0 Hz, 3H).

^{13}C NMR (126 MHz, CDCl$_3$) δ 155.1 (C), 144.2 (C), 144.4 (C), 141.6 (C), 128.9 (CH), 127.9 (CH), 127.3 (CH), 125.9 (CH), 125.2 (CH), 120.1 (CH), 76.7 (C), 71.3 (CH$_2$), 67.8 (CH$_2$), 47.6 (CH), 40.3 (CH$_2$), 34.2 (CH$_2$), 31.8 (CH$_3$).

ESI-HRMS: *m/z* calculated for C$_{26}$H$_{25}$NO$_3$Na$^+$ ([M+Na]$^+$): 422.1727; found: 422.1728.

5.3. Deprotection and Ring Opening of 1,3-Oxazinanes

**N-(3-Hydroxy-3-phenylpropyl)-4-methylbenzenesulfonamide (59a)**
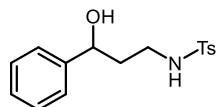
Obtained adapting a reported procedure:[108] the substrate **55a** (158 mg, 0.5 mmol, 1.0 equiv.) was dissolved in MeOH (1 mL) and treated with concentrated HCl 37% (80 µL, 1.0 mmol, 2.0 equiv.). The mixture was heated to 72 °C for 6 h and then to 95 °C for another hour while the MeOH was distilled off. After cooling to room temperature, the mixture was treated with water (5 mL), extracted with toluene, and made basic with excess aq. 50% NaOH. The mixture was taken up in toluene and concentrated under reduced pressure to give a crude product. Further purification by silica gel column chromatography with *n*-hexane/EtOAc mixtures provided the desired product **59a** as a white solid (48 mg, 89%). Spectroscopic data was consistent with the values reported in the literature.[150]

^{1}H NMR (300 MHz, CDCl$_3$) δ 7.68 (d, *J* = 8.3 Hz, 2H), 7.36 – 7.08 (m, 7H), 5.13 (s, 1H), 4.73 (t, *J* = 6.3 Hz, 1H), 3.03 (ddt, *J* = 24.8, 12.7, 6.2 Hz, 2H), 2.36 (s, 3H), 1.78 (q, *J* = 6.1 Hz, 2H).

^{13}C NMR (75 MHz, CDCl$_3$) δ 143.7 (C), 143.3 (C), 136.9 (C), 129.7 (CH, 128.6 (CH$_2$), 127.8 (CH), 127.1 (CH), 125.5 (CH), 73.2 (CH), 40.8 (CH$_2$), 37.7 (CH$_2$), 21.5 (CH$_3$).

ESI-HRMS: *m/z* calculated for C$_{16}$H$_{19}$NO$_3$S$^+$ ([M]$^+$): 304.1013; found: 304.1013.

3-Amino-1-phenylpropan-1-ol (59b)
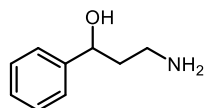
Obtained adapting a reported procedure:[108] a mixture of freshly washed Mg powder (61 mg, 2.5 mmol, 5.0 equiv.) and **55a** (158 mg, 0.5 mmol, 1.0 equiv.) in a 10 mL glass tube was dissolved with a MeOH/THF mixture (5 mL total, 2.5:1 *v/v*) and sonicated at room temperature for 3 hours, until completion of the starting material was observed on TLC. The mixture was filtered over silica, washed with EtOAc (2 × 1 mL) and evaporated under reduced pressure. The crude deprotected product was then dissolved in MeOH (1 mL) and treated with concentrated HCl 37% (80 µL, 1.0 mmol, 2.0 equiv.). The mixture was heated to 72 °C for 6 h and then to 95 °C for another hour while the MeOH was distilled off. After cooling to room temperature, the mixture was treated with water (5 mL), extracted with toluene, and made basic with excess aq. 50% NaOH. The free amine was taken up in toluene and concentrated under reduced pressure to give a crude product. Further purification by silica gel column chromatography with DCM/MeOH mixtures provided the desired product **59b** as a colorless viscous oil (57 mg, 75%). Spectroscopic data was consistent with the values reported in the literature.[151-152]

^{1}H NMR (501 MHz, CDCl$_3$) δ 7.40 – 7.31 (m, 4H), 7.27 – 7.22 (m, 1H), 4.95 (dd, *J* = 8.7, 3.2 Hz, 1H), 3.09 (ddd, *J* = 12.4, 5.9, 4.1 Hz, 1H), 3.03 (br s, 3H), 2.96 (ddd, *J* = 12.7, 9.2, 3.9 Hz, 1H), 1.87 (ddt, *J* = 14.5, 6.0, 3.6 Hz, 1H), 1.77 (dtd, *J* = 14.4, 8.9, 4.0 Hz, 1H).

^{13}C NMR (126 MHz, CDCl$_3$) δ 145.2 (C), 128.4 (CH), 127.2 (CH), 125.8 (CH), 75.5 (CH), 40.6 (CH$_2$), 39.7 (CH$_2$).

## *N*-(3-hydroxy-3-phenylpropyl)-*N*,4-dimethylbenzenesulfonamide (59c)
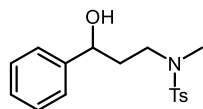
A flame-dried Schlenk flask under argon was charged with **55a** (32 mg, 0.1 mmol, 1.0 equiv.) and dry toluene (1 mL). Diisobutylaluminium hydride (1.2 M in toluene, 0.4 mL, 0.5 mmol, 5.0 equiv.) was then added slowly and the reaction mixture was refluxed overnight, when full conversion of the starting material was observed by TLC. The mixture was cooled down to room temperature and quenched with aq. sat. NH$_4$Cl (5 mL). The phases were separated and the aqueous phase was extracted with EtOAc (3 × 10 mL). The combined organic layers were washed with brine (1 x 10 mL), dried over Na$_2$SO$_4$ and concentrated under reduced pressure. The residue was purified by silica gel column chromatography (*n*-pentane/Et$_2$O 5:1 *v/v*) to yield product **59c** as a yellowish oil (26 mg, 80%). Spectroscopic data was consistent with the values reported in the literature.[153]

^{1}H NMR (400 MHz, CDCl$_3$) δ 7.72 – 7.65 (m, 2H), 7.42 – 7.27 (m, 7H), 4.90 (dd, *J* = 9.1, 4.1 Hz, 1H), 3.50 – 3.45 (m, 1H), 2.92 – 2.86 (m, 1H), 2.78 (s, 3H), 2.66 (s, 1H), 2.44 (s, 3H), 2.02 – 1.76 (m, 2H).

^{13}C NMR (101 MHz, CDCl$_3$) δ 144.2, 143.6, 134.4, 129.9, 128.7, 127.7, 127.6, 125.9, 70.9, 47.3, 37.1, 35.3, 21.3.


3-(Methylamino)-1-phenylpropan-1-ol (59d)
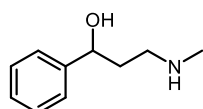
A flame-dried Schlenk flask under argon was charged with LiAlH$_4$ (38 mg, 1.0 mmol, 5.0 equiv.) in 1 mL of dry THF. A solution of **55a** (64 mg, 0.2 mmol, 1.0 equiv.) in dry THF (1 mL) was slowly added to the flask. After refluxing for 3 days (the reduction was monitored by means of TLC), the mixture was quenched with 1.5 mL of water under ice cooling. Then, 2 mL of aq. 20% sodium potassium tartrate were added, and the mixture was stirred at room temperature for 30 min. The phases were separated and the aqueous phase was extracted with EtOAc (3 × 5 mL). The combined organic layers were washed with brine (1 x 5 mL), dried over Na$_2$SO$_4$ and concentrated under reduced pressure to afford product **59d** as a yellowish oil (28 mg, 85%). Spectroscopic data was consistent with the values reported in the literature.[154]

^{1}H NMR (501 MHz, CDCl$_3$) δ 7.43 – 7.31 (m, 4H), 7.30 – 7.24 (m, 1H), 4.96 (dd, *J* = 8.7, 3.2 Hz, 1H), 3.81 (bs, 2H), 2.96 – 2.83 (m, 2H), 2.47 (s, 3H), 1.90 (ddt, *J* = 14.6, 5.8, 3.3 Hz, 1H), 1.79 (dtd, *J* = 14.5, 9.2, 3.8 Hz, 1H).

^{13}C NMR (101 MHz, CDCl$_3$) δ 144.9, 128.39, 127.16, 125.7, 74.9, 50.0, 36.5, 35.7.

5.4. Catalytic Asymmetric Cycloaddition of Olefins with In Situ Generated *N*-Boc-Formaldimine

General Procedure E:
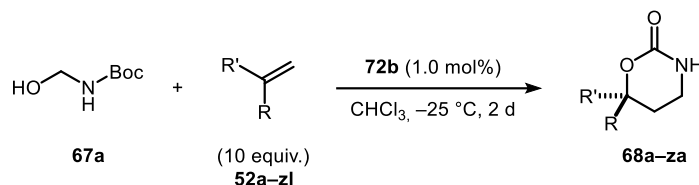
An oven-dried screwcap vial (10 mL) equipped with a magnetic stir bar was charged with carbamate **67a** (74 mg, 0.5 mmol, 1.0 equiv.), olefin **52** (5.0 mmol, 10 equiv.) and dry CHCl$_3$ (1.5 mL). The tube was sealed and cooled down to the respective temperature for 30 min. After this time, a stock solution of catalyst **72b** in 0.1 mL of CHCl$_3$ (1.0 mol%) was added to the previous vial via syringe in one portion. After checking full conversion (TLC monitoring) the reaction was quenched with one equivalent of triethylamine. The mixture was warmed up to rt, suspended on Celite, and further purified by silica gel column chromatography (DCM/MeOH mixtures from 0.5 to 3% *v/v*) to give the desired product **68**.

(*R*)-6-Phenyl-1,3-oxazinan-2-one (68a)
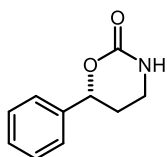
 Obtained following the *General Procedure E,* as a white solid (65 mg, 73%). Spectroscopic data was consistent with the values reported in the literature.[117]

^{1}H NMR (501 MHz, CDCl$_3$) δ 7.43 – 7.30 (m, 5H), 5.96 (s, 1H), 5.35 (dd, *J* = 9.9, 2.8 Hz, 1H), 3.48 (td, *J* = 11.0, 4.9 Hz, 1H), 3.39 (ddt, *J* = 12.0, 5.7, 3.6 Hz, 1H), 2.23 (dq, *J* = 14.0, 3.8 Hz, 1H), 2.09 (dtd, *J* = 14.0, 10.1, 5.5 Hz, 1H).

^{13}C NMR (126 MHz, CDCl$_3$) δ 154.5, 139.1, 128.8, 128.5, 125.8, 78.7, 39.2, 28.9.

HRMS (ESI) calculated for C$_{10}$H$_{11}$NO$_2$Na$^+$ ([M+Na$^+$]): 200.068198, found: 200.068117.

$[a]_T^{20}$ = +50.44 (*c* = 0.23, CHCl$_3$).

HPLC (Chiralpak IC-3, *n*-heptane/*i*-PrOH 50:50, 298 K, 215 nm): t$_R$ (major) = 14.1 min, t$_R$ (minor) = 20.6 min, e.r. = 97:3 (94% e.e.).

Absolute configuration of **68a** was determined by comparison of the optical rotation with available literature data.[155] The absolute configuration of products **68b–t** was assigned by analogy.

(*R*)-6-(4-(Chloromethyl)phenyl)-1,3-oxazinan-2-one (68b)
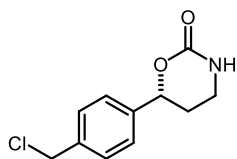
Obtained following the *General Procedure E,* as a white solid (57 mg, 51%).

^{1}H NMR (501 MHz, CDCl$_3$) δ 7.47 – 7.33 (m, 4H), 5.97 (s, 1H), 5.35 (dd, *J* = 9.9, 2.8 Hz, 1H), 4.59 (s, 2H), 3.49 (td, *J* = 11.0, 4.9 Hz, 1H), 3.39 (ddt, *J* = 12.2, 6.1, 3.6 Hz, 1H), 2.22 (dq, *J* = 14.2, 3.9 Hz, 1H), 2.14 – 2.01 (m, 1H).
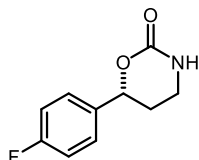
^{13}C NMR (126 MHz, CDCl$_3$) δ 154.4, 139.4, 137.8, 129.0, 126.2, 78.3, 45.9, 39.2, 28.9.

HRMS (ESI) calculated for C$_{11}$H$_{12}$NO$_2$ClNa ([M+Na$^+$]): 248.044876, found: 258.044939.

$[a]_T^{20}$ = +43.29 (*c* = 0.12, CHCl$_3$).

HPLC (Chiralpak IC-3, *n*-heptane/*i*-PrOH 50:50, 298 K, 220 nm): t$_R$ (major) = 16.0 min, t$_R$ (minor) = 20.9 min, e.r. = 98.8:1.2 (97.6% e.e.).

(*R*)-6-(4-Fluorophenyl)-1,3-oxazinan-2-one (68c)

Obtained following the *General Procedure E*, as a white solid (69 mg, 71%).

^{1}H NMR (501 MHz, CDCl$_3$) δ 7.38 – 7.32 (m, 2H), 7.12 – 7.02 (m, 2H), 6.49 (s, 1H), 5.30 (dd, *J* = 10.2, 2.7 Hz, 1H), 3.47 (dddd, *J* = 11.7, 10.7, 4.9, 1.0 Hz, 1H), 3.38 (ddt, *J* = 12.0, 5.6, 3.4 Hz, 1H), 2.18 (ddtd, *J* = 13.9, 4.2, 3.1, 1.0 Hz, 1H), 2.05 (dtd, *J* = 13.9, 10.4, 5.6 Hz, 1H).

^{13}C NMR (126 MHz, CDCl$_3$) δ 162.8 (d, *J* = 246.9 Hz), 154.7, 134.9 (d, *J* = 3.4 Hz), 127.7 (d, *J* = 8.3 Hz), 115.71 (d, *J* = 21.7 Hz), 78.1, 39.1, 28.9.
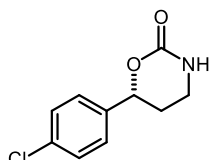
^{19}F NMR (471 MHz, CDCl$_3$) δ -113.53.

HRMS (ESI) calculated for C$_{10}$H$_{10}$NO$_2$FNa ([M+Na$^+$]): 218.058776, found: 218.058696.

$[a]_T^{20}$ = +32.84 (*c* = 0.24, CHCl$_3$).

HPLC (Chiralpak IC-3, *n*-heptane/*i*-PrOH 50:50, 298 K, 209 nm): t$_R$ (major) = 11.8 min, t$_R$ (minor) = 16.6 min, e.r. = 95.5:4.5 (91% e.e.).

(*R*)-6-(4-Fluorophenyl)-1,3-oxazinan-2-one (68d)

Obtained following the *General Procedure E,* as a white solid (58 mg, 55%).

^{1}H NMR (501 MHz, CDCl$_3$) δ 7.36 (d, *J* = 8.5 Hz, 2H), 7.31 (d, *J* = 8.6 Hz, 2H), 6.44 (s, 1H), 5.30 (dd, *J* = 10.1, 2.8 Hz, 1H), 3.51 – 3.43 (m, 1H), 3.38 (ddt, *J* = 12.0, 5.6, 3.5 Hz, 1H), 2.23 – 2.15 (m, 1H), 2.03 (dtd, *J* = 13.9, 10.3, 5.6 Hz, 1H).
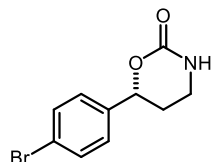
^{13}C NMR (126 MHz, CDCl$_3$) δ 154.5, 137.6, 134.4, 128.9, 127.2, 78.0, 39.1, 28.8.

HRMS (ESI) calculated for C$_{10}$H$_{10}$NO$_2$ClNa ([M+Na$^+$]): 234.029226, found: 234.029267.

$[a]_T^{20}$ = +41.46 (c = 0.16, CHCl$_3$).

HPLC (Chiralpak IC-3, *n*-heptane/*i*-PrOH 50:50, 298 K, 209 nm): t_R (major) = 11.6 min, t_R (minor) = 15.4 min, e.r. = 95.9:4.1 (91.8% e.e.).

(*R*)-6-(4-Bromophenyl)-1,3-oxazinan-2-one (68e)

Obtained following the *General Procedure E,* as a white solid (77 mg, 60%).

^{1}H NMR (501 MHz, CDCl$_3$) δ 7.58 – 7.50 (m, 2H), 7.31 – 7.19 (m, 2H), 6.59 – 6.55 (m, 1H), 5.31 (dd, *J* = 10.1, 2.8 Hz, 1H), 3.49 (tdd, *J* = 10.6, 4.9, 1.1 Hz, 1H), 3.39 (ddt, *J* = 12.0, 5.6, 3.5 Hz, 1H), 2.26 – 2.16 (m, 1H), 2.04 (dtd, *J* = 13.9, 10.4, 5.6 Hz, 1H).
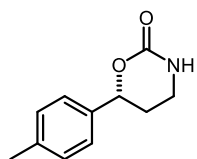
^{13}C NMR (126 MHz, CDCl$_3$) δ 154.5, 138.2, 131.9, 127.5, 122.5, 78.0, 39.0, 28.8.

HRMS (ESI) calculated for C$_{10}$H$_{10}$NO$_2$BrNa ([M+Na$^+$]): 277.978723, found: 277.978836.

$[a]_T^{20}$ = +30.12 (c = 0.17, CHCl$_3$).

HPLC (Chiralpak IC-3, *n*-heptane/*i*-PrOH 50:50, 298 K, 220 nm): t_R (major) = 11.4 min, t_R (minor) = 15.4 min, e.r. = 96.9:3.1 (93.8% e.e.).

(*R*)-6-(*p*-Tolyl)-1,3-oxazinan-2-one (68f)

Obtained by adapting the *General Procedure E*, in Et$_2$O/CHCl$_3$ (3:1 *v/v*) mixture at –30 °C, as a white solid (58 mg, 61%).

^{1}H NMR (501 MHz, CDCl$_3$) δ 7.31 – 7.23 (m, 2H), 7.20 (d, *J* = 7.9 Hz, 2H), 6.92 – 6.89 (m, 1H), 5.31 (dd, *J* = 9.9, 2.8 Hz, 1H), 3.46 (tdd, *J* = 10.4, 4.9, 1.1 Hz, 1H), 3.38 (ddt, *J* = 11.9, 5.5, 3.5 Hz, 1H), 2.37 (s, 3H), 2.23 – 2.14 (m, 1H), 2.06 (dtd, *J* = 13.9, 10.2, 5.6 Hz, 1H).

^{13}C NMR (126 MHz, CDCl$_3$) δ 155.1, 138.2, 136.2, 129.3, 125.7, 78.6, 38.9, 28.7, 21.2.

HRMS (GC-EI) calculated for C$_{11}$H$_{13}$NO$_2$ ([M$^+$]): 191.094079, found: 191.094073.

$[a]_T^{20}$ = +34.06 (c = 0.28, CHCl$_3$).

HPLC (Chiralpak IC-3, *n*-heptane/*i*-PrOH 50:50, 298 K, 225 nm): t_R (major) = 16.3 min, t_R (minor) = 21.9 min, e.r. = 95.5:4.5 (91% e.e.).

(*R*)-6-(4-(*tert*-Butyl)phenyl)-1,3-oxazinan-2-one (68g)
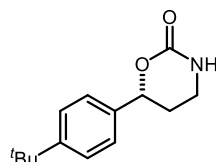
Obtained by adapting the *General Procedure E*, in Et$_2$O/CHCl$_3$ (3:1 *v/v*) mixture at –40 °C, as a white solid (67 mg, 57%).

^{1}H NMR (501 MHz, CDCl$_3$) δ 7.46 – 7.40 (m, 2H), 7.35 – 7.30 (m, 2H), 6.83 – 6.75 (m, 1H), 5.33 (dd, *J* = 9.9, 2.8 Hz, 1H), 3.47 (dddd, *J* = 11.5, 10.2, 4.9, 1.1 Hz, 1H), 3.39 (ddt, *J* =

12.0, 5.6, 3.5 Hz, 1H), 2.21 (dddd, J = 13.5, 6.8, 3.7, 1.8 Hz, 1H), 2.09 (dtd, J = 13.9, 10.1, 5.5 Hz, 1H), 1.34 (s, 9H).

^{13}C NMR (126 MHz, CDCl$_3$) δ 155.1, 151.5, 136.1, 125.6, 125.5, 78.5, 38.9, 34.7, 31.4, 28.6.

HRMS (ESI) calculated for C$_{14}$H$_{19}$NO$_2$Na ([M+Na$^+$]): 256.130798, found: 256.130875.

$[a]_T^{20}$ = +23.73 (c = 0.30, CHCl$_3$).

HPLC (Chiralpak IC-3, *n*-heptane/*i*-PrOH 50:50, 298 K, 209 nm): t$_R$ (major) = 13.4 min, t$_R$ (minor) = 16.9 min, e.r. = 94:6 (88% e.e.).

(*R*)-4-(2-Oxo-1,3-oxazinan-6-yl)phenyl acetate (68h)
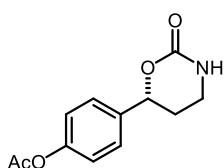
Obtained by adapting the *General Procedure E*, in Et$_2$O/CHCl$_3$ (3:1 *v/v*) mixture at –30 °C, as a white solid (66 mg, 56%).

^{1}H NMR (501 MHz, CDCl$_3$) δ 7.37 (d, J = 8.5 Hz, 2H), 7.09 (d, J = 8.6 Hz, 2H), 6.75 – 6.71 (s, 1H), 5.30 (dd, J = 10.1, 2.7 Hz, 1H), 3.43 (dddd, J = 11.7, 10.6, 4.8, 1.0 Hz, 1H), 3.39 – 3.29 (m, 1H), 2.28 (s, 3H), 2.21 – 2.12 (m, 1H), 2.02 (dtd, J = 13.9, 10.4, 5.6 Hz, 1H).

^{13}C NMR (126 MHz, CDCl$_3$) δ 169.5, 154.8, 150.6, 136.7, 126.9, 121.9, 78.1, 38.9, 28.8, 21.2.

HRMS (ESI) calculated for C$_{12}$H$_{13}$NO$_4$Na ([M+Na$^+$]): 258.073678, found: 258.073665.

$[a]_T^{20}$ = +36.24 (c = 0.15, CHCl$_3$).

HPLC (Chiralpak IC-3, *n*-heptane/*i*-PrOH 50:50, 298 K, 215 nm): t$_R$ (major) = 23.8 min, t$_R$ (minor) = 35.3 min, e.r. = 95.1:4.9 (90.2% e.e.).

(*R*)-6-(3-Methoxyphenyl)-1,3-oxazinan-2-one (68j)

Obtained following the *General Procedure E*, as a white solid (68 mg, 67%).

^{1}H NMR (501 MHz, CDCl$_3$) δ 7.36 – 7.21 (m, 1H), 6.98 – 6.91 (m, 2H), 6.90 – 6.79 (m, 1H), 6.47 (s, 1H), 5.31 (dd, J = 9.8, 2.8 Hz, 1H), 3.82 (s, 3H), 3.47 (dddd, J = 11.7, 10.4, 4.9, 1.2 Hz, 1H), 3.38 (ddt, J = 11.6, 5.5, 3.6 Hz, 1H), 2.26 – 2.17 (m, 1H), 2.07 (dtd, J = 13.9, 10.2, 5.6 Hz, 1H).

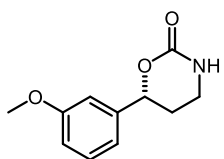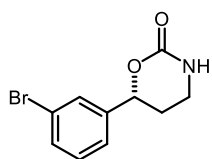^{13}C NMR (126 MHz, CDCl$_3$) δ 159.9, 154.8, 140.8, 129.8, 117.9, 114.0, 111.3, 78.5, 55.5, 39.1, 28.9.

HRMS (ESI) calculated for C$_{11}$H$_{13}$NO$_3$Na ([M+Na$^+$]): 230.078763, found: 230.078873.

$[a]_T^{20}$ = +37.29 (c = 0.12, CHCl$_3$).

HPLC (Chiralpak IC-3, *n*-heptane/*i*-PrOH 50:50, 298 K, 209 nm): t$_R$ (major) = 15.8 min, t$_R$ (minor) = 22.1 min, e.r. = 95.7:4.3 (92% e.e.).

(*R*)-6-(3-Bromophenyl)-1,3-oxazinan-2-one (68k)

Obtained following the *General Procedure E*, as a white solid (55 mg, 43%).

^{1}H NMR (501 MHz, CDCl$_3$) δ 7.48 (t, *J* = 1.9 Hz, 1H), 7.40 (dt, *J* = 7.8, 1.6 Hz, 1H), 7.27 – 7.12 (m, 2H), 6.47 (s, 1H), 5.23 (dd, *J* = 10.1, 2.8 Hz, 1H), 3.41 (dddd, *J* = 11.7, 10.5, 4.9, 1.1 Hz, 1H), 3.32 (ddt, *J* = 11.9, 5.6, 3.4 Hz, 1H), 2.19 – 2.09 (m, 1H), 1.97 (dtd, *J* = 14.0, 10.4, 5.6 Hz, 1H).
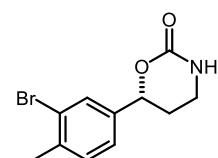
^{13}C NMR (126 MHz, CDCl$_3$) δ 154.4, 141.4, 131.1, 130.4, 128.9, 124.4, 122.9, 77.8, 39.0, 28.9.

HRMS (GC-EI) calculated for C$_{10}$H$_1$NO$_2$Br ([M$^+$]): 254.988954, found: 254.988967.

$[a]_T^{20}$ = +43.77 (*c* = 0.20, CHCl$_3$).

HPLC (Chiralpak IC-3, *n*-heptane/*i*-PrOH 50:50, 298 K, 270 nm): t$_R$ (major) = 11.4 min, t$_R$ (minor) = 15.5 min, e.r. = 97.4:2.6 (94.5% e.e.).

(*R*)-6-(3-Bromo-4-methylphenyl)-1,3-oxazinan-2-one (68l)

Obtained following the *General Procedure E*, as a white solid (68 mg, 71%).

^{1}H NMR (501 MHz, CDCl$_3$) δ 7.49 (d, *J* = 1.8 Hz, 1H), 7.24 – 7.07 (m, 2H), 5.97 (s, 1H), 5.21 (dd, *J* = 10.0, 2.8 Hz, 1H), 3.41 (td, *J* = 11.0, 4.9 Hz, 1H), 3.32 (ddt, *J* = 11.9, 5.6, 3.5 Hz, 1H), 2.33 (s, 3H), 2.17 – 2.09 (m, 1H), 1.98 (dtd, *J* = 14.0, 10.3, 5.6 Hz, 1H).

^{13}C NMR (126 MHz, CDCl$_3$) δ 154.3, 138.5, 138.2, 131.1, 129.7, 125.2, 124.7, 77.7, 39.1, 28.8, 22.8.

HRMS (GC-EI) calculated for C$_{11}$H$_{12}$NO$_2$Br ([M$^+$]): 269.004604, found: 269.004583.

$[a]_T^{20}$ = +40.00 (*c* = 0.12, CHCl$_3$).

HPLC (Chiralpak IC-3, *n*-heptane/*i*-PrOH 50:50, 298 K, 220 nm): t$_R$ (major) = 13.2 min, t$_R$ (minor) = 16.5 min, e.r. = 97.1:2.9 (94.2% e.e.).

(*R*)-6-(*o*-Tolyl)-1,3-oxazinan-2-one (68m)
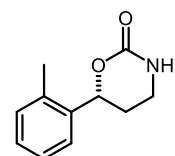
Obtained following the *General Procedure E*, as a white solid (77 mg, 81%).

^{1}H NMR (501 MHz, CDCl$_3$) δ 7.45 (dd, *J* = 7.0, 2.2 Hz, 1H), 7.24 (tt, *J* = 7.3, 4.9 Hz, 2H), 7.17 (dd, *J* = 6.8, 2.1 Hz, 1H), 6.83 – 6.77 (m, 1H), 5.50 (dd, *J* = 10.4, 2.6 Hz, 1H), 3.52 – 3.45 (m, 1H), 3.45 – 3.38 (m, 1H), 2.35 (s, 3H), 2.20 – 2.11 (m, 1H), 2.03 (dtd, *J* = 14.0, 10.7, 5.7 Hz, 1H).

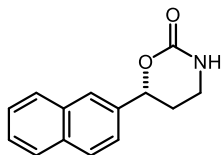^{13}C NMR (126 MHz, CDCl$_3$) δ 155.3, 137.1, 134.4, 130.7, 128.3, 126.5, 125.7, 76.1, 39.3, 27.7, 19.0.

HRMS (ESI) calculated for C$_{11}$H$_{13}$NO$_2$Na ([M+Na$^+$]): 214.083847, found: 214.083794.

$[a]_T^{20}$ = +31.84 (*c* = 0.25, CHCl$_3$).

HPLC (Chiralpak IC-3, *n*-heptane/*i*-PrOH 50:50, 298 K, 209 nm): t_R (major) = 15.7 min, t_R (minor) = 26.9 min, e.r. = 95.8:4.2 (91.6% e.e.).

(*R*)-6-(naphthalen-2-yl)-1,3-oxazinan-2-one (68n)

Obtained following the *General Procedure E*, as a white solid (61 mg, 54%).

^{1}H NMR (501 MHz, CDCl$_3$) δ 7.90 – 7.81 (m, 4H), 7.54 – 7.47 (m, 2H), 7.45 (dd, *J* = 8.6, 1.7 Hz, 1H), 5.82 (s, 1H), 5.52 (dd, *J* = 9.8, 2.9 Hz, 1H), 3.53 (dddd, *J* = 11.5, 10.2, 4.9, 1.2 Hz, 1H), 3.42 (ddt, *J* = 11.6, 5.6, 3.6 Hz, 1H), 2.32 (dqd, *J* = 11.7, 4.0, 2.0 Hz, 1H), 2.18 (dtd, *J* = 14.0, 10.0, 5.5 Hz, 1H).

^{13}C NMR (126 MHz, CDCl$_3$) δ 154.4, 136.4, 133.3, 133.3, 128.7, 128.3, 127.9, 126.6, 126.5, 124.8, 123.4, 78.8, 39.2, 28.9.

HRMS (ESI) calculated for C$_{14}$H$_{13}$NO$_2$Na$^+$ ([M+Na$^+$]): 250.083848, found: 200.083915.

$[a]_T^{20}$ = +50.38 (*c* = 0.13, CHCl$_3$).

HPLC (Chiralpak IC-3, *n*-heptane/*i*-PrOH 50:50, 298 K, 209 nm): t_R (major) = 16.5 min, t_R (minor) = 21.0 min, e.r. = 97:3 (94% e.e.).

(*R*)-6-(4-vinylphenyl)-1,3-oxazinan-2-one (68o)
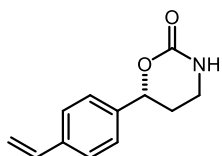
Obtained following the *General Procedure E*, as a white solid (43 mg, 42%).

^{1}H NMR (501 MHz, CDCl$_3$) δ 7.42 (d, *J* = 8.4 Hz, 2H), 7.33 (d, *J* = 8.2 Hz, 2H), 6.71 (dd, *J* = 17.6, 10.9 Hz, 1H), 6.57 – 6.53 (m, 1H), 5.76 (dd, *J* = 17.5, 0.9 Hz, 1H), 5.32 (dd, *J* = 9.9, 2.8 Hz, 1H), 5.27 (dd, *J* = 10.9, 0.9 Hz, 1H), 3.46 (dddd, *J* = 11.6, 10.3, 4.9, 1.1 Hz, 1H), 3.37 (ddt, *J* = 11.8, 5.6, 3.6 Hz, 1H), 2.24 – 2.15 (m, 1H), 2.05 (dtd, *J* = 14.0, 10.2, 5.6 Hz, 1H).

^{13}C NMR (126 MHz, CDCl$_3$) δ 154.81, 138.59, 137.82, 136.32, 126.55, 125.94, 114.57, 78.47, 39.01, 28.76.

HRMS (GC-EI) calculated for C$_{12}$H$_{13}$NO$_2$ ([M$^+$]): 203.094079, found: 203.093985.

$[a]_T^{20}$ = +36.04 (*c* = 0.11, CHCl$_3$).

HPLC (Chiralpak IC-3, *n*-heptane/*i*-PrOH 50:50, 298 K, 254 nm): t_R (major) = 15.0 min, t_R (minor) = 19.6 min, e.r. = 95.4:4.6 (90.8% e.e.).

(*R*)-6-(Thiophen-3-yl)-1,3-oxazinan-2-one (68q)
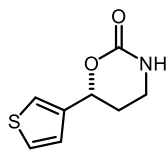
Obtained by adapting the *General Procedure E*, in MTBE at –30 °C, as a white solid (71 mg, 78%).

^{1}H NMR (501 MHz, CDCl$_3$) δ 7.37 – 7.28 (m, 2H), 7.07 (dd, *J* = 5.0, 1.4 Hz, 1H), 6.68 (s, 1H), 5.41 (dd, *J* = 9.5, 2.9 Hz, 1H), 3.48 – 3.32 (m, 2H), 2.24 (dq, *J* = 11.9, 3.8 Hz, 1H), 2.10 (dtd, *J* = 13.9, 9.7, 5.6 Hz, 1H).

^{13}C NMR (126 MHz, CDCl$_3$) δ 154.7, 140.3, 126.7, 125.3, 122.0, 75.3, 38.8, 27.8.

HRMS (ESI) calculated for C$_8$H$_9$NO$_2$SNa ([M+Na$^+$]): 206.024620 found: 206.024649.

$[a]_T^{20}$ = +1.40 (*c* = 0.14, CHCl$_3$).

HPLC (Chiralpak IC-3, *n*-heptane/*i*-PrOH 50:50, 298 K, 233 nm): t$_R$ (major) = 14.3 min, t$_R$ (minor) = 16.6 min, e.r. = 93:7 (86% e.e.).

(*R*)-6-(Benzo[*b*]thiophen-6-yl)-1,3-oxazinan-2-one (68r)

Obtained by adapting the *General Procedure E*, in Et$_2$O/CHCl$_3$ (3:1 *v/v*) mixture at –30 °C, as a white solid (53 mg, 76%).

^{1}H NMR (501 MHz, CDCl$_3$) δ 7.96 – 7.92 (m, 1H), 7.83 (d, *J* = 8.2 Hz, 1H), 7.47 (d, *J* = 5.4 Hz, 1H), 7.37 – 7.30 (m, 2H), 6.28 (s, 1H), 5.47 (dd, *J* = 9.9, 2.8 Hz, 1H), 3.50 (dddd, *J* = 11.6, 10.3, 4.8, 1.1 Hz, 1H), 3.40 (ddt, *J* = 11.9, 5.5, 3.6 Hz, 1H), 2.32 – 2.23 (m, 1H), 2.14 (dtd, *J* = 13.9, 10.2, 5.5 Hz, 1H).
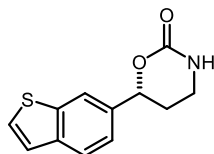
^{13}C NMR (126 MHz, CDCl$_3$) δ 154.6, 140.2, 139.7, 135.4, 127.4, 123.9, 123.7, 122.1, 119.8, 78.8, 39.2, 29.2.

HRMS (GC-EI) calculated for C$_{12}$H$_{11}$NO$_2$S ([M$^+$]): 233.050501, found: 233.050416.

$[a]_T^{20}$ = +52.94 (*c* = 0.14, CHCl$_3$).

HPLC (Chiralpak IC-3, *n*-heptane/*i*-PrOH 50:50, 298 K, 209 nm): t$_R$ (major) = 17.1 min, t$_R$ (minor) = 22.4 min, e.r. = 95.5:4.5 (91% e.e.).

(*R*)-6-(Benzofuran-6-yl)-1,3-oxazinan-2-one (68s)
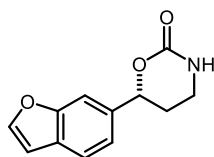
Obtained following the *General Procedure E,* employing **67a** (37 mg, 0.25 mmol, 1.0 equiv.) and 6-vinylbenzofuran (2.5 mmol, 10 equiv.), as a white solid (47 mg, 87%).

^{1}H NMR (501 MHz, CDCl$_3$) δ 7.64 (d, *J* = 2.2 Hz, 1H), 7.62 – 7.54 (m, 2H), 7.23 (dd, *J* = 8.2, 1.5 Hz, 1H), 6.76 (d, *J* = 2.1 Hz, 1H), 6.57 (s, 1H), 5.44 (dd, *J* = 10.0, 2.8 Hz, 1H), 3.49 (td, *J* = 11.1, 4.8 Hz,

1H), 3.40 (ddt, *J* = 11.9, 5.6, 3.5 Hz, 1H), 2.24 (ddt, *J* = 14.1, 5.4, 3.2 Hz, 1H), 2.12 (dtd, *J* = 13.9, 10.2, 5.6 Hz, 1H).

^{13}C NMR (126 MHz, CDCl$_3$) δ 155.08, 154.82, 145.90, 135.75, 127.63, 121.41, 120.63, 109.02, 106.54, 78.83, 39.09, 29.21.

HRMS (GC-EI) calculated for C$_{12}$H$_{11}$NO$_3$ ([M$^+$]): 217.073343, found: 217.073229.

$[a]_T^{20}$ = +41.51 (*c* = 0.11, CHCl$_3$).

HPLC (Chiralpak IC-3, *n*-heptane/*i*-PrOH 50:50, 298 K, 254 nm): t$_R$ (major) = 16.3 min, t$_R$ (minor) = 21.3 min, e.r. = 93:7 (86% e.e.).

(*R*)-6-Ethyl-6-phenyl-1,3-oxazinan-2-one (68u)

Obtained by adapting the *General Procedure E*, employing **67a** (57 mg, 0.4 mmol, 1.0 equiv.) and α-ethylstyrene (4.0 mmol, 10 equiv, in Et$_2$O/CHCl$_3$ (3:1 *v/v*) mixture at –30 °C, as a white solid (59 mg, 71%).

^{1}H NMR (501 MHz, CDCl$_3$) δ 7.38 (dd, *J* = 8.4, 6.9 Hz, 2H), 7.34 – 7.26 (m, 3H), 5.10 (s, 1H), 3.23 (ddt, *J* = 11.9, 6.3, 3.1 Hz, 1H), 2.96 (td, *J* = 11.5, 4.7 Hz, 1H), 2.33 – 2.26 (m, 1H), 2.18 (ddd, *J* = 13.9, 11.5, 5.6 Hz, 1H), 1.95 (ddt, *J* = 25.4, 14.2, 7.1 Hz, 2H), 0.84 (t, *J* = 7.4 Hz, 3H).
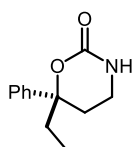
^{13}C NMR (126 MHz, CDCl$_3$) δ 141.6, 128.8, 127.7, 125.0, 37.3, 35.9, 30.6, 7.6. (other signals not detected or observed).

HRMS (ESI) calculated for C$_{12}$H$_{15}$NO$_2$Na ([M+Na$^+$]): 228.099498, found: 228.099418.

$[a]_T^{20}$ = +89.17 (*c* = 0.16, CHCl$_3$).

HPLC (Chiralpak IE-3, *n*-heptane/*i*-PrOH 80:20, 298 K, 209 nm): t$_R$ (minor) = 10.9 min, t$_R$ (major) = 11.7 min, e.r. = 5.3:94.7 (89.4% e.e.).

(*S*)-6-Isopropyl-6-phenyl-1,3-oxazinan-2-one (68v)
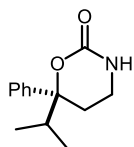
Obtained by adapting the *General Procedure E*, employing **67a** (57 mg, 0.4 mmol, 1.0 equiv.) and (3-methylbut-1-en-2-yl)benzene (4.0 mmol, 10 equiv.), as a white solid (38 mg, 43%).

^{1}H NMR (501 MHz, CDCl$_3$) δ 7.40 – 7.33 (m, 2H), 7.33 – 7.23 (m, 3H), 5.78 (s, 1H), 3.21 (dddd, *J* = 11.7, 5.9, 4.0, 2.0 Hz, 1H), 2.91 (td, *J* = 11.9, 4.6 Hz, 1H), 2.33 (ddt, *J* = 14.0, 4.6, 1.7 Hz, 1H), 2.22 (ddd, *J* = 13.9, 12.3, 5.7 Hz, 1H), 2.08 (hept, *J* = 6.8 Hz, 1H), 0.96 (d, *J* = 6.8 Hz, 3H), 0.85 (d, *J* = 6.9 Hz, 3H).

^{13}C NMR (126 MHz, CDCl$_3$) δ 154.7, 140.6, 128.6, 127.6, 125.7, 86.9, 38.6, 37.2, 27.7, 17.1, 16.7.

HRMS (ESI) calculated for C$_{13}$H$_{17}$NO$_2$Na ([M+Na$^+$]): 242.115148, found: 242.115159.

$[a]_T^{20}$ = +75.47 (c = 0.16, CHCl$_3$).

HPLC (Chiralpak ID-3, *n*-heptane/*i*-PrOH 91:10, 298 K, 209 nm): t$_R$ (major) = 10.6 min, t$_R$ (minor) = 11.7 min, e.r. = 98.7:1.3 (97.4% e.e.).

(*S*)-6-Cyclopentyl-6-phenyl-1,3-oxazinan-2-one (68w)

Obtained by adapting the *General Procedure E*, employing **67a** (34 mg, 0.25 mmol, 1.0 equiv.) and (1-cyclopentylvinyl)benzene (2.5 mmol, 10 equiv.), in Et$_2$O/CHCl$_3$ (3:1 *v/v*) mixture at –30 °C, as a white solid (13 mg, 23%).

^{1}H NMR (501 MHz, CDCl$_3$) δ 7.34 – 7.16 (m, 5H), 5.84 (s, 1H), 3.10 (dddd, *J* = 11.7, 7.1, 4.3, 2.4 Hz, 1H), 2.79 (tt, *J* = 11.5, 5.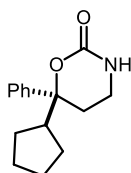5 Hz, 1H), 2.30 – 2.12 (m, 3H), 1.72 (dh, *J* = 11.2, 3.1 Hz, 1H), 1.60 – 1.25 (m, 6H), 1.13 (ddt, *J* = 10.8, 7.3, 4.0 Hz, 1H).

^{13}C NMR (126 MHz, CDCl$_3$) δ 154.9, 142.1, 128.7, 127.5, 125.2, 85.7, 51.1, 37.0, 29.8, 26.7, 26.5, 25.6, 25.2.

HRMS (ESI) calculated for C$_{15}$H$_{19}$NO$_2$Na ([M+Na$^+$]): 268.13080, found: 268.13117.

$[a]_T^{20}$ = +76.77 (c = 0.15, CHCl$_3$).

HPLC (Chiralpak ID-3, *n*-heptane/*i*-PrOH 80:20, 298 K, 220 nm): t$_R$ (major) = 7.3 min, t$_R$ (minor) = 9.2 min, e.r. = 94.8:5.2 (89.6% e.e.).

(*S*)-6-Cyclohexyl-6-phenyl-1,3-oxazinan-2-one (68x)
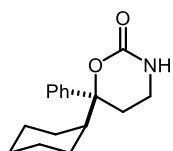
Obtained by adapting the *General Procedure E*, employing **1a** (59 mg, 0.4 mmol, 1.0 equiv.) and (1-cyclohexylvinyl)benzene (4.0 mmol, 10 equiv.), as a white solid (58 mg, 56%).

^{1}H NMR (501 MHz, CDCl$_3$) δ 7.29 (dd, *J* = 8.4, 6.3 Hz, 2H), 7.26 – 7.16 (m, 3H), 5.40 (d, *J* = 3.7 Hz, 1H), 3.13 (dddd, *J* = 11.5, 5.9, 4.0, 2.0 Hz, 1H), 2.84 (td, *J* = 11.9, 4.7 Hz, 1H), 2.26 (ddt, *J* = 14.0, 4.7, 1.7 Hz, 1H), 2.16 (ddd, *J* = 13.9, 12.2, 5.7 Hz, 1H), 1.87 (dt, *J* = 12.7, 3.3 Hz, 1H), 1.64 (dtt, *J* = 14.9, 9.3, 3.1 Hz, 3H), 1.57 – 1.42 (m, 3H), 1.14 – 0.83 (m, 5H).

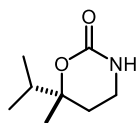^{13}C NMR (126 MHz, CDCl$_3$) δ 154.5, 140.8, 128.5, 127.6, 125.8, 86.9, 48.5, 37.2, 27.5, 26.9, 26.7, 26.6, 26.4, 26.3.

HRMS (GC-EI) calculated for C$_{16}$H$_{22}$NO$_2$ ([M$^+$]): 260.164504, found: 260.164391.

$[a]_T^{20}$ = +76.36 (c = 0.11, CHCl$_3$).

HPLC (Chiralpak ID-3, *n*-heptane/*i*-PrOH 80:20, 298 K, 209 nm): t$_R$ (major) = 8.1 min, t$_R$ (minor) = 8.9 min, e.r. = 96.7:3.3 (93.4% e.e.).

(*R*)-6-Isopropyl-6-methyl-1,3-oxazinan-2-one (68z)

Obtained by adapting the *General Procedure E*, in Et$_2$O/CHCl$_3$ (3:1 *v/v*) mixture at –10 °C, as a white solid (47 mg, 60%).

^{1}H NMR (501 MHz, CDCl$_3$) δ 6.62 (s, 1H), 3.33 (ddqd, *J* = 9.9, 6.8, 5.1, 1.9 Hz, 2H), 1.94 (p, *J* = 6.8 Hz, 1H), 1.90 – 1.81 (m, 1H), 1.71 (dt, *J* = 13.8, 4.9 Hz, 1H), 1.26 (s, 3H), 0.96 (dd, *J* = 35.4, 6.9 Hz, 6H).

^{13}C NMR (126 MHz, CDCl$_3$) δ 154.9, 83.3, 36.6, 36.5, 27.6, 20.2, 17.3, 16.7.

HRMS (ESI) calculated for C$_{15}$H$_{19}$NO$_2$Na ([M+Na$^+$]): 180.099497, found: 180.099440.

$[a]_T^{20}$ = +1.82 (*c* = 0.22, CHCl$_3$).

GC (30.0 m BGB-174), injection temperature: 220 °C, 170 °C iso 30 min, 240 °C iso 10 min, 0.6 bar H$_2$): t$_R$ (major) = 25.0 min, t$_R$ (minor) = 16.6 min, e.r. = 93.2:6.8 (86.4% e.e.).

(*R*)-6-(*tert*-Butyl)-6-methyl-1,3-oxazinan-2-one (68za)
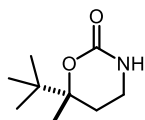
Obtained by adapting the *General Procedure E*, in Et$_2$O/CHCl$_3$ (3:1 *v/v*) mixture at –10 °C, as a white solid (30 mg, 35%).

^{1}H NMR (501 MHz, CDCl$_3$) δ 5.84 (s, 1H), 3.41 (td, *J* = 12.1, 4.7 Hz, 1H), 3.33 (dddd, *J* = 12.0, 6.1, 4.1, 1.7 Hz, 1H), 2.03 (td, *J* = 13.1, 6.4 Hz, 1H), 1.67 (ddt, *J* = 13.6, 4.7, 1.4 Hz, 1H), 1.37 – 1.28 (m, 3H), 1.02 (s, 9H).

^{13}C NMR (126 MHz, CDCl$_3$) δ 154.9, 84.9, 37.8, 36.9, 25.3, 25.0, 18.8.

HRMS (ESI) calculated for C$_9$H$_{17}$NO$_2$Na ([M+Na$^+$]): 194.115150, found: 194.115212.

$[a]_T^{20}$ = +4.92 (*c* = 0.12, CHCl$_3$).

GC (25.0 m Hydrodex beta-TBDAc), injection temperature: 220 °C, 150 °C iso 45 min, 8°C/min, 220 °C, 0.6 bar H$_2$): t$_R$ (major) = 39.1 min, t$_R$ (minor) = 41.3 min, e.r. = 97.8:2.2 (95.6% e.e.).

5.4.1. Absolute Configuration Determination

The absolute configuration of **68a** was determined by comparison of the optical rotation with available literature data.[155] Similarly, the absolute configuration of **68v** was established after transformation to amino alcohol **S5** and comparison of its optical rotation with available literature data.[156] Other products' absolute configurations were assigned by analogy.

Reaction scheme: 3s → (KOH (4.0 equiv.), ^{i}PrOH/H$_2$O (1:1), reflux, 20 h) → 88%, S13
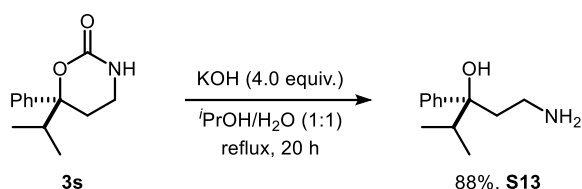
Compound	Measured $[\alpha]_D$	Literature value
3a	$[a]_T^{20} = +50.44$ ($c = 0.23$, CHCl$_3$) (R)	$[a]_T^{20} = +30.20$ ($c = 1.0$, CHCl$_3$) (R)[155]
S13	$[a]_T^{25} = +10.21$ ($c = 0.12$, EtOH) (S)	$[a]_T^{25} = -3.36$ ($c = 3.3$, EtOH) (S)[156]

Table 10. Absolute configuration determination.

5.5. Scale-Up Experiments

5.5.1. Catalyst and Olefin Recovery Experiment

An oven-dried Schleck flask equipped with a magnetic stir bar was charged with carbamate **67a** (735 mg, 5.0 mmol, 1.0 equiv.), olefin **52a** (3.7 mL, 50 mmol, 10 equiv.) and dry CHCl$_3$ (12 mL). The flask was sealed and cooled down to –25 °C for 30 min. After this time, a stock solution of catalyst **72b** in 4 mL of CHCl$_3$ (42 mg, 0.5 mol%) was added dropwise via syringe. After the reaction was completed (TLC monitoring) it was quenched with one equivalent of triethylamine and stirred for 30 min at rt. The reaction crude mixture was transferred to a round-bottomed flask to facilitate manipulation. A short distillation apparatus was attached to the flask and CHCl$_3$ and triethylamine were distilled off the crude under vacuum (100 mbar, rt). The receiving flask was changed and the non-reacted styrene was further recovered by bulb-to-bulb vacuum distillation (94% styrene recovered, 1 mbar, 35 °C). The crude residue was purified by silica gel column chromatography (DCM/MeOH mixtures from 0.5 to 3% *v/v*) to give 545 mg of **68a** as a white solid (62%, e.r. = 96.5:3.5). Fractions containing IDPi catalyst were combined and purified by silica gel column chromatography (*n*-hexane/EtOAc 9:1 to 4:1 *v/v*) to afford a white solid, which was subjected to acidification by filtration over a plug of DOWEX 50WX8 (H-form, eluted with DCM) to obtain the reisolated catalyst **72b** (30 mg, 72%) as a yellowish solid.

Figure 50. Distillation of the non-reacted styrene under vacuum.

5.5.2. Formal Synthesis of (*R*)-Fluoxetine Hydrochloride from Styrene

(*R*)-6-Phenyl-1,3-oxazinan-2-one (68a)
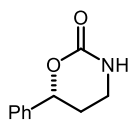
Obtained following the *General Procedure E*: an oven-dried Schleck flask equipped with a magnetic stir bar was charged with carbamate **67a** (2.5 g, 17 mmol, 1.0 equiv.), olefin **52a** (19.5 mL, 170 mmol) and dry CHCl$_3$ (40 mL). The flask was sealed and cooled down to –25 °C for 30 min. After this time, a stock solution of catalyst **72b** in 14 mL of CHCl$_3$ (283 mg, 1.0 mol%) was added dropwise via syringe. After the reaction was completed (TLC monitoring) it was quenched with one equivalent of triethylamine and stirred for 30 min at rt. The mixture was suspended on Celite and further purified by silica gel column chromatography (DCM/MeOH mixtures from 0.5 to 3% *v/v*) to give 2.20 g of **68a** as a white solid (73%, e.r. = 96.5:3.5).

(*R*)-3-(Methylamino)-1-phenylpropan-1-ol (34)
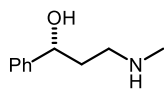
Obtained adapting a reported procedure:[117] to a two-necked round-bottomed oven-dried Schleck flask charged with product **68a** (2.20 g, 12 mmol, 1.0 equiv.) and dry THF (124 mL) was added LiAlH$_4$ (1.4 g, 37 mmol, 3.0 equiv.) under argon at 0 °C. The mixture was refluxed overnight. After cooling down to rt, the reaction was diluted with MTBE (30 mL), and cooled down to 0 °C. LiAlH$_4$ was quenched by a careful addition of water (3 mL), followed by an aqueous NaOH 15% solution (3 mL), and water (15 mL). The mixture was warmed up to rt and stirred for 30 min. Then it was transferred to a separatory funnel and both phases were separated. The aqueous phase was extracted with MTBE (3 x 10 mL). Combined organic phases were washed with brine (1 x 10 mL), dried over anhydrous Na$_2$SO$_4$ and evaporated to give compound **34** as a pure pale yellow oil (1.86 g, 91%) without further purification. Spectroscopic data was consistent with the values reported in the literature.[117]

(*R*)-Fluoxetine hydrochloride (83)
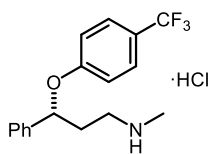
Obtained adapting a reported procedure:[157] in a flame-dried Schlenk under argon atmosphere, (*R*)-3-(methylamino)-1-phenylpropan-1-ol (**34**, 1.60 g, 9.7 mmol, 1.0 equiv.) was dissolved in 9 mL of dry dimethylacetamide. The mixture was cooled down to 0 °C and sodium hydride (60% dispersion in paraffin liquid, 0.46 g, 11.6 mmol, 1.2 equiv.) was added slowly. The mixture was heated to 90 °C for 1.5 h, and an orange solution resulted. To this solution was added 4-chlorobenzotrifluoride (1.92 g, 10.7 mmol, 1.1 equiv.), and the mixture was heated to 105 °C for 2 h. After cooling to rt and dilution with EtOAc (10 mL), the mixture was washed with water (5 mL), and the aqueous layer was separated and extracted with EtOAc (3 x 5 mL). The combined organic phases were washed with sat. aq. NaHCO$_3$ (1 x 10 mL) and brine (1 x 10 mL), dried over anhydrous Na$_2$SO$_4$ and evaporated. The crude free base fluoxetine was dissolved in 10 mL Et$_2$O and acidified with gaseous HCl to afford 3.05 g (91% yield) of (*R*)-fluoxetine hydrochloride as pale yellow crystals. Spectroscopic data was consistent with the values reported in the literature.[157]

^{1}H NMR (501 MHz, CDCl$_3$) δ 9.72 (s, 2H), 7.41 (d, *J* = 8.6 Hz, 5H), 7.36 – 7.22 (m, 5H), 6.90 (d, *J* = 8.5 Hz, 2H), 5.47 (dd, *J* = 8.3, 4.3 Hz, 1H), 3.18 – 3.05 (m, 2H), 2.61 (t, *J* = 5.5 Hz, 3H), 2.57 – 2.39 (m, 2H).

^{13}C NMR (126 MHz, CDCl$_3$) δ 159.8, 139.2, 129.2, 128.6, 126.9 (q, *J* = 3.6 Hz), 125.9, 116.0, 77.1, 46.2, 34.7, 33.1.

^{19}F NMR (471 MHz, CDCl$_3$) δ -61.67.

$[a]_T^{20}$ = –13.8 (*c* = 0.19, CHCl$_3$).

HPLC (Chiralpak IG-3, 70:30 MeOH/20 mM NH$_4$HCO$_3$ aq. pH = 9, 298 K, 220 nm): t$_R$ (major) = 8.8 min, t$_R$ (minor) = 11.1 min, e.r. = 96.5:3.5 (93% e.e.).

5.6. Synthesis of (*S*,*S*)-IDPi Catalysts

(*S*,*S*)-IDPi catalysts **64**, **71**, and **73** were prepared following modified literature procedures.[158-160] Phosphazene reagent **S6** was prepared following reported literature procedures.[161]

4-((3*r*,5*r*,7*r*)-Adamantan-1-yl)phenol (S7)
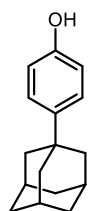
Following a reported procedure:[162] to a solution of phenol (1.00 g, 10.6 mmol. 1.0 equiv.) in trifluoroacetic acid (32 mL) was added 1-adamantol (1.61 g, 10.6 mmol, 1 equiv.) in a two-necked round-bottomed flask under argon. The suspension was stirred for 6 h at rt. After this time, the mixture was diluted with H_2O (50 mL) and the precipitate was filtered off, washed with an aqueous solution of Na_2CO_3 (until pH = 7) and dried to give product **S7** (2.40 g, quant.) as a colorless solid. Spectroscopic data was consistent with the values reported in the literature.[162]

^{1}H NMR (501 MHz, CDCl$_3$) δ 7.30 – 7.16 (m, 2H), 6.78 (d, *J* = 8.7 Hz, 2H), 4.77 (s, 1H), 2.14 – 2.02 (m, 3H), 1.88 (d, *J* = 2.9 Hz, 6H), 1.82 – 1.66 (m, 6H).

4-((3*r*,5*r*,7*r*)-Adamantan-1-yl)phenyl trifluoromethanesulfonate (S8)
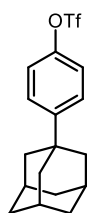
Following a reported procedure:[163] in a flame-dried Schlenk under argon atmosphere, sub-strate **S7** (2.41 g, 10.5 mmol, 1.0 equiv.) was dissolved in 67 mL of dry DCM. The solution was cooled down to 0 °C using an ice/water bath and triethylamine (8.8 mL, 6.0 equiv.) was added. After stirring for 10 min, trifluoromethanesulfonic anhydride (3.5 mL, 21.0 mmol, 2.0 equiv.) was added dropwise. The solution was stirred at 0 °C for 30 min, then warmed up to rt, and quenched with aqueous HCl 10% (50 mL). The layers were separated and the aqueous layer was further extracted with DCM (3 x 20 mL). The combined organic extracts were washed with water (1 x 20 mL), dried over anhydrous Na_2SO_4, filtered, and concentrated. The crude residue was purified by silica gel column chromatography using *n*-hexane/EtOAc (15:1 *v/v*) as eluent to afford 2.53 g (67% yield) of product **S8**. Spectroscopic data was consistent with the values reported in the literature.[163]

^{1}H NMR (501 MHz, CDCl$_3$) δ 7.41 (d, *J* = 8.8 Hz, 2H), 7.20 (d, *J* = 8.8 Hz, 2H), 2.18 – 2.04 (m, 3H), 1.89 (d, *J* = 3.0 Hz, 6H), 1.85 – 1.63 (m, 6H).

^{13}C NMR (126 MHz, CDCl$_3$) δ 151.9, 147.6, 126.9, 120.8, 119.0 (q, $^1J_{CF}$ = 320 Hz, CF$_3$), 43.2, 36.7, 36.4, 28.9.

^{19}F NMR (471 MHz, CDCl$_3$) δ –72.94.

5.6.1. Synthesis of Substituted (*S*)-BINOLs
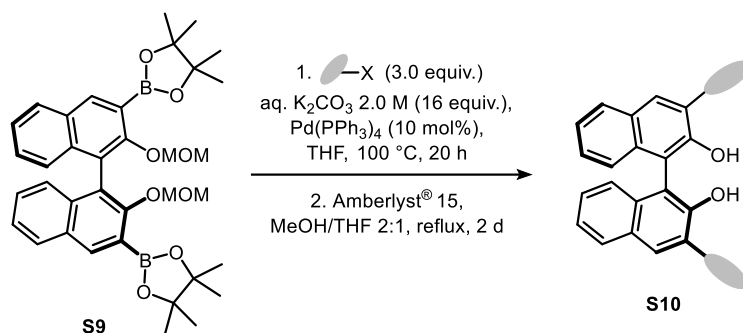
(*S*)-3,3'-bis(4-((3r,5r,7r)-Adamantan-1-yl)phenyl)-[1,1'-binaphthalene]-2,2'-diol (S10b)

A flame-dried Schlenk under argon atmosphere was charged with (*S*)-MOM-BINOL Bpin ester[164] **S9** (626 mg, 1.0 mmol, 1.0 equiv.) and triflate **S8** (1.08 g, 3.0 mmol, 3.0 equiv.). THF (10 mL) and K_2CO_3 (2 M in H_2O, 8 mL, 16 mmol, 16 equiv.) were added and the solution was sparged with argon for 20 min. Subsequently, $Pd(PPh_3)_4$ (116 mg, 0.1 mmol, 10 mol%) was added and the reaction was heated to 100 °C for 20 h. After cooling to rt, the reaction was di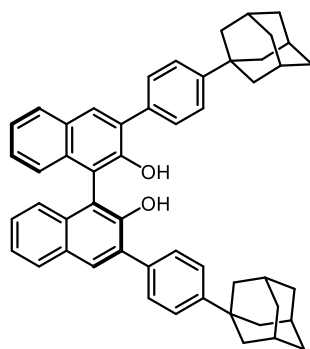luted with water (10 mL) and the aqueous layer was extracted with DCM (3 x 15 mL). The combined organic phases were washed with brine (1 x 15 mL), dried over anhydrous Na_2SO_4, filtered, and concentrated under reduced pressure. The crude residue was purified by silica gel column chromatography using *n*-hexane/EtOAc mixtures as eluent. The pure white-off solid was transferred to a round-bottomed flask and dissolved in 30 mL MeOH/THF 2:1 (*v/v*). 590 mg of Amberlyst® 15 ion-exchange resin were added and the mixture was heated at reflux for 2 days, after which full conversion was confirmed by TLC (*n*-hexane/EtOAc 10:1 *v/v*). The mixture was cooled down to rt and the solid resin was removed by filtration. The crude product was repurified through a short silica gel column chromatography using *n*-hexane/EtOAc mixtures to afford 399 mg (76%) of BINOL **S10b** as a white solid.

^{1}H NMR (501 MHz, $CDCl_3$) δ 8.09 (s, 2H), 7.97 (d, *J* = 8.1 Hz, 2H), 7.79 – 7.73 (d, *J* = 8.4 Hz, 4H), 7.58 – 7.53 (d, *J* = 8.4 Hz, 4H), 7.44 (ddd, *J* = 8.1, 6.7, 1.3 Hz, 2H), 7.36 (ddd, *J* = 8.1, 6.7, 1.3 Hz, 2H), 7.31 – 7.25 (m, 2H), 5.45 (s, 2H), 2.19 (m, 6H), 2.05 (d, *J* = 2.9 Hz, 12H), 1.96 (d, *J* = 2.9 Hz, 2H), 1.93 – 1.71 (m, 10H).

^{13}C NMR (126 MHz, $CDCl_3$) δ 151.9, 151.1, 150.4, 147.5, 134.6, 133.0, 131.3, 130.7, 129.6, 129.4, 128.5, 127.3, 126.9, 125.2, 124.5, 124.3, 120.9, 112.6, 43.3, 43.2, 36.9, 36.7, 36.3, 29.1, 28.9.

HRMS (ESI) calculated for $C_{52}H_{49}O_2$ ([M–H^{−}]): 705.373805, found: 705.373803.

$[a]_T^{20}$ = -4.55 (*c* = 0.13, $CHCl_3$).

5.6.2. Synthesis of (*S*,*S*)-IDPis
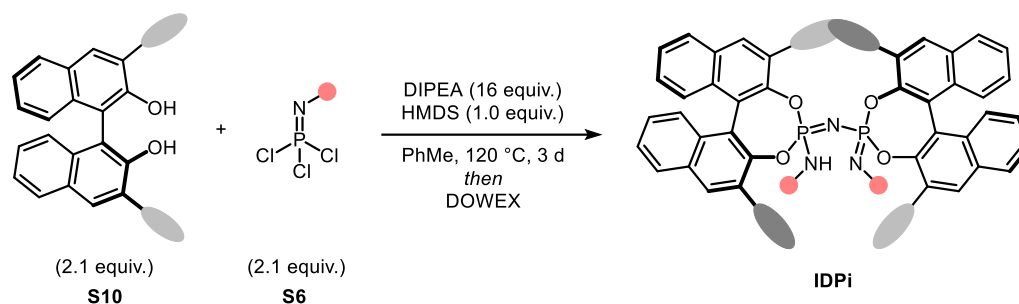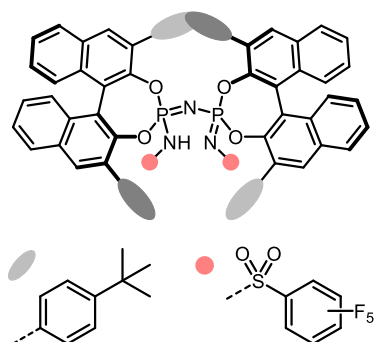
In a flame-dried Schlenk flask under argon, (*S*)-3,3'-bis(4-(tert-butyl)phenyl)-[1,1'-binaphthalene]-2,2'-diol[165] (**S10a**, 1.00 g, 1.81 mmol, 2.1 equiv.) and ((perfluoro-phenyl)sulfonyl)phosphorimidoyl trichloride **S6** (694 mg, 1.81 mmol, 2.1 equiv.) were dissolved in toluene (8.2 mL). Then diisopropylethylamine (2.4 mL, 13.8 mmol, 16 equiv.) was added and the yellow suspension was stirred at rt for 10 min. Hexamethyldisilazane (180 µL, 0.86 mmol, 1.0 equiv.) was added to the reaction mixture, which was further stirred at rt for 10 min, and then heated to reflux for 3 d. After cooling to rt, the mixture was diluted with DCM and quenched with aq. HCl 10%. The aqueous layer was extracted with DCM (3 x 30 mL) and the combined organic layers were dried over anhydrous Na_2SO_4 and concentrated under reduced pressure. Purification by silica gel column chromatography (*n*-hexane/EtOAc 9:1 to 4:1 *v/v*) afforded a white solid, which was subjected to acidification by filtration over a plug of DOWEX 50WX8 (H-form, eluted with DCM) to afford catalyst **72b** (936 mg, 65%) as a yellowish solid. Spectroscopic data was consistent with the values reported in the literature.[166]

(*S*,*S*)-(4-*tert*-Butylphenyl)-C₆F₅ IDPi (72b)

^{1}H NMR (501 MHz, CDCl₃) δ 8.18 (d, *J* = 8.2 Hz, 2H), 8.05 (s, 2H), 8.00 – 7.92 (m, 4H), 7.73 – 7.66 (m, 2H), 7.57 – 7.46 (m, 5H), 7.40 – 7.30 (m, 5H), 6.82 (d, *J* = 8.0 Hz, 4H), 6.52 (d, *J* = 8.1 Hz, 4H), 1.30 (s, 18H), 0.89 (s, 18H).

^{13}C NMR (126 MHz, CDCl₃) δ 151.3, 150.3, 143.8 (dm, *J* = 260 Hz), 143.6 (dt, *J* = 9.4, 5.3 Hz), 142.8 (dm, *J* = 260 Hz), 136.9 (dm, *J* = 257 Hz), 134.5, 133.2, 132.8, 132.5, 132.1, 131.7 (d, *J* = 6.3 Hz), 131.2 (d, *J* = 6.7 Hz), 130.4, 129.4, 129.0, 128.9, 128.3, 127.4, 126.9 (d, *J* = 6.7 Hz), 126.8 – 126.6 (m), 126.1, 124.7, 123.3, 122.7, 117.5 (m), 34.7, 34.4, 31.2.

^{19}F NMR (471 MHz, CDCl₃) δ -134.85 (d, *J* = 22.2 Hz, 4F), -145.89 (t, *J* = 21.7 Hz, 2F), -160.15 (dd, *J* = 22.3, 17.0 Hz, 4F).
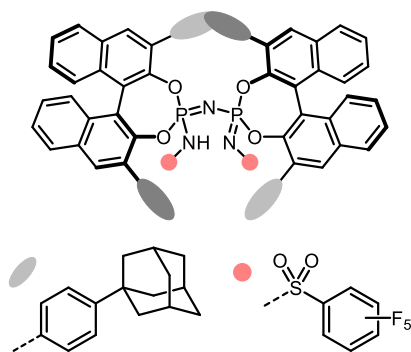
^{31}P NMR (203 MHz, CDCl₃) δ -8.58.

HRMS (ESI) calculated for C₉₂H₇₂F₁₀N₃O₈P₂S₂F₁₀ ([M–H⁻]): 1662.40819, found: 1662.40802.

$[a]_T^{20}$ = +135.48 (c = 0.12, CHCl₃).

LC-MS (50 mm Zorbax SB300-C8, 3.5 µm, 4.6 mm i.d., 1% TFA/MeCN 25:75, 1.0 mL/min, 4.7 MPa, 308 K, 254 nm): t_R = 16.8 min (98% purity).

(*S*,*S*)-(4-(3*r*,5*r*,7*r*)-adamantan-1-yl)phenyl)-C₆F₅ IDPi (74b)

In a flame-dried Schlenk flask under argon, BINOL **S10b** (240 mg, 0.34 mmol, 2.1 equiv.) and ((perfluorophenyl)sulfonyl)phos-phorimidoyl trichloride **S6** (130 mg, 0.34 mmol, 2.1 equiv.) were dissolved in toluene (1.5 mL). Then diisopropylethylamine (450 µL, 2.59 mmol, 16 equiv.) was added and the yellow suspen-sion was stirred at rt for 10 min. Hexamethyldisilazane (34 µL, 0.16 mmol, 1.0 equiv.) was added to the reaction mixture, which was stirred at rt for 10 min, then heated to reflux for 4 d. After cooling to rt, the mixture was diluted with DCM and quenched with aq. HCl 10%. The aqueous layer was extracted with DCM (3 x 10 mL) and the combined organic layers were dried over anhydrous Na₂SO₄ and concentrated under reduced pressure. Purification by silica gel column chromatography (*n*-hexane/EtOAc 9:1 to 4:1 *v/v*) afforded a white solid, which was subjected to acidification by filtration over a plug of DOWEX 50WX8 (H-form, eluted with DCM) to afford catalyst **74b** (47 mg, 15%) as a yellowish solid.

¹H NMR (501 MHz, CDCl₃) δ 8.14 (d, *J* = 8.2 Hz, 2H), 8.03 (s, 2H), 7.94 (d, *J* = 8.3 Hz, 2H), 7.87 (s, 2H), 7.69 (t, *J* = 7.5 Hz, 2H), 7.54 (ddd, *J* = 8.1, 5.5, 2.5 Hz, 2H), 7.49 – 7.43 (m, 6H), 7.40 (d, *J* = 8.4 Hz, 4H), 7.35 – 7.29 (m, 4H), 6.81 (d, *J* = 8.2 Hz, 4H), 6.48 (d, *J* = 8.1 Hz, 4H), 5.07 (bs, 1H), 2.05 – 1.97 (m, 6H), 1.87 (m, 12H), 1.76 – 1.66 (m, 18H), 1.57 – 1.45 (m, 18H), 1.42 – 1.35 (m, 6H).

¹³C NMR (126 MHz, CDCl₃) δ 151.3, 150.6, 134.5, 133.6, 132.8, 132.4, 132.2, 131.7 (d, *J* = 5.8 Hz), 131.2, 130.4, 129.5, 128.9 (d, *J* = 15.2 Hz), 128.3, 127.5, 127.0 – 126.3 (m), 125.5, 124.2, 123.3, 122.5, 42.8, 42.7 36.9, 36.7, 36.2, 35.9, 29.1, 28.9 (other signals not detected or observed).

¹⁹F NMR (471 MHz, CDCl3) δ -134.74 (t, *J* = 22.3 Hz, 4F), -146.11 (t, *J* = 22.3 Hz, 2F), -160.14 (t, *J* = 20.3 Hz, 4F).

³¹P NMR (203 MHz, CDCl₃) δ -8.14.

HRMS (ESI) calculated for C₁₁₆H₉₆F₁₀N₃O₈P₂S₂ ([M–H⁻]): 1974.596000, found: 1974.59597.

$[a]_T^{20}$ = +144.52 (c = 0.11, CHCl₃).

LC-MS (50 mm Zorbax SB300-C8, 3.5 µm, 4.6 mm i.d., 1% TFA/MeCN 10:90, 1.0 mL/min, 4.7 MPa, 308 K, 254 nm): t_R = 3.57 min (99% purity).

5.7. NMR Characterization of Ion Pair VI

Sample preparation

An oven-dried (80 °C, overnight) NMR tube was charged with substrate **67a** (23 mg, 1.0 equiv.) and styrene (**52a**, 180 µL, 10 equiv.) in 0.38 mL CDCl₃. The initial mixture was precooled to –78 °C in a dry ice/ethanol bath. After addition of a solution of catalyst **72b** (10.4 mg, 4.0 mol%) in CDCl₃ (125 µL), the NMR tube was quickly turned upside down, vortexed, and transferred to the precooled NMR probe at 233 K (–40 °C). Afterwards a set of different NMR experiments was performed (see NMR data below) to characterize the intermediate as best as possible.
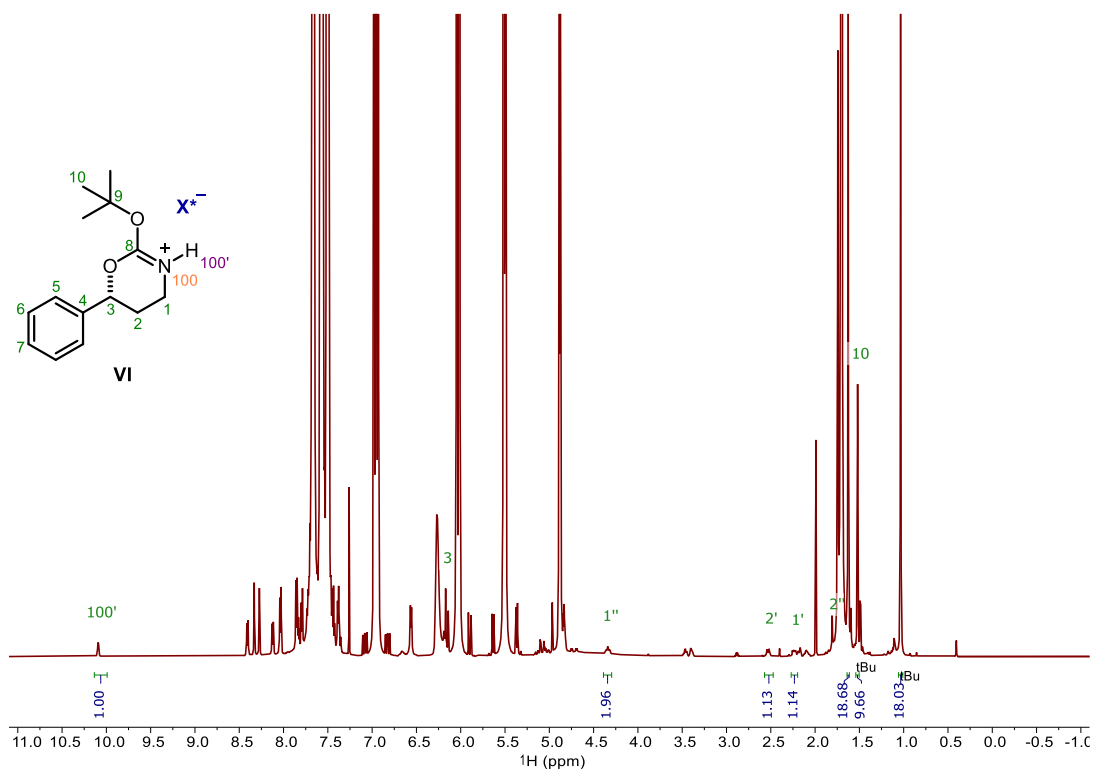
Figure 51. ¹H NMR spectrum of intermediate **VI** (600 MHz, CDCl₃, 233 K).
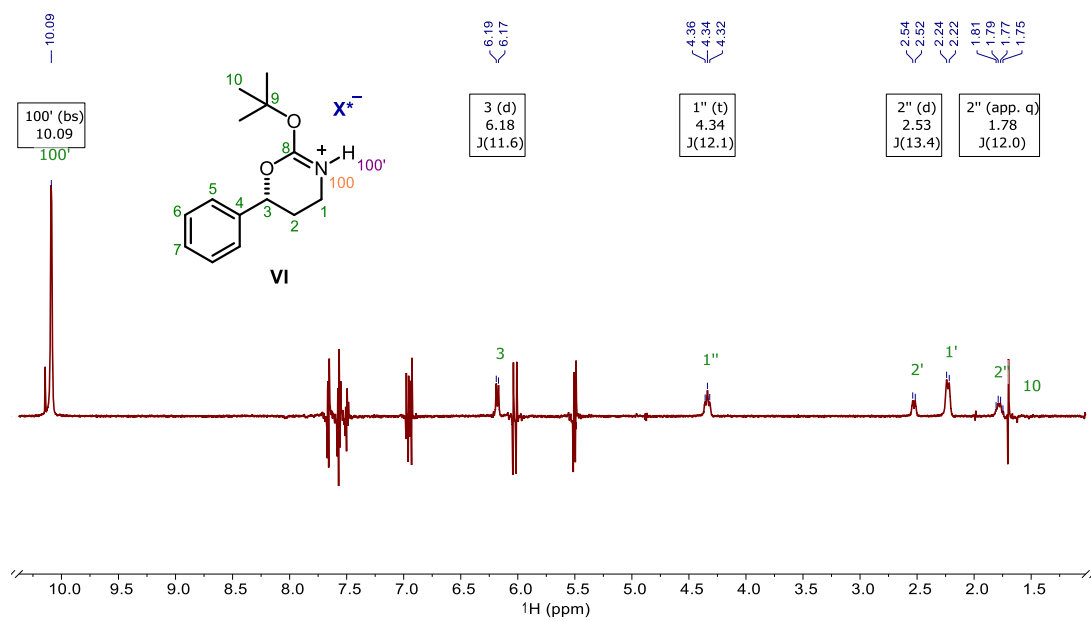
Figure 52. 1D selective TOCSY of intermediate **VI** with excitation of H-100' (spin lock mixing time 150 ms, 600 MHz, CDCl₃, 233 K).
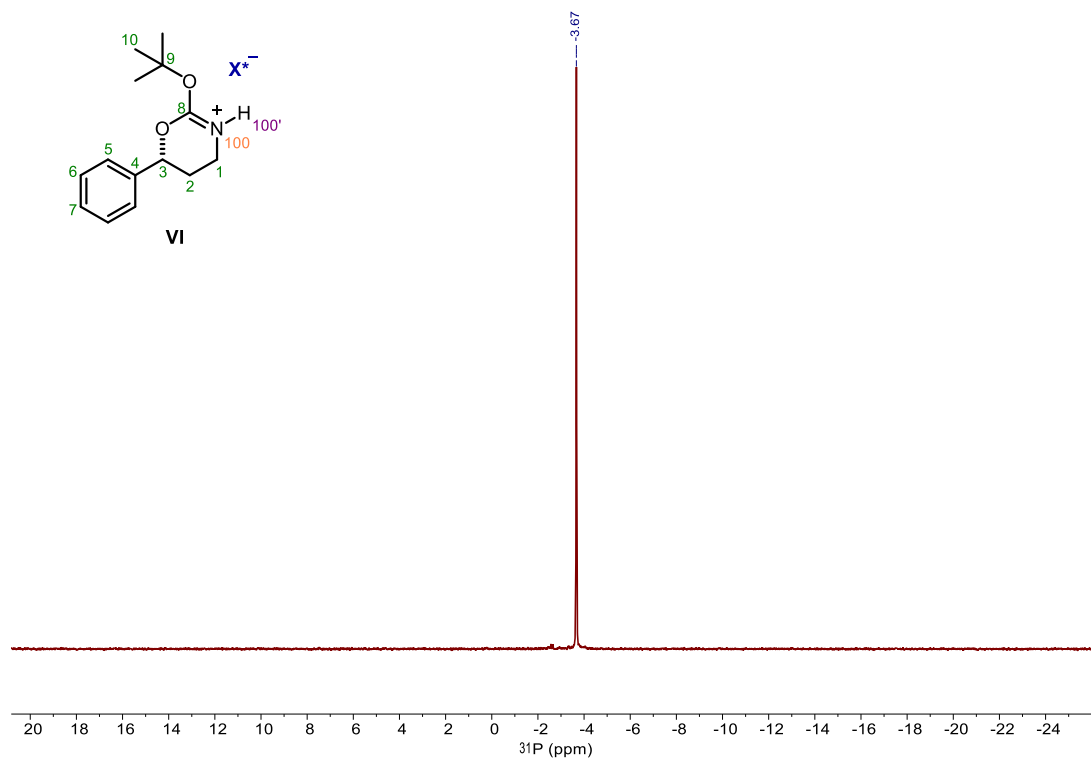
Figure 53. ³¹P NMR spectrum of intermediate **VI** (243 MHz, CDCl₃, 233 K).
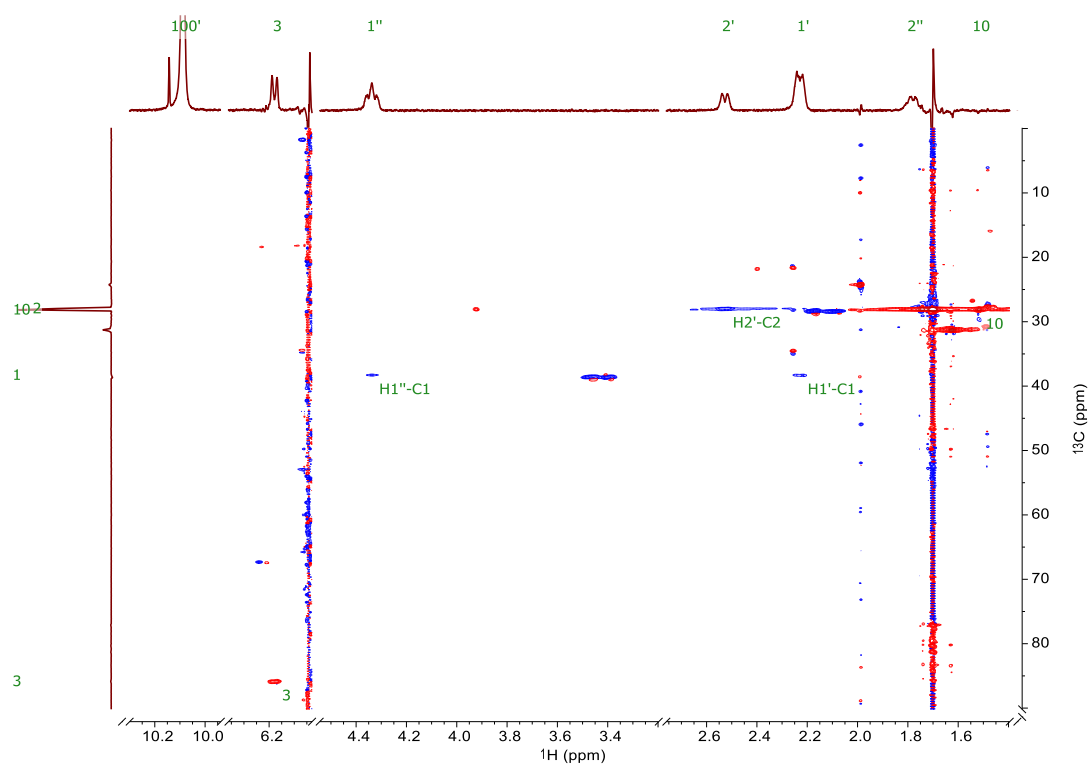
Figure 54. Excerpt of the ^{1}H-^{13}C-edited HSQC NMR spectrum showing relevant cross peaks of intermediate **VI** (600 MHz, CDCl$_3$, 233 K).
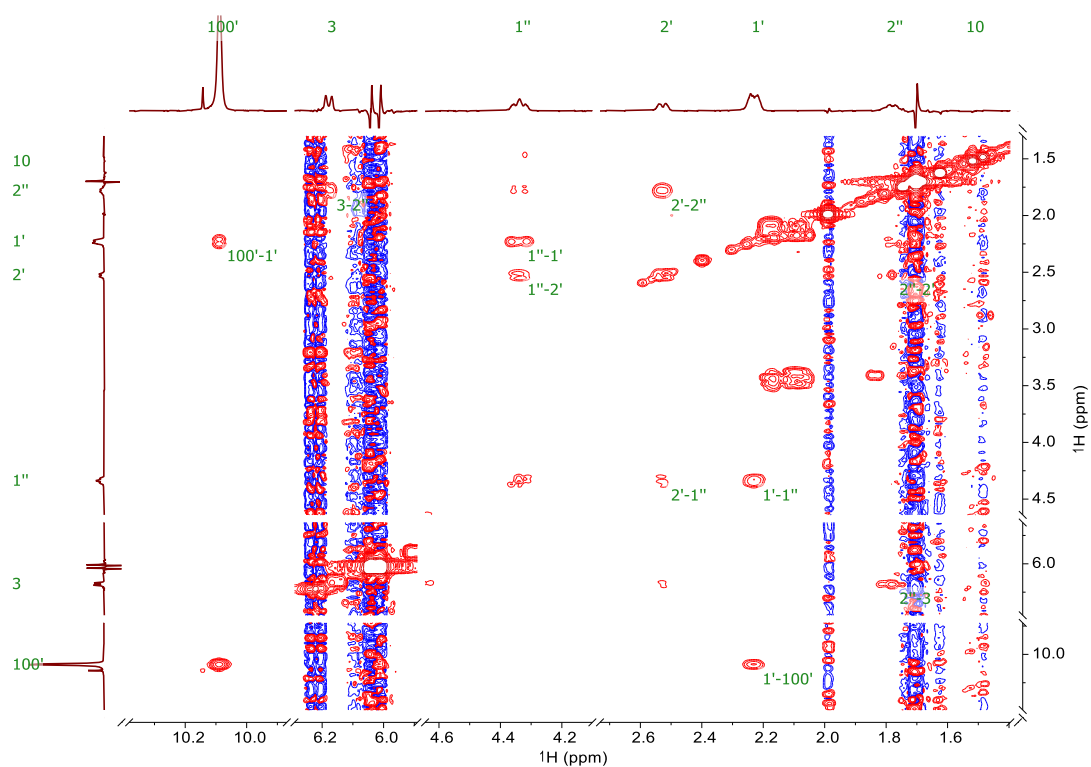
Figure 55. Excerpt of the ^{1}H,^{1}H-COSY NMR spectrum showing relevant correlations of intermediate **VI** (600 MHz, CDCl$_3$, 233 K).
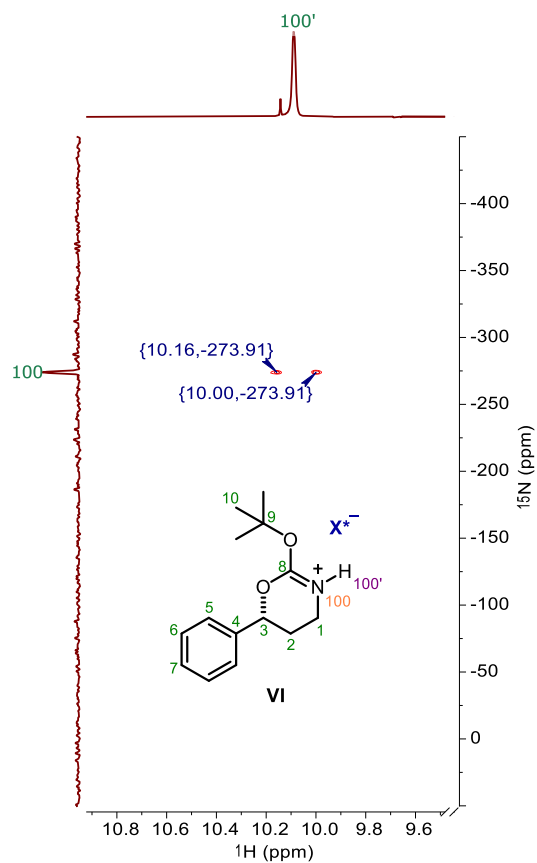
Figure 56. Cross section of the ^{1}H,^{15}N-HMBC spectrum showing the relevant cross peak of intermediate **VI** (600 MHz, CDCl$_3$, 233 K).
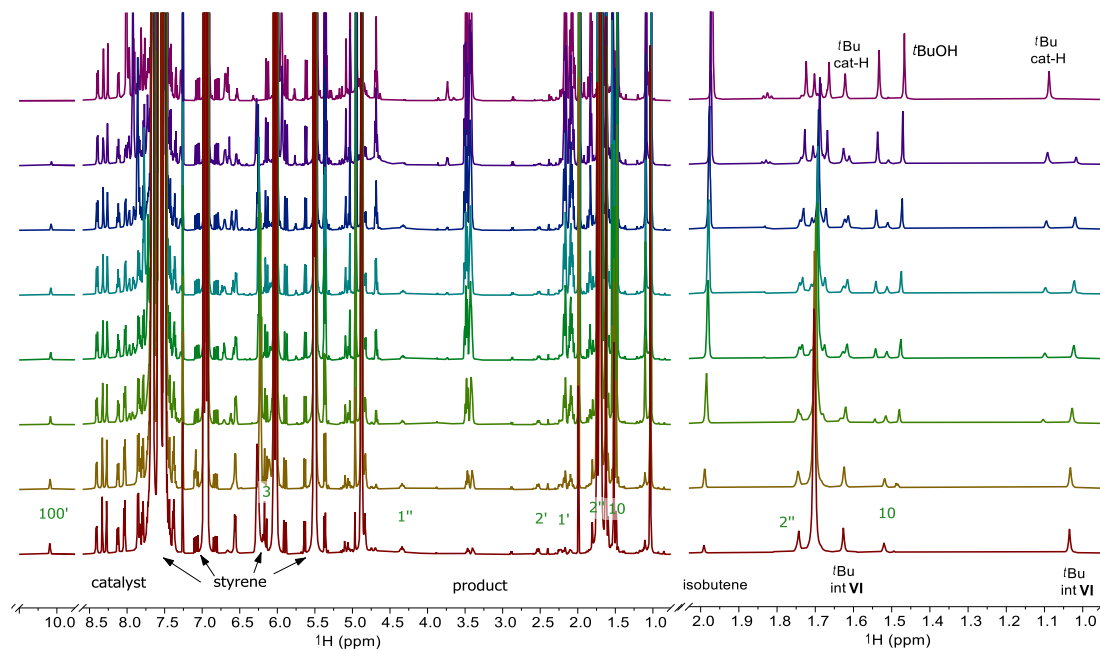
Figure 57. ^{1}H NMR spectra taken at different time points showing the decay of the intermediate **VI** signals as well as the change of signals from the catalyst and product formation (600 MHz, CDCl$_3$, 233 K).
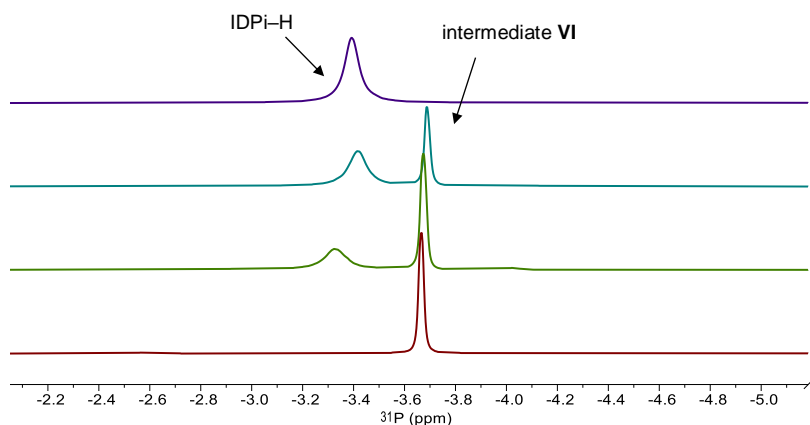
Figure 58. ^{31}P NMR spectra taken at different time points showing the decay of the intermediate **VI** signals as well as the formation of a broadened IDPi–H species (243 MHz, CDCl$_3$, 233 K).


```
Mass to be matched (m/z): 234.14868  charge: 1

Mass tolerance: ±0.005
restriction of atom numbers:
      C        H        N        O
   1-100    1-100     1-3     0-10
Number of calculated formulas: 2
Formula        Diff. (ppm)  theor. m/z
C14 H20 N1 O2        0.77    234.14886
C9 H20 N3 O4       -16.44    234.14483
```

possible elemental composition of m/z 234

reduced mass range m/z 200-250 (pos. ions)

R3: 43(2:36) m(42-46) 685 42% E47849c-00 * GUQ-GA-435-01/ESIpos/CH2Cl2+CH3OH/Exactive/

Figure 59. HRMS of the reaction intermediate **VI**.

6. References

[1]   D. G. Blackmond, *Philos. Trans. Biol. Sci.* **2011**, *366*, 2878–2884.

[2]   L. A. Nguyen, H. He, C. Pham-Huy, *Int. J. Biomed. Sci.* **2006**, *2*, 85–100.

[3]   G.-Q. Lin, Y.-M. Li, A. S. C. Chan, *Principles and Applications of Asymmetric Synthesis*, John Wiley & Sons, **2001**.

[4]   B. List, R. A. Lerner, C. F. Barbas, *J. Am. Chem. Soc.* **2000**, *122*, 2395–2396.

[5]   K. A. Ahrendt, C. J. Borths, D. W. C. MacMillan, *J. Am. Chem. Soc.* **2000**, *122*, 4243–4244.

[6]   O. García Mancheño, M. Waser, *Eur. J. Org. Chem.* **2023**, *26*, e202200950.

[7]   B. Han, X.-H. He, Y.-Q. Liu, G. He, C. Peng, J.-L. Li, *Chem. Soc. Rev.* **2021**, *50*, 1522–1586.

[8]   R. Janoschek, *Chirality – From Weak Bosons to the Alpha-Helix*, Springer Berlin, Heidelberg, **1991**.

[9]   E. J. Ariëns, *Eur. J. Clin. Pharmacol.* **1984**, *26*, 663–668.

[10]   R. U. McVicker, N. M. O'Boyle, *J. Med. Chem.* **2024**, *67*, 2305–2320.

[11]   Catalyst, in *The IUPAC Compendium of Chemical Terminology*, International Union of Pure and Applied Chemistry (IUPAC): Research Triangle Park, NC, **2019**.

[12]   J. von Liebig, *Justus Liebigs Ann. Chem.* **1860**, *113*, 246–247.

[13]   H. Pracejus, *Justus Liebigs Ann. Chem.* **1960**, *634*, 9–22.

[14]   S. Bahmanyar, K. N. Houk, *J. Am. Chem. Soc.* **2001**, *123*, 12911–12912.

[15]   B. List, L. Hoang, H. J. Martin, *Proc. Natl. Acad. Sci.* **2004**, *101*, 5839–5842.

[16]   B. List, *Tetrahedron* **2002**, *58*, 5573–5590.

[17]   J. Seayad, B. List, *Org. Biomol. Chem.* **2005**, *3*, 719–724.

[18]   D. Kampen, C. M. Reisinger, B. List, in *Asymmetric Organocatalysis. Top. Curr. Chem. Vol. 291*, Springer Berlin, Heidelberg, **2010**, pp. 395–456.

[19]   P. Vachal, E. N. Jacobsen, *J. Am. Chem. Soc.* **2002**, *124*, 10012–10014.
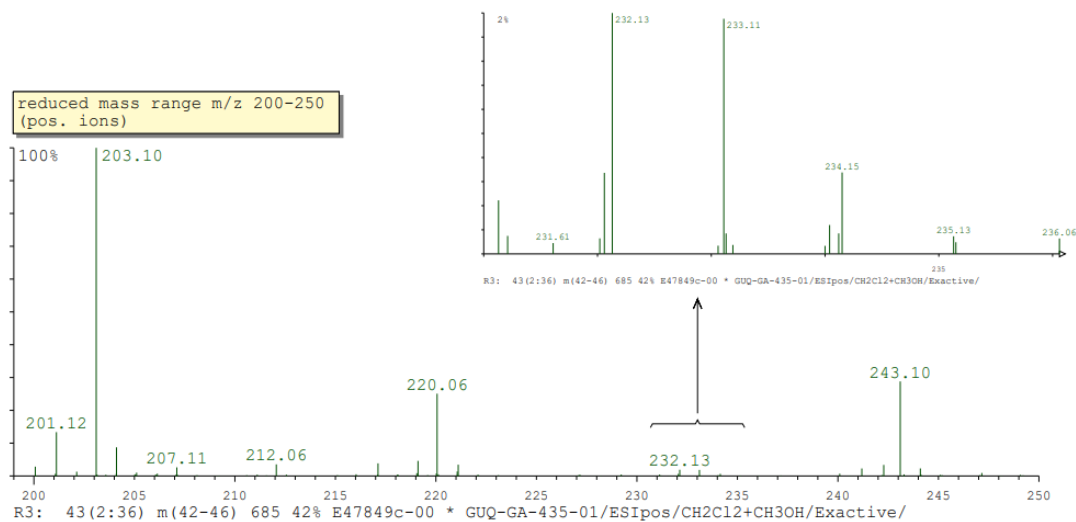
[20]   J. P. Malerich, K. Hagihara, V. H. Rawal, *J. Am. Chem. Soc.* **2008**, *130*, 14416–14417.

[21]   A. G. Doyle, E. N. Jacobsen, *Chem. Rev.* **2007**, *107*, 5713–5743.

[22]   T. Akiyama, J. Itoh, K. Yokota, K. Fuchibe, *Angew. Chem. Int. Ed.* **2004**, *43*, 1566–1568.

[23]   D. Uraguchi, M. Terada, *J. Am. Chem. Soc.* **2004**, *126*, 5356–5357.

[24]   M. Hatano, K. Moriyama, T. Maki, K. Ishihara, *Angew. Chem. Int. Ed.* **2010**, *49*, 3823–3826.

[25]   M. Klussmann, L. Ratjen, S. Hoffmann, V. Wakchaure, R. Goddard, B. List, *Synlett* **2010**, *2010*, 2189–2192.

[26]   K. Kanomata, M. Terada, *Synlett* **2011**, *2011*, 1255–1258.

[27]   S. Hoffmann, A. M. Seayad, B. List, *Angew. Chem. Int. Ed.* **2005**, *44*, 7424–7427.

[28]   A. Kütt, S. Tshepelevitsh, J. Saame, M. Lõkov, I. Kaljurand, S. Selberg, I. Leito, *Eur. J. Org. Chem.* **2021**, *2021*, 1407–1419.

[29]   L. M. Yagupolskii, V. N. Petrik, N. V. Kondratenko, L. Sooväli, I. Kaljurand, I. Leito, I. A. Koppel, *J. Chem. Soc., Perkin Trans. 2* **2002**, 1950–1955.

[30]   D. Nakashima, H. Yamamoto, *J. Am. Chem. Soc.* **2006**, *128*, 9626–9627.

[31]   P. S. J. Kaib, B. List, *Synlett* **2016**, *27*, 156–158.

[32]   P. García-García, F. Lay, P. García-García, C. Rabalakos, B. List, *Angew. Chem. Int. Ed.* **2009**, *48*, 4363–4366.

[33]   M. Treskow, J. Neudörfl, R. Giernoth, *Eur. J. Org. Chem.* **2009**, *2009*, 3693–3697.

[34]   M. C. Benda, S. France, *Org. Biomol. Chem.* **2020**, *18*, 7485–7513.

[35]   A. Berkessel, P. Christ, N. Leconte, J.-M. Neudörfl, M. Schäfer, *Eur. J. Org. Chem.* **2010**, *2010*, 5165–5170.

[36]   M. Mouarrawis, R. Plessius, J. I. van der Vlugt, J. N. H. Reek, *Front. Chem.* **2018**, *6*.

[37]   I. Čorić, B. List, *Nature* **2012**, *483*, 315–319.

[38]   L. Schreyer, R. Properzi, B. List, *Angew. Chem. Int. Ed.* **2019**, *58*, 12761–12777.

[39]   S. Brunen, B. Mitschke, M. Leutzsch, B. List, *J. Am. Chem. Soc.* **2023**, *145*, 15708–15713.

[40]   R. Properzi, P. S. J. Kaib, M. Leutzsch, G. Pupo, R. Mitra, C. K. De, L. Song, P. R. Schreiner, B. List, *Nat. Chem.* **2020**, *12*, 1174–1179.

[41]   H. Zhou, Y. Zhou, H. Y. Bae, M. Leutzsch, Y. Li, C. K. De, G.-J. Cheng, B. List, *Nature* **2022**, *605*, 84–89.

[42]   N. Luo, M. Turberg, M. Leutzsch, B. Mitschke, S. Brunen, V. N. Wakchaure, N. Nöthling, M. Schelwies, R. Pelzer, B. List, *Nature* **2024**, *632*, 795–801.

[43]   W. Xieqing, X. Chaogang, L. Zaiting, Z. Genquan, in *Practical Advances in Petroleum Processing*, Springer New York, **2006**, pp. 149–168.

[44]   Statista, https://www.statista.com/statistics/1067372/global-ethylene-production-capacity/.

[45]   Statista, https://www.statista.com/statistics/1065879/global-propylene-production-capacity/.

[46]   C. Perego, P. Pollesel, in *Advances in Nanoporous Materials, Vol. 1*, Elsevier, **2010**, pp. 97–149.

[47]   B. A. Vaughan, M. S. Webster-Gardiner, T. R. Cundari, T. B. Gunnoe, *Science* **2015**, *348*, 421–424.

[48]   J. Ragan, in *Practical Synthetic Organic Chemistry: Reactions, Principles, and Techniques,* John Wiley & Sons, **2011**, pp. 167–235.

[49]   R. S. Bon, H. Waldmann, *Acc. Chem. Res.* **2010**, *43*, 1103–1114.

[50]   K. B. Sharpless, W. Amberg, Y. L. Bennani, G. A. Crispino, J. Hartung, K. S. Jeong, H. L. Kwong, K. Morikawa, Z. M. Wang, *J. Org. Chem.* **1992**, *57*, 2768–2771.

[51]   G. Li, H.-T. Chang, K. B. Sharpless, *Angew. Chem. Int. Ed.* **1996**, *35*, 451–454.

[52]   H. C. Kolb, M. S. VanNieuwenhze, K. B. Sharpless, *Chem. Rev.* **1994**, *94*, 2483–2547.

[53]   C. D. Díaz-Oviedo, R. Maji, B. List, *J. Am. Chem. Soc.* **2021**, *143*, 20598–20604.

[54]   S. L. Meisel, J. J. Dickert, H. D. Hartough, *J. Am. Chem. Soc.* **1956**, *78*, 4782–4783.

[55]   D. V. Deubel, G. Frenking, *Acc. Chem. Res.* **2003**, *36*, 645–651.

[56]   O. Diels, K. Alder, *Justus Liebigs Ann. Chem.* **1928**, *460*, 98–122.

[57]   S. Kobayashi, K. A. Jørgensen, *Cycloaddition Reactions in Organic Synthesis*, Wiley-VCH Verlag GmbH, **2001**.

[58]   R. Sustmann, *Pure Appl. Chem.* **1974**, *40*, 569–593.

[59]   D. L. Boger, R. P. Schaum, R. M. Garbaccio, *J. Org. Chem.* **1998**, *63*, 6329–6337.

[60]   T. Lipińska, *Tetrahedron* **2005**, *61*, 8148–8158.

[61]   H. Mayr, M. Patz, *Angew. Chem. Int. Ed.* **1994**, *33*, 938–957.

[62]   B. E. Maryanoff, H.-C. Zhang, J. H. Cohen, I. J. Turchi, C. A. Maryanoff, *Chem. Rev.* **2004**, *104*, 1431–1628.

[63]   C. Mannich, W. Krösche, *Arch. Pharm.* **1912**, *250*, 647–667.

[64]   A. Pictet, T. Spengler, *Dtsch. Chem. Ges.* **1911**, *44*, 2030–2036.

[65]   P. Wu, T. E. Nielsen, *Chem. Rev.* **2017**, *117*, 7811–7856.

[66]   A. J. Basson, M. G. McLaughlin, *Tetrahedron* **2022**, *114*, 132764.

[67]   R. R. Schmidt, *Angew. Chem. Int. Ed.* **1969**, *8*, 602–602.

[68]   H. E. Zaugg, *Synthesis* **1984**, *3*, 181–212.

[69]   C. Giordano, G. Ribaldone, G. Borsotti, *Synthesis* **1971**, *2*, 92–95.

[70]   N. Momiyama, H. Okamoto, J. Kikuchi, T. Korenaga, M. Terada, *ACS Catal.* **2016**, *6*, 1198–1204.

[71]   J. Kikuchi, H. Ye, M. Terada, *Org. Lett.* **2020**, *22*, 8957–8961.

[72]   M. Hatano, K. Nishikawa, K. Ishihara, *J. Am. Chem. Soc.* **2017**, *139*, 8424–8427.

[73]   N. Uddin, J. S. Ulicki, F. H. Foersterling, M. M. Hossain, *Tetrahedron Lett.* **2011**, *52*, 4353–4356.

[74]   D. T. Wong, K. W. Perry, F. P. Bymaster, *Nat. Rev. Drug Discov.* **2005**, *4*, 764–774.

[75]   Top 20 Global Products 2012, IMS Health MIDAS, **2012**.

[76]   L. J. Scott, C. M. Perry, *Drugs* **2000**, *60*, 139–176.

[77]   N. Y. Rakhmanina, J. N. van den Anker, *Expert Opin. Drug Metab. Toxicol.* **2010**, *6*, 95–103.

[78]   R. P. Jain, R. M. Williams, *J. Org. Chem.* **2002**, *67*, 6361–6365.

[79]   M.-K. Kim, H.-S. Park, C.-H. Kim, H.-M. Park, W. Choi, *Yeast* **2002**, *19*, 341–349.

[80]   H. Ren, W. D. Wulff, *Org. Lett.* **2013**, *15*, 242–245.

[81]   S. M. Lait, D. A. Rankic, B. A. Keay, *Chem. Rev.* **2007**, *107*, 767–796.

[82]   S. Sakuraba, K. Achiwa, *Synlett* **1991**, *1991*, 689–690.

[83]   C. Liu, L. Zhang, L. Cao, Y. Xiong, Y. Ma, R. Cheng, J. Ye, *Commun. Chem.* **2022**, *5*.

[84]   J.-N. Zhou, Q. Fang, Y.-H. Hu, L.-Y. Yang, F.-F. Wu, L.-J. Xie, J. Wu, S. Li, *Org. Biomol. Chem.* **2014**, *12*, 1009–1017.

[85]   X. Chen, Z.-Q. Liu, C.-P. Lin, Y.-G. Zheng, *Bioorg. Chem.* **2016**, *65*, 82–89.

[86]   B. List, *J. Am. Chem. Soc.* **2000**, *122*, 9336–9337.

[87]   B. List, P. Pojarliev, W. T. Biller, H. J. Martin, *J. Am. Chem. Soc.* **2002**, *124*, 827–833.

[88]   J. W. Yang, C. Chandler, M. Stadler, D. Kampen, B. List, *Nature* **2008**, *452*, 453–455.

[89]   R. Breslow, S. H. Gellman, *J. Am. Chem. Soc.* **1983**, *105*, 6728–6729.

[90]   S. M. Paradine, J. R. Griffin, J. Zhao, A. L. Petronico, S. M. Miller, M. Christina White, *Nat. Chem.* **2015**, *7*, 987–994.

[91]   F. A. Davis, P. M. Gaspari, B. M. Nolt, P. Xu, *J. Org. Chem.* **2008**, *73*, 9619–9626.

[92]   S. Ichikawa, S. L. Buchwald, *Org. Lett.* **2019**, *21*, 8736–8739.

[93]   R. Xu, K. Wang, H. Liu, W. Tang, H. Sun, D. Xue, J. Xiao, C. Wang, *Angew. Chem. Int. Ed.* **2020**, *59*, 21959–21964.

[94]   M. Breugst, H.-U. Reissig, *Angew. Chem. Int. Ed.* **2020**, *59*, 12293–12307.

[95]   W. S. Jen, J. J. M. Wiener, D. W. C. MacMillan, *J. Am. Chem. Soc.* **2000**, *122*, 9874–9875.

[96]   S. D. Karyakarte, T. P. Smith, S. R. Chemler, *J. Org. Chem.* **2012**, *77*, 7755–7760.

[97]   C.-Z. Yao, Z.-F. Xiao, J. Liu, X.-S. Ning, Y.-B. Kang, *Org. Lett.* **2014**, *16*, 2498–2501.

[98]   J.-i. Tateiwa, K. Hashimoto, T. Yamauchi, S. Uemura, *Bull. Chem. Soc. Jpn.* **1996**, *69*, 2361–2368.

[99]   T. Bach, J. Löbel, *Synthesis* **2002**, *2002*, 2521–2526.

[100]   X. Li, C. Li, W. Zhang, X. Lu, S. Han, R. Hong, *Org. Lett.* **2010**, *12*, 1696–1699.

[101]   Y. Ashikari, Y. Kiuchi, T. Takeuchi, K. Ueoka, S. Suga, J.-I. Yoshida, *Chem. Lett.* **2014**, *43*, 210–212.

[102]   I. Colomer, O. Adeniji, G. M. Burslem, P. Craven, M. O. Rasmussen, A. Willaume, T. Kalliokoski, R. Foster, S. P. Marsden, A. Nelson, *Bioorg. Med. Chem.* **2015**, *23*, 2736–2740.

[103]   J.-W. Chang, D.-P. Jang, B.-J. Uang, F.-L. Liao, S.-L. Wang, *Org. Lett.* **1999**, *1*, 2061–2063.

[104]   B. Gadenne, P. Hesemann, J. J. E. Moreau, *Tetrahedron Lett.* **2004**, *45*, 8157–8160.

[105]   F. Carta, A. Scozzafava, C. T. Supuran, *Expert Opin. Ther. Pat.* **2012**, *22*, 747–758.

[106]   İ. Gulçin, P. Taslimi, *Expert Opin. Ther. Pat.* **2018**, *28*, 541–549.

[107]   S. Bookheimer, L. M. Schrader, R. Rausch, R. Sankar, J. Engel Jr., *Epilepsia* **2005**, *46*, 236–243.

[108]   Y. Ni, H. Zuo, H. Yu, Y. Wu, F. Zhong, *Org. Lett.* **2018**, *20*, 5899–5904.

[109]   L. McMaster, *J. Am. Chem. Soc.* **1934**, *56*, 204–206.

[110]   C. D. Egginton, A. J. Lambie, *J. Chem. Soc. C.* **1969**, 1623–1625.

[111]   V. I. Meshcheryakov, M. Y. Moskalik, I. Starke, B. A. Shainyan, *Russ. J. Org. Chem.* **2010**, *46*, 1471–1475.

[112]   C. D. Díaz-Oviedo, *The Catalytic Asymmetric Intermolecular Prins Reaction*, Universität zu Köln, **2022**.

[113]   L. Zhuang, C. M. Tice, Z. Xu, W. Zhao, S. Cacatian, Y.-J. Ye, S. B. Singh, P. Lindblom, B. M. McKeever, P. M. Krosky, Y. Zhao, D. Lala, B. A. Kruk, S. Meng, L. Howard, J. A. Johnson, Y. Bukhtiyarov, R. Panemangalore, J. Guo, R. Guo, F. Himmelsbach, B. Hamilton, A. Schuler-Metz, H. Schauerte, R. Gregg, G. M. McGeehan, K. Leftheris, D. A. Claremon, *Bioorg. Med. Chem.* **2017**, *25*, 3649–3657.

[114]   W. Yang, Y. Wang, A. Lai, C. G. Clark, J. R. Corte, T. Fang, P. J. Gilligan, Y. Jeon, K. B. Pabbisetty, R. A. Rampulla, A. Mathur, M. Kaspady, P. R. Neithnadka, A. Arumugam, S. Raju, K. A. Rossi, J. E. Myers, Jr., S. Sheriff, Z. Lou, J. J. Zheng, S. A. Chacko, J. M. Bozarth, Y. Wu, E. J. Crain, P. C. Wong, D. A. Seiffert, J. M. Luettgen, P. Y. S. Lam, R. R. Wexler, W. R. Ewing, *J. Med. Chem.* **2020**, *63*, 7226–7242.

[115]   Y. F. Wang, T. Izawa, S. Kobayashi, M. Ohno, *J. Am. Chem. Soc.* **1982**, *104*, 6465–6466.

[116]   M. Schulze, *Synth. Commun.* **2010**, *40*, 3415–3422.

[117]   S. Xu, Y. Ping, W. Li, H. Guo, Y. Su, Z. Li, M. Wang, W. Kong, *J. Am. Chem. Soc.* **2023**, *145*, 5231–5241.

[118]   A. Kanwal, U. Afzal, M. Zubair, M. Imran, N. Rasool, *RSC Adv.* **2024**, *14*, 6948–6971.

[119]   N. Balak, I. Elmaci, *Eur. J. Neurol.* **2007**, *14*, 552–561.

[120]   D. W. Robertson, N. D. Jones, J. K. Swartzendruber, K. S. Yang, D. T. Wong, *J. Med. Chem.* **1988**, *31*, 185–189.

[121]   D. W. Robertson, J. H. Krushinski, R. W. Fuller, J. D. Leander, *J. Med. Chem.* **1988**, *31*, 1412–1417.

[122]   J. C. Stevens, S. A. Wrighton, *J. Pharmacol. Exp. Ther.* **1993**, *266*, 964–971.

[123] D. M. Stresser, A. K. Mason, E. S. Perloff, T. Ho, C. L. Crespi, A. A. Dandeneau, L. Morgan, S. S. Dehal, *Drug Metab. Dispos.* **2009**, *37*, 695–698.

[124] H. Liu, L. Song, B. Zhao, Y. Tang, H. Wei, C. Wang, Y. Liu, CN105001102A ed., Zhengzhou University, China, **2015**.

[125] Y. Zhao, H. Zhu, S. Sung, D. J. Wink, J. M. Zadrozny, T. G. Driver, *Angew. Chem. Int. Ed.* **2021**, *60*, 19207–19213.

[126] B. Loev, M. F. Kormendy, *J. Org. Chem.* **1963**, *28*, 3421–3426.

[127] J. M. Risley, R. L. Van Etten, *J. Am. Chem. Soc.* **1979**, *101*, 252–253.

[128] S. Das, B. Mitschke, C. K. De, I. Harden, G. Bistoni, B. List, *Nat. Catal.* **2021**, *4*, 1043–1049.

[129] L. Liu, M. Leutzsch, Y. Zheng, M. W. Alachraf, W. Thiel, B. List, *J. Am. Chem. Soc.* **2015**, *137*, 13268–13271.

[130] H. Mayr, A. R. Ofial, E.-U. Würthwein, N. C. Aust, *J. Am. Chem. Soc.* **1997**, *119*, 12727–12733.

[131] J. Burés, *Angew. Chem. Int. Ed.* **2016**, *55*, 2028–2031.

[132] J. Burés, *Top. Catal.* **2017**, *60*, 631–633.

[133] R. D. Baxter, D. Sale, K. M. Engle, J.-Q. Yu, D. G. Blackmond, *J. Am. Chem. Soc.* **2012**, *134*, 4600–4606.

[134] L. Capaldo, Z. Wen, T. Noël, *Chem. Sci.* **2023**, *14*, 4230–4247.

[135] T. Tsubogo, T. Ishiwata, S. Kobayashi, *Angew. Chem. Int. Ed.* **2013**, *52*, 6590–6604.

[136] W. L. F. Armarego, *Purification of laboratory chemicals*, 8th ed., Butterworth-Heinemann, Woburn, MA, **2003**.

[137] H. Cao, T. Chen, Y. Zhou, D. Han, S. F. Yin, L. B. Han, *Adv. Synth. Catal.* **2014**, *356*, 765–769.

[138] T. Brégent, J. P. Bouillon, T. Poisson, *Chem. Eur. J.* **2021**, *27*, 13966–13970.

[139] A. Gonzalez-de-Castro, J. Xiao, *J. Am. Chem. Soc.* **2015**, *137*, 8206–8218.

[140] A. Tsoukaki, E. Skolia, I. Triandafillidi, C. G. Kokotos, *Eur. J. Org. Chem.* **2022**, *2022*, e202200463.

[141] B. Wolff, Z. W. Qu, S. Grimme, M. Oestreich, *Angew. Chem. Int. Ed.* **2023**, *62*, e202305295.

[142] D. G. Kohler, S. N. Gockel, J. L. Kennemur, P. J. Waller, K. L. Hull, *Nat. Chem.* **2018**, *10*, 333–340.

[143] O. O. Orazi, R. A. Corral, *J. Chem. Soc., Perkin Trans. 1* **1975**, 772–774.

[144] S. Fustero, D. Jiménez, J. Moscardó, S. Catalán, C. del Pozo, *Org. Lett.* **2007**, *9*, 5283–5286.

[145] Y. E. You, L. Zhang, L. Cui, X. Mi, S. Luo, *Angew. Chem. Int. Ed.* **2017**, *56*, 13814–13818.

[146] H. Meyer, A. K. Beck, R. Sebesta, D. Seebach, *Org. Synth.* **2008**, *85*, 287–194.

[147] P. M. Esch, I. M. Boska, H. Hiemstra, R. F. de Boer, W. N. Speckamp, *Tetrahedron* **1991**, *47*, 4039–4062.

[148] N. N. Nasief, D. Hangauer, *J. Med. Chem.* **2014**, *57*, 2315–2333.

[149] N. C. Boaz, N. C. Bair, T. T. Le, T. J. Peelen, *Org. Lett.* **2010**, *12*, 2464–2467.

[150] X. Feng, G. Qiu, S. Liang, J. Su, H. Teng, L. Wu, X. Hu, *Russ. J. Org. Chem.* **2006**, *42*, 496–500.

[151] B. Viswambharan, T. Okimura, S. Suzuki, S. Okamoto, *J. Org. Chem.* **2011**, *76*, 6678–6685.

[152] G. Facchetti, R. Gandolfi, M. Fusè, D. Zerla, E. Cesarotti, M. Pellizzoni, I. Rimoldi, *New J. Chem.* **2015**, *39*, 3792–3800.

[153] J. Song, W.-H. Zheng, *Chem. Commun.* **2022**, *58*, 7392–7395.

[154] G. Mathieu, H. Patel, H. Lebel, *Org. Process Res. Dev.* **2020**, *24*, 2157–2168.

[155] C.-Q. Deng, J. Deng, *Org. Lett.* **2022**, *24*, 2494–2498.

[156] E. Dongala, C. Mioskowski, M. A. Solladié-Cavallo, M. G. Solladié, *C. R. Acad. Sci. Paris. Série C, Sciences Chimiques [0567-6541]* **1973**, *277*, 251–253.

[157] Y. Gao, K. B. Sharpless, *J. Org. Chem.* **1988**, *53*, 4081–4084.

[158] P. S. J. Kaib, L. Schreyer, S. Lee, R. Properzi, B. List, *Angew. Chem. Int. Ed.* **2016**, *55*, 13200–13203.

[159] H. Zhou, R. Properzi, M. Leutzsch, P. Belanzoni, G. Bistoni, N. Tsuji, J. T. Han, C. Zhu, B. List, *J. Am. Chem. Soc.* **2023**, *145*, 4994–5000.

[160] S. Lee, P. S. J. Kaib, B. List, *J. Am. Chem. Soc.* **2017**, *139*, 2156–2159.

[161] H. Zhou, H. Y. Bae, M. Leutzsch, J. L. Kennemur, D. Bécart, B. List, *J. Am. Chem. Soc.* **2020**, *142*, 13695–13700.

[162] Y. Grell, N. Demirel, K. Harms, E. Meggers, *Organometallics* **2019**, *38*, 3852–3859.

[163] M. V. Skorobogatyi, A. V. Ustinov, I. A. Stepanova, A. A. Pchelintseva, A. L. Petrunina, V. L. Andronova, G. A. Galegov, A. D. Malakhov, V. A. Korshun, *Org. Biomol. Chem.* **2006**, *4*, 1091.

[164] Y. Xu, S. Yu, Q. Chen, X. Chen, Y. Li, X. Yu, L. Pu, *Chem. Eur. J.* **2016**, *22*, 12061–12067.

[165] X. Liu, T. Liu, W. Meng, H. Du, *Org. Biomol. Chem.* **2018**, *16*, 8686–8689.

[166] S. Lee, H. Y. Bae, B. List, *Angew. Chem. Int. Ed.* **2018**, *57*, 12162–12166.

7. Appendix

Erklärung/Declaration

Hiermit versichere ich an Eides statt, dass ich die vorliegende Dissertation selbstständig und ohne die Benutzung anderer als der angegebenen Hilfsmittel und Literatur angefertigt habe. Alle Stellen, die wörtlich oder sinngemäß aus veröffentlichten und nicht veröffentlichten Werken dem Wortlaut oder dem Sinn nach entnommen wurden, sind als solche kenntlich gemacht. Ich versichere an Eides statt, dass diese Dissertation noch keiner anderen Fakultät oder Universität zur Prüfung vorgelegen hat; dass sie noch nicht veröffentlicht worden ist sowie, dass ich eine Veröffentlichung der Dissertation vor Abschluss der Promotion nicht ohne Genehmigung des Promotionsausschusses vornehmen werde. Die Bestimmungen dieser Ordnung sind mir bekannt. Darüber hinaus erkläre ich hiermit, dass ich die Ordnung zur Sicherung guter wissenschaftlicher Praxis und zum Umgang mit wissenschaftlichem Fehlverhalten der Universität zu Köln gelesen und sie bei der Durchführung der Dissertation zugrundeliegenden Arbeiten und der schriftlich verfassten Dissertation beachtet habe und verpflichte mich hiermit, die dort genannten Vorgaben bei allen wissenschaftlichen Tätigkeiten zu beachten und umzusetzen. Ich versichere, dass die eingereichte elektronische Fassung der eingereichten Druckfassung vollständig entspricht.

—Mülheim an der Ruhr, December 2024

(María de los Ángeles Guillén Moralejo)

Bisher sind folgende Teilpublikationen/Patenten veröffentlicht worden:

(1) M. Guillén, S. Liu, C. D. Díaz-Oviedo, M. Klussmann, B. List. Acid-Catalyzed Oxy-aminomethylation of Styrenes. *ACS Catal.* **2024**, *14*, 751–756.

(2) M. Guillén, C. D. Díaz-Oviedo, B. List. Process for the Asymmetric Cycloaddition of Alkenes toward 1,3-Amino Alcohols. Application No. EP24184448.9, filed June 25th, 2024.

(3) M. Guillén, M. Leutzsch, B. List. Catalytic Asymmetric Cycloaddition of Olefins with In Situ Generated *N*-Boc-Formaldimine. *J. Am. Chem. Soc.* **2024**, *146*, 32292–32297.

Lebenslauf/CV

María de los Ángeles Guillén Moralejo

Geboren am 25. März 1997 in Barcelona (Spanien)

Staatsangehörigkeit: spanisch

Akademischer Werdegang

Promotion

04.2021–02.2025   Dissertation im Arbeitskreis von Prof. Dr. Benjamin List
Max-Planck-Institut für Kohlenforschung, Mülheim an der Ruhr
Titel: "Catalytic Oxy-aminomethylation of Alkenes"

Hochschulstudium

09.2019–11.2020   Studium Master of Science – Organische Chemie. Masterarbeit im Arbeitskreis von Prof. Dr. Albert Moyano
Universitat de Barcelona, Barcelona (Spanien)
Titel: "Design and Synthesis of New Functionalized Porphyrins for Photoredox Organocatalysis"

09.2015–06.2019   Studium Bachelor of Science – Chemie. Bachelorarbeit im Arbeitskreis von Prof. Dr. Montserrat Corbella
Universitat de Barcelona, Barcelona (Spanien)
Titel: "Effect of Ionic Liquids on the Synthesis and Reactivity of Manganese Complexes with Carboxylate Ligand"